DEVELOPMENT OF RENEWABLE HETEROGENEOUS CATALYSTS FOR PRODUCTION OF LIQUID BIOFUELS

(A THESIS SUBMITTED IN PARTIAL FULFILLMENT OF THE REQUIREMENTS FOR THE DEGREE OF DOCTOR OF PHILOSOPHY)

BY

LAKHYA JYOTI KONWAR

REGISTRATION NO: TZ121501 OF 2012

THE SCHOOL OF ENGINEERING

DEPARTMENT OF ENERGY

TEZPUR UNIVERSITY

NAPAAM-784028

JUNE 2014

ABSTRACT

In light of the constantly increasing crude oil prices and growing environmental concerns, the replacement of fossil and petroleum fuels by renewable alternatives is becoming more and more important. While other renewable sources of energy, such as the sun and wind, can contribute to electricity capacity, in reality the vast majority of motor vehicles (transportation sector and distribution networks) require liquid fuel and will do so for the foreseeable future and therefore any attempts to sustainably power, the world's millions of motor vehicles must include biofuels. Nonetheless, the main drawbacks preventing the large scale commercialization of these fuels are their higher production costs due to: (i) feedstock issues (expensive, food vs. fuel issues) and (ii) involvement of complex multi step synthesis and purification steps.

About 90% of all chemical manufacturing processes require the use of catalysts. Production of biofuels is no exception, as processing of biomass components into fuels and platform chemicals involve large number high energetic chemical and biochemical reactions. The present work focuses on the catalysis aspect of biofuel production. Next to feedstock, catalyst plays the most vital role in any industrial process as it directly affects production route and product cost, quality and yield. It is well accepted fact that uses of heterogeneous catalysts offer several process advantages over the homogeneous counterparts which include easy catalyst separation from product and reusability. However, most of the conventional heterogeneous catalysts (alumina, zeolites, amberlyst, sulfated zirconia etc) have shown poor performance in connection to applications in biofuel production. The main drawbacks are (i) poor activity (narrow pore structures restricting the interaction with large-size biomass building-blocks), (ii) high operational cost associated to the use of such materials and (iii) stability issues (leaching, thermal stability etc). Recently, attention has been given to biomass as renewable catalyst precursors in order to make the synthesis of heterogeneous catalyst "*green*" and "*cost effective*". Within this concept, the carbon based catalysts and bio based CaO were reported, CaO prepared from Ca rich waste sources such as mollusk, snail, shrimp and egg shells have been successfully applied as catalysts for biodiesel production. Similarly, carbon based heterogeneous catalysts have been prepared from a variety of biomass sources such as starch, cellulose, glucose and

agro-industrial wastes. They are considered as ideal catalysts due to desirable features such as low material cost, chemical inertness, high surface area and thermal stability. Such catalysts were generally prepared in two steps: (i) carbonization followed by (ii) surface modification or functionalization with acids or bases.

In view of the above consideration, the present investigation was undertaken with the aim of developing heterogeneous catalysts from renewable sources using locally available bio-wastes. The prepared catalysts were examined for their catalytic activities in biofuel productions, which could eliminate the use of corrosive chemicals such as H_2SO_4, NaOH, KOH etc. thus, make the process environmentally benign, cost effective and greener one.

The work embedded in the thesis is arranged in seven chapters. The theme of the thesis is outlined in the introduction chapter (**Chapter 1**). The role of catalyst and the need for renewable source based '*green*' heterogeneous catalysts in reference to biofuel production are discussed. While, in **Chapter 2** the detailed discussion of various analytical methods used for characterization of the catalytic materials are presented.

In **Chapter 3**, the utilization of post harvest crop residues of *Vigna radiata* plant, *Musa balbisiana pseudo* stem for preparing a highly basic metal/mixed oxide catalyst is demonstrated. The materials were composed mainly of potassium and calcium in the form of oxides and carbonates, responsible for the high alkalinity and catalytic activity of such materials. The chapter also describes their application as a heterogeneous substitute to NaOH in biodiesel production. The *Vigna radiata* derived catalytic materials exhibited highest activity, FAME yield of 92% with 9:1 methanol to oil molar ratio in 8 h reaction time. Although such catalysts are cheap and could substantially reduce the biodiesel production costs, but they have disadvantages related to the reusability and requirement of a large catalyst amount for satisfactory FAME yield. Nonetheless, all the major fuel properties of biodiesel produced over such catalyst confer to the existing norms of biodiesel fuel.

In **Chapter 4,** the preparation, characterization and catalytic applications (in transesterification of vegetable oils) of a highly robust and reusable bio based CaO supported *active carbon* (ACaO) catalyst from *Turbonilla striatula* shells is demonstrated. Under optimized reaction conditions of 120 °C, 40:1 methanol to oil ratio, 11 wt% catalyst and 7 h of reaction time, FAME yield upto 96% could be reached. Although the catalyst

was less active than native CaO, ACaO was highly stable, reusable and maintained its initial activity upto five cycles under the investigated conditions. Consequently the reusability issues of the catalysts discussed in chapter 3 are successfully addressed by employing ACaO catalyst. The high stability of ACaO is attributed to the oxygen-containing groups (-COOH,-OH, lactones etc) present on the surface of active carbon which probably act as anchoring sites for the CaO molecules, thus preventing them from leaching out into the reaction mixture.

In **Chapter 5,** the preparation, characterization and catalytic applications (biodiesel production by simultaneous esterification and transesterification of acidic oils) of highly porous *sulfonated carbon* (Brønsted solid acid) catalysts from de-oiled waste cake (DOWC) residues generated in biodiesel production has been presented. The DOWC based catalytic materials exhibited high acid density, porosity, specific surface area, thermal stability and good reusability and outperformed homogeneous H_2SO_4 under similar conditions. The catalytic activity was found to be dependent on the reaction conditions and initial free fatty acid (FFA) content in oil. Higher FFA content leads to improved mutual solubility of the oil and methanol resulting in increased transesterification activity. Highest FAME yield of 71% was obtained from oil containing 43 wt% FFA in 8 h under mild conditions of 80 °C, 5 wt% catalyst and 43:1 methanol to oil molar ratio.

In **Chapter 6,** the effects of carbon source and preparation method on the structure, acidity and catalytic activity of DOWC based sulfonated carbons are described. The chapter also discusses the effect of catalyst structure on activity and selectivity through simultaneous and comparative evaluation of activities in oleic acid esterification and cellulose saccharification, two opposite but equally imperative reaction involved in biofuel synthesis. In the current work, preparation method strongly influenced the structure and surface properties of DOWC based sulfonated carbons, and hence their catalytic properties. In general, catalysts with a higher porosity, high surface area and acid site density always favor high activity. Use of chemical activation was necessary to facilitate porosity and functional group development, in order to enhance the catalytic performance. Structurally, these carbons are more complicated than previously reported sulfonated carbons and contain phosphates, nitrogen compounds in addition to $-SO_3H$, –COOH, –OH and lactones, typically present in carbohydrate, sugar or resin based sulfonated carbons.

Conventional H_2SO_4 sulfonation fails to produce catalysts with a high $-SO_3H$ density and porosity simultaneously. Radical sulfonation on the other hand was found to be more effective and produced catalysts with tenfold higher $-SO_3H$ densities than H_2SO_4 sulfonation even from graphitic and ordered AC. Carbon source and amount of sulfonating agent influenced efficiency of radical sulfonation, hence $-SO_3H$ density and catalytic activity. A high density of $-SO_3H$ groups resulted in higher esterification rates (FFA conversion upto 96% in 10 h under mild conditions of 65 °C, 3 wt% catalyst and 30:1 methanol to oil molar ratio) while a higher density of surface functional groups –COOH, –OH favored high saccharification activity as well as selectivity towards sugars (sugar yield 50.5 mol C% at 150 °C). Thus, the *Mesua ferrea* Linn. and *Pongamia pinnata* DOWC based catalysts with higher $-SO_3H$ density and surface area were found to be more active in esterification of oleic acid whereas the *Jatropha curcas* cake based catalyst showed better activity and sugar selectivity in cellulose saccharification.

In Chapter 7, the main findings of work embedded in the thesis have been summarized and the prospective scopes for future work/development are discussed.

TEZPUR UNIVERSITY
(A Central University established by an act of Parliament)
Napaam, Tezpur-784028
Dist Sonitpur, Assam, India
Ph: 03712-267004, 267005: Fax: 03712-267005 (6)

Declaration by the candidate

I hereby declare that the thesis entitled "**DEVELOPMENT OF RENEWABLE HETEROGENEOUS CATALYSTS FOR PRODUCTION OF LIQUID BIOFUELS**" being submitted to the Department of Energy, Tezpur University, Assam, India, is a record of original research work carried out by me. The work was carried out at Biomass conversion Laboratory, Department of Energy Tezpur University. Parts of the work were also carried out at Laboratory of Industrial chemistry and Reaction Engineering, Department of Chemical Engineering at Åbo Akademi University between March 2012 and January 2014. I also declare that neither this work as a whole or a part of it has been submitted to any other University or Institute for any other degree or diploma.

All helps received from various sources have been duly acknowledged.

Date: 19-12-14

Place. Tezpur University

Lakhya Jyoti Konwar

(Lakhya Jyoti Konwar)

TEZPUR UNIVERSITY
(A Central University established by an act of Parliament)
Napaam, Tezpur-784028
Dist Sonitpur, Assam, India
Ph: 03712-267004, 267005: Fax: 03712-267005 (6)

Certificate of the Supervisors

This is to certify that the thesis entitled "**DEVELOPMENT OF RENEWABLE HETEROGENEOUS CATALYSTS FOR PRODUCTION OF LIQUID BIOFUELS**" submitted to the Department of Energy, School of Engineering Tezpur University in part fulfillment for the award of the degree of Doctor of Philosophy in Energy is a record of research work carried out by Mr. Lakhya Jyoti Konwar under our supervision.

All help received by him/her from various sources have been duly acknowledged.

No part of this thesis has been submitted elsewhere for award of any other degree.

19/12/14

(Prof. Dhanapati Deka)
Supervisor
Professor
Department of Energy
Tezpur University

19/12/14

(Dr. Ashim J. Thakur)
Co-Supervisor
Associate Professor
Department of Chemical Sciences
Tezpur University

TEZPUR UNIVERSITY
(A Central University established by an act of Parliament)
Napaam, Tezpur-784028
Dist Sonitpur, Assam, India
Ph: 03712-267004, 267005: Fax: 03712-267005 (6)

Certificate of the External Examiner and ODEC

This is to certify that the matter embodied in the thesis entitled "**DEVELOPMENT OF RENEWABLE HETEROGENEOUS CATALYSTS FOR PRODUCTION OF LIQUID BIOFUELS**" submitted by Mr. Lakhya Jyoti Konwar to Tezpur University in the Department of Energy under the school of Engineering in partial fulfillment of the requirement for the award of the degree of Doctor of Philosophy in Energy has been examined by me/us on _____ and found to be satisfactory.

(Prof. D Deka)
Supervisor
Date

External Examiner

Date

(Dr. A.J.Thakur)
Co-Supervisor
Date

DEDICATION

Dedicated in loving memory of my beloved father late Binanda Chandra Konwar.

Your words of wisdom, inspiration and encouragement in pursuit of excellence, still linger on.

Lakhya Jyoti Konwar

ACKNOWLEDGEMENTS

At the very outset I want to express my gratitude to my supervisors, Prof. Dr. D. Deka and Dr. A. J. Thakur for giving me the platform, guidance and the support to carry out the whole work.

I am also grateful to Dr. P. Mäki-Arvela, Prof. Dr. J-P Mikkola and Dr. N. Kumar for their guidance and support during my research visits at Åbo Akademi University.

I also want to express my gratitude to Centre for International Mobility – CIMO (Finland) for providing visiting doctoral fellowship to work at Åbo Akademi University. I am also thankful to the DST, India and the Academy of Finland for the initiation of the research programme between India and Finland and funding some of my research visits.

I am also grateful to all the faculty members, especially Dr. R. A. Prasath of The Center for green energy Technologies, Pondicherry University where I briefly pursued M.Tech. For if it was not for them I would have never chosen energy/bioenergy as a research subject.

I also take this opportunity to thank the doctoral committee members for proper guidance and positive inputs for better outputs.

My heartiest thanks also go to the HoD and all the faculty members of Department of Energy, Tezpur University. I am especially thankful to Dr. R. Kataki and his doctoral students Rahul Singh Chutia and Sarat Ch. Borah for providing the facility and necessary help to carry out some of the initial carbonization experiments.

I am also grateful to the non-teaching staff, research scholars, especially Tapan Borah, Chitta Ranjan Gogoi and T. Lahon of Department of Energy, Tezpur University.

I am also thankful to Laboratory manager Dr. Kari Eränen of Laboratory of Industrial chemistry and Reaction Engineering, Åbo Akademi University for his invaluable help with reactor systems, instruments and timely answers to my practical difficulties.

Dr. Samrat Paul, Department of Energy and SAIF, North East Hill University, Shillong (India) are gratefully acknowledged for TEM analysis. Dr. Andrey Shchukarev of

Department of Chemistry Umeå University (Sweden) is gratefully acknowledged for XPS analysis. I am highly thankful to Ms. Munu Borah, CSIR-NPL for Raman analysis.

I am also thankful to Vice Chancellor, Prof. M. K. Chaudhuri, for encouraging doctoral students like us towards research.

My special thanks also goes to my lab mates, co-authors and friends: Dr. Jutika Boro, Plaban Borah, Pitambar Sedai, Subrata Das, Rahul Singh Chutia, Prasanta Baishya, Pankaj Gogoi, Arup Jyoti Dutta and Bhaskar Saikia for their support, advice and making my time at the university a productive and meaningful one. Working every single day with my lab mates here was a joyful experience and they encouraged me for betterment of my work.

I am thankful to School of Engineering cafeteria for donating waste cooking oil.

Most importantly I am decidedly grateful to my loving mother (Bhairabi Konwar), my brother (Biswadeep Konwar), uncle and aunty (Gita Saikia, Dipen Saikia), my cousins (Dr. Khagorika Saika and Jumoni Saikia) and relatives for their love, endless support, encouragement and giving me strength during ominous times to move forward and complete the work. I also take this opportunity to acknowledge the tremendous faith, moral and at times economic support from my close friends Rupali Das and Jutika ba.

(Lakhya Jyoti Konwar)

TABLE OF CONTENTS

LIST OF TABLES

LIST OF FIGURES

LIST OF SYMBOLS AND ABBREVIATIONS

4-BDS	4-benzenediazoniumsulfonate
AO	Acid oils or high free fatty acid containing oils
ASTM	American Society of Testing of Materials
AOAC	American Oil Chemists' Society
ACaO	CaO supported active carbon
BET	Brunauer–Emmett– Teller
BJH	Barrett-Joyner-Halenda
BtL	Biomass to liquid
$CDCl_3$	Chloroform-d
$d_{(p)}$	Pore diameter
DSC	Differential Scanning calorimetry
DOWC	De-oiled waste cake
DTBG	di-tert-butyl-glycerol
EDX/EDS	Energy-dispersive X-ray spectroscopy
FAAE	Fatty Acid Alkyl Esters
FAME	Fatty Acid Methyl Ester
FFA	Free Fatty Acids
FT	Fischer-Tropsch
FT-IR	Fourier transform infrared spectroscopy
GTBE	glycerol-tertiary-butyl-ether
GHG	Green house gas
GC	Gas chromatography
GC-MS	Gas chromatography mass spectrometry
H_	Hammett strength
HPLC	High precision liquid chromatography
HVO	Hydrotreated vegetable oil or Renewable diesel
IEA	International Energy Agency
IEO	International Energy Outlook

$I_{(D)}/I_{(G)}$	Intensity ratio of D and G band in Raman spectra
JCPDS	Joint Committee on Powder Diffraction Standards
JAC	Active carbon from *Jatropha curcas* DOWC
JACS	Sulfonated active carbon from *Jatropha curcas* DOWC
K	Rate constant
L_a	Graphitic cluster size
MAC	Active carbon from *Mesua ferea* Linn. DOWC
MACS	Sulfonated active carbon from *Mesua ferea* Linn. DOWC
MACHT	Hydrothermally sulfonated *Mesua ferea* Linn. DOWC
MAC-SO_3H	Sulfonated active carbon from *Mesua ferea* Linn. DOWC (Method 1)
MAC-SO_3H*	Sulfonated active carbon from *Mesua ferea* Linn. DOWC (Method 2)
$MACH_2SO_4$	H_2SO_4 sulfonated Active carbon from *Mesua ferea* Linn. DOWC
MTBE	methyl-tertiary-butyl- ether
MB-ash	*Musa balbisiana* ash
MCC	Microcrystalline cellulose
NMR	Nuclear magnetic resonance spectroscopy
NO_x	NO and NO_2
PTSA	p-toluenesulfonic acid
PAC	Active carbon from *Pongamia pinnata* DOWC
PACS	Sulfonated active carbon from *Pongamia pinnata* DOWC
-$PhSO_3H$	Phenyl sulfonic acid
SEM	Scanning electron microscopy
-SO_3H	Sulfonic acid
TIC	Total ion chromatogram
TEM	Transmission electron microscopy
T	Time
T	Temperature
$T_{(max)}$	Thermal stability

TBA	tert-butyl alcohol
TGA	Thermogravimetric analysis
TMS	Tetramethylsilane
TOF	Turnover frequency
TPD	Temperature programmed desorption
$V_{(p)}$	Pore volume
$V_{(mp)}$	Micropore volume
VR-ash	*Vigna radiate* ash
WCO	Waste Cooking Oil
wt.%	Weight percentage
XRD	X-ray Diffraction
XPS	X-ray photoelectron spectroscopy

LIST OF PUBLICATIONS

1. **Konwar, L.J.,** Boro, J. & Deka, D. Review on latest developments in biodiesel production using carbon-based catalysts, *Renew Sust Energ Rev,* **29**, 546–564, 2014.

2. **Konwar, L.J.,** Mäki-Arvela, P., Thakur, A.J., Salminen, E., Kumar, N., Mikkola, J.P. & Deka, D. Towards carbon efficient biorefining: Biomass conversion using multifunctional mesoporous solid acids obtained from biodiesel wastes, *Appl. Catal. B,* Revision Submitted.

3. **Konwar, L.J.,** Das, R., Thakur, A.J., Salminen, E., Mäki-Arvela, P., Kumar, N., Mikkola, J.P. & Deka, D. Biodiesel production from acid oils using sulfonated carbon catalyst derived from oil-cake waste, *J. Mol. Cat. A,* **388–389**, 167-176, 2014.

4. *Boro, J., ***Konwar, L.J.** & Deka, D. Transesterification of non edible feedstock with lithium incorporated egg shell derived CaO as heterogeneous base catalyst for biodiesel production, *Fuel Process Technol,* **122**, 72-78, 2014. (*Equal contribution)

5. Boro, J., **Konwar, L.J.**, Thakur, A.J. & Deka, D. Ba doped CaO derived from waste shells of *T. striatula* (TS-CaO) as heterogeneous catalyst for biodiesel production, *Fuel,* 129, 182–187, 2014.

6. Boro, J., **Konwar, L.J.** & Deka, D. *Vigna radiata* (mung bean) ash as heterogeneous base catalyst for biodiesel production, *J. Bio Eng Biorefin.*, **2**, 54–60, 2013.

7. **Konwar, L.J.,** Boro, J. & Deka, D. Activated carbon supported CaO prepared from waste mollusk shells as heterogeneous catalyst for biodiesel production, *Energ Source Part A.*, (2012, Accepted) (doi:10.1080/15567036.2012.733483)

8. Bora, P., Boro, J., **Konwar, L.J.** & Deka, D. A comparative study of Mesua ferrea L. based hybrid fuel with diesel fuel and biodiesel, *Energ Source Part A.*, (2012, Accepted) (10.1080/15567036.2012.747036)

9. **Konwar, L.J.,** Chutia, R.S., Boro, J., Kataki, R. & Deka, D. Biochar supported CaO as heterogeneous catalyst for biodiesel production, *International Journal of Innovative Research*, **1**(7), 186-195, 2012.

10. Boro, J., **Konwar, L.J.,** Das, S. & Deka, D. Comparative study of CaO derived from waste shells of *Turbonilla Striatula* and commercial CaO for biodiesel synthesis, *Journal of Assam Science Society*, **52**(2), 120-122, 2011.

LIST OF PUBLICATION IN CONFERENCE PROCEEDINGS

1. **Konwar, L.J.,** Sedai, P. & Deka, D. Preparation of activated carbon from de-oiled cake residues of biodiesel production, *Proceedings of Recent challenges for Chemical research and Practices,* November 9-10, 2012, Darrang College, Tezpur, Assam, India.

2. **Konwar, L.J.,** Chutia, R.S., Boro, J., Kataki, R. & Deka, D. Biochar supported CaO as heterogeneous catalyst for biodiesel production, *Proceedings of International Seminar and Workshop on Energy, Sustainability and Development (Special focus on Nanoscience and Nanotechnology)*, October 12-14, 2012, Sibsagar College, Sibsagar, Assam, India.

3. Boro, J., **Konwar, L.J.,** Deka, D. & Thakur, A.J. Review on carbon based catalysts for biodiesel production via transesterification, *Proceedings of International congress on renewable energy (ICORE)*, 2-4 November, 2011, Tezpur University, Assam, India.

4. Shyam, B., **Konwar, L.J.,** Boro, J. & Deka, D. Biodiesel production from mixture of non-edible vegetable oil of North-East India, *Proceedings of International congress on renewable energy (ICORE)*, 2-4 November, 2011, Tezpur University, Assam, India.

5. Boro, J., **Konwar, L.J.**, Das, S. & Deka, D. Comparative study of CaO derived from waste shells of *Turbonilla striatula* and commercial CaO for biodiesel synthesis. *Proceedings of UGC sponsored National Seminar on Frontier Areas of Research in Chemistry*, 24-25 October, 2011, Cotton College, Guwahati, Assam, India.

PARTICIPATION IN CONFERENCES AND WORKSHOPS

1. Summer school 2011 on ***Efficent fossil Energy Technolgies*** organized by Centre for Energy, IIT Guwahati and University of Nottingham, UK, at IIT Guwahati, JULY 4-10, 2011. Poster presented: "*Assessment and Analysis of the Plant oil feedstock available in North East India for biodiesel production*"
2. UGC sponsored National Seminar on ***Frontier Areas of Research in Chemistry*** organised by Cotton College, Guwahati, October 24-25, 2011. Oral presentation: *"Comparative study of CaO derived from waste shells of Turbonilla Striatula and laboratory CaO for biodiesel synthesis*".
3. ***Interntaional Congress on Renewable Energy (ICORE-2011)*** organised by SESI and Tezpur University at Tezpur University, November 2-4, 2011.
4. Finland-India-Sweden seminar encompassing various aspects of "***green chemistry***" within the collaborative project of The Academy of Finland and DST, India, March 2012.
5. International Seminar and Workshop on ***Energy, Sustainability and Development*** (Special focus on Nanoscience and Nanotechnology), Sibsagar College, October 12-14 2012. Oral presentation: "*Biochar supported CaO as heterogeneous catalyst for biodiesel production*".

Chapter 1

Introduction

Chapter 1

1. Introduction

Widely voiced concerns in response to the continuously declining petroleum reservoirs and increasing concerns about the environment has constrained mankind to search for renewable, carbon neutral and environmentally benign alternatives for conventional fuels derived from fossil resources. While other renewable sources of energy, such as the Sun and wind, will contribute to electricity capacity, in reality the vast majority of motor vehicles require liquid fuel and will continue to do so for the foreseeable future and any attempts to sustainably power the world's millions of motor vehicles therefore must include biofuels. Research interest has spiked up tremendously with both the emerging and developed economies pushing forward scientific research for the production and development of biofuels as an alternative for theses 'petrofuels' [1]. There are two crucial aspects to the success of such bio-based products/fuels; (i) feedstock, (ii) process chemistry (catalytic issues). Next to feedstock, catalysts play the most imperative role in any industrial process as their adoption in the processes directly affects the feasible production routes, product costs, product quality and yield. Catalysts are substances that alter (usually increase) the velocity of a chemical reaction without itself being consumed or affected during the process. About 90% of all chemical manufacturing processes and more than 20% of all industrial products require the use of catalysts. Productions of biofuels are no exception as processing of biomass components into fuels and platform chemicals involve large number of high energetic chemical and biochemical reactions. One of the major bottlenecks in current generation biofuel production technology is their reliance on the use of many hazardous and corrosive chemicals, such as NaOH, KOH, HCl, H_2SO_4 etc. as catalysts. This causes not only environmental hazards, increase carbon footprint of such fuels but also negatively impacts the overall process economy as unwanted steps such as purification, product separation, catalyst recovery and waste generation becomes unavoidable. Switching to heterogeneous catalyst may provide a possible solution; this approach however is largely limited by the high cost and low activity of these materials. Therefore, use of renewable materials as heterogeneous catalysts or heterogeneous catalysts synthesized from renewables such as biomass or bio-wastes may successfully

address this issue. The rationale of the thesis was formed after reviewing the current literature on catalyst synthesis and on discovering the possibility of use of 'renewable' (biobased) precursors for this purpose. Finally this chapter concludes with the outline of the thesis.

1.1. An overview of biofuels

By definition the term biofuel refers to solid, liquid and gaseous fuels produced from biomass – organic matter derived from plants or animals. However, there is considerable debate on the classification of biofuels. Biofuels are generally divided into first-, second- and third-generation biofuels, but the same fuel might be classified differently depending on technology maturity, green house gas (GHG) emission balance, physical state or the feedstock used. Thus for simplification, throughout this thesis we will follow the International Energy Agency (IEA) classification of "*conventional*" and "*advanced*" based on the maturity of a technology (Fig. 1.1) [1].

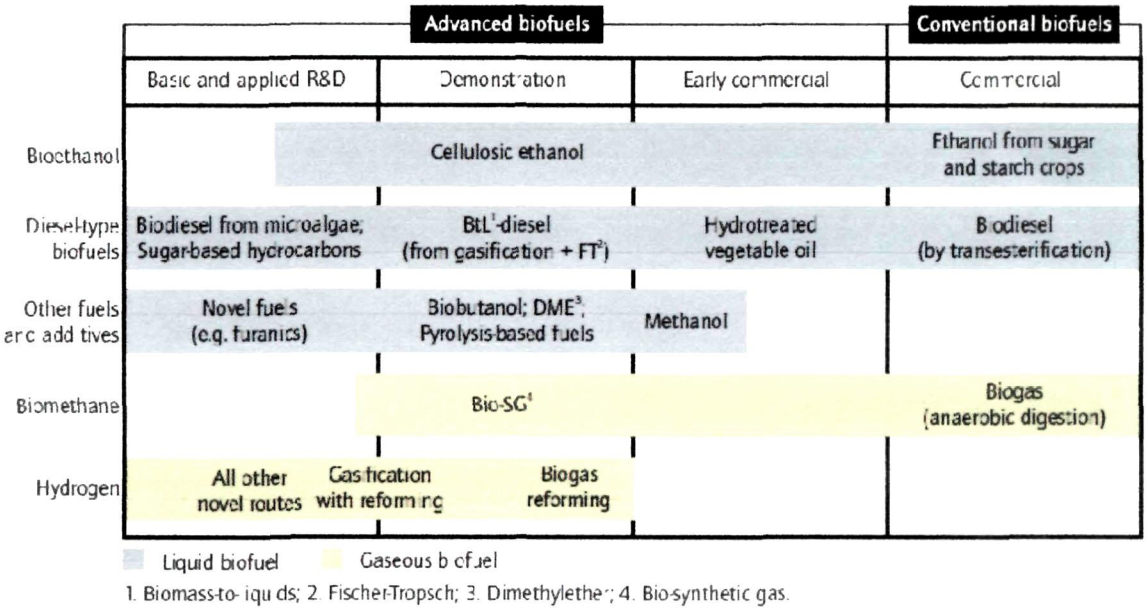

Figure 1.1. The International Energy Agency (IEA) classifications of biofuels, *Adapted from* Technology Roadmaps Biofuels for transport, IEA, (2011) [1]

Conventional biofuel technologies include well-established processes that are already producing biofuels on a commercial scale. These biofuels, commonly referred to as first-generation, include sugar- and starch-based ethanol, oil-crop based biodiesel and

straight vegetable oil, as well as biogas derived through anaerobic digestion. Advanced biofuel technologies are conversion technologies which are still in the research and development (R&D) stage, pilot or demonstration phase, commonly referred to as second- or third-generation. However, it is important to realise that performance and the GHG emission balance of advanced biofuels are not always superior to that of conventional biofuels as these parameters depends on both the feedstock and conversion technology (Fig 1.2) [1].

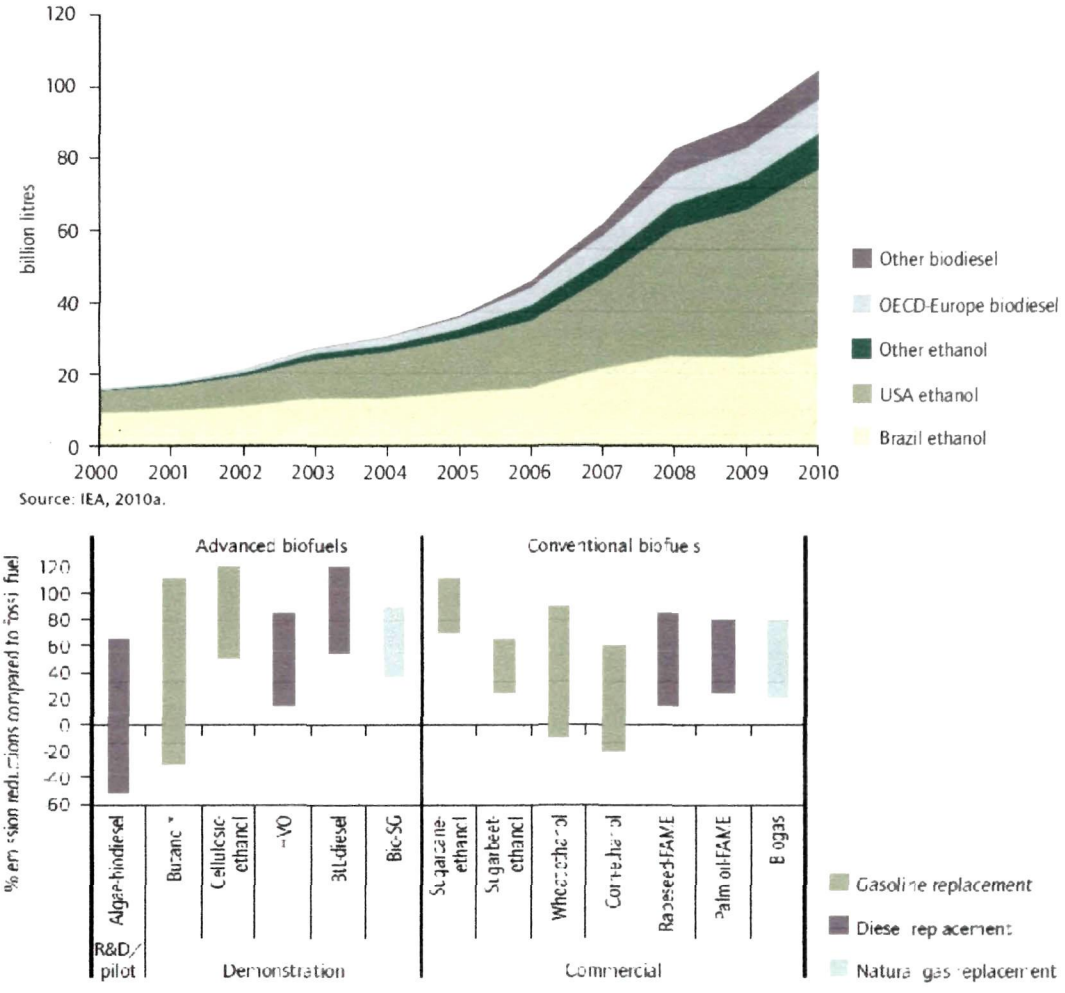

Figure 1.2. Global biofuel production during 2000-2010 (top) and Life-cycle GHG balance of different conventional and advanced biofuels (bottom), *Adapted from* Technology Roadmaps Biofuels for transport, IEA, (2011) [1]

According to a recent report by the IEA, global biofuel production now tops 100 billion litres per year and is expected to increase with the steep rise in crude oil prices (Fig. 1.2). Different fuel types vary in their costs, carbon emissions and impact on land use patterns. The IEA, recently laid out a 'roadmap' to ramp-up the use of biofuels from 2% of global transport fuel today to 27% by the year 2050 which according to IEA could displace enough petroleum to avoid the equivalent of 2.1 gigatonnes of carbon dioxide emission each year if produced sustainably — about as much as net carbon dioxide absorbed by the oceans (Fig. 1.3) [1,2].

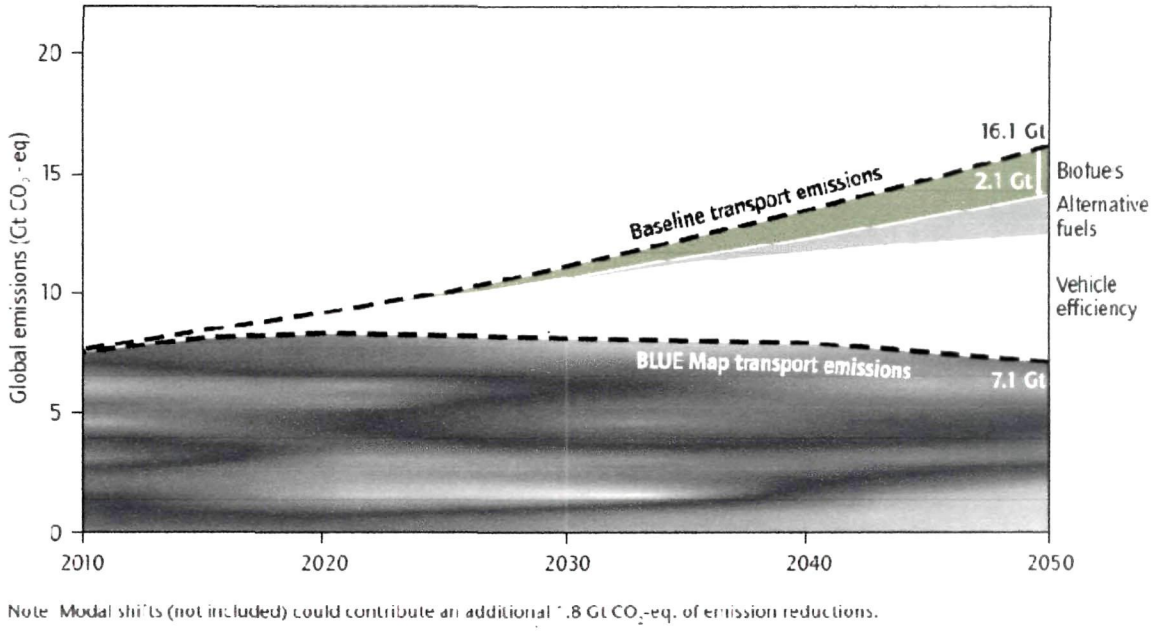

Figure 1.3. Projected contributions of biofuels to emission reductions upto 2050, *Adapted from* Technology Roadmaps Biofuels for transport, IEA, (2011) [1]

Fig. 1.4 shows a simplified schematic representation of the various routes available for processing biomass into fuels and fuel additives. Among the different biomass derived fuels, liquid biofuels such as biodiesel, green diesel or renewable diesel or HVO (hydrotreated vegetable oil) [3,4], bioalcohols [5], Fischer–Tropsch Diesel (from biomass) [6] and glycerol *tert*-butyl ethers (GTBE); a glycerol derived fuel additive [7] are some of the promising alternatives to the petroleum based transportation fuels presently in use. Besides, as these fuels are derived from biomass they are renewable and have significantly lower environmental effect. However, the main drawbacks preventing large scale

commercialization of these alternative fuels are their higher production costs due to involvement of expensive feedstock/raw material, complex multistep synthesis and purification, use of expensive chemicals during processing (as catalysts and purification agents). It is a well accepted fact that in any industrial process the main input to product cost comes from i) raw material/feedstock and ii) process chemistry (production route, chemicals and catalyst used in the process): effects product quality, yield and cost [8,9]. For example, in biodiesel production the main factors contributing to product cost are (a) vegetable oil price and (b) catalyst: properties of catalyst have a direct effect on biodiesel production route, quality and yield [10,11]. Similarly, high feedstock (sugarcane, corn, rice etc) price is main contributing factor to production cost of 1st generation or conventional bioalcohols (bioethanol or sugar ethanol) due to the presence of food vs. fuel conflict. On the other hand, the production of 2nd generation bioethanol (cellulosic ethanol) from lignocellulosic biomass is more energy intensive, complex and requires sophisticated technology: expensive acid resistant high pressure reactors (as the process uses homogeneous acids such as H_2SO_4 at high temperature during pretreatment, hydrolysis steps), modified enzymes catalysts capable of degrading both C5 and C6 sugars and involves multistep separation, purification and recovery process that increases overall production cost. Direct production of liquid fuel from biomass (BtL) using Fischer–Tropsch (FT) synthesis is also possible but more research is still needed in this area. Several European demonstration projects on BtL have been discontinued for various reasons. Another drawback is that the FT process is energy intensive and requires expensive catalysts which increase the processing, maintenance and finally the production cost. Hydrotreating is another method which has been successfully commercialized for production of diesel like hydrocarbons from vegetable oils, but the process is more energy intensive and the initial set up costs are much higher than a conventional biodiesel plant [3,6].

Glycerol is a major byproduct of biodiesel production. The increasing demand and growing biodiesel production is causing a sharp reduction of the market value of glycerol due to excessive production of crude glycerol. Therefore, new applications and value addition process for glycerol are being investigated. Out of the several available value addition processes (hydrogenolysis, etherification, esterification, dehydration, oxidation,

and to name a few) transformation into glycerol *tert*-butyl ethers (GTBE); a fuel additive via etherification with isobutene or *tert*-butyl alcohol (TBA) has been identified as most promising. The reaction can be catalyzed by acidic homogeneous catalysts or by heterogeneous acid catalysts such as zeolites, strong acid ion exchange resins or sulfonic mesostructured silicas and also sulfonated carbons. However, there are only few reported use of sulfonated carbons for *tert*-butylation of glycerol [7]. To summarize, from above discussion it could be concluded that in order to bring down the production costs two areas could be targeted i) look for cheaper feedstocks or ii) substitute some of the expensive chemicals and homogenous catalysts with cheaper and green alternatives.

1.1.1. Biodiesel

Biodiesel is a proven alternative to petrodiesel as a clean-burning renewable alternative fuel already in production on a commercial scale. Currently, biodiesel is regarded the best substitute for petrodiesel due to several reasons. It is derived from vegetable oils or fats which are abundant, commercially viable synthesis process and compatibility with petrodiesel (Table 1.1), not requiring major engine modification and can be distributed using the existing network. The main components of vegetable oils and animal fats are triglycerides or also known as esters of fatty acids attached to a glycerol [4,9,10]. Biodiesel is produced by the alcoholysis of vegetable oils in the presence of a catalyst (usually NaOH or KOH), Scheme 1.1. The main product is fatty acid methyl ester (FAME), known as biodiesel, and the by-product is glycerol (approximately 10%). Usually, excess alcohol is employed to enhance the conversion of triglyceride.

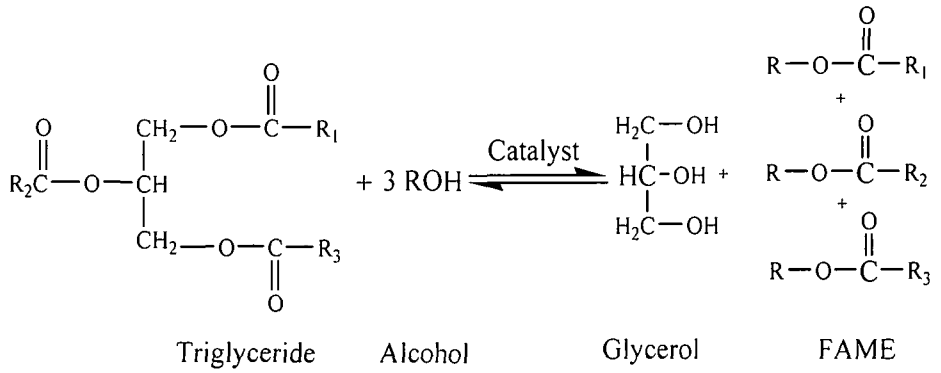

where, R, R_1, R_2 and R_3 represent different fatty acid chains

Scheme 1.1. Schematic representation of biodiesel synthesis.

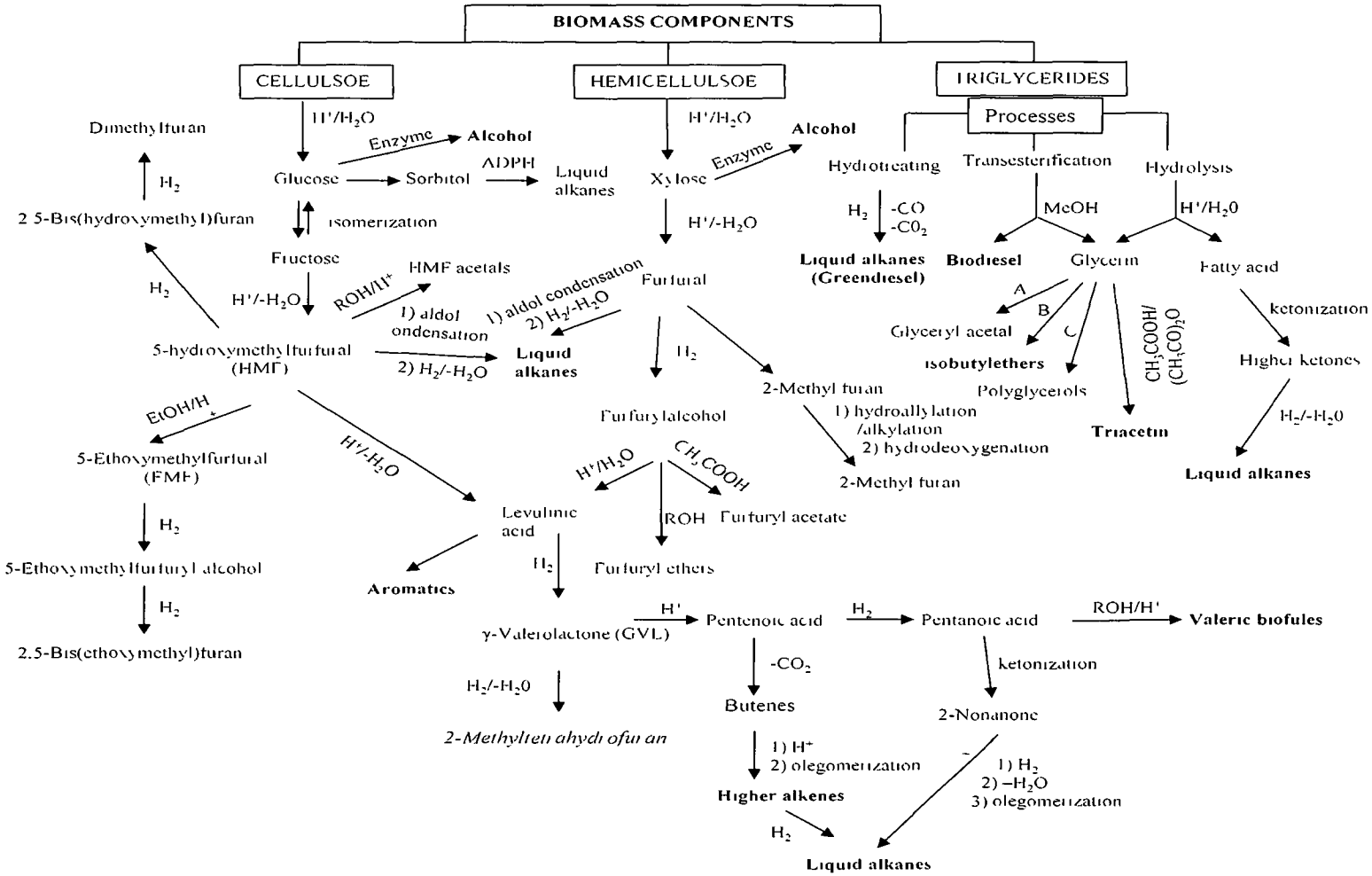

Figure 1.4. Schematic representation of the various paths for obtaining fuels and fuel additives from biomass, where A is RCHO (aldehyde), B is isobutene or *tert*-butylalcohol, C is heat; Adapted from Climent, *et al.* with modifications [3].

While there are advantages of biodiesel over the traditional petroleum based 'fossil' diesel, biodiesel commercialization is limited by production costs: the cost of biodiesel is dominated by the price of the feedstock (refined vegetable oil) [12-14]. Acid oils (AOs) (crude vegetable oils, waste cooking oils, yellow grease etc.) has the potential to serve as attractive low cost biodiesel feedstocks, but the chemical composition of these oils are variable depending on the source. Besides, the presence of moisture and FFA renders conventional NaOH or KOH catalyzed transesterification ineffective for biodiesel production from such oils (Table 1.2) [14]. Therefore, the right choice of raw material and catalyst must always be based on technical, economic aspects for sustainable and cost-effective biodiesel production. In developing countries such as India, use of edible vegetable oils as feedstock is not a viable option as it may give rise to the food vs. fuel conflict [13]. Therefore, with global demand for renewable biofuels gearing up, the investigation of new sources of triglycerides becomes equally important.

Identification of new feedstock will not only increase the feedstock diversity but also add to the economic value of that plant species. Several non-edible feedstock such as *Jatropha curcas*, nahar (*Mesua ferrea* L.), cottonseed oil, karanja (*Pongamia glabra*), fieldpennycress (*Thlaspi arvense* L.), rubber (*Hevea brasiliensis*), microalgae (*Chlorella vulgaris*), terminalia (*Terminalia belerica* R.), mahua (*Madhuca indica*), yellow oleander (*Thevetia peruviana* S.) etc. have already been identified individually as prospective biodiesel feedstock [15-22]. In the Indian scenario, biodiesel has been considered as the most viable biofuel due to the lower implementation costs in comparison to bioalcohols (biobutanol or bioethanol) and wide availability of non-edible oil crops such as *Jatropha curcas* and *Pongamia glabra*.

Table 1.1
Fuel Property Comparison for Ethanol, Butanol, Gasoline, No. 2 Diesel and Biodiesel, [1,95-97]

Property	Ethanol	Butanol	Gasoline	No. 2 Diesel	ASTM Biodiesel (B100)
Chemical Formula	C_2H_5OH	C_4H_9OH	C4 to C12 HC	C3 to C25 HC	C12-C22 FAME
Molecular Weight	46.07	74.12	100–105	≈200	≈270.5
Carbon	52.2	64.75	85–88	84–87	77
Hydrogen	13.1	13.49	12–15	33–16	12
Oxygen	34.7	21.58	0	0	11
Specific gravity, 60 °F/60° F	0.796	0.81	0.72–0.78	0.81–0.89	0.88
Density, lb/gal @ 60° F	6.61		6.0–6.5	6.7–7.4	7.328
Boiling temperature, °F	172	244	80–437	370–650	599 – 662
Reid vapor pressure, psi	2.3	33	8–15	0.2	<0.04
Research octane no.	108	96	90–100	--	--
Motor octane no.	92	78	81–90	--	--
(R + M)/2	100	87	86–94	N/A	--
Cetane no.(1)	--	--	5–20	40–55	47 min
Fuel in water, volume %	100	7.7	Negligible	Negligible	--
Water in fuel, volume %	100	--	Negligible	Negligible	.05% max
Freezing point, °F	-173.2	-130	-40	-40–30[a]	-15–16[a]
Centipoise @ 60 °F	1.19	2.544	0.37–0.44[b]	2.6–4.1	1.9-6.0
Flash point, closed cup, °F	55	95	-45	165	93.0 min
Autoignition temperature, °F	793	343	495	≈600	705-840
Lower heating value (MJ/Kg)	19.6	29.2	32	43.4	≈39[d]
Specific heat, Btu/lb °F	0.57		0.48	0.43	18,145
Stoichiometric air/fuel, weight	9	11.1	14.7[b]	14.7	13.8

[a] Pour Point, ASTM D 97.
[b] Calculated.
[c] Based on Cetane.
[d] Higher Heating Value.

1.1.2. Bioalcohols

Bioalcohols (bioethanol, biopropanol, and biobutanol) are green alternative fuels for internal combustion engines. Bioalcohols (unlike regular alcohols) are always produced by the action of microorganisms and enzymes through the fermentation of sugars derived from starches or cellulose or lignocelluloses (more difficult). Bioalcohols could be divided into two categories:

i). First-generation (or conventional) bioalcohols produced from sugar and starchy crops that can be used for human consumption (common feedstocks include: sugercane, sugar beets, potatoes etc).

ii). Second generation (or advanced) bioalcohols produced from non-food crops, cellulosic and lignocellulosic biomass (i.e. woody stems, branches, bagasse, corncob etc) or from lignocellulosic wastes. Unlike first generation biofuel they do not create problems in regards to the food vs. fuel conflict.

Bioethanol is the most common bioalcohol accounting for more 95% of all the global bioalcohol production. Ethanol presents some distinct advantages over petroleum gasoline for internal combustion engines — primarily in that tailpipe emissions are "cleaner." However, the vast majority of ethanol currently produced in the world comes from food crops such as corn, sugarcane using 1st generation technology. Thus at least some of the on-going inflation in worldwide food prices can be related to the growing portion of the global corn crop that is diverted to fuel production. Thus it becomes more important to switch towards 2nd generation cellulosic-ethanol [1,3,5].

Biobutanol or biobased butanol fuel is a 2nd generation alcohol fuel usually produced by fermentation of biomass via A.B.E. (Acetone-Butanol-Ethanol) process. The process uses *Clostridium acetobutylicum* (popularly known as the Weizmann organism after its discoverer) for degrading sugars. It was originally used for the production of acetone from starch in 1916 by Chaim Weizmann with butanol as a by-product. The process also creates several other by-products in recoverable amounts: acetic, lactic and propionic acids, isopropanol, ethanol and H_2. There are several advantages of butanol over ethanol (Table 1.1) such as: higher energy content, better water tolerance, is less corrosive

than ethanol and better suitability for distribution through existing fuel distribution network. Moreover, in blends with diesel or gasoline, butanol is less likely to separate from this fuel than ethanol if the fuel is contaminated with water [23,24]. According to DuPont (American chemical giant), existing bioethanol plants can cost-effectively be retrofitted to biobutanol production [1,98,99].

2-Propanol is a secondary alcohol that is commonly used as a solvent. There has been an increasing demand for isopropanol production without the use of petroleum products. 2-Propanol has a key role in the polymer industry as a precursor for propylene, which can then be made into polypropylene. 2-Propanol is currently derived from petroleum and with a decreasing availability of petroleum; the need for natural alternatives is rising. Due to recent advances in metabolic engineering, production of bioisopropanol (2-propanaol) has become possible, and is presently considered as a 2nd generation bioalcohol. Researchers at Kyushu University have developed a fermentation process utilizing the TA76 strain of *Escherichia coli* which converts sugars present in biomass to 2-propanaol. Globally, 2-propanol production reached 2,153 thousand metric tons in 2003 with an expected growth rate of 1-3% per year [25,26].

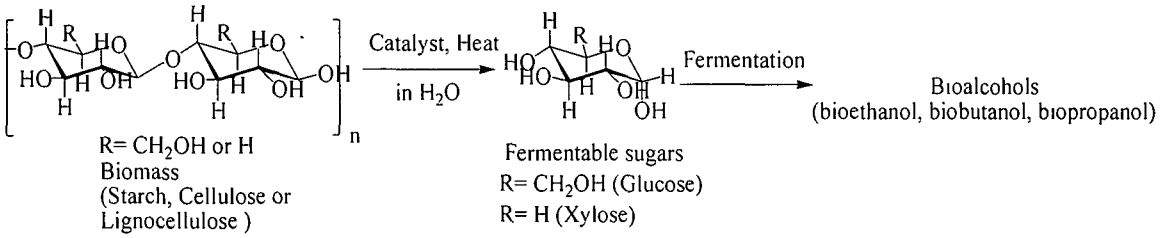

Scheme 1.2. Schematic representation of bioalcohol synthesis

Nonetheless, the production of all bioalcohols (Scheme 1.2) from biomass precedes through the common hydrolysis step in order to covert the cellulosic or lignocellulosic components into sugars. There is significant scope for improvement of this step through incorporation of heterogeneous catalytic approaches which could drastically reduce the production cost of 2nd generation bioalcohols.

1.1.3. GTBE - Glycerol tertiary butyl ethers or glycerol ethers

An increase in production of biodiesel has resulted in the generation of large excess of glycerol in the chemical market and currently only small proportions of this are being further processed. Glycerol has numerous applications in different industrial processes. Its recovery and purification, however, contribute to high production costs and energy consumption. Therefore, new methods of glycerol utilization are desirable. One of the methods is its conversion into glycerol ethers (GTBE). These ethers have been identified as excellent oxygen additives for diesel fuel (including biodiesel). Addition of GTBE to biodiesel also improves the cold flow properties of biodiesel. Oxygenated diesel fuels are of importance to both environmental compliance and efficiency of diesel engines [27]. Commercial opportunity for GTBE as antiknock additive for petrol is also available. Since lead additives are prohibited, methyl-*tertiary*-butyl-ether (MTBE) is mainly used here, but this is hazardous to the environment and has already been partially prohibited in USA. In contrast, GTBE is much more readily biodegradable. They are easily produced by etherification of glycerol and isobutene, in presence of a homogeneous or heterogeneous acidic catalyst (Scheme 1.3) [27,28].

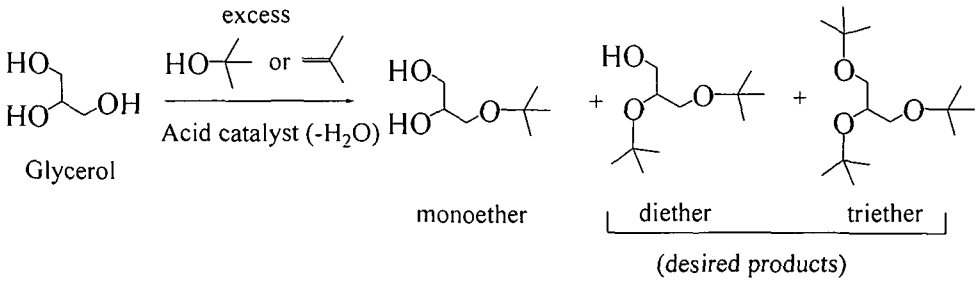

Scheme 1.3. Schematic representation of GTBE synthesis (isomers not shown)

A number of studies on the preparation of glycerol ethers by using different catalytic systems have been reported [7,27]. As a result of the conversion of glycerol to GTBE it can contribute to biofuel market as it is being utilized as a feedstock for biofuel additives.

1.2. Role of catalysts (homogeneous vs. heterogeneous)

Next to the feedstock, catalyst plays the most important role in any industrial process as it directly affects production route and product costs, quality and yield. From Fig. 1.4 it can be seen that both acids and bases have vital catalytic roles in biomass transformation. Acids are crucial catalytic components for majority of the chemical reactions, while the applicability of bases is limited to biodiesel production only. Owing to the advantages of heterogeneous catalysts in terms of separation and reusability over the traditionally used homogeneous catalyst, the industrial research in catalysis (including that for biofuels) has been seen an increasing shift towards heterogeneous catalysis in recent years. Fig. 1.5 shows the schematic comparison of the homogeneous catalytic approach, while Fig. 1.6 shows the heterogeneous one. For example, catalyst research for biodiesel production has seen a shift towards heterogeneous catalysts in recent years. Some of the reported catalysts include supported alkali metal catalysts [29], alkali and alkaline earth oxides, mixed metal oxides, [30,31] dolomites, perovskite type catalysts and zeolites [32], heteropolyacids [33], Amberlyst-15 [34], $H_3PW_{12}O_{40}.6H_2O$ [35], WO_3/ZrO_2 [36] hydrotalcite [37], Sulfated zirconia [38,39] and to name a few [40]. In a recent study, it was reported that for the production of 8000 tonnes of biodiesel, 88 tonnes of sodium hydroxide was required while the use of only 5.7 tonnes of solid supported MgO was sufficient for the production of 100,000 tonnes of biodiesel [62].

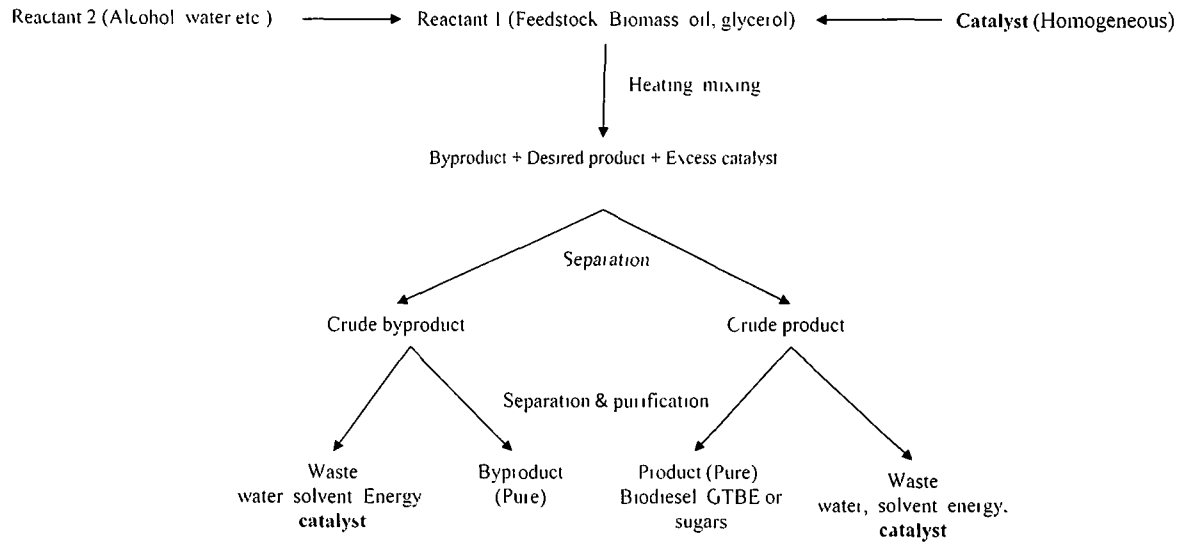

Figure 1.5. Synthesis of biofuels using homogeneous catalytic approach.

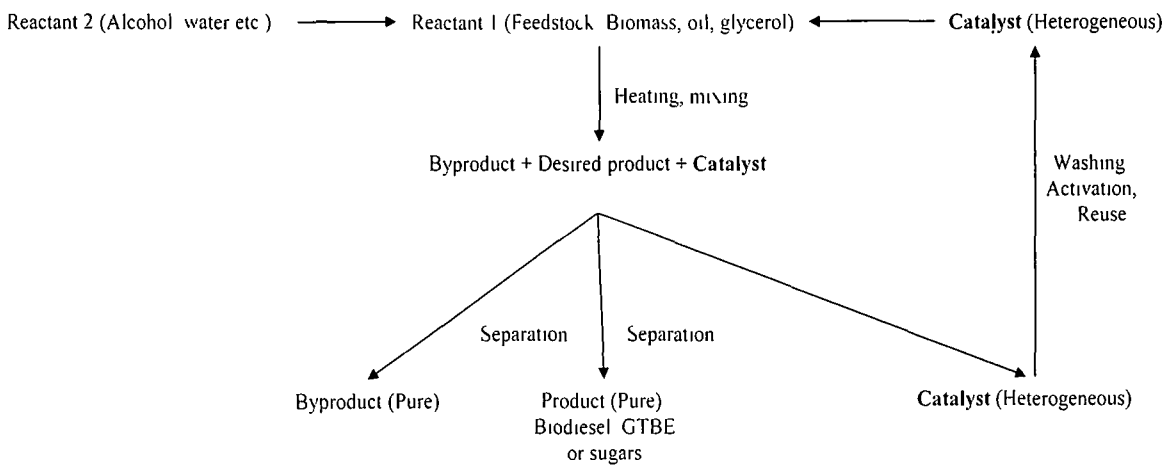

Figure 1.6. Simplified syntheses of biofuels using heterogeneous catalytic approach.

Table 1.2 illustrates an overview on the different aspects of biodiesel production using various types of catalysts. Among the reported heterogeneous catalysts, the calcium-based catalysts, CaO in particular has emerged as a well-known solid base catalyst for biodiesel production due to its low cost and excellent catalytic performance [62]. Apart from the heterogeneous bases, solid acids such as sulfated zirconia [37,38], sulfonated carbons [10,42,43], Amberlyst-15 [34] have also attracted great deal of attention as effective catalysts for biodiesel production from acidic oils (AO) such as crude vegetable oils, waste cooking oils and fatty acid distillates. Studies have shown that the sulfonated carbons and sulfated zirconia are superior catalysts owing to their higher acid strengths; however, they are reported to suffer from loss of catalytic activity upon reuse, particularly the sulfated zirconia [13,44]. In general, the main drawbacks of heterogeneous catalyzed process of biodiesel production are the lower activity of these materials in comparison to the homogeneous counterparts, resulting in slower reactions and in some cases incomplete conversions. Many heterogeneous catalysts are also plagued by leaching, deactivation problems and results in substantial loss of catalytic activity upon reuse. Some well documented examples include sulfated zirconia and CaO. The deactivation CaO is due to the easy leaching of Ca species into the reaction media causing loss of activity. In addition, removal of Ca contaminant from the biodiesel requires additional separation and purification processes that could generate a large amount of waste water to the environment. Nonetheless, they could be easily regenerated or reactivated by simple

calcination. Attempts have been made to reduce Ca leaching by modification with metals such as Li, Ce [41,42]. Similarly, CaO supported on carbon materials (nanoporous carbons, graphitic oxide and activated carbon) have been demonstrated by many researchers to be exhibit superior reusability, improved water and free fatty acid tolerance in comparison to CaO [40,62]. On the other hand, deactivation of sulfated zirconia is caused by the leaching of the active sulfate ions. However, in a recent study, Das *et al.* [39] was able to address the reusability of such catalysts using (ZrO_2) nanostructures. Reusability and low material costs are the most important aspects of heterogeneous catalyst which needs substantial research and improvement in order for them to become commercially successful as there is no point in using an expensive, slow and non-recyclable material as heterogeneous catalyst. Preparation of supported catalyst is a commonly adapted route to overcome these issues by many researchers.

Table 1.2
An overview of biodiesel production by transesterification using different catalysts, *Adapted from* Konwar *et al.* [60]

Type of catalyst	% Yield	Feedstock	Advantage	Disadvantage
Industrially used Homogeneous alkali catalysts (NaOH, KOH)	96-98	Suitable for pretreated/refined vegetable oils	1. Very fast reaction 2. Reactions occur at very mild conditions 3. Cheap and widely available (NaOH, KOH)	1. Requires refined or pretreated vegetable oils as feedstock (FFAs<1wt%) increasing the production cost 2. Sensitive to water and FFAs can cause soap formation if too much catalyst is used. This decrease the biodiesel yield and cause problem during product purification especially generating huge amount of wastewater 3. Catalyst cannot be reused
Heterogeneous alkali catalysts (CaO, ZnO, mixed oxides)	<90	Suitable for pretreated/refined vegetable oils	1. Relatively faster reaction rate compared to acid catalyzed transesterification 2. Reactions are less energy intensive and occur at mild conditions 3. Easy product separation by filtration 4. Catalysts can be reused	1. Requires refined or pretreated vegetable oils as feedstock (FFAs<1wt%) increasing the production cost 2. Sensitive to water and FFAs can cause soap formation if too much catalyst is used. This decrease the biodiesel yield and cause problem during product purification especially generating huge amount of wastewater 3. Leaching of catalyst active sites may result to product contamination 4. Complex and expensive synthesis route
Homogeneous acid Catalysts (H_2SO_4, HCl)	Upto 99	Suitable for waste and crude vegetable oils containing large amount of FFAs	1. Insensitive to FFAs and water content in the oil 2. Can simultaneously catalyse both esterification and transesterification reactions 3. Preferable for low grade feedstock oil with very high FFAs content (e.g. waste	1. Very slow reaction rate for transesterification compared to alkali catalysts 2. Due to corrosive nature of acids like H_2SO_4, HCl especially designed reactors are needed to overcome problem of corrosion on reactor and pipelines 3. Catalyst recovery is difficult

			cooking oil, crude non edible oils) 4. No soap by product is Formed	4. Use of too much catalyst can increases acid value of biodiesel, requiring extensive washings which generates huge amount of wastewater 5 Requires high alcohol/oil ratio.
Heterogeneous acid catalysts (AC supported-SO_3H, SBA-15, HPA etc)	<90	Suitable for waste and crude vegetable oils containing large amount of FFAs	1. Insensitive to FFAs and water content in the oil 2. Can simultaneously catalyze both esterification and transesterification reactions 3 Easy separation of catalyst from product and reusability 4. No soap by product is formed 5. Non corrosive to reactor and reactor parts	1. Slow to very slow reaction rate for transesterification compared to alkali catalysts 2. Complicated and expensive synthesis routes in some cases 3. Energy intensive, requires high alcohol/oil ratio 4. Leaching of catalyst active sites in may result to product contamination
Enzyme (Lipase)	99	Suitable for pretreated/refined vegetable oils as well as waste and crude vegetable oils containing large amount of FFAs	1. Insensitive to FFA and water content in the oil 2. Simple purification step 3. Mild reaction conditions and low alcohol/oil ratio	1. Very slow reaction rate, even slower than acid-catalyzed transesterification 2. High cost, Sensitive to alcohol, typically methanol that can deactivate the enzyme
Ionic Liquids	-	Depends on the nature of IL used; for acidic, waste and crude oils or and for basic, refined or pretreated oils	1. Can act as both solvents and catalyst 2. Easy separation of products 3. Depending upon its chemical properties, Can act as both acid or base catalyst	1. Highly expensive 2. Slow reaction rate compared to conventional catalytic systems even for basic ionic liquids 3. Difficulty in separation of Ionic liquids and glycerin
Carbon based catalysts (sulfonated carbons, amine grafted carbons and supported carbons)	<90	Depends on the nature of catalyst; for acidic, waste and crude oils or and for basic, refined or pretreated oils	1. Reusability 2. Simple synthesis route and Inexpensive 3. High thermal stability 4. Large surface area and uniform distribution of active particles	1. Slow reaction rate 2. Leaching 3. Use of high methanol to oil molar ratio

A similar trend has also been observed in catalyst research for biomass saccharification, the most crucial step in the production of bioalcohols (bioethanol, biobutanol etc.) from cellulosic and lignocellulosic feedstock. So far, H_2SO_4 has been the catalyst of choice for this purpose; however, its utilization has its own drawbacks. The main problems are: corrosion of reactors (requiring constant maintenance), need for additional purification steps to neutralize the excessive catalysts along with waste disposal issues. These limitations significantly lower the attraction of such homogeneous acid-catalyzed process. Therefore, in order to minimize the environmental impact, several alternative green approaches have been developed, such as the use of supercritical water, enzymes, solid acids and ionic liquids [45-52]. Thus far, a great deal of effort has been put towards the degradation of cellulose/lignocelluloses with enzymes [45,46], dilute acids [45,47] and supercritical water [48,49]. Nonetheless, with the exception of solid acids most of these processes still suffer from major drawbacks such as difficulty in separation of products and catalysts, corrosion hazard, and difficulties in controls of enzymes, waste fluids, and reaction conditions. Various solid acids such as: γ-Al_2O_3, H-mordenite, H-beta, H-ZSM5, Sulfated zirconia, Amberlyst-15, SBA-SO_3H, Fe_3O_4-SBA-SO_3H and sulfonated carbon materials have been investigated for their activity in such reactions [50,52]. Onda *et al* [50] has recently shown that heterogeneous catalytic processes for cellulose conversion to glucose is the most effective over sulfonated activated-carbon catalysts with yield upto 50%, greater than the industrially used dilute H_2SO_4 catalyzed process. Among H-form zeolite catalysts, the hydrophobic zeolites with high Si/Al ratios show relatively high yield of glucose. The sulfated zirconia and amberlyst 15 catalysts were reported to show higher activity than the H-form zeolite catalysts, however significant leaching of SO_4^{2-} ions were reported along with by-products formation. Ormsby *et al* [53] in a related study confirmed the effectiveness of a sulfonated biochar catalyst for selective hemicellulose hydrolysis under optimized conditions.

Glycerol etherification has been reported to take place efficiently in the presence of Brønsted acid catalysts. In general, the most suitable catalysts are homogeneous strong acids such as H_2SO_4, *p*-toluenesulfonic acid (PTSA). However, due to the advantages of heterogeneous catalysis, the catalytic activity of many solid acids has also been studied in glycerol etherification. Amongst heterogeneous catalysts commercial acidic resins such as

amberlyst, have been reported to be the most active due to the high density of Brønsted acid sites of the sulfonic groups. However, major limitation on the use of these resins has been due to their relatively low thermal stability (393 K for amberlyst-15, 463 K for amberlyst-70). Many authors also reported the use of zeolites, heteropolyacids, niobia, sulfonic acid- functionalized mesostructured silica and other acidic solids [54,55]. Compared to the conventional resins, sulfonic acid-functionalized mesostructured silica catalysts showed superior activity. However, the materials showed poor reusability with the loss of both activity as well as selectivity [55]. Zeolite H-Y was reported to show good glycerol conversion (88.7%), reusability and high selectivity to DTBG (di-*tert*-butyl-glycerol) [53]. Recently, the sulfonic acid-functionalized carbon materials (or sulfonated carbons) have also been demonstrated to have excellent catalytic behavior in transformations of glycerol, however the reactions with isobutene have been reported to show more favorable results with better selectivity of desired products (diether and triether) [7,58,59].

1.3. Biomass as a catalysts precursor

The catalyst research has been focused mainly on the chemically synthesized ones. However in recent years, with growing environmental, economic concerns and emerging concepts of green chemistry, the utilization of renewable source or bio-based catalysts for chemical transformations has recently gained immense attention [50,60-65]. Fig. 1.7 represents the total U.S. sales of catalyst support materials while Table 1.3 presents a comparison of properties of various types of commercially available heterogeneous catalysts and support materials.

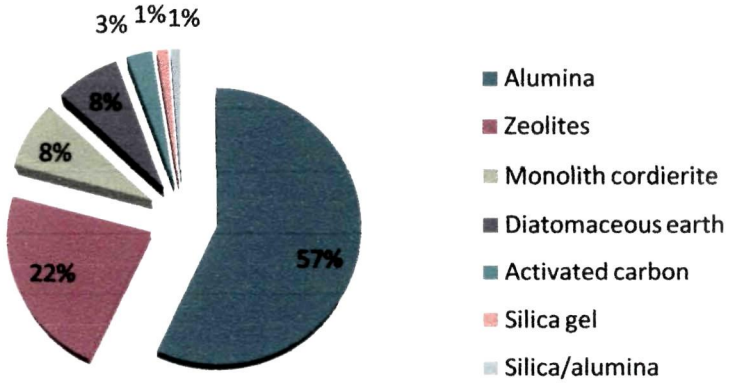

Figure 1.7. Sales of catalyst support materials [60].

Table 1.3
Main features of different types of catalyst supports, *Adapted from* Konwar *et al.* [60]

Carrier	Features
Activated Carbon	Surface area : 800~1,500 m^2/g Heat stability. Can be produced from bio based carbon sources
Alumina	Surface area : 100~300 m^2/g Type α・γ・η are often used as carriers. Reasonable price. Heat resistance. Alkali resistance.
Silica	Surface area : 200~600 m^2/g
Zeolite	Surface area : 350~900 m^2/g Type A・X・Y・Mordenite・Erionite・ZSM-5 are often used as carriers. High controllability of pore size.
Titania	Surface area : 40~100 m^2/g
Magnesia	Surface area : 50~200 m^2/g Basic. Strong adsorption of carbon dioxide and water in air.

In general, the based on literature survey, biomass derived catalytic materials can be classified into two distinct classes:

i). *Metal oxides* or *mixed metal oxide* catalysts derived from alkali rich biomass sources (e.g. CaO prepared from waste shells of egg, shrimps, mollusk etc.) prepared by calcination [64-66] and

ii). *Sulfonated carbon* catalysts, i.e. *Carbon materials* modified with strong acidic groups (such as $-SO_3H$) prepared from biomass or products of biomass origin by carbonization followed by subsequent sulfonation [58-61, 84-89].

Considering that biomass is renewable, abundant, and low-cost, catalysts produced directly from biomass and bio-wastes would own potential advantage. Biomass is

abundantly available and is almost free of cost. It can be processed into a variety of useful products including heterogeneous catalysts. Certain varieties of biomass are rich in alkali and alkaline metals like Na, K, and Ca which make them suitable precursor for synthesizing strong base catalyst. e.g. biomass from domestic waste especially kitchen waste (egg shells, fish shells, crab shells etc.) are rich in Ca and Na. Thus, through careful processing they may be easily converted to their corresponding oxides which could thereafter be employed as base catalysts in reactions such as transesterification, for applications during biodiesel production [62-66]. Recently, Boro *et al.* prepared a highly active CaO catalyst for biodiesel production from waste shells of *Turbonilla striatula,* a variety of mollusk used as a food source by the indigenous people of Assam [62,65,66].

Carbonization is another approach used by researchers to prepare biomass based heterogeneous catalysts. Carbon based materials are considered as ideal catalysts due to desirable features such as: low material cost, high surface area and thermal stability (Table 1.2 & 1.3). Additionally, since the carbon materials can be produced from any biomass or from the agricultural wastes or bio-waste generated in industrial processing, these catalysts are of particular interest. Carbon based catalysts have been usually prepared by functionalizing or immobilizing of carbon surface with acids or bases. Partially carbonized biomass [67-69] (activated carbon, charcoal) can act as a strong support material for a variety of Lewis acids and bases (BF_3, H_2SO_4, $ZnCl_2$ etc), thereby reducing catalyst cost and also makes it renewable and green [70,71]. Biochar or biocarbon is a major byproduct obtained of all major biomass utilization processes such as gasification, carbonisation, pyrolysis etc. The basic structural unit of activated carbon, biochar or biocarbon is closely approximated by the structure of pure graphite. "Activated carbon is a crude form of graphite with a random or amorphous structure which is highly porous over wide range of pore sizes from visible cracks and crevices to cracks and crevices of molecular dimensions". Structurally activated carbon is a disorganized form of graphite due to presence of impurities where the layers are held by carbon–carbon bonds. Its precise atomic structure, however, is unknown. A much more recent suggestion is that activated carbon has a structure related to that of the fullerenes, in other words that it consists of slightly functionalized (with –OH, -COOH groups) curved fragments containing pentagons and other non-hexagonal rings in addition to hexagons, as illustrated in (Fig. 1.8) [72,73].

These features contribute to the structural features of amorphous carbons such as high porosity, thermal stability etc. Besides, due to its close structural resemblance with graphite, it is possible to functionalize some of these fused rings with groups like $-SO_3H$, -PhOH, $-PhSO_3H$, $-NH_2$, -NHR, $-NR_2$ via. chemical reactions [74-82]. This makes it possible to synthesize a diverse class of functionalized acidic and basic chars or amorphous carbons which can be used as heterogeneous catalysts for different chemical reactions. Particularly, the SO_3H functionalized carbons or carbon supported acids have been demonstrated and successfully employed as a green substitute to H_2SO_4 in many commercially important reactions, including reactions associated with biofuel production such as: hydrolysis of lignocelluloses/cellulose, esterification and transesterification oil/free fatty acid (FFA) and glycerol conversion.

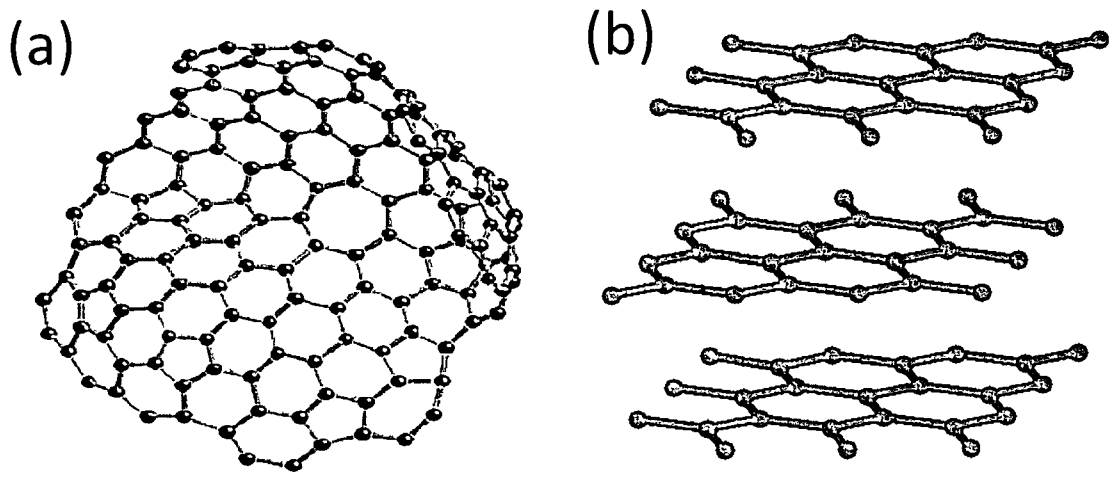

Figure 1.8. Structure of (a) amorphous carbons (i.e biochar or activated carbon) in composition to the structure of (b) graphite, *Adapted from* [72,73].

Amongst the various renewable source based catalysts, the sulfonated carbons have attracted a great deal of attention from the researchers in recent years [59-61]. They are versatile, diverse, promising class of new solid acid catalysts reported to be highly active in a range of acid catalyzed reactions including reactions associated with the production of biofuels such as: FFAs esterification (biodiesel production) [60,61,70,71,73-78], cellulose hydrolysis (bioethanol/bioalcohol production) [9,50,52] and glycerol etherification (diesel additive) [6,45,58-59]. Such catalysts are usually produced by the sulfonation of a incompletely pyrolysed cheap carbon obtained from source such as: sucrose [83], glucose [61,84], starch [85], glycerol [86], biochar [78], wood [75], oil pitch [87], canola meal

[88], corncob [89] etc. Similar sulfonated carbons have also been prepared from more expensive carbon precursors such as phenolic resins [90], carbon foams [91] graphene [92], OMCs [79,93,94] and to name a few [60].

1.4. Rationale of the present work and objectives

As discussed above, one of the major bottlenecks in current generation biofuel production technology is from their reliance on the use of homogeneous acids and bases (NaOH, KOH, H_2SO_4, HCl etc) as catalysts. Owing to the advantages of heterogeneous catalysts in terms of separation and reusability over the traditionally used homogeneous catalyst, switching to heterogeneous catalyst may provide a possible solution. This approach however is largely limited by the high cost and low activity of commercially available heterogeneous catalysts. Therefore, keeping in mind the importance heterogeneous catalysts and biomass as a possible catalyst precursor, the present work has been undertaken with the aim of developing active, cheap, renewable and versatile heterogeneous catalysts from biomass sources (such as bio-wastes, food-wastes and agroindustrial wastes) to substitute some of the conventionally used homogeneous catalyst in biofuel production.

The objectives of the present investigation could be summarized as follows:

i). To identify renewable precursors for catalysts preparation.

ii). To develop heterogeneous catalysts using the renewable precursors.

iii). To characterize the prepared catalysts using standard techniques.

iv). To examine the catalytic activity of the prepared catalytic materials in biofuel production employing esterification, transesterification, etherification, saccharification etc. as model reactions.

1.5. Outline of the thesis

This section provides a detailed outline of all parts of the thesis:

Chapter 1: The theme of the thesis is introduced in this chapter including the importance of biofuels as an energy source, its advantages and shortcomings. It also describes the role of catalysts in the synthesis of biofuels and the need for renewable source based heterogeneous catalysts. A detailed literature survey with regard to utilization of heterogeneous catalysts and renewables as precursors for catalytic materials, synthesis and applications of such materials in the biofuel sector provided rationale of present work and based on which the objectives of the present work were set.

Chapter 2: This chapter gives a detailed account of the various analytical methods: N_2-physisorption, XRD, EDX, organic elemental analysis, FT-IR, Raman analysis and acid-base titrations employed to characterize the catalytic materials. The chapter also discusses the analytical methods used to determine fatty acid composition and physicochemical properties of the vegetable oils used in the study.

Chapter 3: This chapter describes the preparation, characterization of a biomass based *metal/mixed oxide* catalysts from alkali rich wastes (post harvest parts of *Vigna radiata* plant and *Musa balbisiana* pseudo stem) and applications of these materials as a base catalyst for biodiesel production. Properties of the biodiesel prepared in the presence ash catalyst exhibiting maximum conversion are also presented.

Chapter 4: This chapter describes the preparation of biomass based CaO *supported active carbon* catalyst from a food waste (*Turbonilla striatula* shells). The chapter also discusses the characterization and applications of these materials as a reusable base catalyst for biodiesel production.

Chapter 5: This chapter describes the preparation, characterization of an agroindustrial waste based *sulfonated carbon* (solid acid) catalyst with high specific surface area from waste de-oiled cake residues (DOWC) of *Mesua Ferrea* Linn, generated as by-product from biodiesel production. Its application as a solid acid catalyst was successfully demonstrated in the production of biodiesel from acidic oils containing high amounts of free fatty acids. The chapter also discusses the effect of sulfonation conditions, reaction conditions and initial free fatty acid content of oil on biodiesel yield.

Chapter 6: This chapter builds on the preceding chapter and describes the effects of carbon source, preparation method on the structure, acidity and catalytic activity of DOWC based sulfonated carbons. The chapter also discusses the effect of catalyst structure

on activity and selectivity through simultaneous and comparative evaluation of activities in oleic acid esterification and cellulose saccharification, two opposite but equally imperative reaction involved in biofuel synthesis.

Chapter 7: This chapter gives a summarized comparison of the outcomes of all the chapters and also discusses the prospective for future work/development.

1.6. References

1. Technology Roadmaps Biofuels for transport, IEA, 2011.
2. Fairley, P., Introduction: Next generation biofuels, *Nature*, **474**, S2–S5, 2011.
3. Climent, M. J. et al. Conversion of biomass platform molecules into fuel additives and liquid hydrocarbon fuels, *Green Chem.*, **16**, 516-547, 2014.
4. Maa, F. & Hanna, M. A. Biodiesel production: a review, *Bioresour. Technol.*, **70**(1), 1-15, 1999.
5. Demirbas, A. Bioalcohols as Alternatives to Gasoline, *Energ Source Part A.*, **31**(12), 1056-1062, 2009.
6. Tijmensen, M. J.A. et al. Exploration of the possibilities for production of Fischer Tropsch liquids and power via biomass gasification, *Biomass Bioenergy.*, **23**(2), 129-152, 2002.
7. Gonçalves, M. et al. Glycerol Conversion Catalyzed by Carbons Prepared from Agroindustrial Wastes, *Ind. Eng. Chem. Res.* **52**, 2832–2839. 2013.
8. Kondili, E.M. & Kaldellis, J.K. Biofuel implementation in East Europe: Current status and future prospects, *Renew Sust Energ Rev*, **11(9)**, 2137-2151, 2007.
9. Vasudevan, P. T. & Briggs, M. Biodiesel production—current state of the art and challenges, *J Ind Microbiol Biot*, **35**, 421–430, 2008.
10. Hara, M. Biomass conversion by a solid acid catalyst, *Energy Environ Sci.* **3**, 601–607, 2010.
11. Luque, R. *et al.* Biofuels: a technological perspective, *Energy Environ Sci.*, **1**, 542-564, 2008.

12. Zheng, S. et al. Acid-catalyzed production of biodiesel from waste frying oil, *Biomass Bioenergy*, **30**(3), 267–272, 2006.

13. Lotero , E. et al. Synthesis of Biodiesel via Acid Catalysis, *Ind. Eng. Chem. Res.* **44**(14), 5353–5363, 2005,

14. Zhang, Y., et al. M. Biodiesel production from waste cooking oil: 1. Process design and technological assessment. *Bioresour Technol.*, **89**, 1–16, 2003.

15. Kumar, A. & Sharma, S., Potential non-edible oil resources as biodiesel feedstock: An Indian perspective. *Renew Sust Energ Rev,* **15** (4), 1791–1800, 2011.

16. Moser, B.R. et al. Production and evaluation of biodiesel from Field Pennycress (Thlaspi arvense L.) oil. *Energy Fuels,* **23**, 149-155, 2009.

17. Ramadhas, A.S. et al. Characterization and effect of using rubber seed oil as fuel in the compression ignition engines. *Renew Energ,* **30**, 795-803, 2005.

18. Scragg, A.H. et al. The use of a fuel containing Chlorella vulgaris in a diesel engine. *Enzym Microb Technology,* **33**, 884-889, 2003.

19. Chakraborty, M. et al. Investigation of terminalia (Terminalia belerica Robx.) seed oil as prospective biodiesel source for North-East India. *Fuel Process Technol,* **90**, 1435–1441, 2009.

20. Puhan, S. et al. Mahua oil (Madhuca Indica seed oil) methyl ester as biodiesel-preparation and emission characteristics. *Biomass Bioenergy,* **28**, 87-93, 2005.

21. Deka, D. C. & Basumatary, S. High quality biodiesel from yellow oleander (Thevetia peruviana) seed oil. *Biomass Bioenergy,* **35**, 1797-1803, 2011.

22. Singh, S.P. & Singh, D. Biodiesel production through the use of different sources and characterization of oils and their esters as the substitute of diesel: A review. *Renew Sust Energ Rev,* **14,** 200–216, 2010.

23. Ezeji, T.C. et al. Bioproduction of butanol from biomass: from genes to bioreactors, *Curr Opin Biotech,* **18** (3), 220-227, 2007.

24. Berezina, O.V. et al. Microbial producers of butanol. *Appl Biochem Micro+*, **48**(7) 625-638, 2012.
25. Hanai, T. et al. Engineered Synthetic Pathway for Isopropanol Production in Escherichia coli, *Appl. Environ. Microbiol.*, **73**(24),7814, 2007.
26. Jojima, T. et al. Production of isopropanol by metabolically engineered Escherichia coli, *Appl Microbiol Biotechnol*, **77**, 1219–1224, 2008.
27. Jamróz, M.E. et al. Mono-, di-, and tri-tert-butyl ethers of glycerol: A molecular spectroscopic study, *Spectrochim Acta A.*, **67**(3–4), 980–988, 2007.
28. Demirbas, A. *Biofuels: Securing the Planet's Future Energy Needs*, Springer, New York, 2010.
29. Xie, W. et al. Soybean oil methyl esters preparation using NaX zeolites loaded with KOH as a heterogeneous catalyst. *Bioresour Technol.*, **98,** 936–939, 2007.
30. Kawashima, A. et al. Development of heterogeneous base catalysts for biodiesel production. *Bioresource Technol.*, **99**, 3439–3443, 2008.
31. Singh, A.K. & Fernando, S.D. Transesterification of soybean oil using heterogeneous catalysts, *Energy Fuels.*, **22**, 2067–2069, 2008.
32. Brito, A. et al. Zeolite Y as a heterogeneous catalyst in biodiesel fuel production from used vegetable oil. *Energy Fuels.*, **21**, 3280–3283, 2007.
33. Alsalme, A. et al. Heteropoly acids as catalysts for liquid-phase esterification and transesterification. *Appl. Catal., A.*, **349 (1-2)**, 170–176, 2008.
34. Rahman Talukder, M.M. *et al.* Comparison of Novozym 435 and Amberlyst 15 as Heterogeneous Catalyst for Production of Biodiesel from Palm Fatty Acid Distillate. *Energy Fuels.*, **23**(1),1-4, 2009.
35. Zhang, X. et al. Heteropolyacid nanoreactor with double acid sites as a highly efficient and reusable catalyst for the transesterification of waste cooking oil. *Energy Fuels.*, **23,** 4640–4646, 2009.
36. Park, Y.M. et al. Esterification of used vegetable oils using the heterogeneous WO_3/ZrO_2 catalyst for production of biodiesel. *Bioresour Technol.*, **101,** 59–61, 2010.

37. Woodford, J.J. et al. Better by design: nanoengineered macroporous hydrotalcites for enhanced catalytic biodiesel production, *Energy Environ Sci.*, 5, 6145-6150, 2012.

38. Furuta, S. et al. Biodiesel fuel production with solid superacid catalysis in fixed bed reactor under atmospheric pressure, *Catal. Commun.*, **5**(12), 721–723, 2004.

39. Das, S.K. & El-Safty, S.A., Development of Mesoscopically Assembled Sulfated Zirconia Nanoparticles as Promising Heterogeneous and Recyclable Biodiesel Catalysts, *ChemCatChem*, **5**(10), 3050–3059, 2013.

40. Lam, M.K. et al. Homogeneous heterogeneous and enzymatic catalysis for transesterification of high free fatty acid oil (waste cooking oil) to biodiesel: A review. *Biotechnol. Adv.*, **28**, 500–518, 2010.

41. Kawashima, A. et al. Acceleration of catalytic activity of calcium oxide for biodiesel production, *Bioresour Technol.*, **100**(2), 696–700, 2009.

42. Thitsartarn, W. & Kawi, S. An active and stable $CaO–CeO_2$ catalyst for transesterification of oil to biodiesel, *Green Chem.*, **13**, 3423-3430, 2011.

43. Nakajima, K. & Hara, M. Amorphous carbon with SO_3H groups as a solid brønsted acid catalyst. *ACS Catal.* **2**(7): 1296–1304, 2012.

44. Chen, X., et al. Direct Synthesis of Mesoporous Sulfated Silica-Zirconia Catalysts with High Catalytic Activity for Biodiesel via Esterification, *J. Phys. Chem. C*, **111**(50), 18731–18737, 2007.

45. Fan, L. T. et al. In, Cellulose Hydrolysis, Springer, Biotechnol. Monographs. Berlin, 1987, pp. 57-50

46. Zhang, Y.P. & Lynd, L.R. Toward an aggregated understanding of enzymatic hydrolysis of cellulose: Non-complexed cellulase systems. *Biotechnol. Bioeng.*, **88**, 797–824, 2004.

47. Mok, W. S. L. et al. Productive and parasitic pathways in dilute acid hydrolysis of cellulose. *Ind. Eng. Chem. Res.*, **31**, 94-100, 1992.

48. Sasaki, M. et al. Dissolution and Hydrolysis of Cellulose in Subcritical and Supercritical Water, *Ind. Eng. Chem Res.*, **39**, 2883–2890, 2000.

49. Sasaki, M. et al. Kinetics of cellulose conversion at 25 MPa in sub- and supercritical water, *AIChE J.*, **50**, 192–202, 2004.

50. Onda, A. et al. Selective hydrolysis of cellulose into glucose over solid acid catalysts, *Green Chem.*, **10**, 1033–1037, 2008.

51. Amarasekara, A.S. & Owereh, O.S. Hydrolysis and decomposition of cellulose in Brønsted acidic ionic liquids under mild conditions, *Ind. Eng. Chem. Res.*, **48**(22), 10152–10155, 2009.

52. Lai, D. et al. Hydrolysis of cellulose into glucose by magnetic solid acid, *ChemSusChem.* **4**, 55–58, 2011.

53. Ormsby, R. et al. Hemicellulose hydrolysis using solid acid catalysts generated from biochar, *Catal. Today.*, **190**, 89–97, 2012.

54. Klepácová, K. et al. Etherification of glycerol and ethylene glycol by isobutylene. *Appl. Catal., A.*, **328**, 1-13, 2007.

55. Oliveira, L. C. A. et al. Modified niobia as a bifunctional catalyst for simultaneous dehydration and oxidation of glycerol. *Appl. Catal. B.*, **117**, 29-35, 2012.

56. Melero, J. A. et al. Acid-catalyzed etherification of bio-glycerol and isobutylene over sulfonic mesostructured silicas. *Appl. Catal. A*, **346**, 44-51, 2008.

57. Frusteri, F. et al. Catalytic etherification of glycerol by tert-butyl alcohol to produce oxygenated additives for diesel fuel, *Appl. Catal. A*, **367**(1–2), 77–83, 2009.

58. Janaun, J. & Ellis, N. Glycerol Etherification by tert-Butanol Catalyzed by Sulfonated Carbon Catalyst. *J. Appl. Sci.* **10**, 2633, 2010.

59. Zhao, W. et al. Etherification of Glycerol with Isobutylene to Produce Oxygenate Additive Using Sulfonated Peanut Shell Catalyst, *Ind. Eng. Chem. Res.*, **49** (24), 12399–12404, 2010.

60. Konwar, L.J. et al. Review on latest developments in biodiesel production using Carbon-based catalysts, *Renew Sust Energ Rev*, **29**, 546–564, 2014.

61. Toda, M., et al. Green chemistry – biodiesel made with sugar catalyst. *Nature,* **438**,178, 2005.

62. Konwar, L.J. et al. Activated carbon supported CaO prepared from waste mollusk shells as heterogeneous catalyst for biodiesel production, *Energ Source Part A.*, In press, doi:10.1080/15567036.2012.733483

63. Boro, J. et al. *Vigna radiata* (mung bean) ash as heterogeneous base catalyst for biodiesel production, *J. Bioprocess Eng. Biorefinery*, **2**, 54–60, 2013.

64. Wei, Z. et al. Application of waste eggshell as low-cost solid catalyst for biodiesel production. *Bioresour Technol.*, **100,** 2883–2885, 2009.

65. Boro, J. et al. Solid oxide derived from waste shells of Turbonilla striatula as a renewable catalyst for biodiesel production. *Fuel Process. Technol.* **92**, 2061–2067, 2011.

66. Boro, J. et al. A review on solid oxide derived from waste shells as catalyst for biodiesel production. *Renew Sust Energ Rev,* **16**, 904– 910, 2012.

67. Schröder, E. et al. Activated Carbon from Waste Biomass, *Progress in Biomass and Bioenergy Production*, **18**, 333-356, 2011.

68. Ahmedna, M. et al. Production of granular activated carbons from select agricultural by-products and evaluation of their physical, chemical and adsorption properties. *Bioresour Technol.,* **71**, 113–123, 2000.

69. Ahmadpour, A. & Do, D.D. The preparation of activated carbon from macadamia nutshell by chemical activation, *Carbon*, **35**, 1723–1732, 1997.

70. Hara, M. Environmentally Benign Production of Biodiesel Using Heterogeneous Catalysts, *ChemSusChem.*, **2**, 129–135, 2009.

71. Maciá-Agulló, J. A. et al. Synthesis of Carbon-based Solid Acid Microspheres and Their Application to the Production of Biodiesel, *ChemSusChem.*, **3**(12), 1352–1354, 2010.

72. Keiluweit, M. et al. Dynamic molecular structure of plant biomass-derived black carbon (biochar), *Environ. Sci. Technol.*, **44**(4), 1247–1253, 2010.

73. Harris, P.J.F. et al. Imaging the atomic structure of activated carbon. *J. Phys.: Condens. Matter*, **20**, 362201-362205, 2008.

74. Mo, X. et al. A novel sulfonated carbon composite solid acid catalyst for biodiesel synthesis, *Catal. Lett.*, **123**(26), 1–6, 2008.
75. Hara, M. Biodiesel production by amorphous carbon bearing SO_3H, COOH and Phenolic OH Groups, solid Brønsted acid catalyst, *Top. Catal.*, **53**, 805–810, 2010.
76. Okamura, M. et al. Acid-catalyzed reactions on flexible polycyclic aromatic carbon in amorphous carbon, *Chem. Mater.*, **18**, 3039–3045, 2006.
77. Aldana-Pérez, A. et al. Sulfonic groups anchored on mesoporous carbon Starbons-300 and its use for the esterification of oleic acid, *Fuel,* **100,** 128–138, 2012.
78. Yu, J. et al. Development of Biochar-based Catalyst for Transesterification of Canola Oil, *Energy Fuels*, **25**, 337–344, 2011.
79. Wang, X. et al. ordered mesoporous carbon as a stable and highly active protonic acid catalyst. *Chem. Mater.,* **19,** 2395-2397, 2007.
80. Villa, A. et al. Amino-functionalized carbon nanotubes as solid basic catalysts for the transesterification of triglycerides. *Chem. Commun.,* 4405–4407, 2009.
81. Villa, A. et al. Transesterification of triglycerides using nitrogen-functionalized carbon nanotubes. *ChemSusChem.*, **3**(2), 241–245, 2010.
82. Yuan, C. et al. Amino-grafted graphene as a stable and metal-free solid basic catalyst. *J. Mater. Chem.* **22**, 7456–7460, 2012.
83. Peng, L. et al. Preparation of sulfonated ordered mesoporous carbon and its use for the esterification of fatty acids, *Catal. Today.*, **150**, 140-146, 2010.
84. Zong, M.H. et al. Preparation of a sugar catalyst and its use for highly efficient production of biodiesel. *Green Chem.*, **9**, 434, 2007.
85. Budarin, V. et al. Starbons: New Starch-Derived Mesoporous Carbonaceous Materials with Tunable Properties, *Angew. Chem. Int. Ed.*, **45**, 3782-3786, 2006.
86. Devi, B.L.A.P. et al. Glycerol-based Carbon Catalyst for the Preparation of Biodiesel. *ChemSusChem.*, **2**(7), 617–620, 2009.
87. Shu, Q. et al. Synthesis of biodiesel from waste vegetable oil with large amounts of free fatty acids using a carbon-based solid acid catalyst, *Appl Energy*, **87**(8), 2589–2596, 2010.
88. Rao, B.V.S.K. et al. Carbon-based solid acid catalyst from de-oiled canola meal for biodiesel production, *Catal Commun.*, **14**, 20–26, 2011.

89. Arancon, RA. et al. Valorisation of corncob residues to functionalised porous carbonaceous materials for the simultaneous esterification/transesterification of waste oils. *Green Chem.*, **13,** 3162-3167, 2011.
90. Chang, B. et al. Soft-template synthesis of sulfonated mesoporous carbon with high catalytic activity for biodiesel production, *RSC Adv.*, **3**, 1987-1994, 2013.
91. Ordomsky, V.V. et al. Foam supported sulfonated polystyrene as a new acidic material for catalytic reactions, *Chem. Eng J.*, **207–208,** 218–225, 2012.
92. Ji, J. et al. Sulfonated graphene as water-tolerant solid acid catalyst. *Chem. Sci.*, **2**,484–487, 2011.
93. Liu, R. et al. Sulfonated ordered mesoporous carbon for catalytic preparation of biodiesel. *Carbon,* **46**, 1664 –1669, 2008.
94. Geng, L. et al. Efficient carbon-based solid acid catalysts for the esterification of oleic acid. *Catal. Commun.*, **13**, 26–30, 2011.
95. http://www.afdc.energy.gov/afdc/fuels/properties.html
96. http://www.biodieselgear.com/documentation/NBB_Biodiesel_brochure.pdf
97. http://www.methanol.org/Health-And-Safety/Technical-Bulletins/Technical-Bulletins/UsingPhysicalandChemicalPropertiestoManageFlam-(1).aspx
98. http://www.bp.com/liveassets/bp_internet/alternative_energy/alternative_energy_english_new/STAGING/local_assets/downloads_pdfs/b/bp_biobutanol_factsheet_apr13.pdf
99. www2.dupont.com/Production_Agriculture/en_US/assets/downloads/pdfs/BP_DuPont_Fact_Sheet_Biobutanol.pdf/

Chapter 2

Experimental

Chapter 2

A detailed account of the common methodologies and analytical techniques used in characterization of the catalytic materials are presented in this chapter. The methods used for determining fatty acid composition, vegetable oils and biodiesel properties are also discussed in this chapter. Particulars of the methods used for catalyst preparation, reaction product analysis and additional characterizations have been provided in the subsequent chapters individually.

2.1. Methodologies and raw material selection

Based on this idea outlined in Chapter 1, two types of materials were identified, collected and utilized as precursors for the preparation of catalytic materials as listed below:

i). Alkali rich materials: Pseudo stem of banana tree (*Musa balbisiana*) and plant residue of Mung bean (*Vigna radiata*) utilized for preparing the mixed oxide type catalysts, described in Chapter 3.

ii). Carbon rich materials: Waste shells of *Turbonilla striatula* (rich in chitin), Chapter 4 and de-oiled cake (lignocellulose) from non-edible oil seeds rich in utilized for preparing supported active carbon (AC) catalysts, described in Chapter 5 and 6.

The specific details of the origin and source of collection of the raw materials have been discussed separately in each chapter. Those raw materials rich in alkali, alkaline metals were mainly suitable for preparation of metal oxide or mixed metal oxide type catalysts by simple calcinations, on the other hand the materials rich in carbon were employed for the preparation of carbon based catalysts (*supported carbon* and *sulfonated carbons*) by carbonization and surface modification (Fig. 2.1). Fig. 2.2 shows the flow diagram of the general methodology adopted in the study.

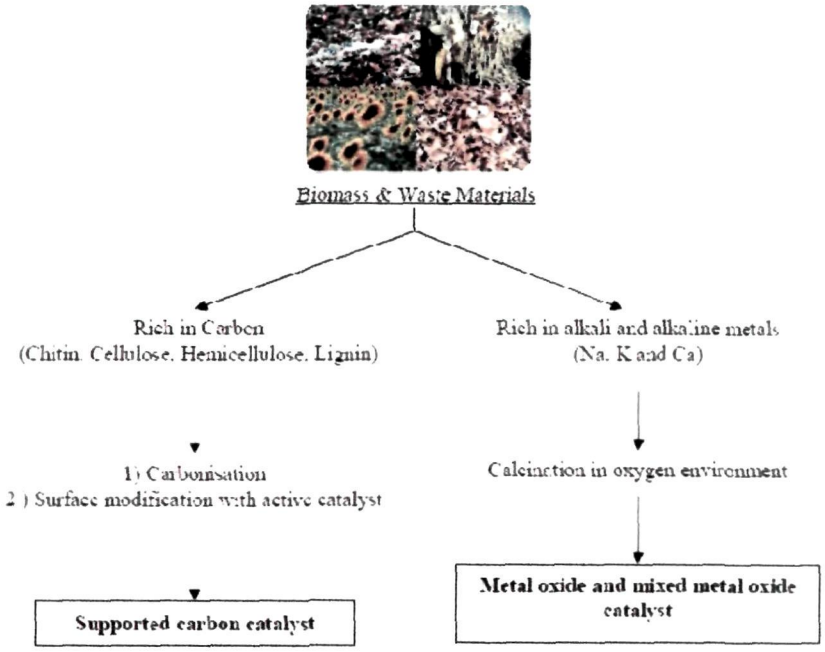

Figure 2.1. General schematic representations for preparation of heterogeneous catalysts from biomass and waste materials

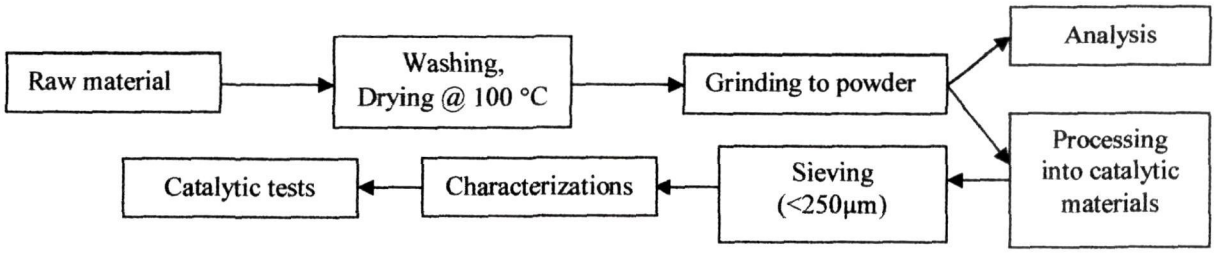

Figure 2.2. The flow diagram representing the methodology adopted in the study.

2.2. Analytical methods used in characterization of catalytic materials

2.2.1. N_2 adsorption-desorption

The specific surface area, pore size, micropore volume and total pore volume of the catalytic materials were determined by N_2 physisorption at liquid nitrogen temperature (Carlo-Erba instruments, sorptometer 1900 or ASAP® 2020 Accelerated Surface Area and Porosimetry Analyzer, USA). The specific surface area (S_{BET}) was determined by the BET equation (P/P0 = 0.05–0.3). The pore size distribution was determined from the desorption branch of the isotherm using the Barrett-Joyner-Halenda (BJH) theory. The micropore volume was calculated via the Dubinin—Radushkevich equation. The samples were

pretreated at 120 °C while degassing (~0.1 Pa). In case of the sulfonated carbons discussed in Chapter 5 & 6 the pretreatment temperatures were varied between 120-200 °C to detect if any leaching occurred at elevated temperatures.

2.2.2. Powder XRD

The powder X-ray diffractograms of catalytic materials as well as their precursors were recorded on a Rigaku miniflex diffractometer (Cu-Kα radiation, λ=1.5406 Å) in 2θ range 10–70° at a scanning rate of 2° min^{-1} to determine the structural features and elemental composition of the materials.

2.2.3. SEM and EDX

The morphological features of the catalytic materials were studied by means of Scanning Electron Microscopy (Jeol, JSM-6290LV). EDX analyses were also performed (Jeol, JSM-6290LV) to determine the elemental composition of the supported active carbon and mixed oxide type catalysts. EDX element mapping (C, O and S) of the carbon catalyst were recorded to get an overview of the distribution of various acid sites (-$PhSO_3H$, -OH and -COOH) on the surface of catalyst.

2.2.4. TEM

Transmission Electron Microscopy (TEM) images were obtained (Jeol, JEM-2100, 200 kV) to examine the structural features and porosity of the catalytic materials. The samples were homogenously suspended in ethanol by sonnicating for 5 min and deposited straight away on a copper grid for analysis.

2.2.5. Elemental analysis

Elemental analyses (Thermo Scientific FLASH 2000 and Model PR 2400 Series II Perkin Elmer) were performed in order to determine the chemical composition of the carbon materials (sulfonated carbons and activated carbon) and the biomass precursors (de-oiled cake waste, cellulose etc.).

2.2.6. FT-IR analysis

The chemical composition and the presence of different functionalities in the catalytic materials were studied by means of FT-IR spectroscopy (KBr pellet, Nicolet

Impact 410). KBr pellet of samples were prepared by mixing finely powdered pre-dried sample (particle size <200-μm) and spectroscopic grade KBr (particle size 20-40-μm) in 1000:1 (w/w) ratio, followed by pressing on a standard evacuated 13 mm hydraulic press. Sample pellets were run versus a blank KBr pellet in the reference beam to cancel KBr impurity bands, mainly H_2O bands.

2.2.7. Raman analysis

Laser Raman spectroscopy (Renishaw InVia laser Raman microscope) was used to study the structural features of the carbon materials (activated carbons and sulfonated carbons) in order to investigate structural change taking place in the materials due to sulfonation. The green 514 nm laser excitation was used to induce the Raman spectrum and the angle between the laser beam and the sample was varied in the range 0-25° to minimize Rayleigh scattering effects.

2.2.8. Thermo gravimetric analysis

The thermal stability of the prepared catalysts were investigated via thermogravimetric analysis (Model TGA-50 & DSC-60, Shimadzu) from room-temperature to 600 °C at a ramping rate of 10 °C min^{-1} under N_2 flow rate of 1 ml/min.

2.2.9. Basicity measurements

The Hammett indicator method was used to determine the basic strength of the catalytic materials (metal oxide catalyst). The method of Hammett indicator-benzene carboxylic acid (0.02 mol/L anhydrous methanol solution) titration was used to measure the basicity of the catalysts. Approximately 300 mg of a sample was shaken with 1 mL solution of Hammett indicator diluted in methanol and left to equilibrate for 2 h. The color of the medium (catalyst) was then noted. The Hammett indicators used in the study were bromothymol blue ($H_- = 7.2$), phenolphthalein ($H_- = 9.8$), 2, 4-dinitroaniline ($H_- = 15.0$) and 4-nitroaniline ($H_- = 18.4$). All the indicator solutions were prepared in methanol.

2.2.10. Acid site density measurements

The acid site densities of the carbon materials were determined by titration method as follows: 40 mg of a carbon sample was added into an aqueous solution of sodium hydroxide (0.01 mol L^{-1}, 20 mL). Then, the suspension was dispersed by stirring with a

magnetic stirrer for 4 h uniformly, at room temperature. After centrifugal separation at 6000 rpm, the supernatant solution was titrated by an aqueous solution of hydrochloric acid (0.01 mol L^{-1}) using phenolphthalein as an indicator. The $-SO_3H$ densities of sulfonated carbons were estimated from elemental analysis assuming that all S present in the carbon samples were due to $-SO_3H$ groups.

2.3. Determination of fatty acid compositions of vegetable oils

Synthesis-grade methanol (≥99% assay and ≤0.2% water content), Na_2SO_4 (99.5%, anhydrous), NaCl (99.5%), H_2SO_4 (98%), n-heptane (HPLC grade) and all necessary solvents were purchased from Merck Limited, Mumbai, India and were used as received. The standards for biodiesel analysis (37-componet FAME Mix, C4-24), methyl heptadecanoate (99.5%) were purchased from Sigma Aldrich. Fried soybean oil (acid value, 0.5 mg KOH g^{-1}, free fatty acid ~0.3%) was collected from School of Engineering canteen, Tezpur University, Assam, India. The oil seeds used in the study namely, *Mesua ferrea* L. *Jatropha curcas* and *Pongamia Pinnata* were purchased from Kaliabor Nursery, Nagaon (Assam), India. Oils were extracted by Soxhlet extraction using hexane as solvent.

Fatty acid composition of the vegetable oils were determined by gas chromatography of the corresponding methyl esters on a TRACE™ 1300 (Thermo Scientific) gas chromatograph equipped with FID detector and TRACE™ TR-FAME GC column. The methyl esters were prepared according to AOCS Official Method 1998; Ce 1e62 and Ce 2e66 [1]. The individual components were identified by comparison of retention times of the standard FAME mix and the wt% of the individual components were calculated based on internal standard (C17:0, methyl heptadecanoate). The column temperature was held at 50 °C for 2 min, then heated to 200 °C @10°C/min then to 300 °C @5°C/min and held for 10 min at this temperature. The carrier gas used was helium and the flow rate was maintained at 1 mL/min. Fig. 2.3. shows the representative gas chromatograph of the C4-C24 FAME Mix used for identification of individual fatty esters.

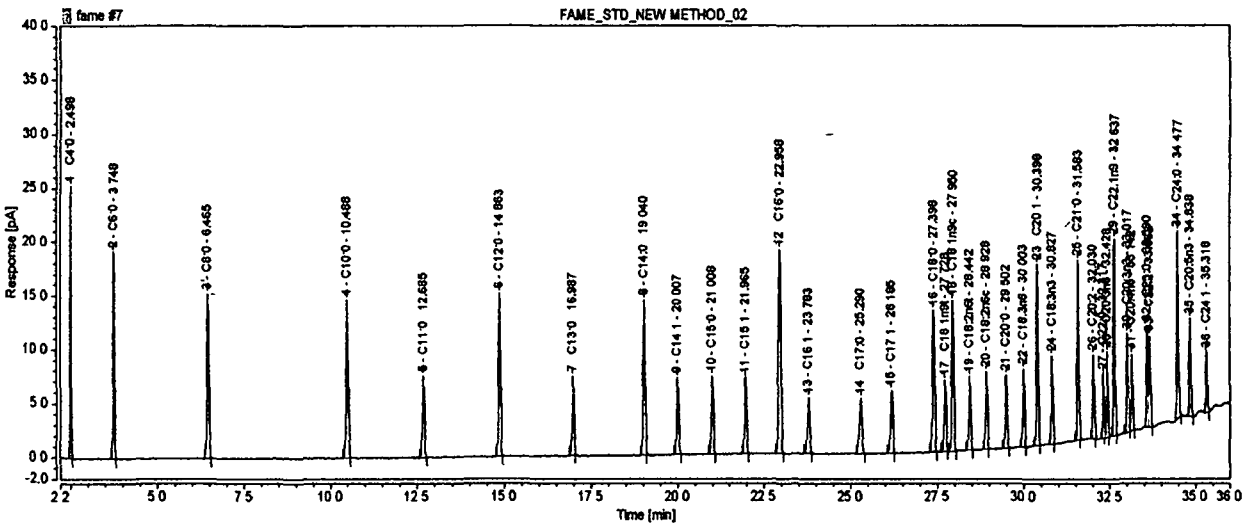

Figure 2.3. The representative Gas Chromatogram of C4-C24 FAME Mix used for identification of individual fatty esters.

2.4. Vegetable oil and Biodiesel analysis

2.4.1. Acid value

The acid number is a measure of the amount of carboxylic acid groups in a chemical compound such as a fatty acid. Acid values of the various vegetable oils and FAMEs were determined as per ASTM D 664 [2]. 0.2 – 0.5g of oil was mixed with ethanol and then heated on a water bath to dissolve the sample. This solution was titrated against 0.1M KOH using phenolphthalein as indicator. The acid value was determined as follows:

$$\text{Acid value } (mg\,KOH/g) = \frac{A \times M \times 56.1}{W} \qquad (ii.i)$$

Where,

A = ml of 0.1M KOH consumed by sample

M = molarity of KOH

W = weight in grams of the sample

The acid value was converted to weight percentage of free fatty acid (FFA) using the following relation:

$$\text{Acid value } (mg\,KOH/g) = 1.989 \text{ x Free fatty acids wt\% (as oleic acid)} \qquad (ii.ii)$$

2.4.2 Water content

Water content was determined by volumetric Karl Fischer (KF) titration (ASTM D 6304-07) using HYDRANAL ® reagents as described elsewhere [2]. In a typical process, HYDRANAL® Composite 2 was used as a titration agent. Ethanol-based, HYDRANAL® CompoSolver E (30 mL) was placed in the titration vessel and titrated to dryness with HYDRANAL® Composite 2. The biodiesel sample (5 mL), precisely measured using differential weighing, is injected into the titration vessel and titrated similarly.

2.4.3. Iodine value

Iodine value was determined according to AOAC official method 993.20 [3]. 0.5g of oils was weighed into conical flask and 20ml of carbon tetrachloride was added to dissolve the oil. 25ml of Wij's reagent was added to the flask using a measuring cylinder in a fume chamber. Stopper was then inserted and the content of the flask was vigorously swirled. The flask was then placed in the dark for 35minutes. At the end of this period, 20ml of 10% aqueous potassium iodide and 100ml of water were added using a measuring cylinder. The content was titrated with 0.1M sodium thiosulphate solution. Few drops of 1% starch indicator were added and the titration continued by adding the sodium thiosulphate drop wise until coloration disappeared after vigorously shaking. The same procedure was used for the blank test. The Iodine Value (I.V) is given by the expression:

$$Iodine\ Value(\text{mg } I_2\ g^{-1}) = \frac{12.69 \times C \times (V_1 - V_2)}{M} \qquad (ii.iii)$$

where,

C = concentration of sodium thiosulphate,

V_1 = volume of sodium thiosulphate used for blank,

V_2 = volume of sodium thiosulphate used for determination

M = mass of sample

2.4.4. Density

Density of was measured according to ASTM D287-92. This test method is based on the principle that the gravity of a liquid varies directly with the depth of immersion of a body floating in it. The floating body, which was graduated by API gravity units in this

method, is called an API hydrometer. The API gravity is read by observing the freely floating API hydrometer and noted the graduation nearest to the apparent intersection of the horizontal plane surface of the liquid with the vertical scale of the hydrometer, after temperature equilibrium was reached. The temperature of the sample was read from a separate accurate ASTM thermometer in the sample or from the thermometer which was an integral part of the hydrometer (thermo hydrometer) [2].

2.4.5. Viscosity

Viscosity was determined by falling-ball viscometer (Haake, Type C). It meets the requirements of the German DIN 53015 as well as ISO 12058 standards. The sample to be measured was pulled into the syringe without bubbles and placed into the temperature controlled holder of the HAAKE MicroVisco 2 unit. The sample reached the test temperature after approx. 5 min, and the measuring ball was pulled in the upper start position by means of a magnet. The ball then rolls down the wall of the syringe, which was inclined (15°C) to avoid bouncing. The fall of the ball was delayed by the resistance of test fluids. The falling ball time was proportional to its viscosity. The test result was the falling time for a defined distance which was measured electronically and converted into viscosity units by the stored calibration factors [2]. The dynamic viscosity η (in mPa.s) was calculated using the following equation:

$$\eta\ (\mathrm{mPa.s}) = K\left(\rho_1 - \rho_2\right) \times t \qquad (ii.iv)$$

where,

K = ball constant in mPa.s.cm^3/g.s

ρ_1 = density of the ball in g/cm^3

ρ_2 = density of the liquid to be measured at the measuring temperature in g/cm^3

t = falling time of the ball in seconds

The dynamic viscosity η can be converted to the kinematic viscosity ν by the following equation:

$$\nu\ (\mathrm{mm2/s}) = \frac{\eta}{\rho} \qquad (ii.v)$$

ν = kinematic viscosity (mm^2/s) (1 mm^2/s = 1 cSt); η = dynamic viscosity (mPa.s);

ρ = density of the liquid sample (g/cm^3)

2.4.6. Calorific value

Calorific value was measured in an oxygen auto bomb calorimeter according (SE-1AC/ML) to ASTM D2015 standard method. An oxygen – bomb was pressurized to 3 Mpa with an oxygen container. The bomb was fired automatically after the jacket and a bucket temperature equilibrates to within acceptable accuracy of each other [2].

2.4.7. Flash point

Flash point of biodiesel was determined according to ASTM D93-12 which corresponds to the standard test methods for flash point by pensky-martens closed cup tester. 70 ml of a sample was heated in a closed cup with a predetermined temperature rate. A test flame was lowered into the vapor space at regular intervals to observe a flash, the so called 'Closed Cup Flash Point [2].

2.4.8. Cloud point

The cloud point of biodiesel was determined according to ASTM D 2500. To determine the cloud point, the oil sample was cooled and examined visually until first cloud was appeared [2].

2.5. References

1. Official method Ce 1e62: fatty acid composition by gas chromatography. In Official methods and recommended practices of the AOCS. Champaign, IL, USA: *American Oil Chemists Society*, 2004.
2. Boro, J. Development of heterogeneous catalysts from biomass for biodiesel production, Ph.D, thesis, Tezpur University, India, 59-64, 2013.
3. AOAC official method 993.20 iodine value of fats and oils Wijs method. *AOAC Official Methods of Analysis*, **41**, 7–9, 1995.

Mixed oxide catalysts from pseudo stem of banana tree (Musa balbisiana) and post harvest residue of Mung bean (Vigna radiata) plant

Chapter 3

Chapter 3

In this chapter, the ashes obtained from post harvest crop residues of two alkali rich plants viz. *Vigna radiata* and *Musa balbisiana* have been proposed as alternative heterogeneous base catalysts for transesterification of vegetable oils.

3.1. Introduction

As already outlined in Chapter 1, catalyst research in biofuel production has been focused mainly on the chemically synthesized ones, but catalysts prepared straightway using biomass as raw materials have rarely been reported. Considering the complex organomineral structure of plants consisting both organic and inorganic components, the scope of using plant martial as catalyst precursor is enormous. The main biochemical constituents of plants viz. carbohydrates, proteins and lipids are made up of C, H, N and O. In addition, plants also contain variable amounts of organic and inorganic salts. The plant cell walls contain pectin—a negatively charged polysaccharide which tends to attract Ca^{2+} and other positively charged ions. It is often referred to as 'calcium pectate' and particularly concentrated in the middle lamellae of the cell walls. Weier *et al.* [1] and Amott *et al.* [2] observed that nutrients and mineral cations such as sodium and potassium chlorides, sulphates, phosphates, tartrates, malates and citrates dissolved themselves in the sap and protoplasm. Plants also contain cellular calcium oxalate crystals, usually concentrated in the leaves. Silica (as opal) is another compound which is widespread in the plant kingdom and is particularly rich in the grasses. Crystalline $CaCO_3$ is another inorganic compound commonly found in plants [3,4].

Therefore, when a plant material is fully burnt, its constituents undergo various changes. Organic matter is mostly released as CO_2 while inorganic salts such as e.g., chlorides and sulphates alter due to their anions denaturing or disappearing as gases; some salts (silica in conjunction with alkaline salts) undergo melting processes. The net result of these interactions is a product mix of partly new and partly old compounds with varying elemental percentages [5], broadly reflecting the non-volatile (inorganic) elements present in the original plant matter. For example, Ca from the cellular mineral (carbonate or oxalate) and the cell walls ('pectate') is transformed to CaO on burning, which further

recrystallised as carbonate, once it has absorbed enough moisture and CO_2 from the air [6]. To summarize, it is accepted that the ash is composed mainly of carbonates, oxides and hydroxides of alkali metals (Na or/ and K); but in most cases, it contains other water soluble non alkali substances such as some chlorides to form glassy slag; while some compounds e.g. calcium and potassium oxidize and remain as solid; a small proportion (e.g., silica on its own) remain unchanged. The presence of these constituents gives plant ash a strongly alkaline character, a feature highly desirable for catalytic applications.

The aim of this work was to develop a heterogeneous base catalyst straightway from biomass for applications in biodiesel production. The chapter demonstrates the use of banana pseudo stem (*Musa balbisiana*) and post harvest Mung bean plant residues (*Vigna radiata)* as the raw material for preparing mixed oxide type (ash) catalysts by simple calcination at 500-900 °C. *Vigna radiata* is mostly grown as kharif crop in India. After the collection of seeds of mung beans, the plant residue is treated as a waste and considered of no importance. Similarly, banana tree parts (peels, pseudo stems and leaves) are major left over after harvesting of fruit. In this study, these discarded plant materials were utilized as raw materials for catalyst preparation. The selection was based on the previously reported high alkalinity of ash obtained from these plants. Deka *et al.* [7] have recently reported the utility of banana ash obtained from trunks *Musa balbisiana* C. as heterogeneous catalyst in transesterification of refined *Thevetia peruviana* S. oil. However, no information was provided on the physicochemical and morphological features of the catalytic material.

3.2. Materials and Methods

3.2.1. Materials

The pseudo stem of *Musa balbisiana* and post harvest residues of *Vigna radiata* plants were collected from households located near Tezpur University, Assam, India (Fig. 3.1). Anhydrous Na_2SO_4, NaCl, KOH, synthesis-grade methanol (≥99% assay and ≤0.2% water content) and all analytical grade solvents and chemicals were purchased from Merck, Mumbai, India Ltd and used as received. Waste cooking oil (used soybean oil) was collected from School of Engineering's canteen, Tezpur University, Assam, India. Prior to use, the oil was centrifuged to remove solid impurities and dried over anhydrous Na_2SO_4. Properties of the oil along with its fatty acid composition are presented in Table 3.1.

Table 3.1

Selected physicochemical properties and fatty acid composition of waste soybean oil utilized in the study

Properties	Test method	Parameter
Acid value (mg KOH g^{-1})	ASTM D 664	0.94
Water content (ppm)	ASTM D 6304-07	398
Iodine value (mg I_2 g^{-1})	AOAC official method 993.20	139
Viscosity (cSt at 40 °C)	ISO 12058	33.98
Density (kgm^{-3})	EN 14078	901
Fatty acid (wt %)		
Palmitic (C16:0)		3.1
Palmitoleic (C16:1)		-
Stearic (C18:0)		2.7
Oleic (C18:1)		27.98
Linoleic (C18:2)		59.1
Linolenic (C18:3)	Gas chromatography	6.55
Arachidic (C20:0)		-
Gadoleic (C20:1)		-
Behenic (C22:0)		-
Erucic (C22:1)		-
Others		-

3.2.2. Preparation of Catalyst

The collected plant materials were chopped into small pieces, dried to remove moisture and grinded in a laboratory Wiley mill followed by further drying in an oven at 110 °C for 72 h. The powered biomass samples were finally burnt to ashes in a muffle furnace at 500 °C, 700 °C and 900 °C for 2 h to obtain the alkali rich catalytic materials. The ashes were passed through a 0.8 mm sieve to separate the larger particles, dried overnight at 120 °C and stored in air tight containers.

Figure 3.1. The precursors used for preparation of ash (mixed metal oxide type) catalysts (a) *Vigna radiata* plant and (b) *Musa balbisiana* pseudo stem.

3.2.3. Catalyst Characterizations

The catalytic materials were characterized by XRD, N_2 adsorption-desorption, SEM, EDX, FT-IR techniques as discussed in Chapter 2. The basicity was determined by using Hammett indicators as described in Chapter 2.

3.2.4. Catalytic tests

Reactions were performed in a two neck 250 ml round bottom flask, equipped with a magnetic stirrer, a thermometer and a reflux condenser (Fig. 3.2). Initially, a mixture of methanol and ash catalyst (<250 μm, outgassed at 100±5°C for 24 h) was preheated at 40 °C under magnetic stirring for 1 h followed by addition of preheated waste soybean oil. The reaction mixture was then vigorously stirred at 600 rpm and refluxed at different temperatures for different time period. After the reaction, the catalyst was separated from the biodiesel product by filtration and the excess methanol was removed in a rotary evaporator. Glycerin was removed by gravity separation and the upper product layer was analyzed by ^{1}H and ^{13}C NMR after washing three times with saturated aqueous sodium chloride and drying over anhydrous sodium sulfite. Reusability studies were conducted with spent catalyst under identical reaction conditions. The recovered catalyst was not subjected to any pretreatment such as washing prior to use.

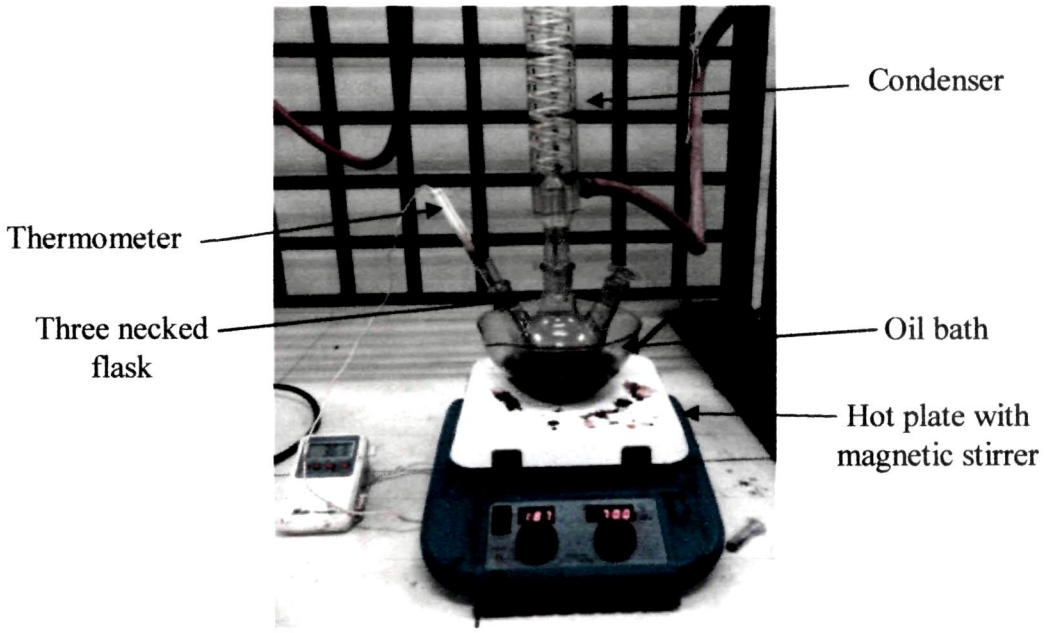

Figure 3.2. Schematic representation of the experimental setup used in catalytic tests

^{1}H NMR spectra were recorded on a Jeol JNM-ECS400 NMR spectrometer at 25.5 °C with $CDCl_3$ as a solvent and Tetramethylsilane (TMS) as an internal standard, respectively. Oil conversions, as methyl ester content, $C_{MEster}(\%)$ were determined by comparing area of methoxy protons of the methyl ester (~3.6 ppm) and α-methylene protons (~2.3 ppm) [8]. The NMR spectra were processed using "ACD NMR Processor Academic Edition" [9].

$$C_{MEster}(\%) = \frac{2\times A}{3\times B} \times 100 \qquad (iii.i)$$

A = integral of methoxy methyl ester peak at 3.6 ppm

B = integral of α-methylene peak at 2.3 ppm

3.3. Results and discussion

3.3.1. Catalyst Characterization

3.3.1.1. *Basicity measurements*

Basicity is one of the most important parameter influencing transesterification activity. Efficient transesterification of vegetable oils requires strong bases capable of abstracting proton from CH_3OH and forming active methoxy species. Both the ash catalysts reported here were found to be strongly basic ($9.8 < H_- < 18.4$) according to Hammett indicator tests. According to Masoud *et al.* [10], group I alkali metal hydroxides such as NaOH, KOH and group II metal oxides like CaO, BaO, SrO showed high transesterification activity owing to their high basicity.

3.3.1.2. *Powder X-ray diffraction patterns*

The XRD patterns of the optimum ash catalysts obtained from both sources indicated that they were a complex mixture of K and Ca compounds in the form of oxides, carbonates, chlorides, sulfates and silicates (Fig. 3.3). Oxides and carbonates were the most dominant species, as the strongest peaks corresponding to K_2O and K_2CO_3 were observed at 2θ = 25, 26, 31, 33, 41, 44, 46 (JCPDS reference no 00-026-1327 and 00-16–820). In addition, peaks observed at 2θ = 30, 39, 43, 47 (JCPDS reference code 01-085-0514) were assigned to CaO. While, the several small peaks corresponding to KCl, K_2SO_4, K_2MgSiO_4

(JCPDS reference no 004-0587, 002-0626, 021-0982, respectively) confirmed the presence of these species in trace quantities. However, with the increase of calcination temperature, the peak intensities corresponding to K_2O and K_2CO_3 were found to be reduced; which could be attributed to the decomposition of these compounds at higher calcination temperatures, Fig. 3.3 (a). The XRD patterns of *Musa balbisiana* ash (MB-ash) also indicated that, K_2CO_3 was in hydrated form ($K_2CO_3.1.5H_2O$) in these materials, Fig.3.3 (b) [11]. Thus, the presence of these alkaline compounds may be attributed to the highly basic nature of ash.

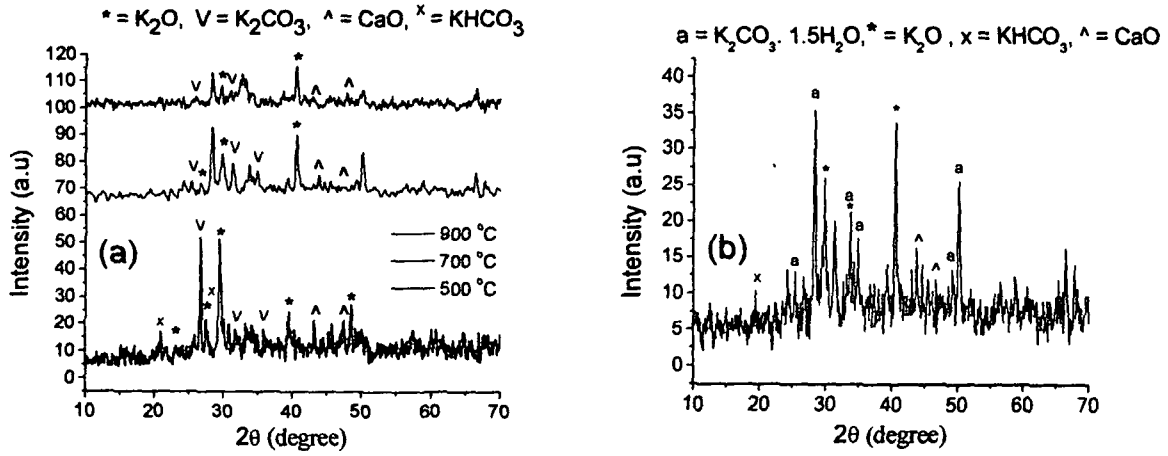

Figure 3.3. X-ray powder diffraction patterns of ash catalysts obtained from (a) *Vigna radiata* at different calcination temperatures and (b) *Musa balbisiana* at 500 °C.

3.3.1.3. *EDX analysis*

EDX studies strongly complimented the findings of XRD and indicated that dominant elements in both the materials were C (44-48 wt %) and O (37-39 wt%) followed by K (7-5.5 wt%) and Ca (4-4.5%) along with some traces of Mg, Si, O, Cl and S (Fig. 3.4). The presence of C and O were also found to support the existence of the metallic oxides and carbonates. However, the percentage of K (7 wt%) and Ca (4.5 wt%) were found to be higher in *Vigna radiata* ash (VR-ash) in comparison to MB-ash with 5.5 wt% K and 4 wt% Ca respectively.

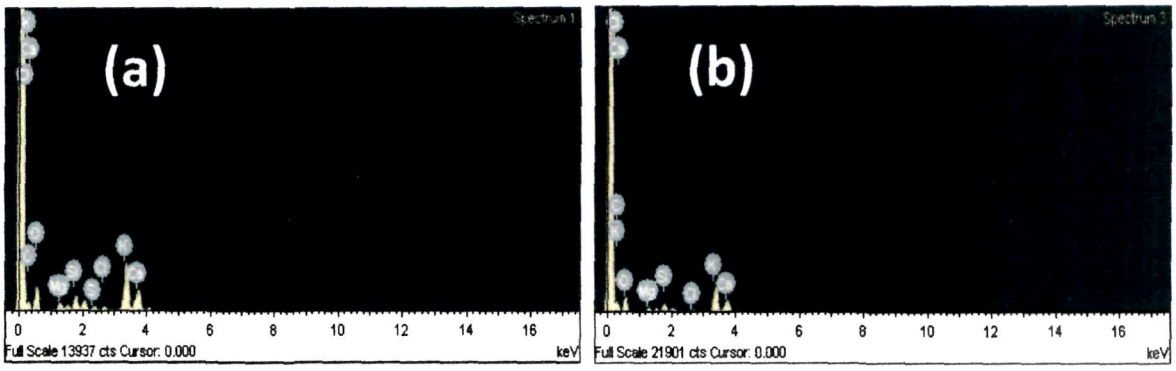

Figure 3.4. EDX spactra of ash catalysts obtained from (a) *Vigna radiata* and (b) *Musa balbisiana.*

3.3.1.4. *FT-IR analysis*

The FT-IR patterns of the ash catalysts also strongly support the results of XRD and EDX analyses. The bands around 2400-2000 cm^{-1} were attributed to the stretching vibrations of M–O–K bonds, where M= Si, Mg, etc. The peaks around 1000 cm^{-1} were attributed to the overlapping C–O and Si–O–Si stretching's whose presences are also confirmed from the XRD pattern shown in Fig. 3.2 [12-14]. Strong absorptions at 550 cm^{-1} may be due to characteristic Ca–O and K–O stretching. While, the asymmetrical bands around 2300 cm^{-1} may be due to the presence of CO_2. The additional CO_2 peaks around 1300–1400 cm^{-1} could be assigned to the presence of carbonates, formed due to the adsorption of atmospheric CO_2 onto metal oxides such as K_2O, (Fig. 3.5).

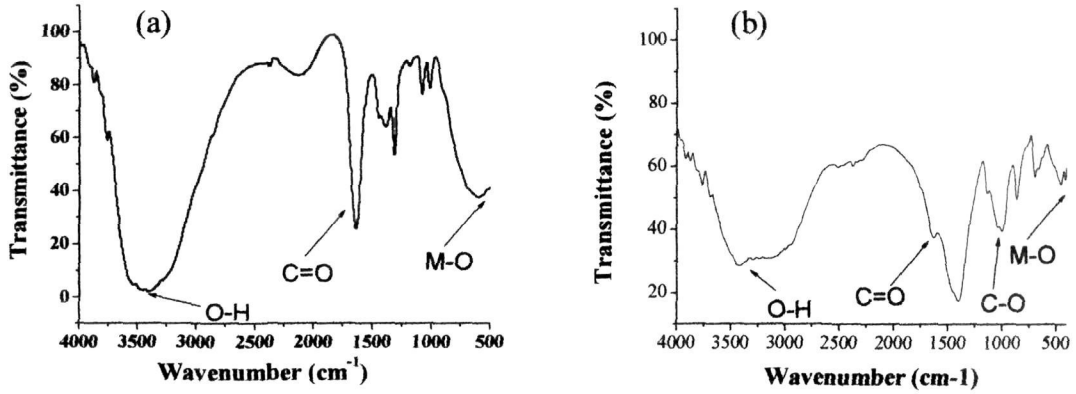

Figure 3.5. FT-IR patterns of ash catalysts obtained from (a) *Vigna radiata* and (b) *Musa balbisiana.*

3.3.1.5. *BET specific surface area measurements*

The BET specific surface areas of the catalysts were extremely low, 6 m^2/g and 5 m^2/g for MB-ash and VR-ash respectively. Similar values were also reported for alkaline oxide (CaO) derived from waste shells by Boro *et al.* [15]. Generally, a linear relationship exists between the surface areas and the catalytic activity as catalysts with larger surface area facilities better interaction between catalyst active sites and reactants. However, in the present case the effect of active site basic strength and density overweight's the contribution from surface area [10-13].

3.3.2. Catalytic activity

In terms of catalytic performance, both catalysts exhibited lower activity than NaOH, KOH or CaO presumably due to the lower basicity of these materials in conjunction to their low specific surface areas. A high catalyst loading was always needed to get high FAME yields. Nonetheless, the catalytic materials derived from *V. radiata* exhibited considerably higher activity, 92% FAME yield in comparison to the MB derived catalysts giving a maximum yield of 84% under identical reaction conditions (Table 3.2). The superior activity of VR-ash may be attributed to the presence of larger amounts of active species: K, Ca oxides. Therefore, VR-ash was chosen as a representative catalyst for optimization of reaction parameters.

Table 3.2

Comparison of catalytic activities of the two ash catalysts

Catalyst	K (wt%) [a]	Ca (wt%) [a]	S_{BET} [b] (m^2/g)	$FAME_{max}$ [c] (wt%)
* VR-ash	7	4.5	5	92
*VR-ash (MeOH filtrate)	-	-	-	47
* VR-ash (spent, 3rd use)	3	3.5	-	20
* MB-ash	5.5	4	6	84
* MB-ash (spent, 3rd use)	3.1	3.3	-	18
**NaOH	-	-	-	99
**KOH	-	-	-	99
TS-CaO [15]	-	36.34	8.35	93.3

[a] Based on EDX; [b] specific surface area determined by BET method (P/P_0 = 0.05–0.3);

[c] Based on ^1H NMR.

Reaction conditions: Catalyst loading *40 wt.% or **1 wt.% of oil; methanol to oil molar ratio of 12:1; reaction time 8 h; reaction temperature 70 °C.

3.3.3. Optimization of reaction Parameters

3.3.3.1. *Effect of catalyst amount*

Reactions were performed for 6 h with varying amounts of catalyst (VR-ash) ranging from 10–60 wt% (Fig. 3.6) and the fixed methanol to oil ratio of 9:1. It was observed that maximum oil conversion of 90% was obtained when the reaction was carried out with 40 wt% catalyst, much higher than values typically reported heterogeneous catalyst [15]. But, the catalyst preparation is easy, cheap and eco-friendly as it only involves calcination of waste materials without any chemical modifications. The required high catalyst loading may be attributed to the low density of basic sites and low specific surface area of the material. However, the low surface area was also advantageous as it could minimize the risk of catalyst poisoning by adsorption of reactants onto catalyst surface. It is also worth mentioning that when catalyst was prepared at higher calcination temperatures the yield decreased significantly and was found to be almost negligible for catalytic materials prepared at 900 °C due to the decomposition of active sites i.e. the oxides, hydroxides and chlorides of potassium at such elevated temperatures [16].

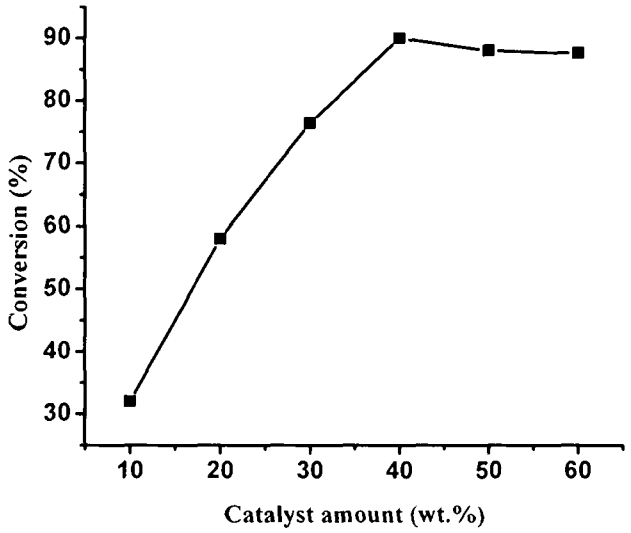

Figure 3.6. Effect of catalyst amount on oil conversion. Conditions: The molar ratio of methanol to oil was 9:1, temperature was 65±5 °C and reaction time was 6 h.

3.3.3.2. *Effect of methanol to oil molar ratio*

Reactions were carried out at different methanol to oil molar ratios with optimum catalyst amount for 6 h. From the results presented in Fig. 3.7, it can be observed that the maximum oil conversion was obtained with 9:1 methanol/oil molar ratio beyond which the FAME yield was found to be decreased slightly. In general, a high methanol amount is expected to favor the transesterification in forward direction as it is an equilibrium reaction. However, in the current experiments, the reduced FAME yield may be due to the reverse transesterification catalyzed by the same base leading to the formation of mono- and diglycerides.

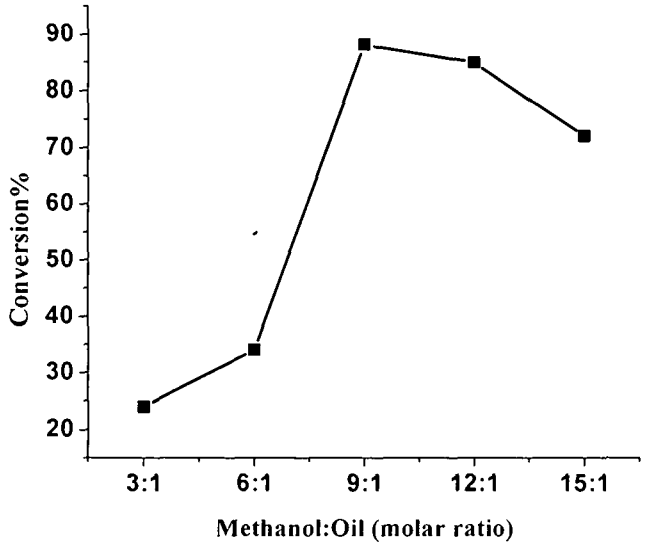

Figure 3.7. Effect of methanol to oil molar ratio on conversion of oil. Conditions: The catalyst loading was 40 wt.%, temperature was 65±5 °C and reaction time was 6 h.

3.3.3.3. *Effect of reaction time and temperature*

The effect of reaction time on oil conversion was investigated using the optimum catalyst loading of 40 wt% and methanol to oil molar ratio of 9:1. For this, the reaction was performed for 10 h and the conversion was monitored at a regular interval of 1 h (Fig. 3.8). The best conversion of 92% was obtained at 8 h of reaction beyond which the reaction reached equilibrium and conversion remained constant. Thus, the time required for the VR-

ash was found to be higher than the homogeneous catalyzed process and similar to the previously reported heterogeneous catalyzed systems [17]

Reactions were also performed at different temperatures ranging from 60–80 °C under the conditions as above. From the experiments, it was observed that the best yield could be obtained at 65-70 °C and beyond this temperature the reaction almost remained constant or decreased slightly possibly due to loss of methanol from the system. Hence, 65 ±5 °C was considered as the optimum reaction temperature in the present investigation.

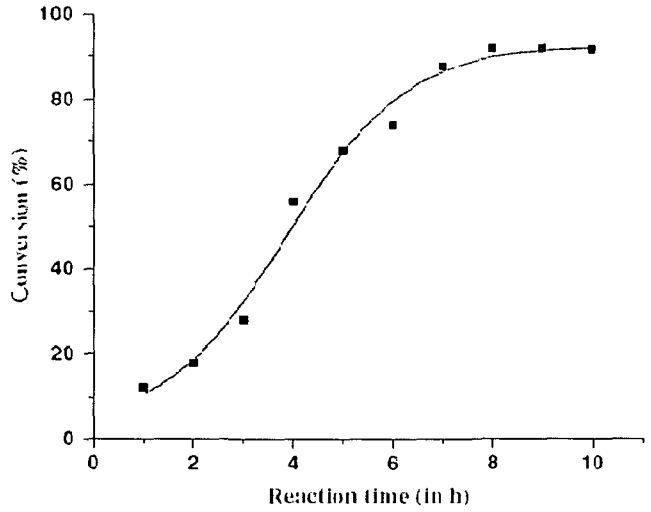

Figure 3.8. Effect of reaction time on conversion. Conditions: The catalyst loading was 40 wt%, molar ratio of 9:1 and temperature was 65±5 °C.

3.3.3.4. *Deactivation of ash catalyst*

Catalyst deactivation was studied by conducting reusability tests under optimized reaction conditions (9:1 methanol to oil ratio; 8 h reaction time). After the completion of the reaction, the catalyst was recovered by filtration and reused for the next cycle without any purification at the same reaction conditions. The catalyst was used consecutively three times and the deactivation results are presented in Figure 3.9. From the Fig. 3.9, it is seen that the catalytic activity decreases sharply after each cycle with total loss of 75% of its activity at 3rd cycle. The decrease in activity was probably due to the leaching out of potassium and calcium into the reaction media (Table 3.2). This observation is further supported by the catalytic effect of hot methanol filtrate (~47% oil conversion, Table 3.2)

of VR-ash catalyst. Another reason contributing to this loss could be the blockage or poisoning of active sites due to the absorption of reactants and glycerin onto the surface of the catalyst.

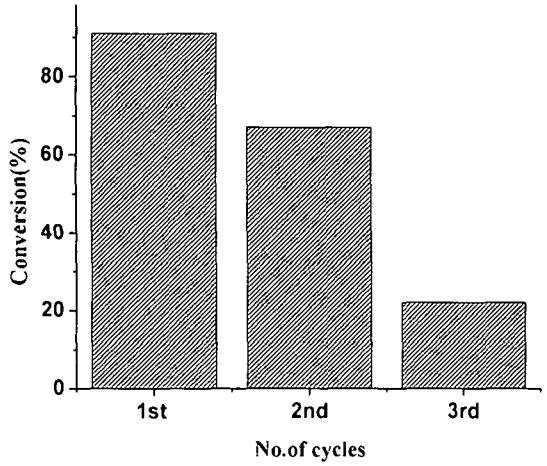

Figure 3.9. Deactivation of ash catalyst upon reuse. Conditions: The catalyst loading was 40 wt%, molar ratio of 9:1, temperature was 65±5 °C and reaction time was 8 h.

3.3.4. Biodiesel analysis

Fuel properties of the biodiesel were analysed according to standard methods described below. From the results presented in Table 3.3, it is seen that the biodiesel produced by using VR-ash catalyst shows similar fuel properties to the conventionally obtained biodiesel and within the limits of ASTM D6751 standards.

Table 3.3

Selected fuel properties soybean FAME produced in presence of VR-ash catalyst

Properties	Test method	ASTM D6751 (biodiesel)	Obtained values	Reported values [21]
Acid value (mg KOH g^{-1})	ASTM D 664	0.5	0.08	0.04 ± 0.01
Density (kgm^{-3})	ASTM D287-92	-	860	-
Viscosity (cSt at 40 °C)	ISO 12058	1.9-6.0	4.3	4.12 ± 0.01
Calorific value (KJ/g)	ASTM D2015	33–40	39.71	39.72–40.08
Flash point (°C)	ASTM D93	100–170	<135	-
Cloud point (°C)	ASTM D2500	−3.0 to 12	4.3	1 ± 1

The biodiesel was also characterized by means of ^{1}H and ^{13}C NMR spectroscopy {Fig. 3.10(a) and Fig. 3.10 (b)}. The appearance of characteristic peaks of methoxy protons ~3.6 ppm and disappearance of the signals of glyceridic backbone near 4-4.2 ppm in Fig. 3.10(a) was consistent with the formation of methyl esters. The formation of biodiesel was also confirmed by the appearance of —OCH_3 carbon peaks at 50.68 ppm in Fig. 3.10 (b), indicative of the formation of methyl esters [18-20].

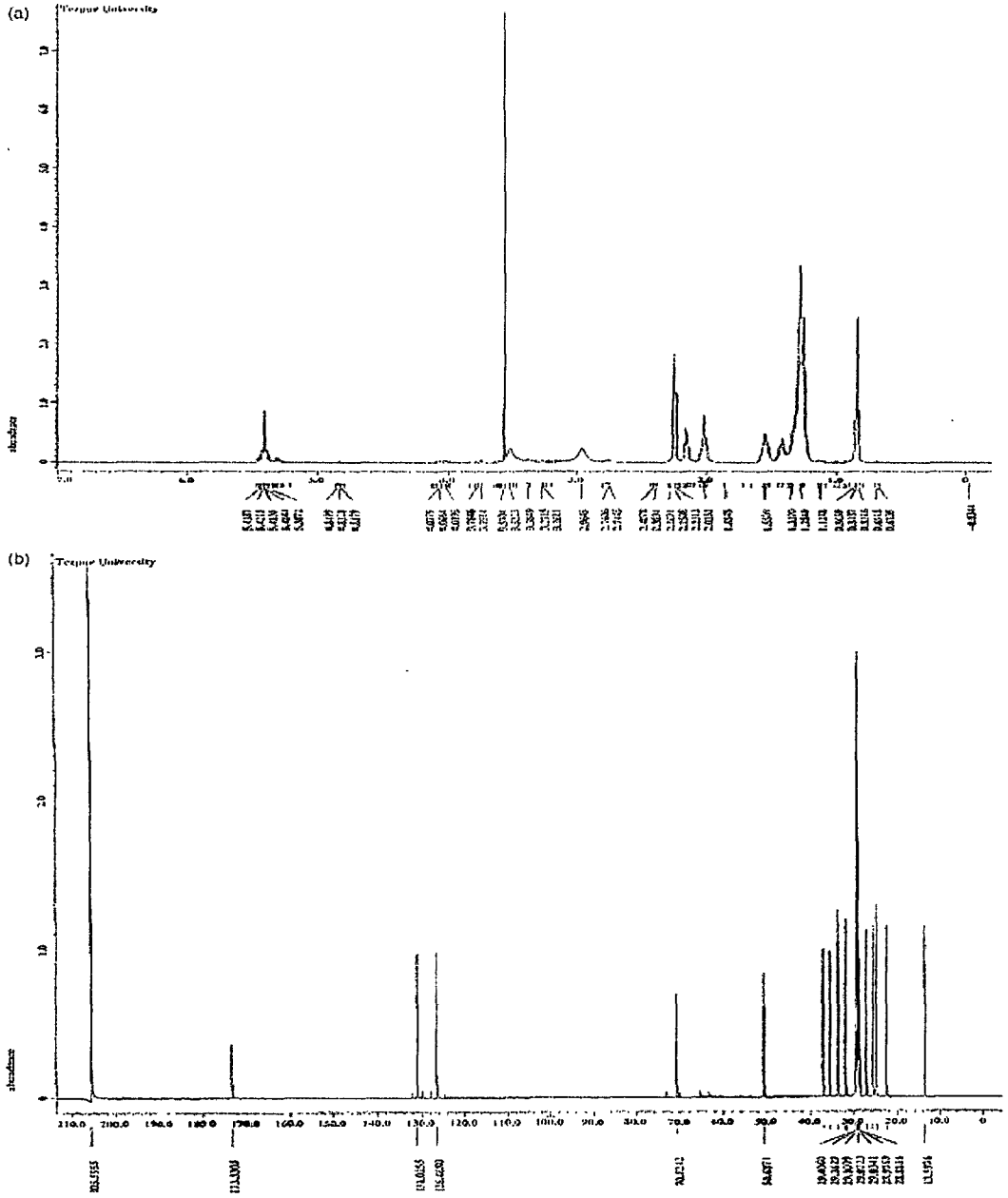

Figure 3.10. (a) ^{1}H NMR and (b) ^{13}C NMR spectra of biodiesel obtained over *Vigna radiata* ash

3.4. Conclusion

In conclusion, the ashes obtained by calcining *Vigna radiata* residues and *Musa balbisiana* pseudo stem were successfully employed as heterogeneous catalysts in biodiesel production. The ash materials were found to be composed mainly of potassium and calcium in the form of oxides and carbonates responsible for the high alkalinity and catalytic activity of such materials. The catalytic activity ash was found to be dependent mainly on the concentration of such active species. The material with the higher amount of such species, those obtained from *Vigna radiata* exhibited highest transesterification activity. Maximum FAME yield of 92% was achieved over this catalyst using 9:1 methanol to oil molar ratio in 8 h reaction time. Although such catalysts are cheap and could substantially reduce the biodiesel production costs, but they have disadvantages related to the reusability and requirement of a large catalyst amount for satisfactory FAME yield. The materials showed sever deactivation upon reuse most likely due to the easy leaching of these active species. Nonetheless, all the major fuel properties of biodiesel produced over such catalyst confer to the existing norms of biodiesel fuel.

3.5. References

1. Arnott, H. J. & Pautard, F. G. E. Calcification in plants, in *Biological Calcification: Cellular and Molecular Aspects.* Schraer, H., eds., Appleton Century Crofts, New York, 1970, 375–446.
2. Weier, T. E. et al. *Botany: An Introduction to Plant Biology*, Wiley, Chichester. 1982.
3. Setoguchi, H., et al. Calcification in higher plants with special reference to cystoliths, in *Origin, Evolution and Modern Aspects of Biomineralization in Plants and Animals*, Crick, R. E., eds, Plenum, New York, 1989. 409–418.
4. Fahn, A. *Plant Anatomy*, Pergamon, Oxford, 1982.
5. Etiégni, L. & Campbell, A. G. Physical and chemical characteristics of wood ash. *Bioresour Technol.*, **37**, 173–178, 1991.
6. Sanderson, D. C. W. & Hunter, J. R. Composition and variability in vegetable ash. *Science and Archaeology*, **23**, 27–30, 1981.

7. Deka, D.C. & Basumatary, S. High quality biodiesel from yellow oleander (Thevetia peruviana) seed oil. *Biomass Bioenergy*, **35**(5), 1797–1803, 2011.
8. Gelbard, G. et al. ^{1}H nuclear magnetic resonance determination of the yield of the transesterification of rapeseed oil with methanol, *J Am Oil Chem Soc*, **72**(10), 1239-1241, 1995.
9. http://www.acdlabs.com/resources/freeware/nmr_proc
10. Masoud, Z. Activity of solid catalysts for biodiesel production: A review. *Fuel Fuel Process. Technol.*, **90**, 770–777, 2009.
11. Qiu, P. et al. Characterization of KF/c-Al_2O_3 catalyst for the synthesis of diethyl carbonate by transesterification of ethylene carbonate. *Catal Lett*, **137**, 232–238, 2010.
12. Luki´c, I. et al. Alumina/silica supported K_2CO_3 as a catalyst for biodiesel synthesis from sunflower oil. *Bioresour Technol.*, **100**, 4690–4696, 2009.
13. Stork, W. H. J. & Pott, G. T. Studies of compound formation on alkali/.gamma.-aluminum oxide catalyst systems using chromium, iron, and manganese luminescence. *J. Phys. Chem.* **78,** 2496–2506, 1974.
14. Axelsson, O. & Paula, J. Reactive evaporation of potassium in CO_2 and the formation of bulk intermediates. *J. Vac. Sci. Technol. A,* **12**(1), 158–160, 1994.
15. Boro, J. et al. Solid oxide derived from waste shells of *Turbonilla striatula* as a renewable catalyst for biodiesel production. *Fuel Process. Technol.* **92**, 2061–2067, 2011.
16. Sharma, M. et al. Wood ash as a potential heterogeneous catalyst for biodiesel synthesis. *Biomass Bioenergy* **41**, 94–106, 2012.
17. Teng, G. et al. Transesterification of soybean oil to biodiesel over heterogeneous solid base catalyst. *Energy Fuel* **23**, 4630–4634, 2009.
18. Peterson, G. R. & Scarrah, W. P. Rapeseed oil transesterification by heterogeneous catalysis. *J. Am. Oil Chem. Soc.* **61**, 1593–1597, 1984.
19. Tariq, M., et al. Evaluation of biodiesel–diesel blends quality using ^{1}H NMR and chemometrics. *Fuel Process. Technol.*, **92,** 336–341, 2011.
20. Monteiro, M. R., et al. Determination of biodiesel blend levels in different diesel samples by ^{1}H NMR. *Fuel,* **88,** 691–696, 2009.

21. Moser, B.R. Influence of blending canola, palm, soybean, and sunflower oil methyl esters on fuel properties of biodiesel, *Energy Fuels*, **22** (6), 4301–4306, 2008.

CaO Supported Active carbon catalyst

Chapter 4

Chapter 4

Chapter 4 describes the synthesis, characterization and application of a CaO supported active carbon (AC) catalyst prepared from waste shells of *Turbonilla striatula* (TS) in biodiesel production. The work discussed in this chapter was carried out with the aim of overcoming the reusability issues of the ash catalysts discussed in previous chapter.

4.1. Introduction

Though the ash catalysts described in Chapter 3 were capable of transesterifying vegetable oils with good FAME yields and addressed some of the issues of homogeneous biodiesel catalysis, but the materials suffered from stability/reusability issues and requirement of large catalyst amounts. Thus, to overcome these disadvantages a new approach was adopted for the fabrication of bio-based catalysts with improved reusability. The lower activity of ash catalysts reported in the previous chapter could be mainly attributed to the low density of active sites and low specific surface area resulting in diffusion limitations. While, the poor reusability/stability was primarily associated with the leaching of active K and Ca oxides and carbonates into the reaction mixture [1].

CaO is the most successful alkali earth metal oxide to be employed as a catalyst in biodiesel production. It is considered as one of the most promising heterogeneous base catalysts because of its low cost, high basic strength and proven activity at mild temperature and atmospheric pressures. Moreover, it possesses relatively less environmental impacts as it can be synthesized from calcium rich biomass sources. Several studies have been conducted with CaO as the catalyst for biodiesel production via transesterification. Recently, CaO was prepared from various calcium rich waste materials such as shells of mollusk and egg and it was demonstrated that the CaO prepared from the shells exhibited the same catalytic activity as the commercially available CaO [2,3]. In a recent work, the successful utilization of waste shells of TS for the preparation of CaO and its subsequent utilization as a biodiesel catalyst was demonstrated by Boro *et al.* [3]. However, the CaO catalysts (irrespective of their source) are found to suffer from deactivation issues resulting from the partial solubility of CaO in MeOH and glycerin [4]. Attempts have been made to overcome the reusability/stability issues by methods such as:

selective doping with metals like Li, Ce, Ba, immobilisation of CaO into porous supports and so on [5-10]. Recently, we found substitutional doping with Li and Ba was partially effective for improving the reusability/stability of egg and TS shell based CaO catalysts [7,8]. In contrast, Zu *et al.* [9] reported substantial improvements in reusability and stability of CaO by its immobilisation onto porous carbon-supports with no substantial drop of activity even after successive reuse during transesterification of triacetin with methanol. The authors further improved their work and successfully applied a similar approach to prepare highly stable graphite oxide supported CaO catalyst. The catalyst was also successfully applied in transesterification of soybean oil with methanol to produce high quality biodiesel with FAME content > 98 wt% even after multiple reaction cycles [10]. Chitin is one of the main structural components present in shells of mollusks, snails. Due to its presence, the exoskeletons of arthropods could be easily transformed to AC [11]. AC, also known as porous carbon, has been widely used as an adsorbent in the separation and purification of gas or liquid. It has a large surface area which allows catalyst particles to disperse over it uniformly and effectively and it is reported that the surface characteristic of activated carbon generally does not changed at high temperature or pressure [12-13]. Consequently, use of AC as a catalyst support is assumed to be a perfect choice for the study.

Therefore, combining the knowledge of our previous work (TS as a CaO source) and superiority of carbon materials as a catalyst support [11-13], in this chapter an attempt was made to prepare a CaO supported AC catalyst in which both support and active material were prepared from the waste shells of TS. Since, organic fraction of the shells was composed of mostly of chitin and inorganic fraction of $CaCO_3$; in principle it could also be processed into high grade AC through careful processing. The choice of TS as a raw material for catalyst synthesis provides a promising way of preparing a "green catalyst" as it comes entirely from biomass. Besides that its utilization also fulfills the aim to integrate low-cost catalyst and environmentally benign biodiesel production.

4.2. Materials and methods

4.2.1. Materials

Waste shells of *Turbonilla striatula* (TS) were obtained from a local household of Chirang district of Assam, India. Synthesis-grade methanol (≥99% assay and ≤0.2% water content) and all necessary solvents were purchased from Merck Limited, Mumbai, India and were used as received. The same vegetable oil discussed in Chapter 3 was used in catalytic tests (Table 2.1).

4.2.2. Preparation of catalyst

CaO *supported activated carbon* catalyst was synthesized from waste shells of *Turbonilla striatula* (TS) (Fig. 4.1).

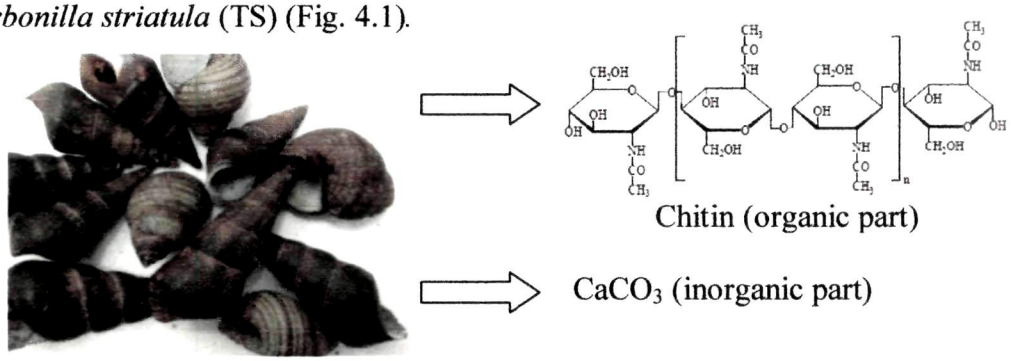

Figure 4.1. The precursor used for the preparation of active carbon supported CaO.

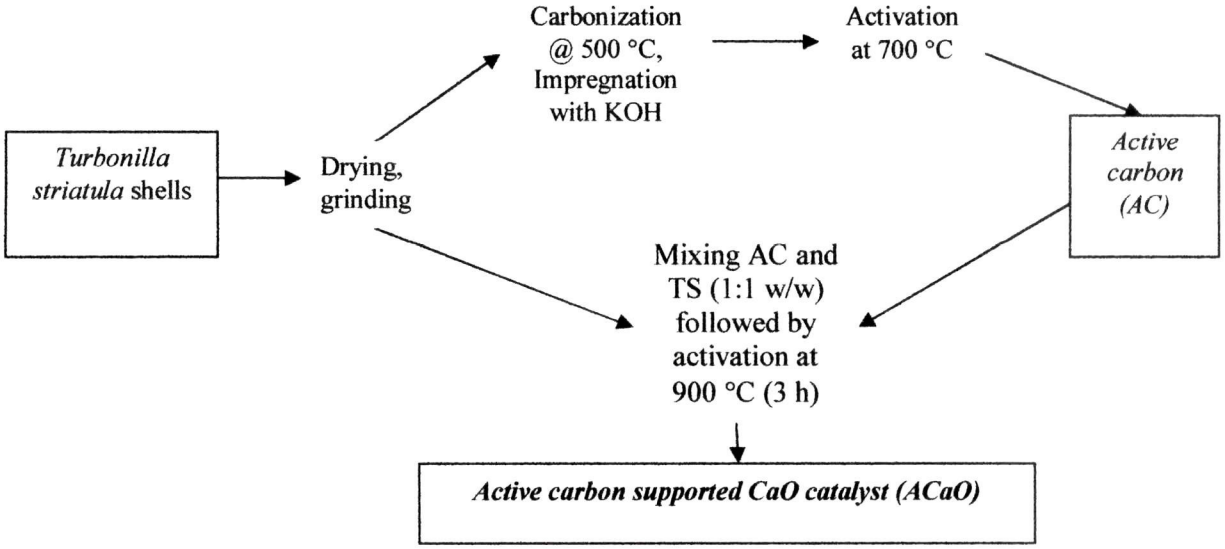

Scheme 4.1 Schematic representation for the preparation of supported CaO catalyst

The waste shells of TS were first washed with deionized water several times and dried at 120 °C for 24 h in an oven. After drying, it was crushed and grinded to powder and

passed through a 0.8 mm sieve. The collected powder was placed in a horizontal stainless steel reactor followed by heating in a furnace at a rate of 10 °C/min at 500 °C for 2 h under N_2 flow. The final product was mixed with aqueous KOH under mechanical stirring for 4 hr and then dried at 130 °C for 4 h. The dried mixture was placed in a furnace under N_2 flow of 100 cm^3/ min and heated at a rate of 10 °C/min for 3 h at 700 °C. The resulting activated carbon (AC) samples were then washed several times with deionized water, followed by 0.1 N HCl and distilled water to remove any inorganic impurities. Finally, the AC was dried at 120 °C for 24 h. In next step, AC support was mixed uniformly with ground and dried shells of TS (1:1 ratio w/w) followed by activation at 900 °C for 3 h to form CaO particles within the AC pores and obtained the CaO supported activated carbon catalyst (ACaO). The final product ACaO was sieved through a standard 250-μm (ASTM No. 60) and stored in an air tight container for further uses (Scheme 4.1).

4.2.3. Catalyst Characterizations

The catalytic materials were characterized by XRD, FT-IR, SEM, EDX, N_2-Physisorption and Hammett indicators as discussed in Chapter 2.

4.2.4. Catalytic tests

Catalytic tests were performed in batch mode in a round bottomed flask, equipped with magnetic stirring and a reflux condenser as discussed in Chapter 3. Oil conversions in terms of methyl ester content were determined by obtaining ^{1}H NMR spectra of samples periodically withdrawn from the reaction mixture as per the method described by Gelbard *et al.* [14]. The details of ^{1}H NMR analysis method have been discussed in Chapter 3.

4.3. Results and discussion

4.3.1. Catalyst characterizations

4.3.1.1. *Basicity and surface area measurements*

The basicity of the CaO supported ACaO catalyst and shell derived CaO were determined using the Hammett indicator tests. It was observed that the catalysts, ACaO and CaO changed the colour of phenolphthalein (H_- = 8.2) from colorless to pink, the colour of indigo carmine (H_-=12.2) from blue to green and the colour of 2,4-dinitroaniline (H_- = 15) from yellow to mauve, but failed to change the colour of 4-nitroaniline (H_- =

18.4). Therefore, the basic strengths of both the catalysts were 15< H_<18.4 and they were considered as strong bases for transesterification reactions similar to pure CaO (Table 4.1).

The specific surface area of the KOH activated TS-shell (AC) carbon was found to be 200 m^2/g, much lower than commercial ACs (>500 m^2/g). The low surface area can be explained by the presence of Ca containing impurities formed within the AC pores during carbonization. Upon CaO immobilization, the surface area of AC reduced to 82 m^2/g (60%), which confirmed that AC pores were filled by the CaO particles (active phase).

Table 4.1

Basicity and surface area of ACaO, shell-CaO and AC

Catalyst	[a] S_{BET} (m^2/g)	H_
AC	200	-
shell-CaO	8.35	15 < H_ < 18.4
ACaO	82	15 < H_ < 18.4

[a] Surface area determined using BET equation P/Po (0.005-0.3)

4.3.1.2. *X-ray powder diffraction patterns*

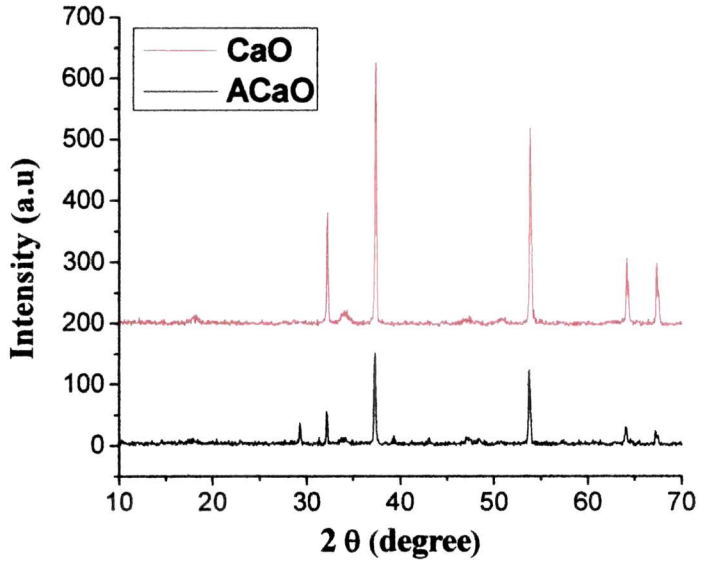

Figure 4.2. Powder XRD patterns of ACaO in comparison to shell derived CaO.

The incorporation of CaO into support materials was confirmed from the X-ray powder diffraction patterns of ACaO catalyst presented in Fig 4.2. The diffraction peaks

that appeared around 2θ = 17, 21, 28, 30, 37, 38, 44, 46, 48, 51, 53, 56, 64, 67 correspond to JCPDS file no. 01-085-1799 were assigned to carbon. On the other hand, the peaks corresponding to 2θ = 32, 37, 53, 64, 67 were due to CaO (JCPDS file no. 01-077-2376). This indicates that the catalyst used during the investigation was composed mainly of carbon and calcium oxide.

4.3.1.3. *EDX analysis*

To strengthen the findings of XRD, the elemental composition of the catalytic martial was also determined by EDX analysis. According EDX analysis, the major constituent elements present in the ACaO catalyst were calcium, carbon and oxygen having weight % of 27, 18 and 55 respectively (Fig. 4.3). This indicates that 1 g of catalytic material is made up of 0.034, 0.007 and 0.012 moles of oxygen, calcium and carbon respectively, which corresponds to additional 0.027 mole of oxygen on ACaO after accounting for all the CaO. This indicate the presence of numerous oxygen containing functional groups in the AC support as at 900 °C TS completely transforms to CaO [3,8].

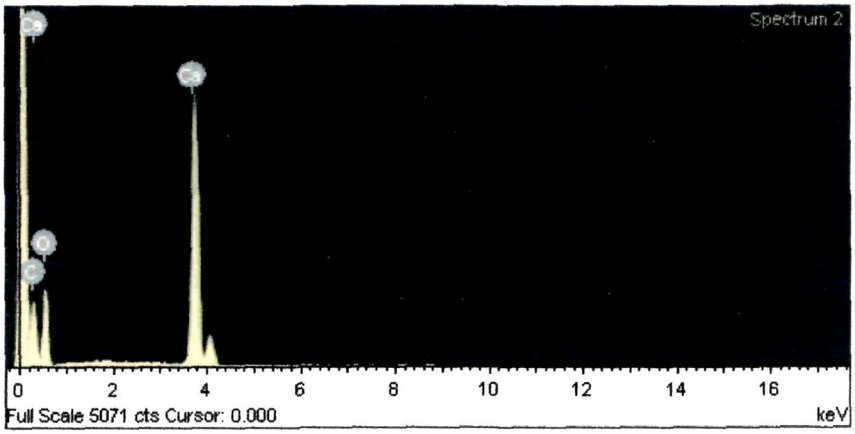

Figure 4.3. EDX spectrum of ACaO catalyst.

4.3.1.4. *SEM analysis*

The morphology of the catalyst particles were studied by SEM. The SEM images of the activated carbon (AC) and ACaO catalyst (Fig. 4.4) showed that the original structure of AC was not disrupted even after CaO loading. The CaO particles distinctly filled up the most of the pores of the support indicated that the CaO species were dispersed on the surface of activated carbon (AC). The pore filling was also indicated by the 60% reduction in specific surface area of AC following CaO loading (Table 4.1).

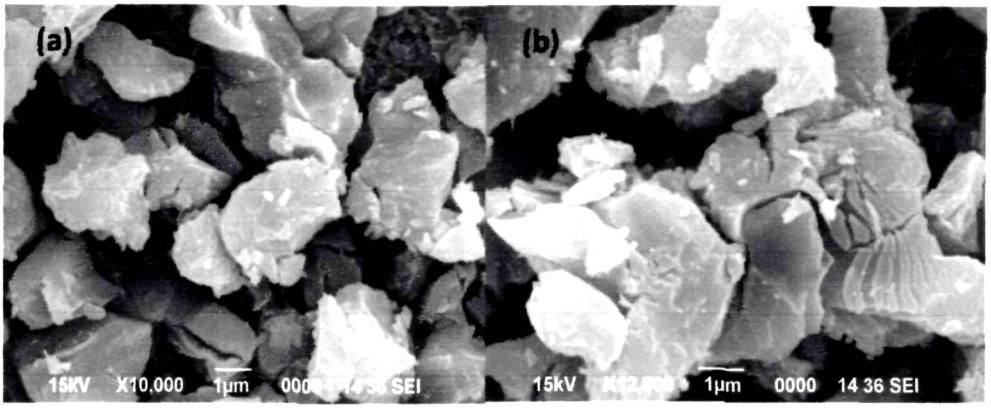

Figure 4.4. SEM images of (a) AC and (b) ACaO particles.

4.3.1.5. *FT-IR analysis*

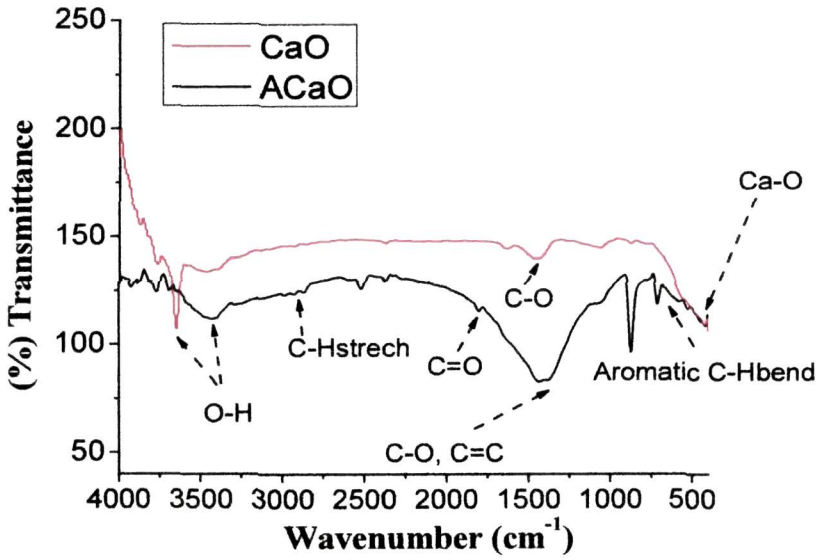

Figure 4.5. FT-IR patterns of TS shell derived CaO in comparison to ACaO.

The FT-IR spectra of ACaO showed the presence of characteristic CaO bands similar to the CaO (TS shell derived CaO), indicated the presence of well dispersed CaO particles in the catalyst surface. The characteristic (Ca-O) stretching at (400-500 cm^{-1}), CO_3^{2-} stretching frequency at (1450 cm^{-1}) in the ACaO spectrum confirmed the immobilisation of CaO onto the carbon framework of active carbon support, while the peaks at (770 cm^{-1}) and (2870 cm^{-1}, 2925 cm^{-1}) were attributed to aromatic C-H bending and stretching frequencies of carbon framework respectively (Fig. 4.5.).

4.3.2. Influence of reaction parameters

4.3.2.1. *Effect of reaction temperature*

The various reaction parameters affecting conversion were also optimized to achieve maximum oil conversion. The reaction temperature was optimized by performing experiments in the temperature range of 50-130 °C at fixed methanol to oil molar ratio of 40:1 and 10 wt% catalyst in 8 h reactions (Fig. 4.6). The results showed a steady increase in oil conversion with increasing reaction temperature upto 100 °C beyond which it remained almost fixed. Thus, the optimal reaction temperatures were found to be 100-120 °C, values much higher than our previous study. It is a well established fact that the low activity of heterogeneous catalysts system is mainly due to the mass transfer limitations performing the reaction at high temperature. Generally, higher reaction temperature favours the collision between the reactants and also in two-phase liquid reaction system such as methanol and oil the increased reaction temperature improves miscibility of methanol and oil phases which reduce mass transfer limitations resulting into improved conversion of oil.

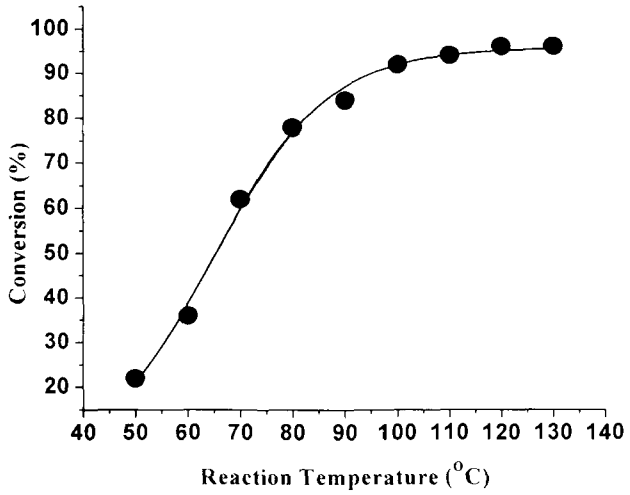

Figure 4.6. Effect of reaction temperature on conversion of oil. Conditions: The methanol to oil molar ratio was 40:1 and 10 wt% catalyst in 8 h reactions.

4.3.2.2. *Effect of molar ratio*

To study the effect of methanol to oil molar ratio, reactions were performed at varying methanol to oil ratio from 6:1 to 52:1 at 120 °C using 10 wt% catalyst in 8 h. The

conversion was found to increase steadily with increasing methanol to oil ratio upto 40:1 beyond which it was found to remain almost unchanged (Fig. 4.7). The lower activity of ACaO in comparison graphite oxide-supported CaO may be attributed to its lower specific surface area and narrow pore structure [9]. At ratios lower than 40:1, ester yields were <85% possibly due to the use of reflux setup where methanol could easily escape from the system at the elevated temperatures. Studies have shown that higher methanol amount drives the transesterification towards forward direction as it is an equilibrium driven reaction [15,16].

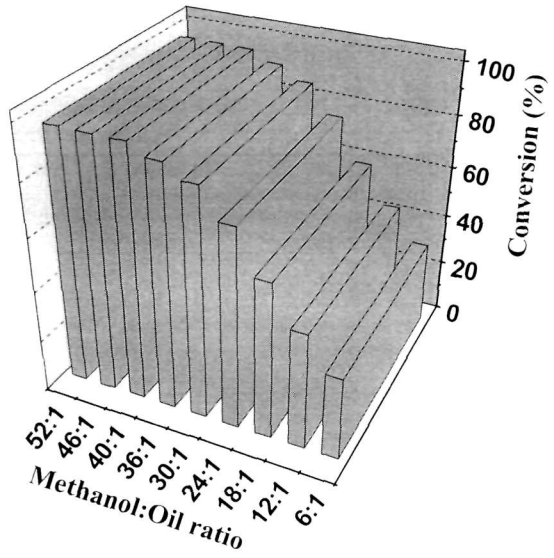

Figure 4.7. Effect of methanol to oil molar ratio. Conditions: The temperature was 120 °C and 10 wt% catalyst in 8 h reactions.

4.3.2.3. *Effect of catalyst amount*

Another factor which determines the conversion is the amount of catalyst used during the reaction. In this study, the catalyst amount was varied from 1-17 wt% by fixing the other reaction parameters to optimum values (Fig. 4.8). In the present investigation, a steady increase in oil conversion was observed with the increase of catalyst amount from 1-11wt%, after that it was found to remain constant. Hence, 11wt% was taken as the optimal catalyst amount. The lower conversions obtained at low loadings could be related to the absence of sufficient active sites.

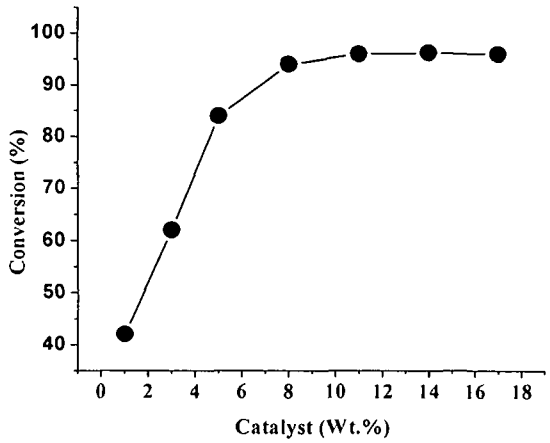

Figure 4.8. Effect of catalyst amount (wt% with respect to oil) on conversion of oil. Conditions: The temperature was 120 °C, methanol to oil molar ratio was 40:1 and 10 wt% catalyst in 8 h reactions.

4.3.2.4. *Effect of reaction time*

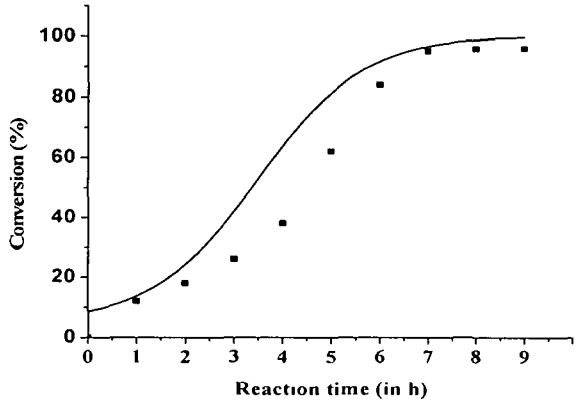

Figure 4.9. Effect of the different reaction time on conversion of oil. Conditions: The temperature was 120 °C, methanol to oil molar ratio was 40:1 and 10 wt% catalyst in 8 h reactions.

The effect of time on conversion was also investigated employing optimal methanol to oil molar ratio, catalyst amount and reaction temperature. The results presented in Fig 4.9 shows a steady increase in conversion with reaction time attaining equilibrium at 7 h. The initial lag and the sigmoidal time vs. conversion plot is consistent with poor mass transfer effects during initial hours of reaction which is due immiscibility

of methanol and oil forming a two-phase liquid reactant system, an effect well documented for vegetable oil transesterification in literature [16].

4.3.2.5. *Effect of reuse (catalyst stability)*

In order to examine the stability of catalyst, deactivation studies were conducted by reusing the catalyst repeatedly upto 5 cycles under same reaction conditions. To conduct reusability studies, the catalyst particles were recovered by filtration followed by washing with methanol for several times, oven drying at 100 °C and re-used for the next cycle. The result presented in Fig. 4.10 shows that the catalyst exhibits excellent stability and retains almost 99% of its initial activity even at the 5^{th} reaction cycle. Accordingly, the ACaO catalyst showed superior stability upon reuse unlike CaO [1], Ba doped CaO [7], Li doped CaO [8] and ash catalysts (Chapter 3). The high stability of such materials may be attributed to the oxygen-containing groups (-COOH,-OH, lactones etc) present on the surface of AC that probably act as anchoring sites for the CaO molecules, thus prevented them from leaching out into the reaction media as also reported by Zu *et al.* [9-10] for carbon supported CaO catalysts.

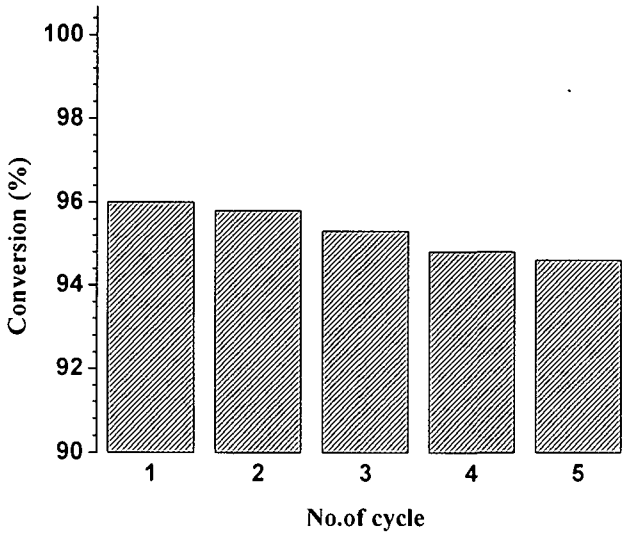

Figure 4.10. Effect of reuse (catalyst deactivation). Conditions: The temperature was 120 °C, methanol to oil molar ratio was 40:1 and 10 wt% catalyst in 8 h reactions.

4.3.3. Mechanism of base catalyzed transesterification

The generally accepted mechanism of transesterification in the presence of strongly basic homogeneous catalysts such as KOH, NaOH or heterogeneous alkali and alkaline earth oxides or carbonates consists of the following four steps:

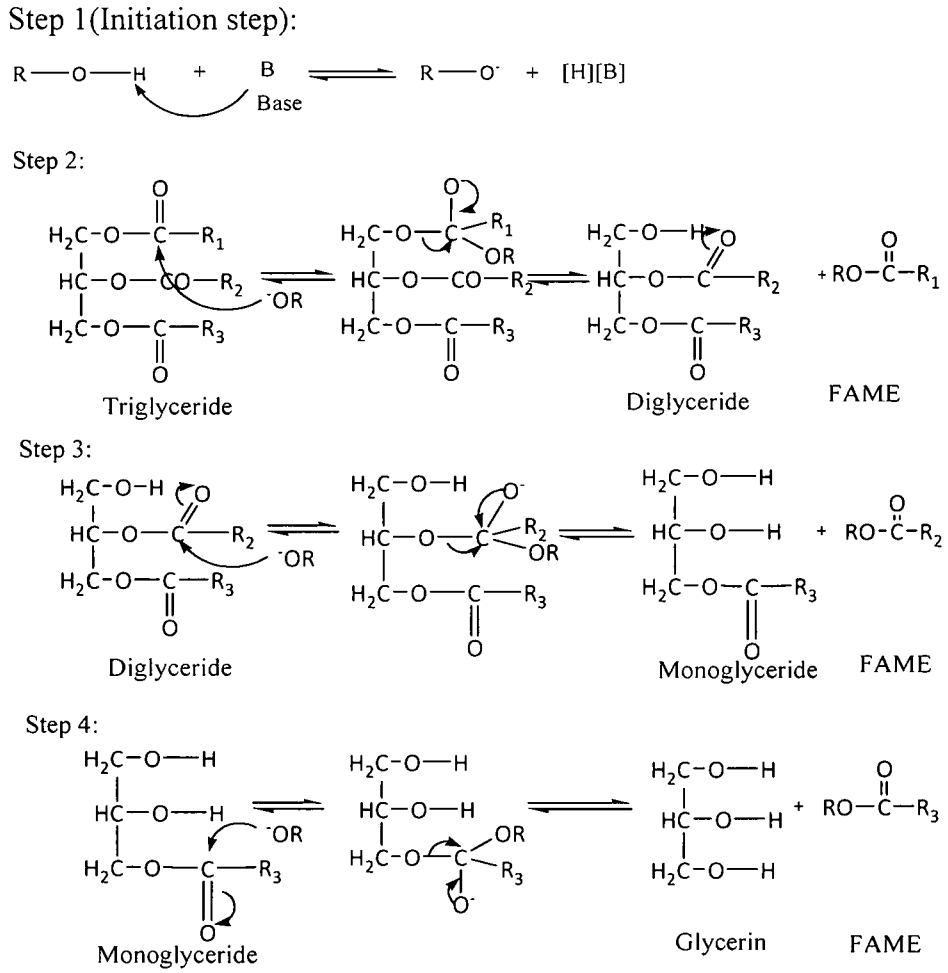

Scheme 4.2 General mechanism of base catalyzed transesterification

A catalyst is crucial for the formation of active ^{-}OR species, a higher concentration of both the catalyst and alcohol means a high concentration of ^{-}OR and consequently a faster reaction. In general, a catalyst is usually used to improve the reaction rate and biodiesel yield while excess alcohol is used to shift the equilibrium towards the product. The actual transesterification process consists of a sequence of three consecutive reversible reactions, which include conversion of triglycerides to diglycerides, followed by the conversion of diglycerides to monoglycerides. Finally, the monoglycerides convert into

glycerin and yield one ester (FAME) molecule in each step [9]. This is represented in three steps in Scheme 4.2.

4.4. Conclusion

In conclusion, waste shells of TS were successfully utilized as a raw material for preparation of a highly robust supported CaO catalyst (ACaO). Catalyst was prepared by physical mixing of the finely powdered TS shells with TS shell derived AC, followed by heat treatment at 900 °C to generate the active CaO particles. ACaO was successfully employed in the transesterification of used soybean oil. Under optimum reaction conditions of 120 °C, 40:1 methanol to oil ratio, 11 wt% catalyst and 7 h of reaction time, FAME yields upto 96% was reached. Although, less active than native CaO catalyst, ACaO was highly stable and maintained 99% of its initial activity even at 5^{th} successive reaction cycle. Consequently the stability and reusability issues of the ash catalysts and neat CaO were successfully addressed by ACaO.

4.5. References

1. Boro, J. et al. Vigna radiata (mung bean) ash as heterogeneous base catalyst for biodiesel production, *J. Bio Eng Biorefin.*, **2**, 54–60, 2013.
2. Boro, J. et al. A review on solid oxide derived from waste shells as catalyst for biodiesel production. *Renew Sust Energ Rev*, **16**, 904– 910, 2012.
3. Boro, J. et al. Solid oxide derived from waste shells of Turbonilla striatula as a renewable catalyst for biodiesel production. *Fuel Process. Technol.*, **92,** 2061–2067, 2011.
4. Kouzu, M. & Hidaka, J. Purification to remove leached CaO catalyst from biodiesel with the help of cation-exchange resin, *Fuel,* **105**, 318–324, 2013.
5. Kawashima, A. et al. Acceleration of catalytic activity of calcium oxide for biodiesel production, *Bioresour Technol.*, **100**(2), 696–700, 2009.
6. Thitsartarn, W. & Kawi, S. An active and stable CaO–CeO_2 catalyst for transesterification of oil to biodiesel, *Green Chem.*, **13**, 3423-3430, 2011.

7. Boro, J. et al. Transesterification of non edible feedstock with lithium incorporated egg shell derived CaO as heterogeneous base catalyst for biodiesel production, *Fuel Process Technol,* **122,** 72-78, 2014.

8. Boro, J. et al. Ba doped CaO derived from waste shells of T striatula (TS-CaO) as heterogeneous catalyst for biodiesel production, *Fuel,* **129**, 182–187, 2014.

9. Zu, Y. et al. CaO Supported on Porous Carbon as Highly Efficient Heterogeneous Catalysts for Transesterification of Triacetin with Methanol, *Energy Fuels,* **24**, 3810–3816, 2010.

10. Zu, Y. et al. Graphite oxide-supported CaO catalysts for transesterification of soybean oil with methanol, *Bioresour Technol.,* **102**, 8939–8944, 2011.

11. Amuda, O.S. et al. Removal of heavy metal from industrial wastewater using modified activated coconut shell carbon, *Biochem. Eng. J.* **36**, 174–181, 2007.

12. Mohan, D. & Pittman Jr., C. U. Activated carbons and low cost adsorbents for remediation of tri- and hexavalent chromium from water, *J. Hazard. Mater.*, **137,** 762–811, 2006.

13. Baroutian, S. et al. Potassium hydroxide catalyst supported on palm shell activated carbon for transesterification of palm oil, *Fuel Process Technol.*, **91**, 1378–1385, 2010.

14. Gelbard, G. et al. ^{1}H nuclear magnetic resonance determination of the yield of the transesterification of rapeseed oil with methanol, *J. Am. Oil Chem. Soc.*, **72**(10), 1239-1241, 1995.

15. Meher, L.C. et al. Technical aspects of biodiesel production by transesterification—a review, *Renew Sust Energ Rev*, **10**(3), 248–268, 2006.

16. Freedman, B., et.al. Transesterification kinetics of soybean oil, *J. Am. Oil Chem. Soc.* **63(10)**, 1375–80, 1986.

Sulfonated carbon catalysts based on de-oiled cake waste I: Synthesis and applications in biodiesel production

Chapter 5

Chapter 5

In this chapter, the synthesis, characterization and catalytic applications of a sulfonated carbon (Brønsted solid acid) catalyst from de-oiled waste cake residues (DOWC) of *Mesua Ferrea* Linn. seeds are discussed. Catalytic performance was evaluated in biodiesel production by simultaneous esterification and transesterification of acidic oils (AOs) containing 8-43 wt% free fatty acids (FFA) in comparison to homogeneous H_2SO_4.

5.1. Introduction

The catalysts discussed in Chapter 3 and 4 are chiefly alkali and alkaline earth oxides and their high activities in transesterification are related to their strong basicity ($15<H_-<18.4$). However, one of the major drawbacks of such strongly basic catalysts (both homogeneous and heterogeneous) is their low tolerance towards FFA and H_2O causing soap formation. These impurities are commonly present in low cost biodiesel feedstock such as crude vegetable oils and waste cooking oil. Although successful transesterification of fried soybean oil obtained from university cafeteria was demonstrated in Chapter 3 and 4 but it should be noted that the FFA content in the said oil was only 0.5 wt %. The FFA content in waste cooking oils are variable from source to source and depends on the extent of reuse, as the common practice in the university cafeteria was to use the oil for once only, therefore the low acidity of the oil was well explained. In a broader context, the applicability of the catalytic materials discussed in previous chapters is limited only to biodiesel production from low FFA containing oils.

Thus the objective of Chapter 5 is shifted towards solid acid catalysts for utilization of acidic oils (AO)s. AO such as crude vegetable oils, waste cooking oils and yellow grease have the potential to serve as an attractive feedstock due to their lower cost. Conventional vegetable oil refining is not considered a practical solution as it drastically increases the cost of biodiesel product. Esterification on the other hand, has been demonstrated to reduce the FFA levels of AOs in a cost effective manner. Nevertheless, requirement of large quantities of methanol and elevated FFA contents are the main factors affecting the economics of FAME production from AOs. Currently, concentrated H_2SO_4 is employed in acid oil pretreatment, at commercial scale, due to its proven activity and low

cost. However, the use of mineral acids comes along with many drawbacks such as the requirement of specialized acid resistant reactors to overcome corrosion problems and requirement of multiple washing steps after the reaction in order to remove the unreacted H_2SO_4 [1-5]. To overcome these limitations, the use of heterogeneous acids such as zeolites [6], heteropolyacids [7], Amberlyst-15 [8], $H_3PW_{12}O_{40}.6H_2O$ [9], WO_3/ZrO_2 [10] and sulfonated carbon catalysts [5,11-14] have been suggested. Nevertheless, the applicability most of the conventional solid acids (e.g. zeolites, Amberlyst etc.) at industrial scale have been limited by their high costs, low activity and poor reusability. The low activity is connected to the narrow pore structures restricting the interaction with large-size biomass building-blocks (triglycerides, long chain fatty acids, carbohydrates etc). Consequently, the sulfonated carbon catalysts could be considered as a viable alternative to H_2SO_4 owing to their low material cost and high catalytic activity. The true beauty of the bio-derived carbons lies in the fact that such materials can be integrated into existing concepts of biorefining. After the introduction of sulfonated carbons by Hara et al. [11], several reports on the preparation and catalytic applications of similar catalysts from different sources followed: vegetable oil asphalt [14], glucose [15,18], sucrose [17], starch [19], glycerol pitch [20], corncob [21], biochar [13], polymeric resins [22,23] and to name others [16]. Sulfonated carbons are undoubtedly the best examples of bio-derived catalysts available in literature; a great deal of work has been performed with sulfonated carbons, which include optimization of preparatory conditions and new catalytic applications. Typically, these catalysts are prepared in two steps via sulfonation of incompletely pyrolysed biomass: (i) carbon precursors are directly pyrolyzed and (ii) sulfonated with concentrated/fuming H_2SO_4 at high temperatures (Scheme 5.1).

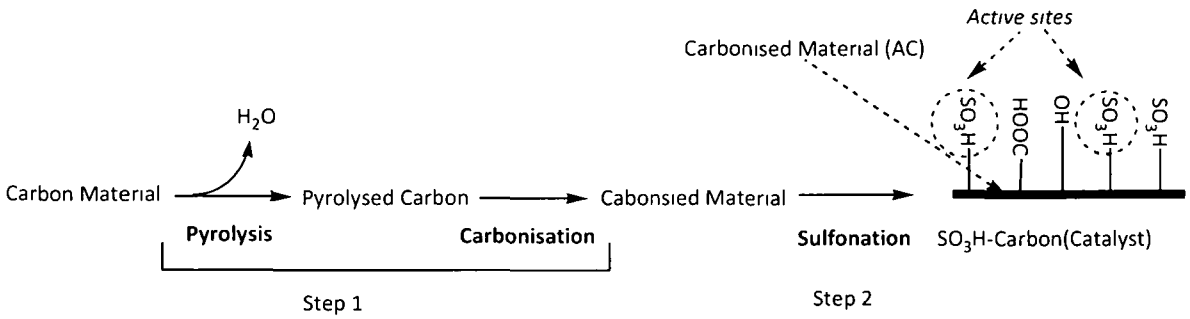

Scheme 5.1. General method for Preparation of SO_3H-carbon catalysts, Konwar *et al.* [16].

However, this simple process usually produces sulfonated carbons with low specific surface area, low acid density and poor reusability. Such carbon catalysts are also difficult to disperse in liquid-phase reaction mixtures [18]. Recently, it has been established that sulfonation is more efficient with 4-benzenediazoniumsulfonate instead of H_2SO_4 due to high degree of sulfonation and use of mild reaction conditions which preserves the structural integrity of the carbon surface upon sulfonation as well as improved reusability due to the high stability of the C-SO_3H bonds [22, 23].

The goal of the present investigation was to transform de-oil waste cake residues (DOWC) (from non-edible oil seeds of *Mesua ferrea* L.), a by-product from biodiesel production, into carbon-based solid acid for applications in biodiesel production from acidic oils (AO). The porous carbonaceous material was prepared by chemical activation of DOWC and it was subsequently sulfonated via covalent functionalization/grafting with 4-benzenediazoniumsulfonate to obtain the solid acid catalyst (Scheme 5.2). In order to investigate the influence of the sulfonation conditions on catalyst activity, two different experimental conditions were adopted upon catalyst preparation: Method 1 introduces H_3PO_2 assisted synthesis [22] whereas method 2 depicts the spontaneous approach [23]. The catalytic activities of the resulting materials were studied in esterification/transesterification of various AOs containing 8.17-43.73 wt% FFAs with methanol. The influence of FFA concentration, MeOH-to-AO molar ratio, reaction temperature and catalyst loading were studied in order to determine the optimal reaction parameters.

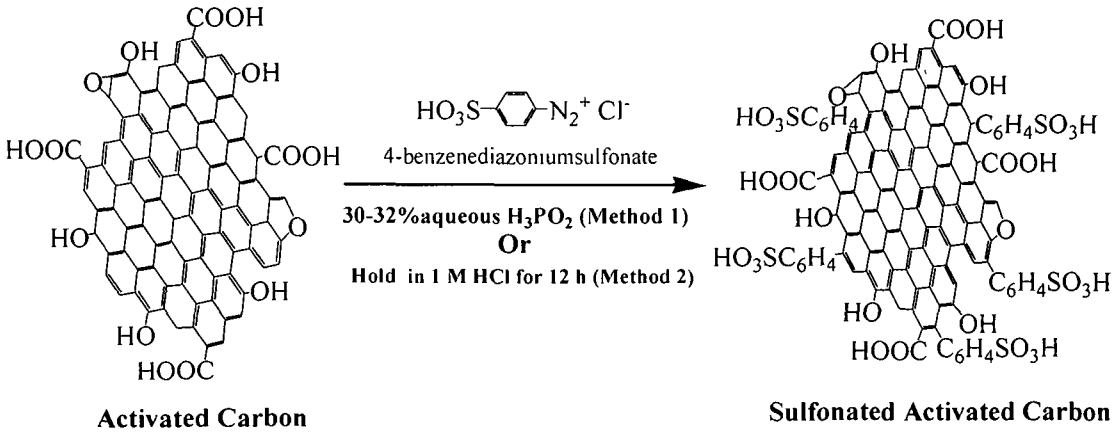

Activated Carbon **Sulfonated Activated Carbon**

Scheme 5.2. Sulfonation of activated carbon with 4-benzenediazoniumsulfonate.

Over the next years, the use of non-edible oils from sources such as *Jatropha Curcas* and *Pongamia Pinnata* are expected to increase in order to meet the feedstock requirements for growing biodiesel demand. Biodiesel production using such oils is likely to generate large quantities of solid wastes in the form of de-oiled waste cakes (DOWCs), the main by-product after oil recovery by pressing and solvent extraction. Albeit a good source of protein, they cannot be considered as a food source due to the presence of anti-nutritional components. As an example, DOWC from *Jatropha Carcus* seeds contain phorbol ester, a highly toxic compound in high concentrations. Similarly, *Pongamia Pinnata* oil and its DOWC are reported to contain a toxic compound, karanjin in high concentrations [21]. For these reasons and environmental concerns, disposal of such bio-waste (DOWC) using conventional methods such as direct burning, conversion into manure or cattle feed becomes problematic. Therefore, more cost-effective and eco-friendly methods are required for their safe disposal without adversely effecting biodiesel production. Since, DOWCs can be basically considered as lignocellulosic biomass, they could similarly be converted into higher value-added products such as activated carbon, biochar, charcoal as well as biogas or bioethanol for use in the non-food sector [22,23]. Utilization of lignocellulosic agricultural residues for preparing activated carbons has already been identified as a cost effective method for waste disposal [24]; extending this concept to the by-products from biodiesel production is of great interest due to low cost of execution and from the possible application of these activated carbons during biodiesel production itself (for waste water treatment, oil treatment or as catalyst through modifications such as sulfonation or metal modification). Additionally, the demand for activated carbons ensures generation of additional revenue from potential wastes. Currently, there are no reports in open literature on the utilization of DOWC generated from biodiesel production for preparing active carbon based catalysts. Utilization of activated carbon support generated from by-products of biodiesel production (Scheme 5.3) as catalysts would not only help to reduce the cost of biodiesel production, but also to increase the environmental viability through complete utilization of starting biomass.

Mesua ferrea L. is a commonly found and slowly growing hardwood tree in the wet tropical parts of India and Asian subcontinent. *Mesua ferrea* L. oil has significant potential as a feedstock for biodiesel production owing to its oleic acid rich seeds with high oil

content (~75 %). Currently, the oil has no use due to its bitter taste and toxicity. With proper and careful planning, *Mesua ferrea* L. could emerge as a major non-edible oil crop similar to *Jatropha curcas*, *Pongamia pinnata* and, consequently, play a major role in meeting the feedstock demand for sustainable biodiesel production, especially in counties like India and other countries in Asian subcontinent [24]. The use of such non-edible vegetable oil as feedstock is expected to increase to meet the growing demands of biodiesel. The above mentioned environmental issues will result in production of large quantities of solid waste in the form of oil-cake waste (DOWC) which creates disposal problems because conventionally used disposal methods such as conversion of waste into cattle feed or manure are not suitable owing to the toxic nature of DOWC, resulting from the presence of anti-nutritional components. Moreover, direct burning is not efficient and appropriate flue-gas cleaning facilities will be needed to minimize pollution. Therefore, cost effective and eco friendly methods are required for disposal of this waste which does not adversely affect the economy of biodiesel production. The use of DOWC as starting material for catalyst production can partly address issues concerning waste disposal and it can simultaneously help to generate revenue from a potential waste. These products can have applications in several fields such as soil nutrition, water purification and catalysis in general.

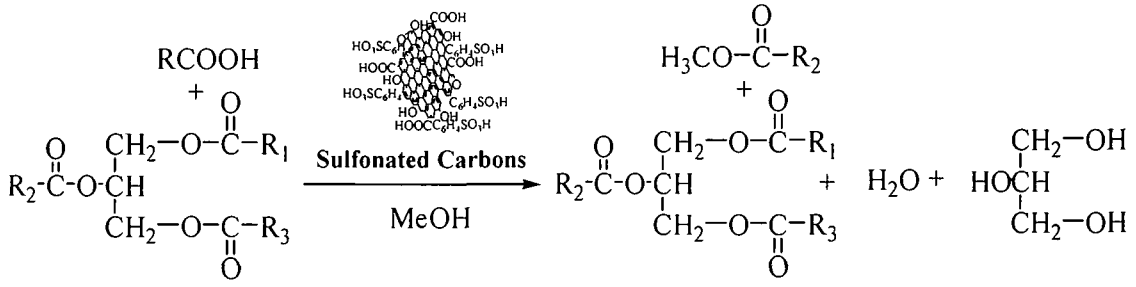

Acid oils (Triglycerides + FFAs) **FAME + Triglycerides** **Glycerin (Trace)**

where, R, R_1, R_2 and R_3 represent different fatty acid chains

Scheme 5.3. Pretreatment (esterification/transesterification) of acid oils using sulfonated carbons as catalysts.

5.2. Materials and methods

5.2.1. Materials

The acid oils (AOs) used in this study were extracted from non-edible seeds of *Mesua ferrea* L. and *Jatropha curcas* via Soxhlet extraction. The oil seeds were purchased from Kaliabor Nursery, Nagaon (Assam), India. The extracted oils were kept at 150-170 °C in an oven for 24 h in order to increase their FFA levels. The fatty acid composition of oils were determined by Gas chromatography and presented in Table 5.1. The FFA content in crude *Jatropha curcas* and *Mesua ferrea* L. oil were found to be 8.17 wt% and 14.4 wt% respectively. The acid oil containing 43.73 wt% of free fatty acid (FFA) was prepared by means of hydrolyzing a portion of *Mesua ferrea* L. oil. Deoiled cake wastes from *Mesua ferrea* L. seeds were collected, ground and passed through Standard ASTM sieve (Mesh No. 60, 0.25 mm) and used as a precursor for the preparation of porous carbon (Fig. 5.1). Ortho-phosphoric acid (88%), sulfanilic acid (99%), $NaNO_2$ (98%), anhydrous Na_2SO_4 (99.5%), H_2SO_4 (98%), HCl (35%), acetonitrile (99.5%) and acetone (99.5%) were purchased from Merck India Ltd., Mumbai and used as received. The H_3PO_2 (30-32%) aqueous solution was purchased from Sisco Research Laboratories Pvt. Ltd. India.

Table 5.1

Fatty acid composition of vegetable oils used in the study

Fatty acid (wt %)	*Jatropha curcas*	*Mesua ferrea* Linn.
Palmitic (C16:0)	7.7	11.29
Palmitoleic (C16:1)	-	0.25
Stearic (C18:0)	2.2	9.18
Oleic (C18:1)	53.51	44.66
Linoleic (C18:2)	36.99	16.82
Linolenic (C18:3)	0.5	-
Arachidic (C20:0)	-	1.21
Gadoleic (C20:1)	-	-
Behenic (C22:0)	-	0.62
Erucic (C22:1)	-	11.16
Others	-	4.78

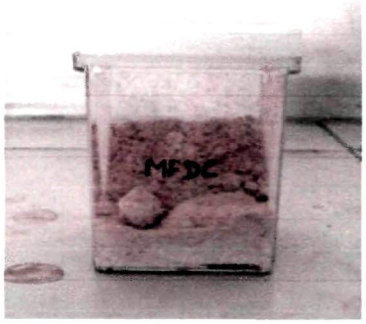

⇨ Lignocellulosic waste, also contains protein

Figure 5.1. The *Mesua ferrea* L. de-oiled cake waste used as precursors for preparation of sulfonated carbon catalysts

(70 mL) *Mesua ferrea* L. oil was refluxed with 9 g NaOH for 3 h. The oil phase was treated with 50% (v/v) sulfuric acid at 60 °C for 2 h. The brown crude oil was further treated with active clay to adsorb the residues, and settled in separating funnel and washed to pH 4–5. The upper layer was collected and dried over anhydrous Na_2SO_4. The concentration of FFAs in the obtained oil was 43.73% on weight basis.

5.2.2. Catalyst preparation

In the present study, chemical activation with phosphoric acid was applied in catalyst preparation since it was reported to facilitate high porosity development, at low temperatures (450-500 °C) under the self-generated atmospheres [25]. In a typical process, 20 g of finely powdered DOCW was soaked in 50% ortho-phosphoric acid in 2:1 (w/w) impregnation ratio for 24 h. The resulting material was then transferred to a silica crucible and calcined in a muffle furnace at 500 °C for 1 h in the self-generated atmosphere. The black solid produced was consequently washed with 180-200 mL double distilled water, HCl (0.01 mol L^{-1}) and finally with 1000-1500 mL hot double distilled water until pH of 6-7, followed by drying in an oven at 110 °C to obtain the Mesua–derived activated carbon (MAC). The yield was 30%, on weight basis. As the next step, the carbonized materials were powdered using a mortar and pestle. Sulfonation was achieved by covalent attachment of 4-benzenediazoniumsulfonate radicals, under two different methods shown in Scheme 5.2 [22,23].

5.2.2.1. Sulfonation method 1

4-benzenediazoniumsulfonate was synthesized by diazotization of sulfanilic acid. In a typical reaction sulfanilic acid (5.2 g, 0.03 mol) was dispersed in 1 M HCl aqueous solution (300 mL) in a threenecked ground flask. The flask was moved to an ice water bath, and the temperature was controlled at 3–5 ° C with continuous stirring. Thereafter, 10% excess of $NaNO_2$ (33 mL, aqueous solution) was added dropwise, a clear solution was obtained after all the $NaNO_2$ was added. After stirring for another 1 h at the same temperature, the white precipitate of 4-benzenediazoniumsulfonate formed was filtered off, washed with deionized water and moved to a three-necked ground flask with deionized water (200 mL) and ethanol (120 mL). Then, AC (MAC, 3 g) was added maintaining the temperature at 3–5 °C. Subsequently, 30-32 % H_3PO_2 aqueous solution (100 mL) was added. After stirring for 30 min, another 50 mL of H_3PO_2 aqueous solution was added and allowed to stand for another 1 h with occasional stirring. The obtained sulfonated AC (MAC-SO_3H) was intensively washed first with acetone and distilled water and then dried in the vacuum overnight [22].

5.2.2.2. Sulfonation method 2

4-benzenediazoniumsulfonate was synthesized by diazotization of sulfanilic acid as described in section 5.2.2.1. The sulfonation was achieved by mixing MAC (3 g) and an aqueous solution containing 0.03 mol 4-benzenediazoniumsulfonate (prepared as described above) in 1 M HCl and holding the suspension at 5 °C for 12 h. After filtration and thorough washing with acetone and distilled water the sulfonated carbon (MAC-SO_3H*) was obtained [23]. All the sulfonated carbons were dried in oven at 110 °C, finely powdered using a mortar and pestle and sieved through an ASTM no 60 sieve to make particles size below 250 μm prior to use.

5.2.3. Catalyst characterization

The carbonaceous materials were characterized by means of elemental analysis, SEM, TEM, FT-IR, Raman spectroscopy, XRD and TGA. The surface area and micropore volume of the carbon catalysts were determined by means of N_2-physisorption (Carlo-Erba instruments, sorptometer 1900) at -196 °C, the details of the characterization techniques

are found in Chapter 2. The acid densities of the carbons were determined by titration method as described in Chapter 2. The -SO_3H densities of sulfonated carbons were based on elemental analysis assuming that all sulphur present in the carbon samples was due to -SO_3H groups.

5.2.4. Catalytic tests

Catalytic tests were performed in batch mode in two different reactors as shown Fig. 5.2, a 3-neck round bottomed flask, equipped with magnetic stirring and a reflux condenser for temperatures up to 65 °C (Fig. 5.2(a)). While, reactions at higher temperature (80–100 °C) were performed in a custom made 200 ml stainless steel autoclave equipped with digital temperature indicator and magnetic stirring (Fig. 5.2(b)). In a typical reaction, 0.2–0.65 g (particle size <250 μm, outgassed at 105±5 °C for 24 h) of catalyst was added to methanol (0.0678–0.4941 mol), stirred and heated to desired reaction temperature which was followed by addition of acid oil (10 g).At selected time intervals, 0.1 ml aliquots were withdrawn from the reaction mixture and centrifuged at 6000 rpm for 2 min and its acid value determined by titration using standard KOH (0.01 mol L^{-1}). The FFA C_{Est} (%) conversion was determined from acid values using equation (v.i).

$$C_{Est}(\%) = \frac{(C_i - C_t)}{C_i} \qquad (v.i)$$

where, C_i is the initial acid value and C_t is the acid value measured at time t. Acid value was measure using the equation below:

$$Acid\ value\ (\text{mg KOH g}^{-1}) = \frac{(56.1 \times N \times V)}{W} \qquad (v.ii)$$

where, N is the strength of KOH solution, V is volume of KOH consumed and W is the weight of sample taken.

Transesterification activity and FFA conversion were also measured by ^{1}H NMR spectroscopy using equation (i) (Chapter 3). The conversion of acid to esters was also confirmed by decreased intensity of unmerged peak of the FFA triplet in the spectra of products (2.38 ppm) and appearance of the characteristic methyl ester peak [26]. Overall oil conversion (as methyl ester content) were determined by comparing methoxy protons of the methyl ester (~3.6 ppm) and α-methylene protons (~2.3 ppm) as discussed in

Chapter 2 [27]. Therefore, by subtracting the esterification yield (in terms of methyl ester) from total ester yield obtained from ^{1}H NMR, the transesterification yield was calculated.

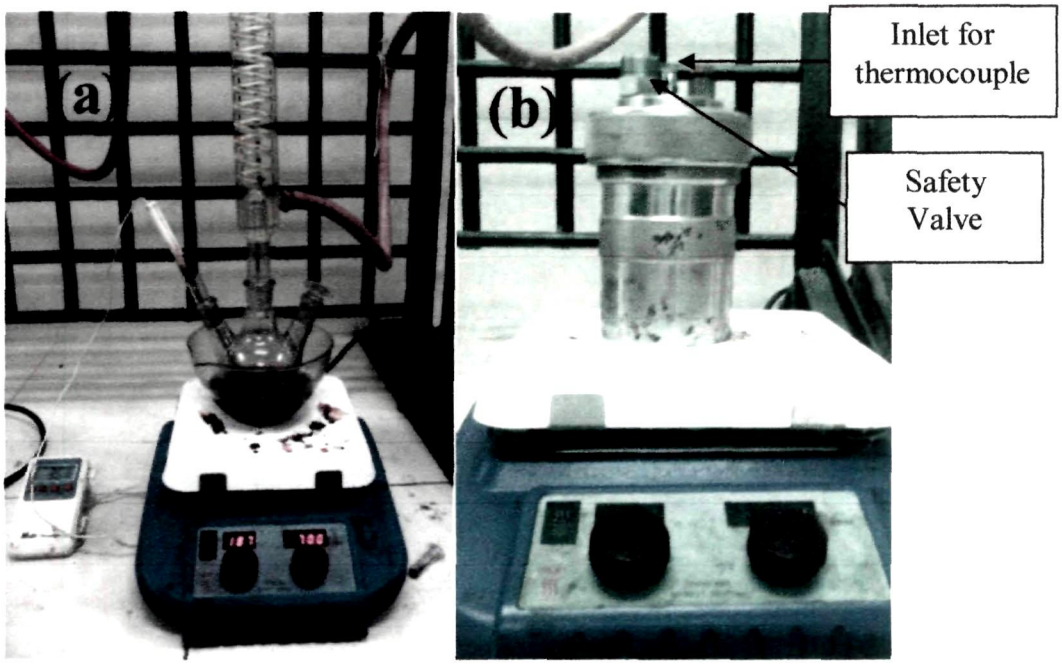

Figure 5.2. The (a) glass reactor and (b) custom made 200 mL autoclave used in catalytic tests.

5.3. Results and Discussion

5.3.1. Catalyst Characterizations

5.3.1.1. *Elemental analysis and textural properties*

The elemental analysis and textural properties of the porous carbon materials before and after sulfonation are shown in Table 5.2 and 5.3, respectively. The presence of $-SO_3H$ groups on the surface of the sulfonated carbons could be observed from their higher O/S atom ratios (>3:1) (Table 5.2). From the results depicted in Table 5.3, it could be seen that sulfonation also resulted in an increase in acid site density and reduction of specific surface area due to attachment of $-PhSO_3H$ groups on the carbon surface. The specific surface area and acid site density of the sulfonated carbons were found to be affected by the sulfonation method applied. With the sulfonated MAC-SO_3H catalyst, the acid density increased by 16% from 2.032 mmol H^+ g^{-1} to 2.426 mmol H^+ g^{-1} while for MAC-SO_3H* increase was by 8% only (Table 5.3). Thus sulfonation in presence of H_3PO_2 (method 1) was more efficient which resulted in higher $-SO_3H$ density and catalytic

activity. Nevertheless, upon comparison to the sulfonated carbons prepared by concentrated H_2SO_4 treatment, the pore structure and surface morphology of the catalysts remained unaltered despite sulfonation and only slight reduction in the specific surface area was observed. Thus, relatively high catalytic activity was observed even with comparatively low -SO_3H densities compared to H_2SO_4 treated catalysts [11-13][17-19][21].

Table 5.2

Elemental analysis of carbon materials

Sample	C	H	N	O[a]	S	O/S
Mesua ferrea L. DOWC	48.63	7.38	3.65	40.34	-	-
MAC	70.28	2.82	3.19	23.54	-	-
MAC-SO_3H*	66.01	1.23	3.14	28.37	1.23	23.06
MAC-SO_3H	54. 65	3.73	4.49	34.76	2.35	14.79
MAC-SO_3H (spent)	55.15	2.98	4.23	35.48	2.15	16.50

[a] by difference (ash free basis)
MAC = *Mesua ferrea* L. DOWC based activated carbon
MAC-SO_3H = *Mesua ferrea* L. DOWC based activated carbon sulfonated by method 1
MAC-SO_3H* = *Mesua ferrea* L. DOWC based activated carbon sulfonated by method 2
(spent) catalyst recovered after fifth cycle of *Jatropha curcas* oil esterification

Table 5.3.

Properties of sulfonated carbons and their catalytic activities

Catalysts	Total acid density [a] / (mmol g^{-1})	-SO_3H density [b] (mmol g^{-1})	Specific Surface area (m^2 g^{-1})	Micro Pore volume (cm^3g^{-1})	L_a [c] (nm)	Esterification activity	
						C_{Est} (%)	k (h^{-1})
MAC	2.032	-	777	0.28	5.47	11	-
MAC-SO_3H*	2.215	0.384	696	0.24	5.41	97	0.60
MAC-SO_3H	2.426	0.735	556	0.20	4.89	99	0.65
MAC-SO_3H (spent)	2.416	0.672	-	-	-	90	-
Starch-SO_3H [18]	4.130	1.500	n.r	n.r	n.r	≤95	n.r
Oil pitch-SO_3H [14]	2.040	2.210	8	n.r	n.r	95	n.r
Corncob-SO_3H [21]	n.r	0.160	80	n.r	n.r	n.r	n.r

[a] based on titration,
[b] based on elemental analysis,
[c] average size of polycyclic aromatic carbon sheets (graphitic clusters)
n.r = not reported,
(spent) = catalyst recovered after fifth cycle of Jatropha oil esterification
Reaction conditions: 80 °C, 6 h, 43:1 (methanol to oil molar ratio), esterification of crude Jatropha oil (containing 8.17 wt% FFA)

Sulfonated carbons dispersed well in water, methanol and other polar solvents. Dispersibility was found to be dependent on the total density of hydrophilic surface functional groups (-COOH, -OH and $-SO_3H$). The better dispersibility of sulfonated carbons in comparison to the unsulfonated ones was due to presence of $-SO_3H$ groups in addition to -COOH, -OH groups (polar groups). The high catalytic activity of sulfonated carbons has been previously related to -COOH, -OH groups on their surface acting as anchoring sites for attaching polar substrates such as MeOH, H_2O and FFAs [15, 16].

High dispersibility clearly suggested carbons exhibiting higher amounts of acid sites as well as high surface functional group density and hence, better activity in esterification. In the present study the presence of hydrophilic functional groups to be helpful in catalyst recovery as catalyst particles preferentially remained in the polar, upper MeOH layer allowing its easy separation after reaction (Fig. 5.3).

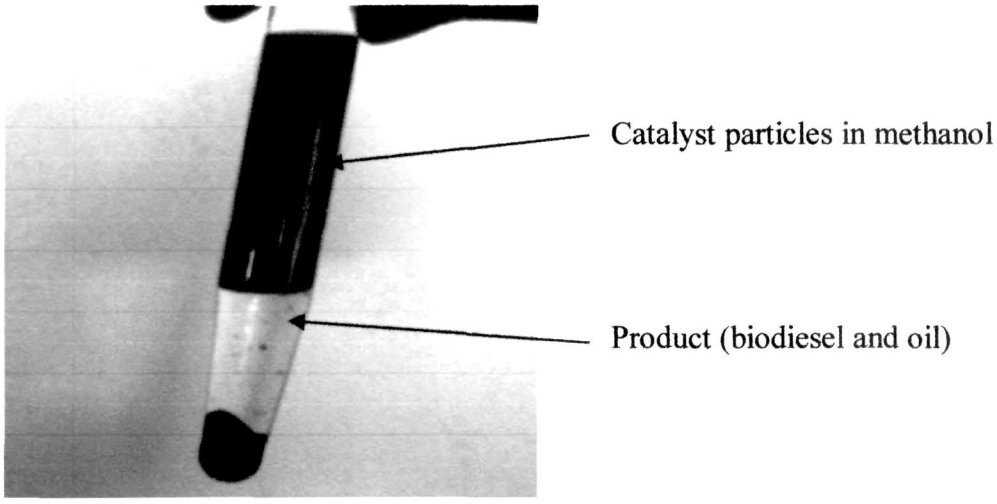

Figure 5.3. Spontaneous separation of hydrophilic catalyst particles from non-polar product mixture (biodiesel ab bnd oil).

5.3.1.2. *SEM and TEM analysis*

The high porosity and irregular particle shapes of the carbon materials are clearly visible in SEM images (Fig. 5.4). The SEM pictures also show that the morphology of the carbon material remains mostly unaffected by sulfonation with 4-benzenediazoniumsulfonate. The presence of randomly arranged aromatic/graphitic carbon

sheets with irregular pore structures is clearly visible in TEM micrographs of MAC-SO_3H samples. The size of the catalyst particles in Fig. 5.5 is about 348 nm.

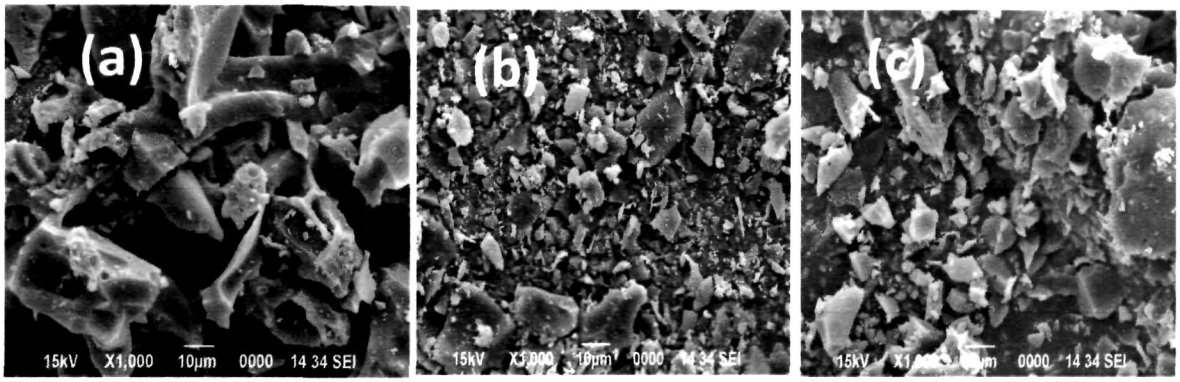

Figure 5.4. SEM images of the carbonaceous materials (a) MAC, (b) MAC-SO_3H* and (c) MAC-SO_3H.

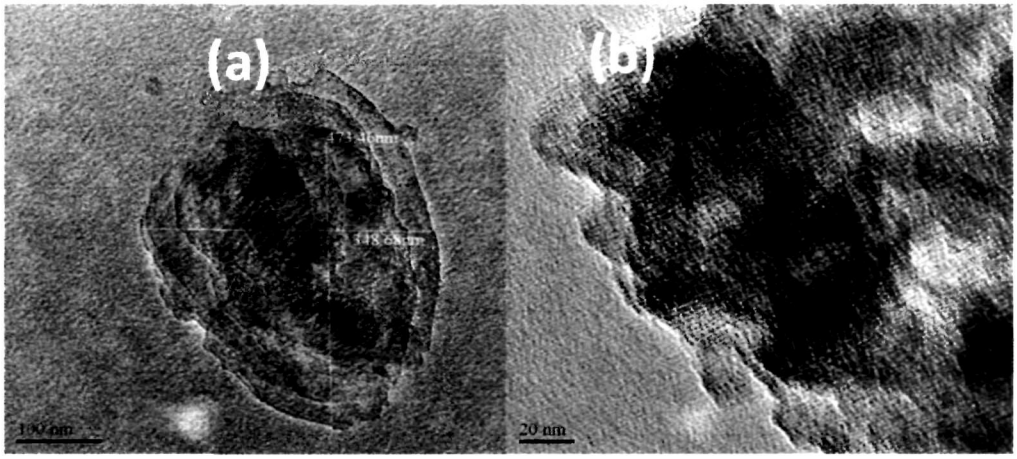

Figure 5.5. TEM images of the carbon catalyst MAC-SO_3H under different magnifications (a) 100 nm and (b) 20 nm.

5.3.1.3. *FT-IR analysis*

FT-IR spectra of the carbon catalysts are illustrated in Figure 5.6. All the materials exhibited the typical bands of carbonyl groups (C=O, near 1700 cm^{-1}) and characteristic peaks of incompletely carbonised materials, near 1580 cm^{-1} attributable to aromatic ring modes. The bands appearing at 1185 cm^{-1} (P=O stretching) and 1075 cm^{-1} (P-OC stretching) in the non-sulfonated carbons were due to incorporation of H_3PO_4 in MAC as a result phosphoric acid activation [28]. The appearance of additional bands at 1097 cm^{-1} and 1008 cm^{-1} (S=O stretching) and 1176 cm^{-1}, 1171 cm^{-1} and 1275 cm^{-1} (stretching in -SO_3H along with P=O stretching) in the FT-IR spectra of the sulfonated carbons were

consistent with the presence of -SO_3H groups [23]. The higher S=O and -SO_3H peak intensities of MAC-SO_3H compared to MAC-SO_3H* were also consistent with its higher -SO_3H density in the former. These characteristic bands for S=O and -SO_3H were also clearly visible in the FT-IR spectra of the spent catalyst supporting the high reusability and stability of covalent C-$PhSO_3H$ bonds.

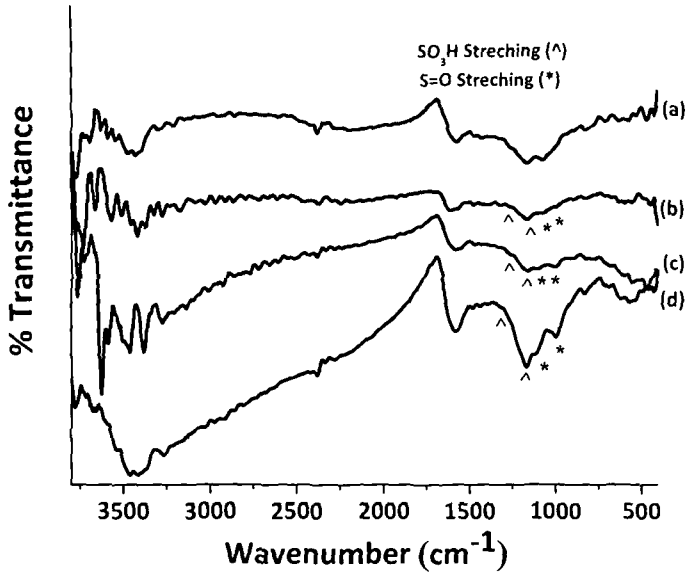

Figure 5.6. FT-IR spectra of porous carbons, (a) MAC, (b) Spent MAC-SO_3H, (c) MAC-SO_3H and (d) MAC-SO_3H*.

5.3.1.4. *Raman analysis*

The Raman spectra of all carbon samples displayed two characteristic bands at around 1339 cm^{-1} and 1600 cm^{-1}, respectively, corresponding to the defects induced in the D band and the first-order scattering of the E_{2g} mode for sp^2 carbon lattice (G band). Usually, the I(D)/I(G) intensity ratio of amorphous carbon could be used as a tool to evaluate the structural changes during such chemical processing. In our study, the I(D)/I(G) intensity ratio of sulfonated carbons (MAC-SO_3H and MAC-SO_3H*) was found to be slightly higher than that of the parent carbon (MAC), due to the introduction of abundant -$PhSO_3H$ groups to the sp^2 carbon network (Fig. 5.7). The G band of the active carbon shifted from 1600 cm^{-1} to 1582 cm^{-1} caused by sulfonation due to increased disorder in carbon framework. The average graphitic cluster size (L_a) in MAC, MAC-

SO_3H and MAC-SO_3H* were calculated from I(D)/I(G) intensity ratios as 5.47, 5.41 and 4.89 nm suggesting that sulfonation resulted in a reduction in the graphitic cluster size [29].

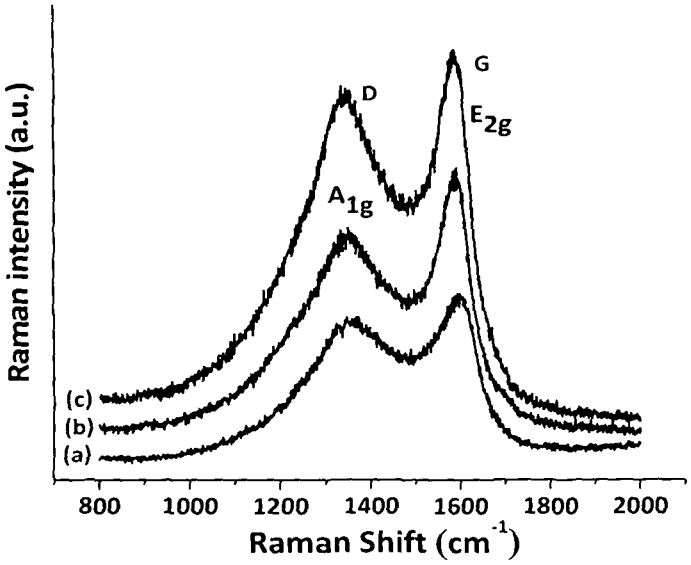

Figure 5.7. Raman spectra of porous carbons, (a) MAC, (b) MAC-SO_3H* and (c) MAC-SO_3H.

5.3.1.5. X-ray *Powder diffraction analysis*

The X-ray diffraction (XRD) patterns, illustrate the amorphous nature of the carbonaceous materials (Fig. 5.8). All the carbon samples (sulfonated and unsulfonated) exhibited similar, broad and weak C(002) and C(101) diffraction peaks around 2θ=15-30° and 40-50° respectively. These regions correspond to an amorphous carbon structure with randomly oriented aromatic carbon sheets [13][18,19]. Upon sulfonation, the peak intensities further decreased and were found to be the lowest for MAC-SO_3H. The decreased peak intensities were due to attachment of abundant -$PhSO_3H$ groups to the sp^2 carbon network leading to an increased disorder among graphitic carbon sheets. The graphitic carbon content in the carbon samples were estimated in terms of d spacing of C(002) peak using the equation suggested by (Maire & Mering, 1970) [30]. The calculations suggest that d spacing in the sulfonated carbons (0.354 and 0.358 nm) were slightly higher than that for the unsulfonated carbons (0.349 nm) indicating an increase in

amorphous character after sulfonation. This change is due to increased disorder in carbon sheets resulting from attachment of -$PhSO_3H$ functional groups and is in agreement to the findings of Raman analysis [30,31].

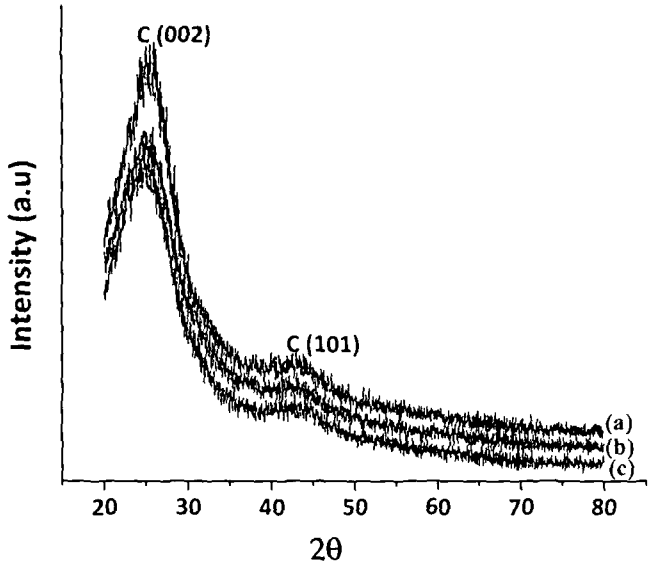

Figure 5.8. X-ray powder diffraction patterns of carbon materials, (a) MAC, (b) MAC-SO_3H* and (c) MAC-SO_3H.

5.3.1.6. *Thermogravimetric analysis*

The thermal stability of the prepared catalysts were investigated by selecting the sulfonated (MAC-SO_3H) as the reference in thermogravimetric analysis (TGA) under N_2 flow. Its behaviour was compared to that of pure Mesua activated carbon (MAC). As shown in Fig. 5.7, the catalyst demonstrated excellent thermal stability up to 242 °C under inert atmosphere. The initial ~10 % weight loss in the region of 0-100 °C was due to loss of water. From 242-380 °C there was a marginal weight loss, followed by a steady and gradual loss of weight until 600 °C. The ~9% weight loss in the temperature region of 242-380 °C could be attributed to the loss of -$PhSO_3H$ groups, as this region was absent in MAC. The catalyst is thermally stable at temperatures close to 240 °C under oxygen-free conditions (Fig. 5.9).

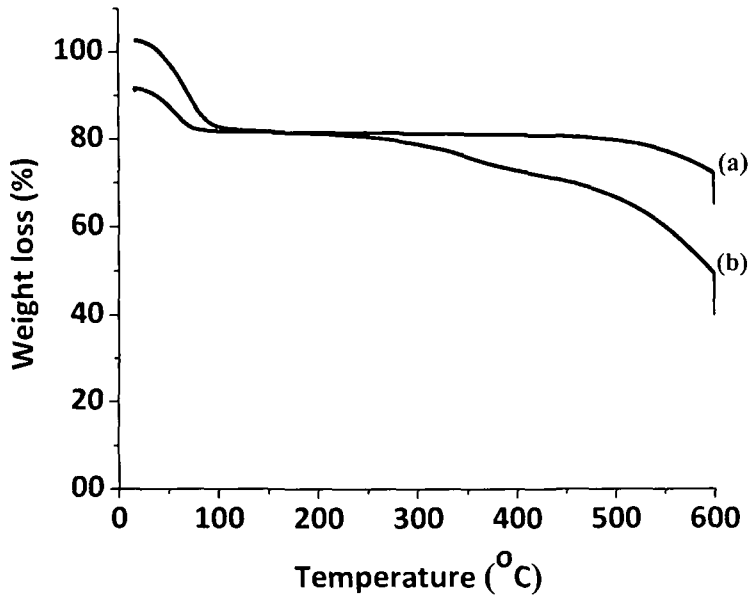

Figure 5.9. TGA patterns of (a) MAC and (b) MAC-SO_3H catalysts.

5.3.2. Catalytic activity

5.3.2.1. *Esterification of free fatty acids*

5.3.2.1.1. *Effect of catalyst loading*

With the sulfonated carbon catalysts MAC-SO_3H and MAC-SO_3H*, the conversion of FFA in acid oils was 99 % and 97 %, respectively at 80 °C within 8 h. The unsulfonated carbon catalyst (MAC) gave rise to only 11 % FFA conversion in 8 h (Fig. 5.10). Both sulfonated carbons showed high catalytic activity even exceeding that of an equivalent amount of H_2SO_4 in the esterification of crude *Jatropha curcas* oil (8.17 wt% FFA). This high activity of the sulfonated carbons could be due to the presence of hydrophilic surface functional groups (-COOH, -OH and -SO_3H) present in the carbon materials acting as anchoring sites for attachment of polar substrates like MeOH and FFAs [16,18,32]. Moreover, the higher activity of MAC-SO_3H compared to MAC-SO_3H* is due to its higher density of strong acid sites (-SO_3H). Furthermore, due to poor mass transfer of solid acid catalysts, a high catalyst loading is needed to gain a high FFAs conversion [33]. Therefore, in the present study, the esterification experiments were performed at 80 °C with methanol to oil molar ratio of 43:1 by varying catalyst amount in the range 2-6.5 wt % (w/w of AO) using crude *Jatropha curcas* oil (8.17 wt% FFA) as AO feedstock. The use of 5 wt%

catalyst resulted in the highest activity for both catalysts and increasing catalyst loading beyond 5 wt% had no significant effect on FFA conversion (Fig. 5.10). Furthermore, similar observations were reported earlier by Guo *et al.* in the esterification of FFAs [33]. Similar conversions were also obtained upon esterification of hydrolysed *Mesua ferrea* L. oil containing 43.7 wt% FFA under the same reaction conditions using 5 wt% MAC-SO_3H.

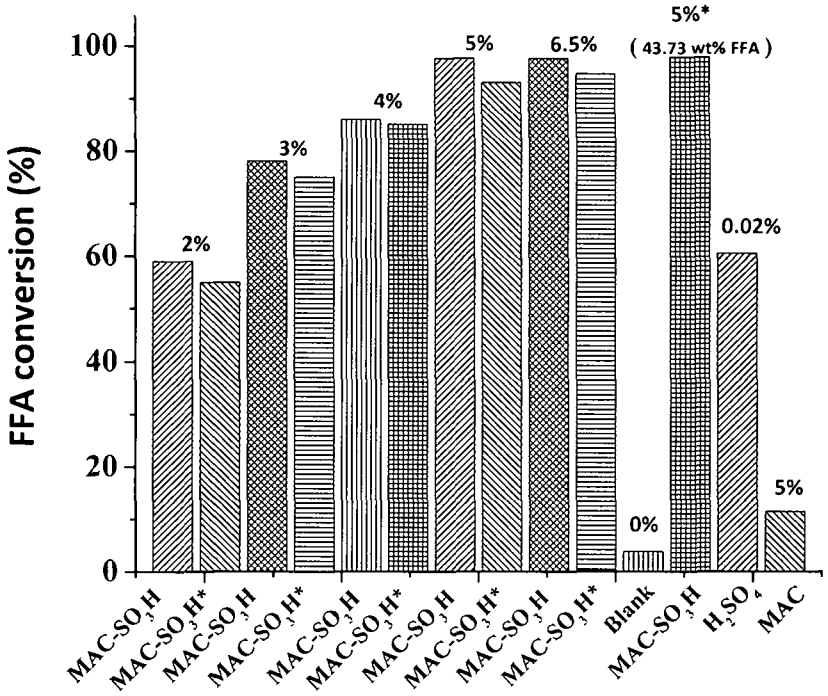

Figure 5.10. Effect of catalyst amount on free fatty acid (FFA) conversion. Conditions: The reaction temperature was 80 °C and the reaction time was 8 hours. Methanol to acid oil molar ratio of 43:1 was applied.

5.3.2.1.2. *Effect of reaction temperature*

The influence of temperature was studied in the esterification of crude *Jatropha curcas* oil (8.2 wt% FFA) applying methanol-to-oil molar ratio of 43:1 and using 5 wt% catalyst by varying the reaction temperature from 50 °C to 100 °C. Increased temperature resulted in increased esterification rates, as expected (Fig. 5.11). However, it was concluded that 80 °C was suitable reaction temperature since no significant differences in FFA conversion for reactions conducted at 80 °C or 100 °C were observed.

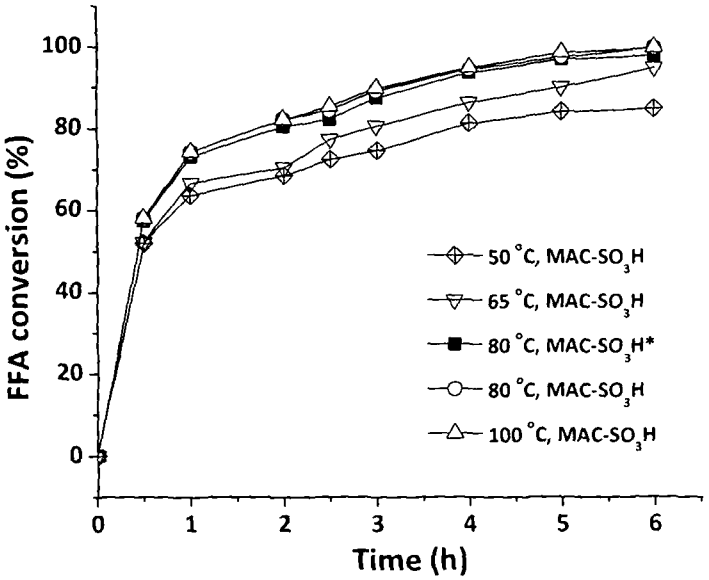

Figure 5.11. Free fatty acid (FFA) conversion as a function of time. Effect of reaction temperature on free fatty acid (acid oil containing 8.2 wt% of FFA) conversion. Conditions: The catalyst loading was 5 wt% and methanol to acid oil molar ratio was 43:1.

5.3.2.1.3. *Effect of methanol-to-oil molar ratio*

In acid catalysed pre-treatment of acidic oils, very large quantities of MeOH (a molar ratio of 70:1-260:1, depending on the FFA content) are required to drive the reaction forward and thus reduce the amount of FFAs to desirable levels of less than 2 wt%. [34,35]. Since the solid acid-catalyzed esterification of fatty acids with methanol exhibits similar kinetic behaviour to the homogeneous acid catalyzed reaction [36-38], the molar ratio of methanol to acid oil is expected to be one of the most important variables affecting the FFA conversion. Because esterification is an equilibrium reaction, an excess of methanol is required to force the reaction towards the formation of FAME. The influence of methanol-to-oil molar ratio on FFA conversion upon esterification/pre-treatment of both crude *Jatropha curcas* oil (8.2 wt% FFA) and hydrolysed *Mesua ferrea* L. oil (43.7 wt% FFA) at 80 °C using 5 wt% MAC-SO_3H as a catalyst was studied (Fig. 5.12). It was shown that only about 44% conversion was obtained when using methanol-to-oil molar ratio of

6:1 in the pretreatment of Mesua oil. However, the use of higher methanol to oil molar ratios (≥10.75:1) resulted in enhanced esterification rates and FFA conversions up to 95% were obtained. The maximum conversion of Mesua oil esterification was obtained with methanol to oil molar ratio of 21.5:1. Analogously for Jatropha oil esterification, FFA conversion also increased when methanol-to-oil ratio was increased from 21.5:1 to 43:1. The maximum conversion of 99% for Jathropa oil was obtained at rather high methanol-to-oil molar ratio (43:1). Additionally, since esterification rate for Mesua oil was much higher than that for Jatropha oil, there was strong effect of initial FFA level on catalytic activity (Fig. 5.10).

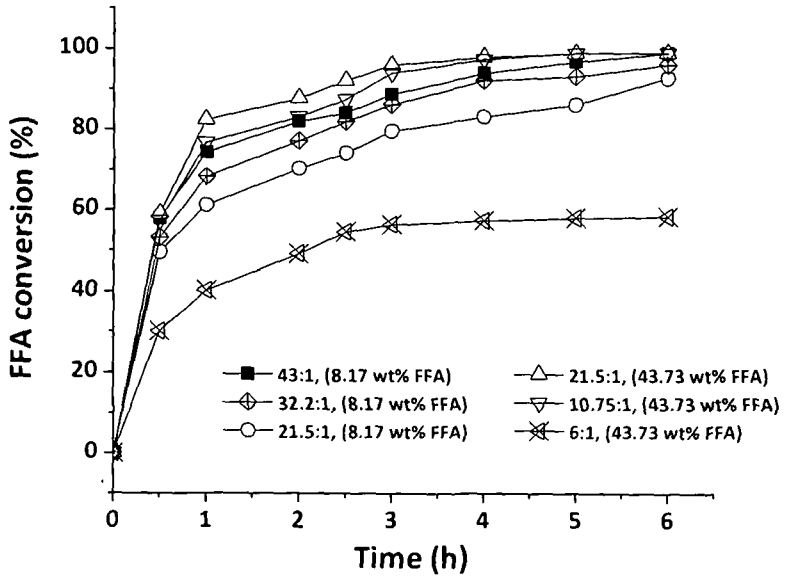

Figure 5.12. Free fatty acid (FFA) conversion as a function of time. The effect of methanol-to-acid oil molar ratio on FFA conversion. Conditions: The reaction temperature was 80 °C and the catalyst (MAC-SO_3H) loading was 5 wt%.

5.3.2.1.4. *Effect of initial FFA concentration*

In order to properly investigate the relationship between the initial FFA concentration and the methanol to oil molar ratio for esterification, a screening similar to that carried out by Diaz-Felixa *et al.* was conducted [37]. Three different acid oils containing ~ 8.2 wt%, 14.4 wt% and 43.7 wt% of FFA respectively were studied. Moreover, the molar ratios of methanol and oil applied were 10.75:1, 21:1 and 43:1, respectively. The reaction temperature was kept constant (80 °C) and 5 wt% of MAC-SO_3H catalyst loading was applied. It was illustrated that high methanol to oil molar ratios and a high initial FFA levels in AOs led to higher FFA conversions. The most appropriate explanation for this behavior is the better solubility of methanol in AOs having high FFA content and the immiscibility of methanol to oil having a low FFA content. Molar ratio of 43:1 was required for complete esterification of acid oil containing 8.17 wt% FFA and to reduce FFA content below 2 wt%. On the other hand, a molar ratio of 10.75:1 was sufficient to complete the esterification of oil containing 43.73 wt% FFAs, resulting from the improved miscibility of methanol and oil. This behavior was a consequence of the ampiphilic character of FFA, making it soluble in both methanol and triglyceride phases and therefore its affinity for methanol or triglyceride was mainly dependent on their concentration in reaction mixture. A lower initial FFA concentration in AO resulted in most of the FFA to remain in the triglyceride phase. Methanol to oil molar ratio for AO pretreatment should be based on the initial FFA level in AO. These results agreed well with the studies of Diaz-Felixa *et al.* on H_2SO_4 catalyzed pretreatment of yellow grease (Fig. 5.13) [37].

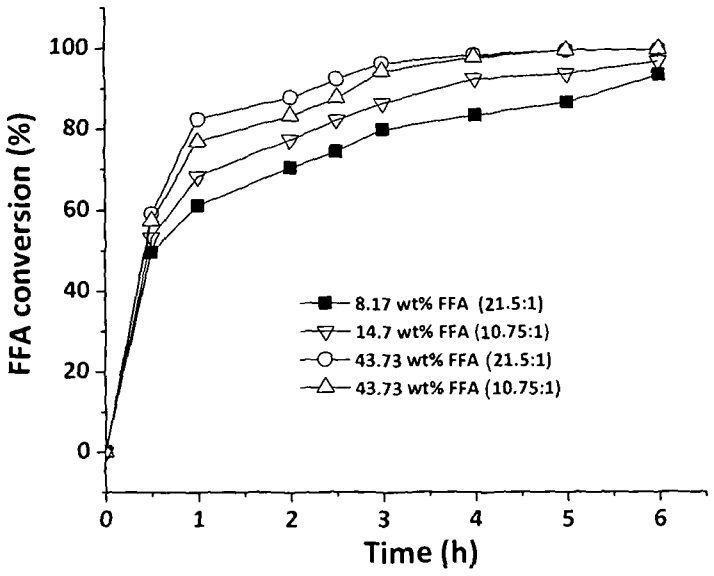

Figure 5.13. Free fatty acid (FFA) conversion as a function of time. With different initial amounts of FFA. Conditions: The reaction temperature was 80 °C and the catalyst (MAC-SO_3H) loading was 5 wt%.

5.3.2.2. *Transesterification of crude acid oil*

The transesterification activities of sulfonated carbons were measured by subtracting the esterification yields (in terms of methyl ester) from the total methyl ester content in final product mixture determined by ^1H NMR (Fig. 5.14). The results from transesterification experiments were summarized in Fig. 5.15. Transesterification of *Jatropha curcas* oil (8.7 wt% FFA) with sulfonated carbon catalysts exhibited low transestefication activity with methyl ester molar yields of only 1.8 % and 1.7 %, respectively. However, with hydrolysed Mesua oil containing 43.7 wt% FFA, the total methyl ester yield was 71 %, out of which approximately 28% was due to transesterification.

The increased transesterification activity was as a consequence of increased mutual solubility of methanol and AO due to higher initial FFA levels in the oil. According to literature the transesterification activity could be greatly improved by carrying out reactions at elevated temperatures in pressurized systems [38].

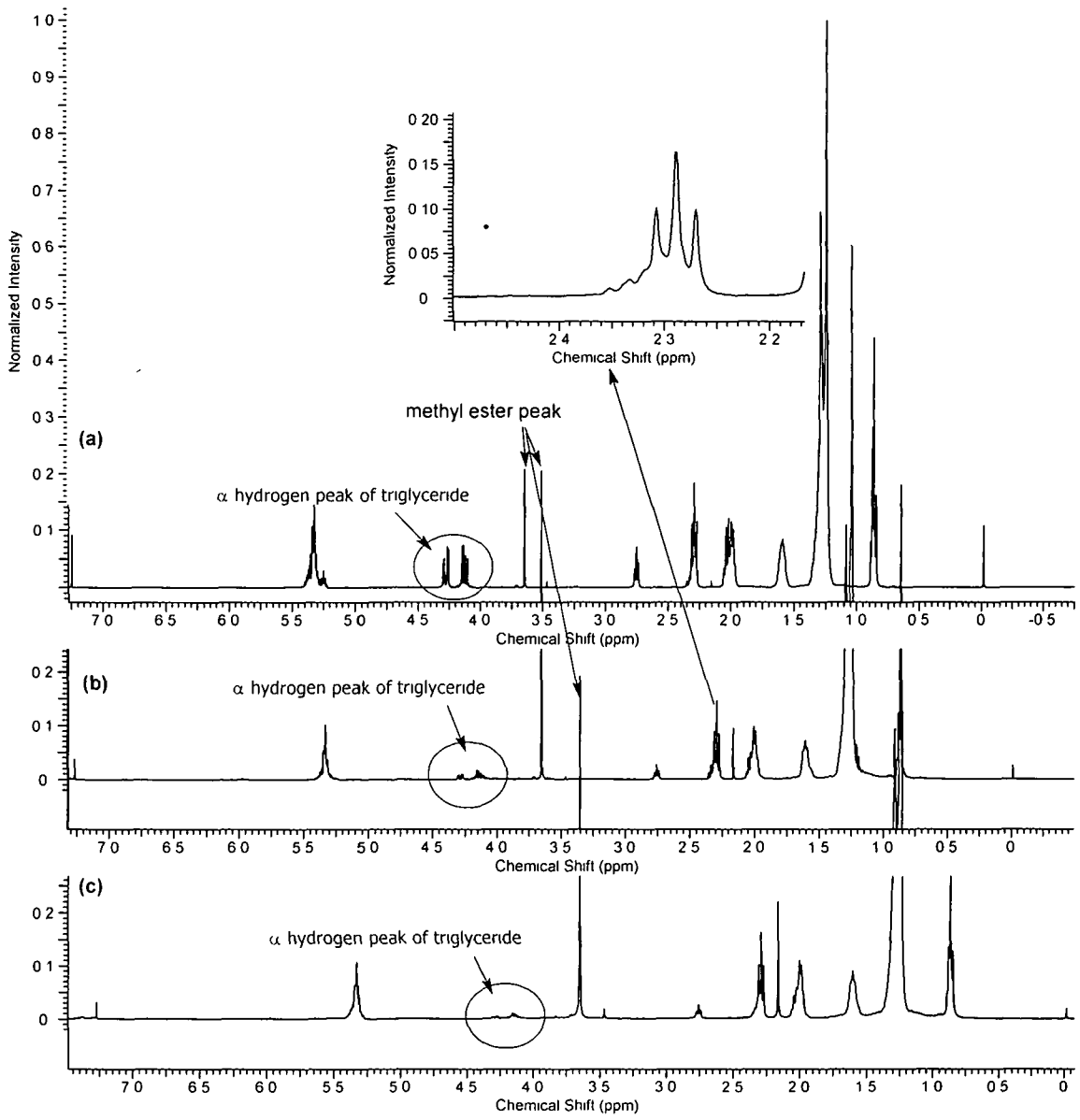

Figure 5.14. ^{1}H NMR (a) showing increased total (esterification + transesterification) yield when using AO with 43.7wt% FFA (b) Effect of reuses on transesterification (reduced yield) at fifth cycle using AO with 43.7wt% FFA (c) Showing low transesterification yield when using AO with 8.17wt% FFA, (insert shows decreased intensity of unmerged FFA triplet at 2.38 ppm); Reaction conditions: 5% MAC-SO_3H catalyst, methanol-to-oil molar ratio 43:1, T = 80 °C, t = 8 h.

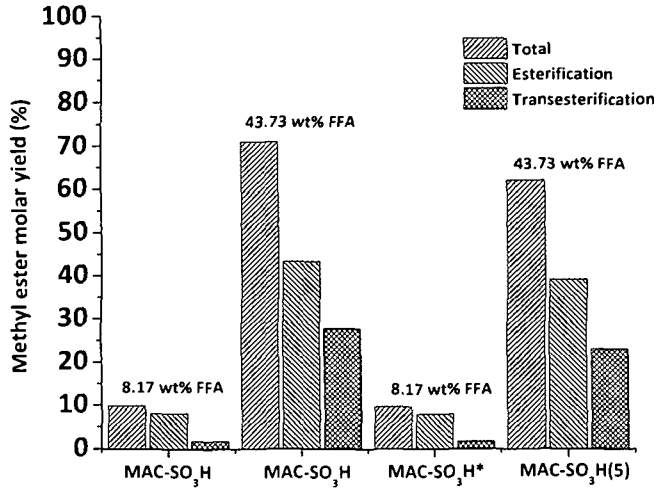

Figure 5.15. Comparison of esterification and transesterification activities. Conditions: The reaction temperature was 80 °C, the reaction time was 8 h, the catalyst loading was 5 wt% and methanol to acid oil molar ratio was 43:1.

5.3.2.3. *Catalyst reusability*

The reusability and stability of the sulfonated carbon catalysts were investigated with MAC-SO_3H catalyst (Fig. 5.16). The catalyst was applied in the pretreatment of crude *Jatropha curcas* and hydrolyzed *Mesua ferrea* L. oil at 80 °C. Overall about 9% activity loss was observed at the 5th cycle. Nevertheless, the sulfonated carbons reported here demonstrated better performance than that observed in the case of sulfonated carbons prepared by sulfuric acid treatment (direct sulfonation method). Many reports claim the loss of 30-40% activity after the second cycle [13, 21]. These findings were also consistent with the sulfur content of the spent catalyst (2.15 wt%), which showed that it retained 92 % of –SO_3H groups after five successive cycles. Moreover, characteristic peaks of –SO_3H groups could also be observed with FT-IR analysis. No peaks corresponding to polyaromatic species (~7.5-7.7 ppm) were found in the ^{1}H NMR of the reaction mixtures at any stage which further supported high stability of the prepared carbons [39]. Nevertheless, even at the fifth cycle the catalyst was capable of reducing the FFA concentration of crude Jatropha oil to 0.82 wt% - lower than the limit of 2 wt% required for base catalyzed transesterification [4].

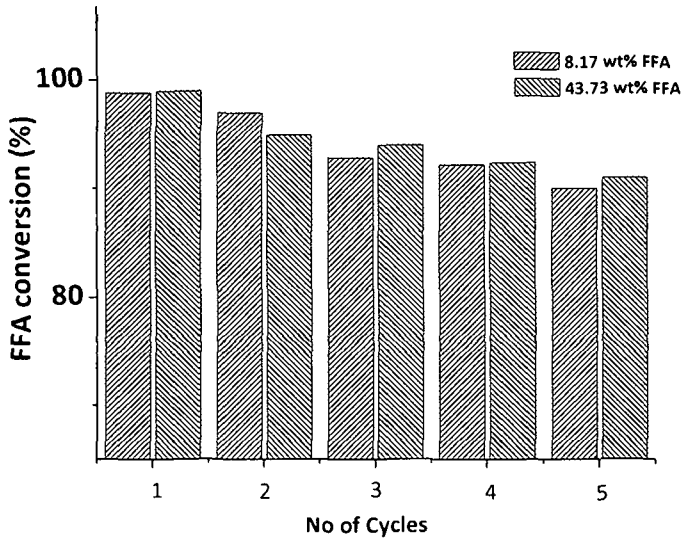

Figure 5.16. Deactivation of the MAC-SO_3H catalyst (FFA conversion was illustrated for five consecutive cycles). Conditions: The reaction temperature was 80 °C, the reaction time was 8 h, the catalyst loading was 5 wt% and methanol to acid oil molar ratio was 43:1.

The loss of transesterification activity was relatively high (~17.5% shown for AO with 43.7 wt% FFA) probably due to partial blocking of the catalyst pores by reactants restricting the entry of large triglyceride molecules into the active sites. The loss of transesterification activity could be clearly seen from the increased intensity of α-hydrogen peaks of triglyceride and reduced intensity of methyl ester peaks in ^{1}H NMR spectrum of product from the fifth cycle (Fig. 5.14).

5.3.2.4. *Kinetic studies*

The FFA conversions followed pseudo 1st order kinetics. In the presence of excess methanol the results showed good fitting to 1st order reaction kinetics and a linear relation was observed in the time vs. ln(1-FFA) plots (Fig. 5.17). Using the 1st order kinetic plots the rate constants (k) for the reactions were determined from the slopes (Table 5.3) [30,35].

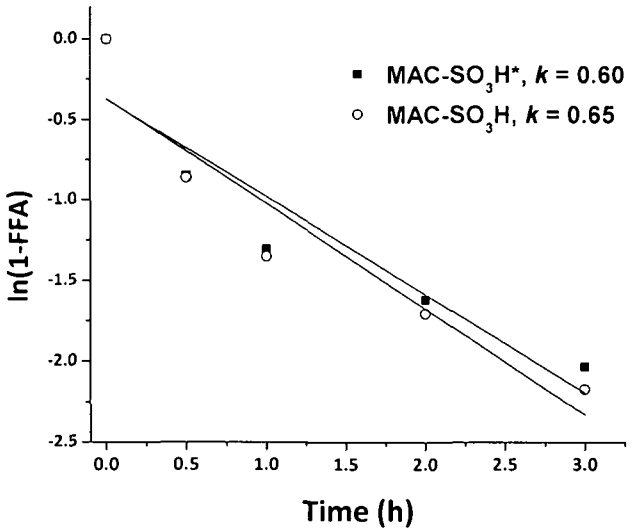

Figure 5.17. 1st order fittings of FFA esterification over the sulfonated carbons; Conditions: 5 wt% catalyst, molar ratio of methanol to AO 43:1, T = 80 °C.

5.3.2.5. *Proposed mechanism*

Mechanistically the reaction could be assumed to closely resemble the H_2SO_4 case in the presence of excess methanol with the Brønsted acidic (-SO_3H groups) acting as active sites and as proton donor in the reaction. Therefore, the esterification /transesterification could be assumed to comprise of the following steps Scheme 5.4: Step (1): Formation of an Catalyst-Substrate intermediate (I); Step (2): Formation of a tetrahedral intermediate (II) by the nucleophilic attack of methanol on the positive carbon centre; Step (3): The rearrangement of the proton of methanol hydroxyl to the carbonyl oxygen of FFA or triglyceride in tetrahedral intermediate (II); Step (4): Dehydration of the tetrahedral intermediate (III) forming one mole of methyl esters (biodiesel), one mole of H_2O or glycerin and regeneration of active sites. The sequence is further repeated with diglycerides and monoglycerides to producing two moles FAME, one mole monoglyceride and one mole glycerin in the process.

Step 1 (initiation):

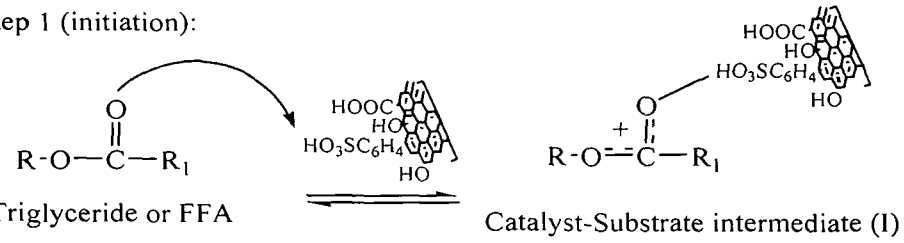

Triglyceride or FFA

Catalyst-Substrate intermediate (I)

Step 2 (Nucelophilic attack by methanol/alcohol to (I)):

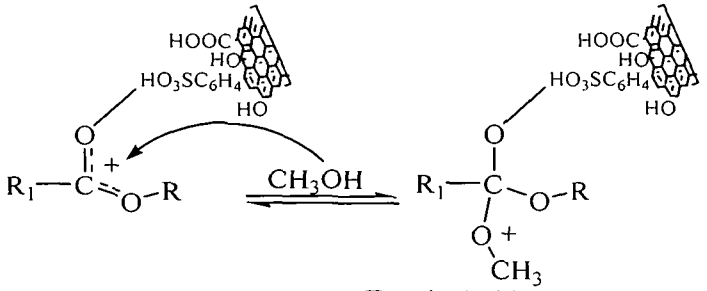

Tetrahedral intermediate (II)

Step 3 (Rearrangement of proton):

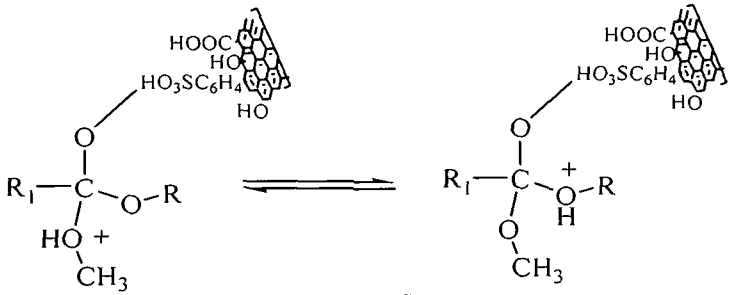

Rearranged tetrahedral intermediate (III)

where, R= H

or

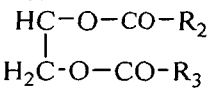

and R_2 and R_3 represent different fatty acid chains

Step 4 (Dehydration of Tetrahedral intermediate (III)):

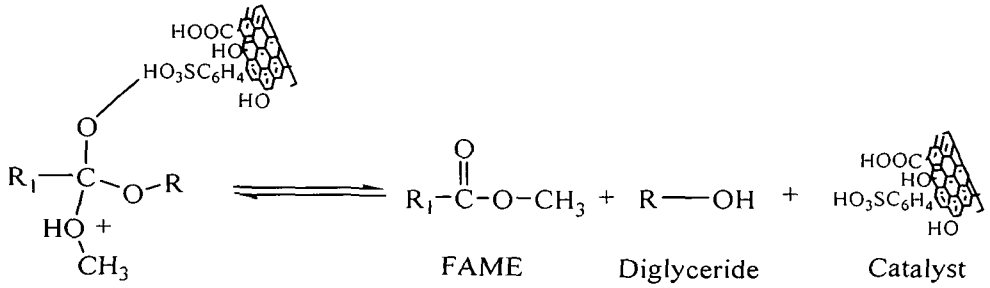

FAME Diglyceride Catalyst

Scheme 5.4. Proposed reaction mechanism for simultaneous esterification and transesterification of FFA and fatty glycerides over sulfonated carbons.

5.4. Conclusions

A highly active and robust carbon based Brønsted solid acid catalyst was developed from de-oiled cake waste. It was employed for the efficient pretreatment of AOs containing 8.2-43.7 wt% FFA. The prepared catalyst exhibited high acid density, porosity, specific surface area, thermal stability and good reusability. Sulfonation method played an important role in determining strong acid site (-SO_3H) density and hence catalytic performance. In our study, MAC-SO_3H sulfonated via method 1, H_3PO_2 aided sulfonation was found to be more efficient (99% FFA conversion) compared to MAC-SO_3H* catalyst prepared by spontaneous sulfonation method. Transesterification activity was low for both catalysts when the initial FFA level was low. Higher initial FFA level resulted in an increased transesterification activity resulting from the increased mutual solubility of methanol and AO, with FAME yields reaching 71% for oil containing 43 wt% FFA. In addition, the reported catalyst could also be used repeatedly without severe decrease in its catalytic activity resulting from strong covalent attachment between -$PhSO_3H$ groups and the carbon material. Since sulfonated carbons exhibited high acid exchange capacity, excellent thermal stability (240 °C) and reusability. They may be considered as a promising waste-derived substitute to H_2SO_4 for the pretreatment and possibly it can be used for one step biodiesel synthesis from acidic oils under suitable reaction conditions.

5.5. References

1. Zheng, S. et al. Acid-catalyzed production of biodiesel from waste frying oil. *Biomass Bioenergy,* **30**(3), 267–272, 2006.
2. Lotero, E. *et al.* Synthesis of biodiesel via acid catalysis. *Ind. Eng. Chem. Res.*, **44**(14), 5353–5363, 2005.
3. Zhang, Y. et al. Biodiesel production from waste cooking oil: 1. Process design and technological assessment. *Bioresour Technol.*, **89**,1–16, 2003.
4. Dorado, M.P. et al. An alkali-catalyzed transesterification process for high free fatty acid waste oils. *Transactions of ASAE,* **45**(3), 525–529, 2002.
5. Lam, M.K. et al. Homogeneous heterogeneous and enzymatic catalysis for transesterification of high free fatty acid oil (waste cooking oil) to biodiesel: A review. *Biotechnol. Adv.* **28**, 500–518, 2010.

6. Brito, A. et al. Zeolite Y as a heterogeneous catalyst in biodiesel fuel production from used vegetable oil. *Energy Fuels*. **21**, 3280–3283, 2007.
7. Alsalme, A. et al. Heteropoly acids as catalysts for liquid-phase esterification and transesterification. *Appl. Catal., A*, **349**, 170–176, 2008.
8. Rahman Talukder, M.M. et al. Comparison of Novozym 435 and Amberlyst 15 as heterogeneous catalyst for production of biodiesel from palm fatty acid distillate. *Energy Fuels*. **23**(1), 1-4, 2009.
9. Zhang, X. et al. Heteropolyacid nanoreactor with double acid sites as a highly efficient and reusable catalyst for the transesterification of waste cooking oil. *Energy Fuels*, **23**, 4640–4646, 2009.
10. Park, Y.M. et al. Esterification of used vegetable oils using the heterogeneous WO_3/ZrO_2 catalyst for production of biodiesel. *Bioresour Technol.*, **101**, 59–61, 2010.
11. Toda, M., et al. Green chemistry – biodiesel made with sugar catalyst. *Nature*, **438,** 178, 2005 4. M. Hara, *et al. Angew. Chem , Int. Ed.*, **43**, 2955, 2004.
12. Hara, M. Biodiesel production by amorphous carbon bearing SO_3H, COOH and phenolic oh groups, a solid brønsted acid catalyst. *Top Catal.*, **53**, 805–810, 2010.
13. Yu, J.T. et al. Development of biochar-based catalyst for transesterification of canola oil. *Energy Fuels.*, **25**, 337–344, 2010.
14. Shu, Q. et al. Synthesis of biodiesel from waste vegetable oil with large amounts of free fatty acids using a carbon-based solid acid catalyst. *Appl Energy.*, **87**(8), 2589–2596, 2010.
15. Okamura, M. *et al.* Acid-catalyzed reactions on flexible polycyclic aromatic carbon in amorphous carbon. *Chem. Mater.*, **18,** 3039-3045, 2006.
16. Konwar, L. J. *et al.* Review on latest developments in biodiesel production using Carbon-based catalysts, Renew Sust Energ Rev, **29,** 546–564, 2014.
17. Peng, L. *et al.* Preparation of sulfonated ordered mesoporous carbon and its use for the esterification of fatty acids. *Catal. Today.*, **150**, 140-146, 2010.
18. Zong, M.H. *et al.* Preparation of a sugar catalyst and its use for highly efficient production of biodiesel. *Green Chem,* 7, 434–437, 2007.

19. Budarin, V. *et al.* Starbons: New starch-derived mesoporous carbonaceous materials with tunable properties. *Angew. Chem. Int. Ed.*, **45**, 3782-3786, 2006.

20. Devi, B.L.A.P. *et al.* A Glycerol-based carbon catalyst for the preparation of biodiesel. *ChemSusChem.*, **2**(7), 617–620, 2009.

21. Arancon, R.A. *et al.* Valorisation of corncob residues to functionalised porous carbonaceous materials for the simultaneous esterification/transesterification of waste oils. *Green Chem.*, 13, 3162-3167, 2011.

22. Liu, R. *et al.* Sulfonated ordered mesoporous carbon for catalytic preparation of biodiesel. *Carbon*, **46**, 1664 –1669, 2008.

23. Geng, L. *et al.* Efficient carbon-based solid acid catalysts for the esterification of oleic acid. *Catal. Commun.*, **13**, 26–30, 2011.

24. De, B.K. & Bhattacharyya, D.K. Biodiesel from minor vegetable oils like karanja oil and nahor oil. *Fett Lipid*, **101**(10), 404–406, 1999.

25. Vernersson, T. *et al.* Arundo donax cane as a precursor for activated carbons preparation by phosphoric acid activation. *Bioresour Technol,* **83**, 95–104, 2002.

26. Satyarthi, J.K. *et al.* Estimation of Free Fatty Acid Content in Oils, Fats, and Biodiesel by 1H NMR Spectroscopy. *Energy Fuels*; **23,** 2273–2277, 2009.

27. Gelbard, G. *et al.* ^{1}H nuclear magnetic resonance determination of the yield of the transesterification of rapeseed oil with methanol, *J. Am. Oil. Chem. Soc.*, **72**(10), 1239-1241, 1995.

28. Puziy, A.M. *et al.* Synthetic carbons activated with phosphoric acid - I. Surface chemistry and ion binding properties, *Carbon,* **40**(9), 1493–1505, 2002.

29. Ferrari, A.C. & Robertson, J. Interpretation of Raman spectra of disordered and amorphous carbon. *Phys. Rev. B: Condens. Matter*, **61**(20), 14095- 14107, 2000.

30. J. Maire, & J. Mering, *Chemistry and Physics of Carbon,* Walker, P.L., eds, Marcel Dekker, 1970, 125-189.

31. Zhao, J. *et al.* Structural evolution in the graphitization process of activated carbon by high-pressure sintering. *Carbon,* **47,** 744 –751, 2009.

32. Nakajima, K. & Hara M. Environmentally benign production of chemicals and energy using a carbon-based strong solid acid. *J Am Ceram Soc*, **90,** 3725–34, 2007.

33. Guo, F. *et al.* Synthesis of biodiesel from acidified soybean soapstock using a lignin-derived carbonaceous catalyst. *Appl Energy*, **98,** 47–52, 2012.

34. Ghade, S. & Raheman H. Biodiesel production from mahua (Madhuca indica) oil having high free fatty acids. *Biomass Bioenerg.*, **28,** 601–605, 2005.

35. Canakci, M. & Gerpen V. Biodiesel production from oils and fats with high free, fatty acids. *Transactions of ASAE*, **44**(6), 1429–36, 2001.

36. Yin, X. *et al.* Comparison of four different enhancing methods for preparing biodiesel through transesterification of sunflowers oil. *Appl Energy,* **91**, 320–325, 2012.

37. Diaz-Felixa, W. *et al.* Pretreatment of yellow grease for efficient production of fatty acid methyl esters. *Biomass Bioenerg.*, **33**, 558-563, 2009.

38. Shu, Q. *et al.* Reaction kinetics of biodiesel synthesis from waste oil using a carbon-based solid acid catalyst. *Chin. J Chem Eng.* **19**(1), 163–168, 2011.

39. Moa, X. *et al.* Activation and deactivation characteristics of sulfonated carbon catalysts. *J Catal.*, **254**, 332–338, 2008.

Sulfonated carbon catalysts based on de-oiled cake waste II: The effect of carbon source on structure and activity

Chapter 6

Chapter 6

In this chapter, the effects of carbon source and preparation method on the structure, acidity and catalytic activity of deoiled waste cake (DOWC) based sulfonated carbons have been studied. The chapter also presents comprehensive characterization of the DOWC based catalytic materials by means of XPS and NH_3-TPD in addition to the standard characterization methods discussed in Chapter 2. Further, the chapter discusses the effect of catalyst structure on activity and selectivity through simultaneous assessments in oleic acid esterification and cellulose saccharification, two opposite but equally imperative reaction involved in biofuel synthesis.

6.1. Introduction

Biofuels such as biodiesel and bioalcohols are considered the most promising renewable alternative to the presently used fossil based liquid fuels [1]. Vegetable oils and fats are the most common feedstocks used for biodiesel production while bioalcohols (bioethanol/biobutanol) are produced from starchy biomass sources as well as from lignocellulosic biomass using 2^{nd} generation technology; their production involves two opposite reactions, namely esterification and hydrolysis catalyzed by same acid (H_2SO_4). Next to feedstock, catalysts play the most important role in such chemical transformations by affecting the overall process chemistry, product costs and economics. The current generation technology for biofuel production relies on the use of homogenous acid such as H_2SO_4 as a catalyst during many crucial steps which is a major concern for their commercialization [2]. In recent years, utilization of renewable source or bio-based catalysts for chemical transformations has gained a great deal of attention due to environmental as well as economic concerns [3,4,5]. Among the various renewable source based catalysts, the sulfonated carbons in recent years have emerged out as promising heterogeneous substitute to H_2SO_4. They are a diverse, promising class of novel solid acid catalysts active in a range of acid catalyzed reactions including many important reactions associated with the production of biofuels such as: FFAs esterification (biodiesel production) [4,5], cellulose hydrolysis (bioethanol/bioalcohol production) [5] and glycerol etherification (diesel additive) [6]. They are considered as model catalysts owing to

features such as high mechanical and thermal stability, chemical inertness, high activity and low material cost. A number of preparation methods and applications of sulfonated carbons have been reported in the literature. Such catalysts are generally produced via sulfonation of incompletely pyrolysed carbonaceous sources such as: sucrose [7], glucose [4,8], starch [9], glycerol [10], biochar [11], wood [12], oil pitch [13], canola meal [14] and corncob [15], to name a few. Further, similar sulfonated carbons can also be prepared from more expensive carbon precursors such as phenolic resins [16], carbon foams [17] graphene [18] and OMCs [19,20]. Considering that biomass is renewable, abundant and low-cost; sulfonated carbons produced directly from biomass and bio-wastes attract more advantages. To summarize, in most studies the carbon precursors were directly pyrolyzed and sulfonated with a strong sulfonating agents such as concentrated H_2SO_4 or fuming H_2SO_4 (except Ref. 17,19,20 mentioned above) in a two-step approach. However, sulfonated carbons produced by this simple process were reported to exhibit low specific surface area (as the carbons were un-activated), acid density and poor reusability; all features non-favorable when considering catalytic applications. Furthermore, since the sulfonation step was carried out employing large amounts of concentrated acids at a high temperature (150-250 °C), the approach cannot reasonably be called an eco-friendly process. Additionally, the efficiency of sulfonation was reported to decrease when more ordered or rigid carbons were used: e.g. graphite, activated carbons or carbons prepared by high temperature treatment (500-900 °C) [4-5,8-9,14-15]. Therefore, it is very difficult to prepare sulfonated carbons that simultaneously possess a high specific surface area and $-SO_3H$ density when applying the conventional sulfonation approach (with H_2SO_4). Recently, it has been shown that sulfonation could be more efficient when using 4-benzenediazoniumsulfonate radicals instead of H_2SO_4 due to a rapid sulfonation, use of mild conditions and preservation of structural, morphological features upon sulfonation. This approach has been found particularly helpful for preparing/designing sulfonated carbons with features such as high specific surface area, acid exchange capacity and large pores. Additionally, sulfonated carbons prepared by this method were found to be more suitable for long term use due to their superior reusability [19-20]. Nevertheless, although numerous reports are found on the production of biofuels using sulfonated carbons from wastes, so far no report on the utilization of by-products from biodiesel production could

be found in open literature for making sulfonated carbons; additionally all the reported carbons were prepared by means of an H_2SO_4 treatment.

The work discussed in this chapter builds on the chapter 5 which has confirmed the versatility of sulfonated carbons prepared from DOWC of *Mesua ferrea* L. for pretreatment of acid oils to esterify the fatty acids upon biodiesel production. The work was undertaken with the aim of investigating the structure, effects of carbon source and preparation method on the physicochemical and catalytic features of DOWC sulfonated carbons employing DOWC residues obtained from different non-edible oil seeds: *Jatropha curcas*, *Pongamia pinnata* and *Mesua ferrea* L. respectively, all associated with biodiesel production.

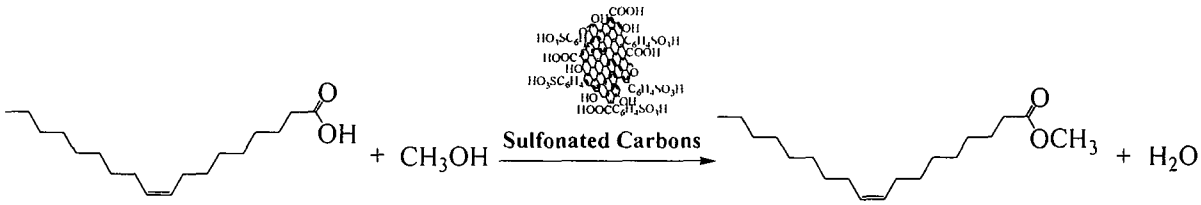

Scheme 6.1. Esterification of oleic acid with methanol.

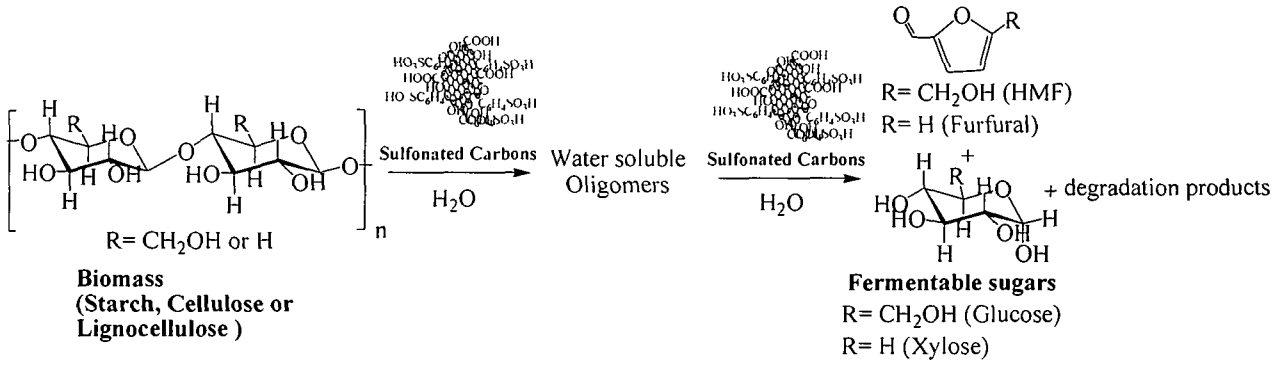

Scheme 6.2. Hydrolysis of cellulose/biomass into fermentable sugars.

The utilization of carbon support generated from by-products of biodiesel production as catalysts can not only help to reduce the production cost of biodiesel, but also increases the environmental viability through complete utilization of starting biomass [22-24]. The use of potentially unwanted and toxic DOCW derived from non-edible oil

(*Mesua ferrea* L.) seeds to produce sulfonated carbon catalysts was successfully demonstrated in our earlier work [25]. However, the above oil seed is significant to the Asian subcontinent only. Therefore, in this work, an attempt was made to produce similar carbon catalysts using DOCW obtained from two additional sources, namely *Jatropha curcas* and *Pongamia pinnata*, the most potent oil seed feedstock for biodiesel production. Thus, the effects of carbon source and preparation/sulfonation method on the structure, acidity and activity of DOWC based sulfonated carbons were investigated by changing the preparatory conditions and the catalytic activities were simultaneously studied in two opposite but equally important reactions involved in biofuel synthesis, namely oleic acid (most common fatty acid in vegetable oils) esterification (Scheme 6.1) as well as cellulose hydrolysis (Scheme 6.2).

6.2. Materials and methods

6.2.1. Materials

Jatropha curcas, *Pongamia pinnata* and *Mesua ferrea* L. seeds were purchased from Kaliabor Nursery, Nagaon (Assam), India. The seeds were allowed to dry in sunlight and then in an oven at 110 °C to remove all traces moisture prior to removal of the kernels and oil extraction. Oil was extracted by Soxhlet extraction using hexane as a solvent. De-oiled waste cakes (DOWCs) were collected (Chemical composition, Table 6.1), ground and passed through Standard ASTM sieve (Mesh No. 60, 250 μm) prior to carbonisation (Fig. 6.1). Ortho-phosphoric acid (88%), Oleic acid (pure, acid value 200 mg KOH/g), sulfanilic acid (99%), $NaNO_2$ (98%), anhydrous Na_2SO_4 (99.5%), H_2SO_4 (98%), HCl (35%), acetone (99.5%), methanol (99.9%), ethanol (99.9%), 1-Propanol (99.5%) and 1-ethyl-3-methylimidazolium chloride (>99%) were purchased from Merck and used as received. Microcrystalline cellulose was purchased from Sigma Aldrich. The H_3PO_2 (30-32%) aqueous solution was purchased from Sisco Research Laboratories Pvt. Ltd. India. All the chemicals were used as received without any further treatments.

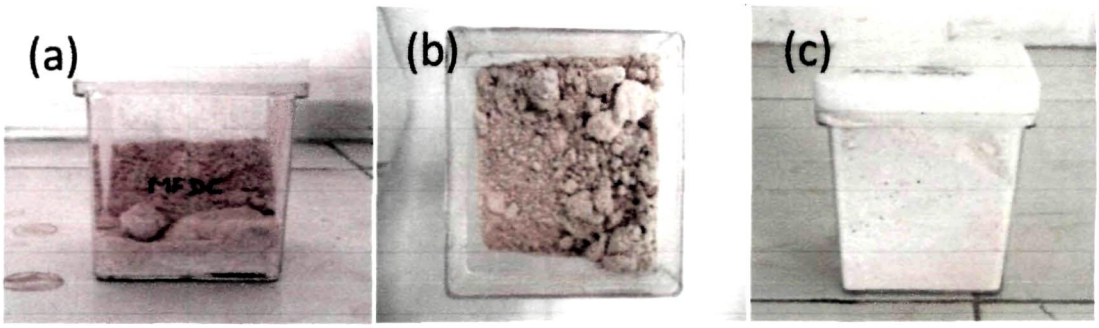

Figure 6.1. The de-oiled waste cakes (DOWC) used as precursors for preparation of sulfonated carbon catalysts (a) *Mesua ferrea* L. (b) *Pongamia pinnata* and (c) *Jatropha curcas*

6.2.2. Catalyst preparation

To determine the effect of preparation method on catalyst structure (surface acid sites, porosity etc), three different approaches were adopted for transforming DOWC into sulfonated carbon catalysts.

6.2.2.1. Method 1 (Radical or electrochemical sulfonation)

The DOWCs were subjected to an activation with 50% (v/v) phosphoric acid as reported in our previous work to prepare the activated carbon (AC), the details of which can be found elsewhere [24,25]. The AC yields were recorded to be 36%, 35% and 20% on dry weight basis for *M. ferrea*, *P. pinnata* and *J. curcas* de-oiled cakes, respectively. Consequently, these AC's were designated as MAC, PAC and JAC, respectively. Further, hereupon M, P and J represent the respective carbon precursor used (M for *Mesua ferrea* Linn, P for *Pongamia pinnata* and J for *Jatropha curcas* DOWC, respectively). The carbonized materials were powdered using a mortar and pestle and sieved through an ASTM no 60 sieve to prepare particles with an average size of ≤250 μm.

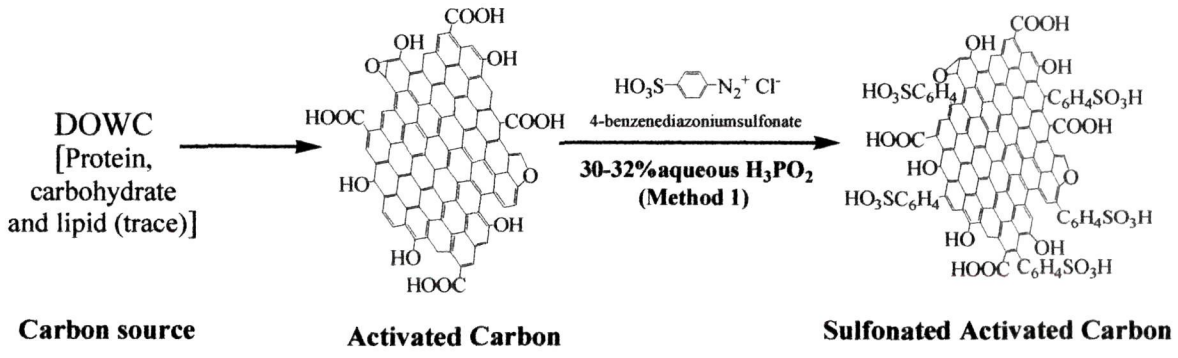

Scheme 6.3. Preparation of sulfonated carbons (radical or electrochemical route).

Sulfonation was achieved by covalent attachment of 4-benzenediazoniumsulfonate radicals in the presence of H_3PO_2 as discussed in our earlier work with some modifications (Scheme 6.3) [25]. In a typical process, sulfanilic acid (15.2 g, 0.086 mol) was dispersed in 1 M HCl aqueous solution (300 mL) in a three necked flask. Then the flask was moved to an ice water bath, and the temperature was controlled at 3–5 °C with continuous stirring. Followed by an addition of 10% excess of 1 M $NaNO_2$ (90 mL, aqueous solution) dropwise, a clear solution was obtained after all the $NaNO_2$ was added. After stirring for another 1 h at the same temperature, the white precipitate of 4-benzenediazoniumsulfonate formed was filtered off, washed with deionized water and transferred to a 500 mL beaker containing deionized water (200 mL) and ethanol (60 mL). To this mixture, 1.5 g AC was added maintaining the temperature at 3–5 °C, followed by subsequent addition of 30-32 % H_3PO_2aqueous solution (100 mL). After stirring for 30 min, another 50 mL of H_3PO_2 was added and allowed to stand for another 1 h (or until evolution of N_2 had ceased) with occasional stirring. The obtained sulfonated carbons were intensively washed with acetone and distilled water and then dried in the vacuum overnight and labeled as PACS (derived from *Pongamia pinnata* DOWC), MACS (derived from *Mesua ferrea* L. DOWC), JACS (derived from *Jatropha curcas* DOWC), respectively [19].

6.2.2.2. Method 2 (Direct sulfonation)

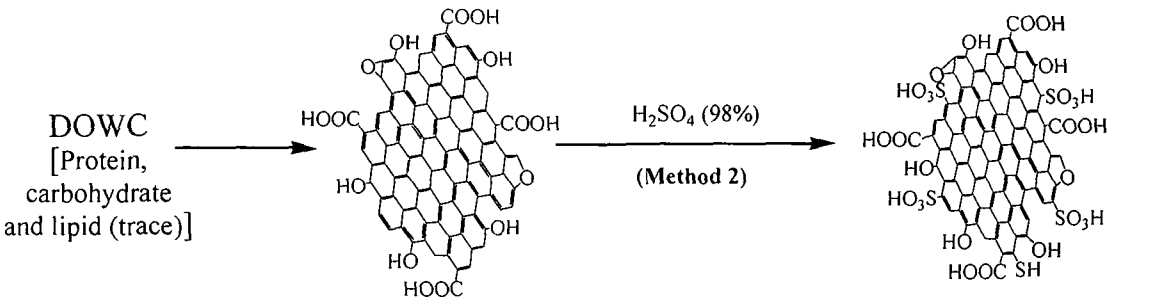

Scheme 6.4. Preparation of sulfonated carbons (direct sulfonation).

Sulfonated carbons were also prepared by direct sulfonation of DOWC based ACs (using MAC as reference) by conc. H_2SO_4 (98%) treatment as reported elsewhere (Scheme 6.4) [12]. In a typical process, 20g sulfuric acid (98%) was mixed with 1 g MAC and

refluxed at 150 °C for 8 h. The obtained black products ($MACH_2SO_4$) were filtered, thoroughly washed with acetone and deionised water and then dried in the vacuum overnight. Similar to the ACs all the sulfonated materials were powdered and sieved to particles size ≤250 μm prior to use.

6.2.2.3. Method 3 (Hydrothermal sulfonation)

These carbons were prepared by one step hydrothermal treatment of DOWC (*Mesua ferrea* L. as a reference) with conc. H_2SO_4 (98%) as reported elsewhere (Scheme 6.5) [26]. In a typical hydrothermal synthesis, a mixture 5 g of DOWC and 25 g conc. H_2SO_4 (98%) were heated in a 200 mL Teflon-lined autoclave at 180 °C for 24 h. 20g sulfuric acid (98%) was mixed with 1 g MAC and refluxed at 150 °C for 8 h [26]. The obtained black products (MACHT) were filtered, thoroughly washed with acetone and deionised water and then dried in the vacuum overnight. Similar to the ACs all the sulfonated materials were powdered and sieved to particles size ≤250 μm prior to use.

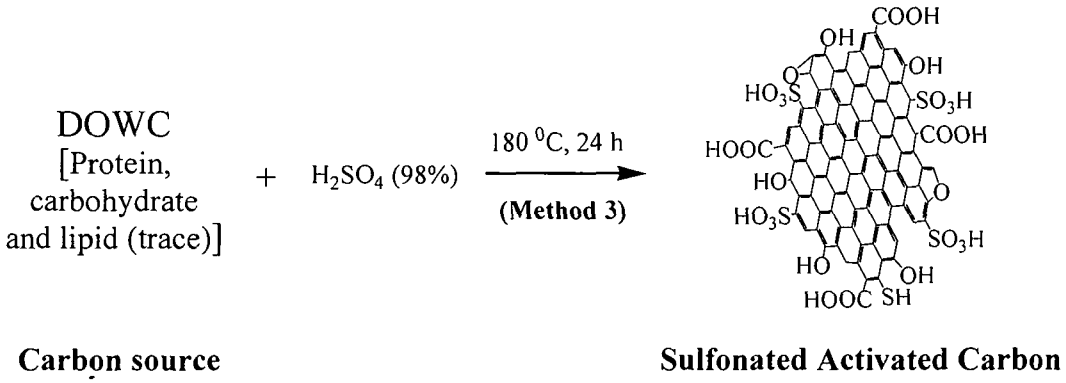

Scheme 6.5. Preparation of sulfonated carbons (hydrothermal sulfonation).

6.2.3. Catalyst Characterization

The catalytic materials were characterized by N_2-physisorption, elemental analysis, SEM, TEM, FT-IR, Raman spectroscopy, XRD and TGA. The details of the characterization techniques are given in Chapter 2. The acid densities of the carbons were determined by titration method as described in Chapter 2. The $-SO_3H$ densities of sulfonated carbons were based on elemental analysis assuming that all sulphur present in the carbon samples was due to $-SO_3H$ groups. In addition to the characterizations discussed

in Chapter 2, the carbon materials were also characterized by means of XPS and ammonia temperature-programmed adsorption-desorption measurements.

6.2.3.1. *XPS analysis*

The elemental composition and the oxidation state of surface functionalities, including the presence of $-SO_3H$ and phosphate groups were evaluated by X-ray photoelectron spectroscopy on a Kratos Axis Ultra DLD spectrometer with a monochromatized Al Kα X-ray source that was operated at 14 kV, 300 W. The analyzer pass energy was 17.9 eV and the energy step was 0.1 eV. The vacuum chamber base pressure was 10^{-9} mbar.

6.2.3.2. *Ammonia temperature programmed adsorption-desorption measurements*

The surface acidities were also measured by the ammonia temperature-programmed adsorption-desorption (AutoChem 2910, Micromeritics) and compared with the results obtained by titration. 0.1 g sample was placed in an adsorption vessel (U-shaped) and activated at 120 °C in He flow for 2 h (heating rate 10 °C/min). Then the sample was cooled to 100 °C in He flow. At this temperature, 5% NH_3 in He was passed through the sample for 1 h followed by cooling to 50 °C in He flow. TPD was carried out from 50 to 500 °C at a heating rate of 10 °C/min with He flow rate of 35 ml/min. After each TPD measurements, the amount of ammonia adsorbed was estimated from the calibration curve obtained from varying volumes of ammonia in He. Further, the acid site densities of the catalytic materials were determined by titration method as reported previously [25].

6.2.4. Evaluation of catalytic properties

6.2.4.1. *Oleic acid esterification*

Oleic acid esterification studies were performed in a 100 mL three necked flask equipped with a magnetic stirring and a digital thermometer in an oil bath. Reactions were performed with 3wt% catalyst loading at methanol reflux temperature with varying alcohol to oil molar ratios (5-30). In a typical reaction, 0.15 g of catalyst (particle size <250 μm, pre dried at 150 °C) was added to methanol/ethanol/2-propanol, stirred (250 rpm) and heated to 64 °C and followed by an addition of 5 g preheated oleic acid. At selected time intervals, 0.1 ml aliquots were drawn from the reaction mixture centrifuged at 6000 rpm

for 3 min to separate the catalyst particles. The acid value of the lower ester layer was determined by titration (in triplicates) after removal of excess methanol with standard KOH (0.01 mol L^{-1}) solution [25]. The conversion was calculated as:

$$C_{Est}(\%) = \frac{(C_i - C_t)}{C_i} \qquad (vi.i)$$

where, C_i is the initial acid value and C_t is the acid value measured at time t.

The ester formation was also verified by ^{1}H NMR analysis of reaction mixtures following completion of reaction on a Jeol JNM-ECS400 NMR spectrometer at 25.5 °C using $CDCl_3$ as solvent and TMS as the internal standard, respectively [27].

Based on the conversion results, the rate constant, k and turn over frequency (TOF) were calculated as reported elsewhere [20]. The TOFs were calculated according to the equation below.

$$\text{TOF} = \frac{k \times C}{n_S} \qquad (vi.ii)$$

where, C denotes the initial amount of oleic acid (in mmol) loaded into the reactor and n_s is the amount of strong acid (-SO_3H) sites on the catalyst loaded into the reactor, based on elemental analysis.

6.2.4.2. *Cellulose hydrolysis*

The hydrolysis reactions were performed in batch mode in 2 mL mini autoclaves (Fig. 6.2) on a hot plate at temperatures of 100 °C, 120 °C and 150 °C, respectively under autogenous pressure. In a typical reaction, 0.01 g of cellulose, 0.01 g of catalyst (particle size <250 μm) and 1 mL distilled water were loaded into the autoclaves, heated to desired reaction temperature for 24 h. After completed reaction, the mini-reactors were immediately cooled under tap water to quench the reaction. The reaction mixture were taken out and centrifuged to separate the solids (containing catalyst and the unreacted cellulose). Thereafter, the liquid phase was analyzed by means of High-Precision Liquid Chromatography, (Hitachi HPLC LaChromUltra) equipped with Aminex HPX-87C column. The individual products were identified using commercially available standard compounds and the yield was calculated following the equation reported by Onda *et al.* [28]:

$$Yield\ (C\ \%) = \frac{moles\ of\ sugar\ or\ HMF \times 6}{moles\ of\ C\ in\ cellulose} \times 100 \qquad (vi.iii)$$

Conversions were based on the weight difference between unreacted cellulose and cellulose fed into the reactor.

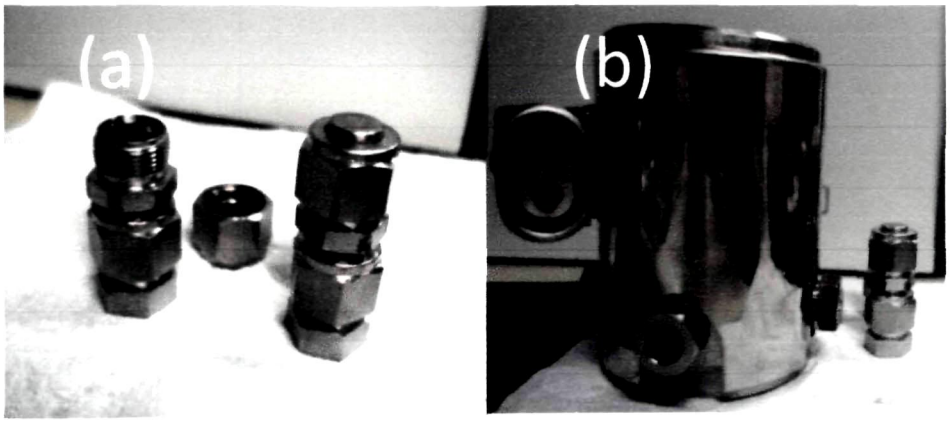

Figure 6.2. Digital images of (a) miniautoclaves used in cellulose/biomass saccharification tests (b) comparison of a minireactor with a standard 35 ml autoclave.

Amorphous cellulose was prepared by Ionic liquid treatment as follows: In a typical process, 0.5 g microcrystalline cellulose (MCC) was dissolved in 9.5 g 1-ethyl-3-methylimidazolium chloride in a test tube and heated at 130 °C for 1.5 h on an oil bath with occasional stirring. Cellulose was regenerated by adding double distilled water to the resulting solution, separated by filtration and dried at 100 °C.

6.3. Results and Discussion

6.3.1. Catalyst characterization

6.3.1.1. *Powder XRD analysis*

The X-ray powder diffractograms (XRD) of the DOWC based sulfonated carbons demonstrate the amorphous nature of these materials (Fig. 6.3). All carbon samples exhibit a similar broad and weak (002) diffraction peak near 2θ=15-30°, with varying intensities corresponding to an amorphous carbon structure with randomly oriented polycyclic aromatic carbon sheets. The broad and least intense, 002 peak was recorded for sulfonated

carbons prepared by one step hydrothermal method, indicating a highly functionalized and amorphous structure, while it was more prominent for chemically activated carbons. In addition, in sulfonated carbons obtained from phosphoric acid activated Mesua and Poongamia DOWC, the additional (101) graphitic structure peak at 2θ=35-50° appeared,

Table 6.1

Chemical composition of de-oiled cakes and the corresponding activated carbons

Properties	de-oiled cake			activated carbon		
	Mesua ferrea Linn	*Pongamia pinnata*	*Jatropha curcas*	MAC	PAC	JAC
Elemental analysis (Wt %)						
C	48.6	43.7	42.5	77.3	76.4	53.38
H	7.4	6.6	5.4	2.82	2.39	3.12
N	3.6	3.2	10.7	3.2	3.1	7.40
O+P[a]	40.3	46.5	41.4	16.7	18.1	34.2
Proximate analysis (Wt %)						
Moisture	4.1	3.8	4.4	21.9	19.6	16.3
Volatile matter	82.6	80.1	74.1	n.d	n.d	n.d
Fixed carbon	8.4	11.9	16.6	11.9	n.d	n.d
Ash	4.8	4.1	4.9	1.1	1.8	1.9

[a] Based on difference (ash free basis); MAC = *Mesua ferrea* Linn deoiled cake AC; PAC = *Pongamia pinnata* de-oiled cake AC; JAC = *Jatropha curcas* AC; n.d = not determined.

these variations in XRD patterns were strongly suggestive of the influence carbon precursor and carbonisation method on catalyst structure and morphology (Fig. 6.3) [13][18,19]. The non-sulfonated materials (Figure not shown) also exhibited similar XRD patterns indicating that carbon samples did not undergo any morphological changes during sulfonation process [25].

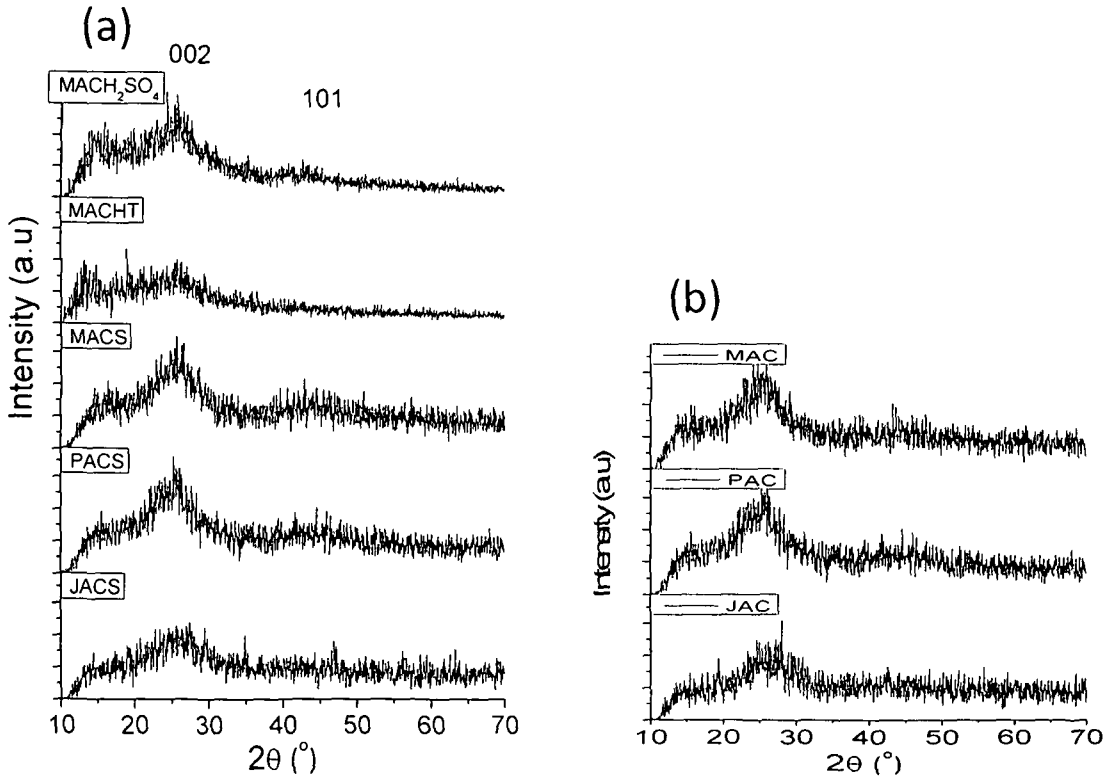

Figure 6.3. Powder X-ray diffraction patterns of the (a) DOWC based sulfonated carbons in comparison to the (b) non-sulfonated forms.

6.3.1.2. FT-IR analysis

The FT-IR spectra of all carbons samples (Fig. 6.4) exhibited the typical bands of carbonyl groups (C-O, C=O, near 1700 cm^{-1}) and characteristic peaks of incompletely carbonised materials, near 1580 cm^{-1}attributable (C=C) to aromatic ring modes with varied absorbance. The incorporation of N and P into AC structure and the presence of phosphorus and nitrogenous compounds were recognized by the appearance of a broad phsopahate band between 1300 and 900 cm^{-1} and characteristic nitrile band near 2360 cm^{-1} in all the spectra [29,30]. The sharper C=O bands for carbon samples obtained from Jatropha cakes and hydrothermally prepared MACHT in comparisons to those obtained by phosphoric acid activation of *M ferrea* and *P pinnata* cakes were consistent with their higher acid densities (–COOH groups) and functionalized structure. The high –COOH density of MACHT was also consistent with the presence of a broad overlapping C-H and O-H signal at 2500-3300 cm^{-1}. While, the shaper C=O bands in $MACH_2SO_4$ in comparison to MAC confirmed that sulfonation using H_2SO_4 created weak acid groups like -COOH in

addition to $-SO_3H$ groups and in good agreement with the literature (Fig. 6.4) [4,10,13]. The presence of additional bands at 1110-1118 cm^{-1} and 1003-1018 cm^{-1} (S=O stretching), 1171-1175 $cm^{-1}$and 1267-1270 cm^{-1} (stretching in $-SO_3H$) confirmed the presence of $-SO_3H$ groups on the surface of sulfonated carbons [9,18,20,25].

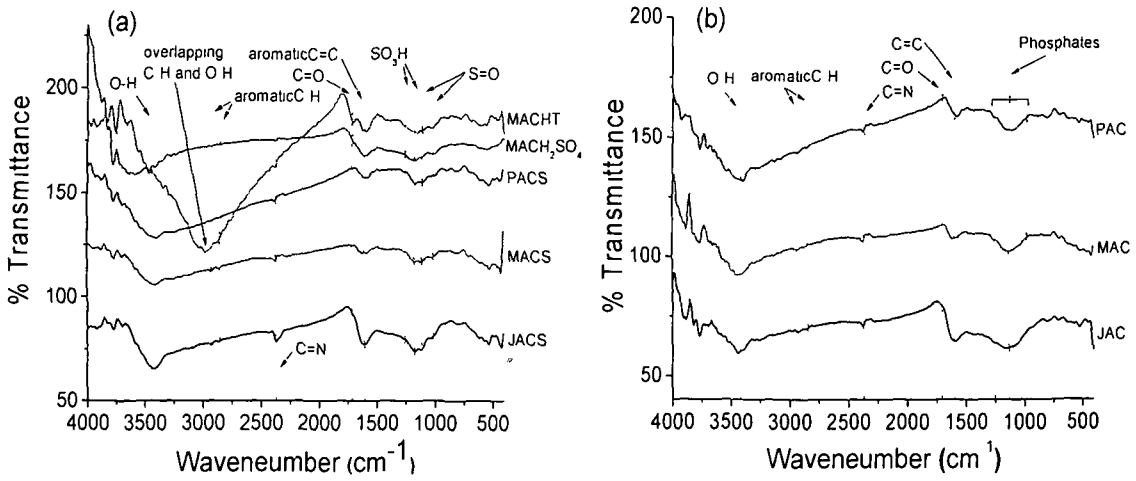

Figure 6.4. FT-IR patterns of (a) DOWC derived sulfonated carbon materials in comparison to their (b) non-sulfonated forms.

6.3.1.3. X-ray photoelectron spectroscopy

The XPS spectra of all DOWC-based sulfonated carbons obtained by different methods indicated the presence of C, O, S in addition to N, P, Fig. 6.5(a). Although the XPS patterns resembled those previously reported for sulfonated carbons [4,11,13]. The carbons reported here are structurally much more complicated due to incorporation of P and N during activation. As evident from high-resolution XPS spectra of C1s, N1s and O1s excitations, they show a much complicated envelope and indicate the presence of several carbon species, Fig. 6.5(b)-(e). The spectra were deconvoluted several components listed in Table 6.2 [31]. The C1s region was resolved into five key components (Fig. 6.5); the main peak at 284.3-284.5 eV was assigned to sp2 -hybridized graphite-like carbon (C-Csp2), the peak at 285.5-285.9 eV was assigned to the overlapping signal of C=N sp2 carbon and C=C sp3 carbon, while the small peaks centred at 286.8-287.2, 287.8-288.1 and 288.2-288.8 eV were attributed to C-O, C=O and –COO corresponding to the various surface functional groups. The N1s region (Fig. 6.5) was deconvoluted into four main

Table 6.2

Deconvolution of XPS peaks of the different carbon materials

Peak	Assignment	JAC Position (eV)	JACS Position (eV)	PAC Position (eV)	PACS Position (eV)	MAC Position (eV)	MACS Position (eV)	$MACH_2SO_4$ Position (eV)
C1s	C=C, sp2	284.6	284.6	284.4	284.3	284.3	284.3	284.5
	C=N sp2 and C=C sp3	285.7	285.8	285.6	286	285.5	285.7	286
	C-O	287.2	287.3			286.8	287.1	287.2
	C=O	288.4		287.1	287	288.1		
	COO		288.8	288.2	288.1	289	288.8	288.9
	Satellite	289.7, 291.6	291.1	290.3	290.6	290.9	291	291
O1s	=O in carbonyl, carboxyl, phosphates and sulfates	530.7	530.8	530.5	530.8	530.4	530.9	530.7
	-O-	532.8	532.5	532.4	532.5	532	532.6	532.1
	Chemisorbed O + H_2O	536	534.5	536.8	534.6	533.5		533.3
N1s	Pyridinic N	398.4	398.3	398.2	398.1	398.3	398.2	398.2
	pyrrolic N	400	400	399.9	399.8	399.8	399.9	400.1
	quaternary N	401.2	401.8	401.2	401.3	400.9	401.3	401.5
	N oxide of pyridine N	403.1		403.1	403	404.2	402.6	403.3
P2p	Phosphates and pyrophosphates	133.4	134.7	133.3	133.2	133.4	133.1	133.2
S2p	thiol or –SH							163.8
	C-SO_3^-		167.2		167.2		167.3	
	sulphate or -SO_3H		168.1		168.3		168.3	167.1

components; the lowest binding energy peak at 398.1-398.3 eV originated from the presence of pyridinic nitrogen, while the peaks at 399.3 eV, 401 eV and 402.4 eV were ascribed to pyrrolic, quaternary and N-oxide of pyridinic nitrogen respectively. The higher percentage of these species in Jatropha cake derived materials was attributed to the

presence of ~11% N (high protein content) which upon carbonisation formed carbon nitride like films (Table 6.1) [32]. Generally, the S2p photoelectron peak (163-168 eV) is of particular significance in these materials and has been used to confirm the presence of –SO_3H groups. In this study, the materials sulfonated by radical/electrochemical method exhibited a single peak at 168 eV, assigned to the bound –SO_3H groups, while those prepared by conc. H_2SO_4 treatment exhibited an additional thiolate peak near 163 eV. The presence of thiolate peak was also reported by Shu *et al.* [13] for oil pitch derived carbons obtained by a similar process, but interestingly authors assumed all S to be –SO_3H causing an overestimation of the strong acid (–SO_3H) sites. The possible explanation for the presence of –SH groups could be related to the formation of weak acid sites and accredited to surface oxidation of the some of the aliphatic hydrocarbons or surface –OH groups on carbon frameworks to -COOH resulting from the strongly oxidative, dehydrating properties of –SO_3H/H_2SO_4 under these conditions. The possibility of elemental sulfur was ruled out as none of the non-sulfonated materials (AC) exhibited the thiolate peak. This observations further strengthened the advantages of 4-benzenediazoniumsulfonate over conc. H_2SO_4 as a sulfonating agent. Consequently, the sulfonated carbons reported in this study are structurally more complex and contain pyridine like N groups and phosphates incorporated in their carbon frameworks in addition to -SO_3H –OH, -COOH and lactones found in carbohydrate or resin derived sulfonated carbons. The non-sulfonated carbons also exhibited similar XPS patterns, only difference being the absence of S2p peak.

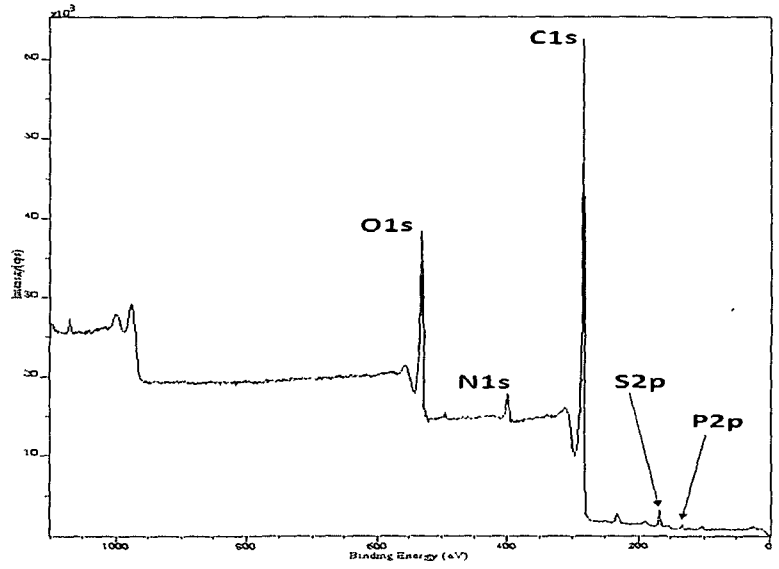

Figure 6.5. (a) Representative XPS spectra of DOWC derived sulfonated carbon (PACS).

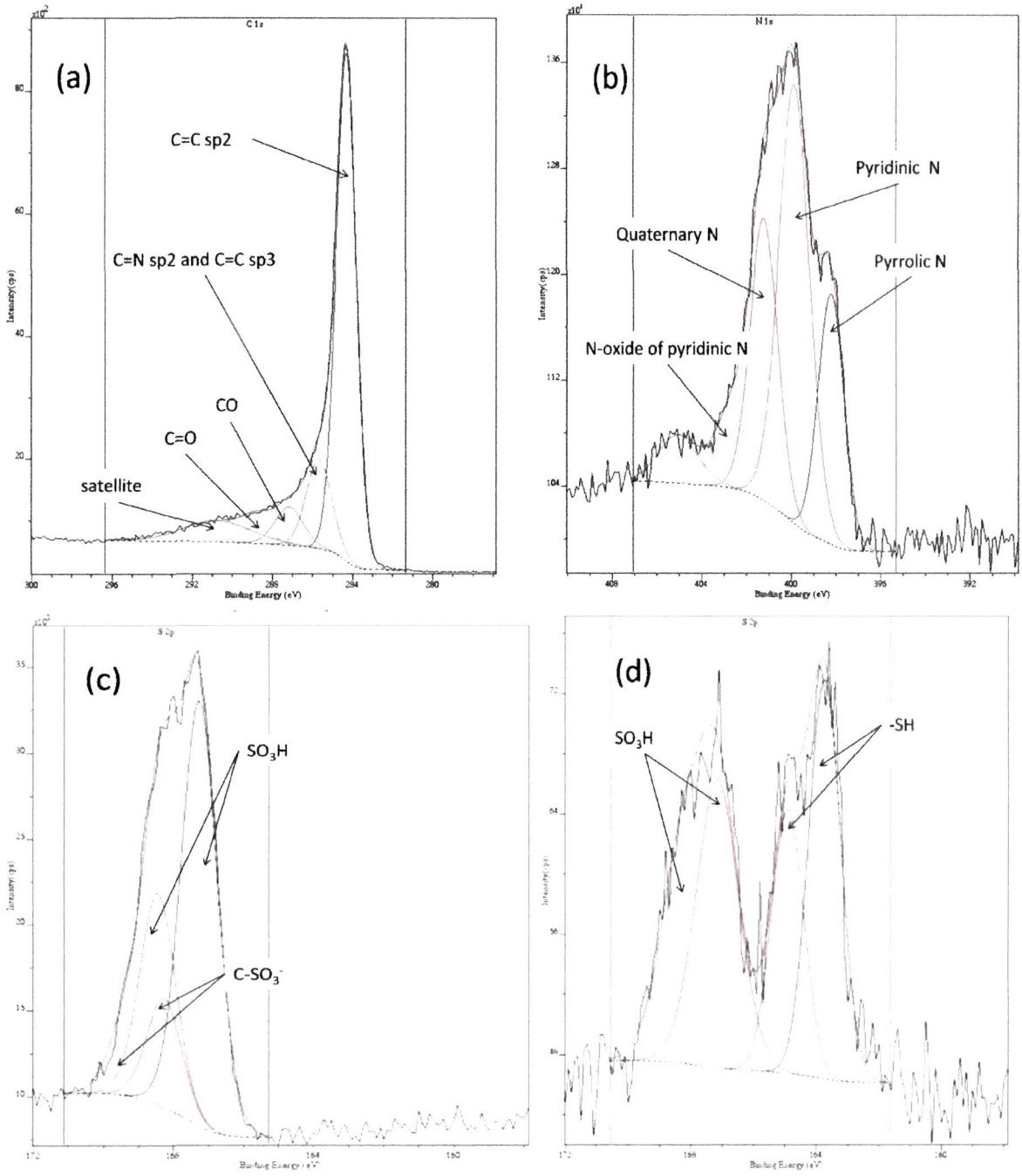

Figure 6.5. Deconvoluted high-resolution XPS spectra of DOWC derived sulfonated carbons (b) C1s peak, (c) N1s peak (d) S2p peak of MACS, and, (e) S2p peak of $MACH_2SO_4$.

Table 6.3

Overview of the surface and textural characteristics of the different carbon materials

Catalyst	S_{BET} [a]/ $m^2 g^{-1}$	$V_{(p)}$ [b] /cm^3g^{-1}	$d_{(p)}$ [c]/ nm	$V_{(mp)}$ [d]/ cm^3g^{-1}	$I_{(D)}/I_{(G)}$	L_a [e]/ nm	Acid density/ mmol g^{-1}			$T_{(max)}$ [f] (°C) in N_2
							$-SO_3H$ [f]	Total[g]	Total[h]	
JAC	423	0.32	3.93	0.15	0.79	5.56	-	3.24	4.34	n.d
PAC	914	0.77	5.4	0.35	0.64	6.72	-	2.58	2.01	n.d
MAC	786	0.63	3.72	0.28	0.86	5.07	-	1.91	1.76	460
JACS	93	0.23	3.9	0.13	0.86	4.9	1.5	3.96	6.20	240
PACS	483	0.46	3.84	0.17	0.66	6.68	1.59	3.62	5.86	248
MACS	468	0.40	3.7	0.17	0.90	4.85	1.62	3.59	5.63	243
$MACH_2SO_4$	690	0.61	3.7	0.26	0.86	5.07	0.16	2.01	n.d	n.d
MAC-SO_3H [25]	556	n.r	n.r	0.19	n.r	4.89	0.73	2.426	n.r	242
MACHT	<1	-	-	-	n.d	n.d	1.7	3.2	n.d	n.d

[a] Specific surface area calculated via the Brunauer-Emmett-Teller (BET) model; [b] Total pore volume at P/P0 = 0.95; [c] maximum pore diameter calculated from the Barrett-Joyner-Halenda (BJH) plot; [d] micropore volume via the Dubinin—Radushkevich equation; [e] $L_a = C(\lambda)/(I_{(D)}/I_{(G)})$ where $C(\lambda) = 4.4$ nm; [f] Based on EDX; [g] Based on titration; [h] Based on NH_3-TPD measurements; [i] Based on TGA; n.d = not determined; n.r = not reported.

6.3.1.4. Raman analysis

The Raman spectra of all carbon samples exhibited the characteristic amorphous carbon peaks at 1339 cm^{-1} and 1600 cm^{-1}, corresponding to the defects induced vibrations (D-band) and the tangential C-C stretching vibration (G-band) due to integrity of hexagonal carbon or the first-order scattering of the E_{2g} mode for sp^2 carbon lattice (Fig. 6.6). The intensity ratio of D and G band, $I_{(D)}/I_{(G)}$ is a measure of the degree of structural order and has been used as an to detect structural changes (disordering, clustering etc) in carbon materials due thermal annealing, sulfonation and oxidation [25,33]. In line with our previous findings upon sulfonation with 4-benzenediazoniumsulfoante, the $I_{(D)}/I_{(G)}$ intensity ratio of AC increased by 3-7% due to incorporation of additional $-PhSO_3H$ groups on carbon frameworks which caused the intensity of defects induced vibrations to increase, while the same changes were not observed for carbons obtained by direct

sulfonation (Table 6.3) most likely due to the less effective functionalization of $-SO_3H$. In addition, based on these intensity ratios the graphitic cluster sizes (L_a) in the carbon samples were estimated using the Knight formula (Table 6.3) [18,33].

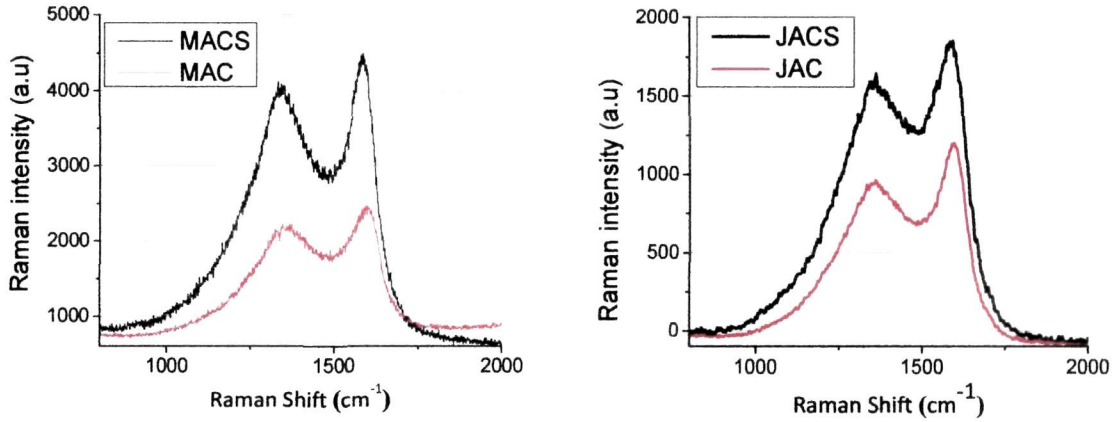

Figure 6.6. Raman spectra the carbon materials showing changed $I_{(D)}/I_{(G)}$ intensity ratio upon sulfonation with 4-benzenediazoniumsulfonate.

6.3.1.5. N_2 physisorption and surface properties

Comparison of textural and surface properties of the carbon materials presented in Table 6.3, shows strong effect of carbon precursor and preparation method on the said properties. The chemically activated carbons were a mixture of mesoporous and microporous particles, while hydrothermally obtained carbon was essentially non-porous and exhibited specific surface area <1 m^2/g. Under identical conditions, the surface area and porosity development in chemically activated carbons were mainly affected by the carbon precursor; those obtained from *P. pinnata* and *M. ferrea* DOWCs exhibiting much higher specific surface area 914 m^2/g and 786 m^2/g and mesopore content than the *J. curcas* cake based carbons (423 m^2/g) (Table 6.3 and Fig. 6.7). Sulfonation was also evident from the reduction in pore volume and specific surface area as shown in Table 6.3. Sulfonation using 4-benzenediazoniumsulfonate reduced pore volume by 28-40% and specific surface area by 300-400 m^2/g (Fig. 6.7). On the other hand, in case of carbons sulfonated by H_2SO_4, such changes were not observed indicating less successful incorporation of $-SO_3H$ groups on carbon surface. Thus, such sulfonation was considered to be less effective [7,20,34-36]. From (Fig. 6.7), it is seen that sulfonation occurred in

meso and micro pores equally, JACS being the only exception where micropores were preferentially filled. However, no significant reduction in average pore diameters was observed for both sulfonation methods.

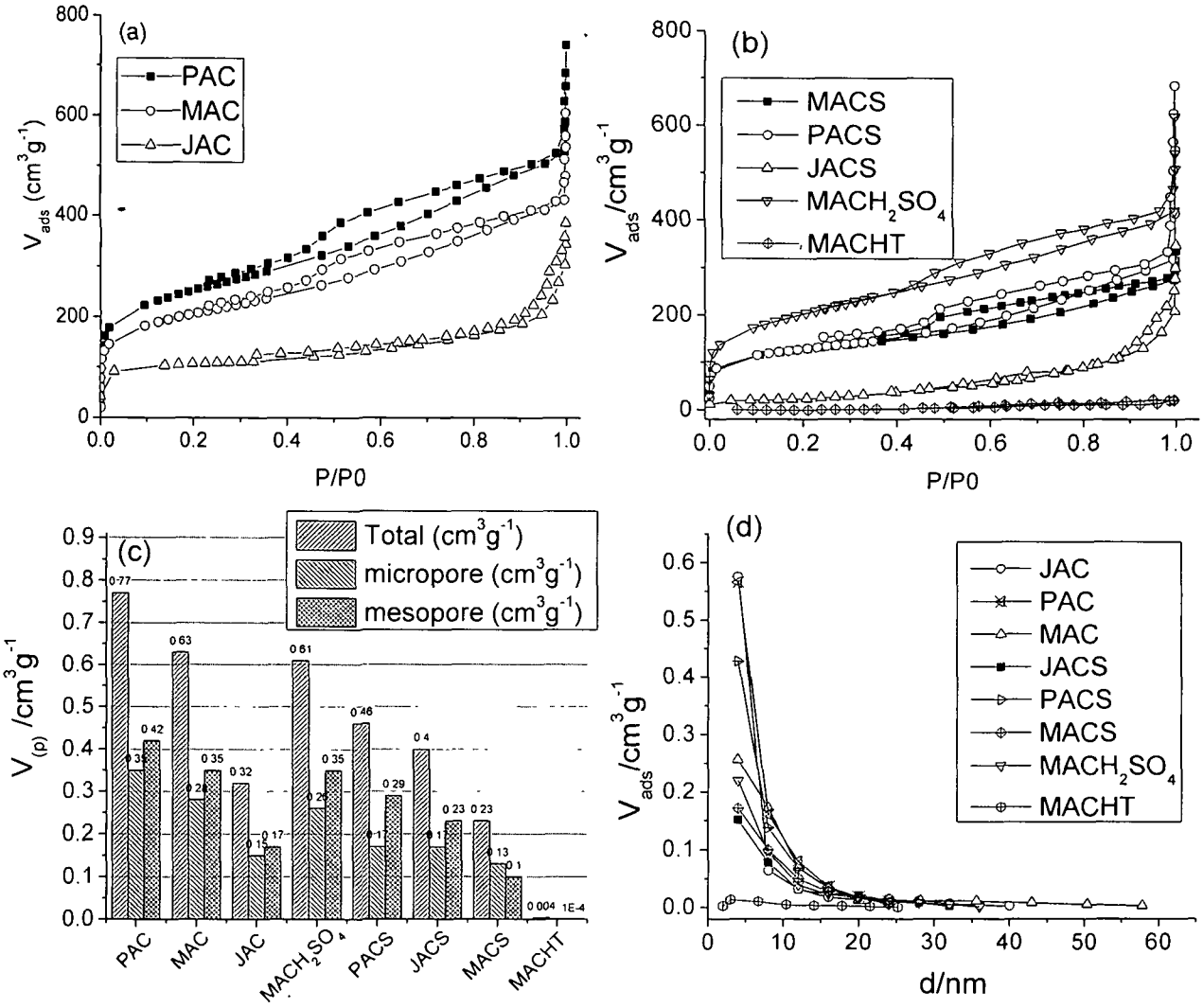

Figure 6.7. The N_2 adsorption-desorption isotherms of carbon materials (a) before (b) after sulfonation, (c) the corresponding pore volumes and (d) pore-size distributions.

Subsequently, dispersibilities of sulfonated carbons were studied in the investigated reactions media viz. methanol and H_2O. Dispersibility was dependent on density of hydrophilic functional groups on carbon surface (-COOH, -OH and $-SO_3H$) rather than

surface area. Fig. 6.8 shows a comparison of the dispersibility of sulfonated carbons prepared by radical sulfonation in comparison to their non-sulfonated derivatives. The better dispersibilities of sulfonated carbons in comparison to the unsulfonated ones were due to presence of -$PhSO_3H$ groups in addition to surface functional groups (-COOH, -OH etc). The catalytic activity of sulfonated carbons has also been related to the amounts of -COOH, -OH groups on their surface acting as anchoring sites for attaching polar substrates like methanol and FFAs. Thus, a higher dispersibility is expected to enhance catalytic activity [4,5,13,20].

6.3.1.6. $-SO_3H$ density

The elemental compositions of the activated carbons prepared by phosphoric acid activation (AC) are summarized in Table 6.1 in comparison to the corresponding carbon precursors (DOWCs). The presence of S and 15-21% increase in the acid site density of the sulfonated materials were consistent with the success of sulfonation process (Table 6.3). The increased C content of the carbonized materials and consequently, a comparison to the carbon sources also confirmed the success of chemical activation. The $-SO_3H$ density in the carbon materials was strongly influenced by the sulfonation method. The order of the $-SO_3H$ density was found to be MACHT> MACS> PACS> JACS> MAC-SO_3H> MACH_2SO_4. Comparison of the $-SO_3H$ densities (Table 6.3) and C contents (Table 6.1) revealed a linear relation between the two parameters for the carbons sulfonated by 4-benzenediazoniumsulfonate. The increase in $-SO_3H$ density with increased C content could be credited to the availability of more aromatic carbon sheets with a less functionalized framework (–COOH and –OH groups) and hence abundant sites for functionalization of 4-benzenediazoniumsulfonate radicals. On the contrary, the directly sulfonated MAC H_2SO_4 (H_2SO_4 treated) exhibited the lowest -SO_3H density as it was difficult for H_2SO_4 to react with the more rigid and ordered frameworks of AC. Okamura *et al.* [5] has demonstrated that non-graphitic carbon and graphitic carbons have different abilities to attach the $-SO_3H$. The non-graphitic carbon is easier to be attached with the $-SO_3H$ group, so a carbon material with more non-graphitic carbon will have more amounts of $-SO_3H$ upon sulfonation with H_2SO_4. Nonetheless, successful sulfonation of ordered carbon materials has been demonstrated with stronger sulfonating agents (fuming H_2SO_4,

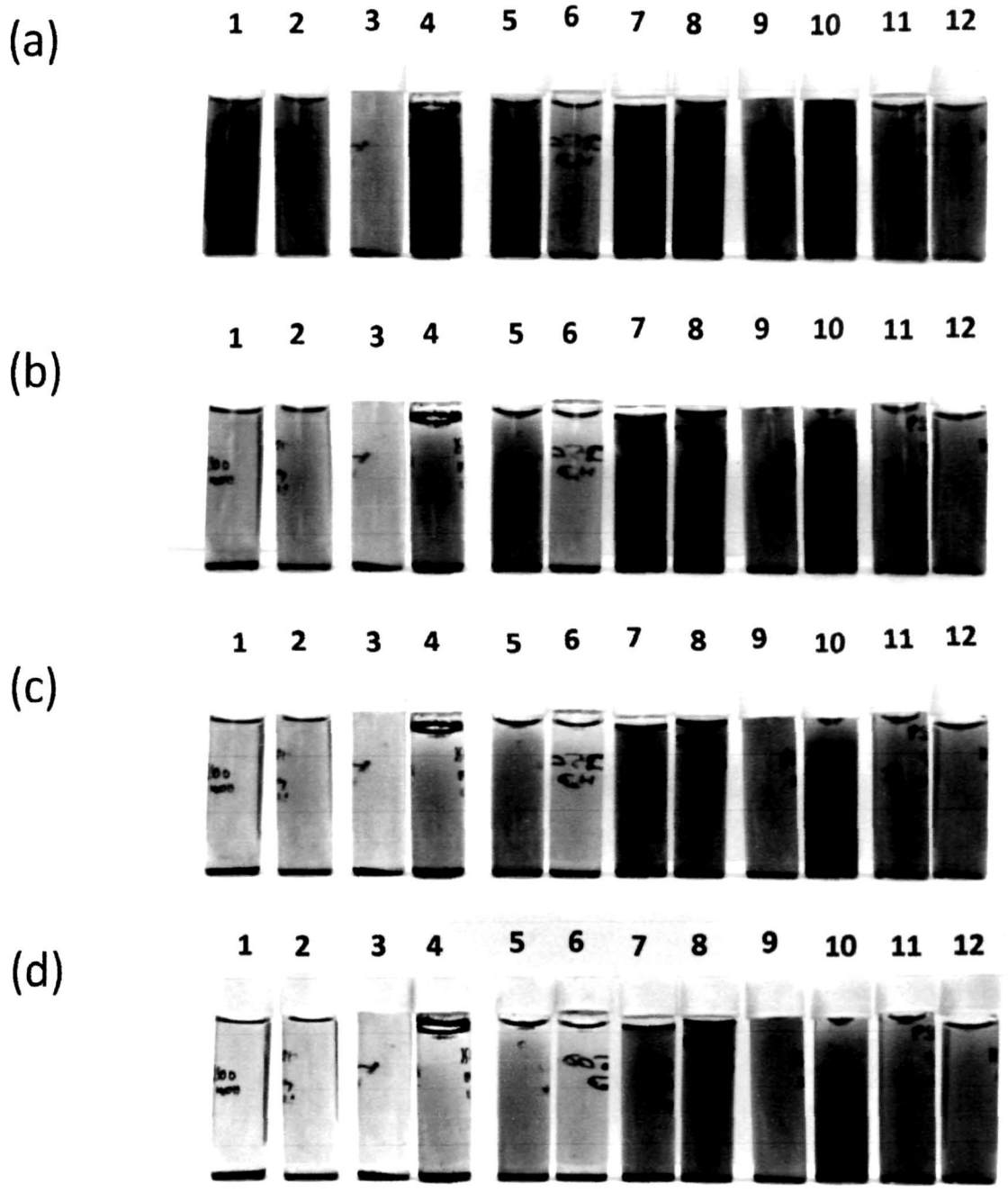

Figure 6.8. Digital images showing the dispersibility of carbon materials (a) 0 min, (b) 30 min, (c) 60 min and (d) 120 min; Sample code: 1 (JAC, CH_3OH), 2 (PAC, CH_3OH), 3 (MAC, CH_3OH), 4 (JAC, H_2O), 5 (PAC, H_2O), 6 (MAC, H_2O), 7 (JACS, CH_3OH), 8 (PACS, CH_3OH), 9 (MACS, CH_3OH), 10 (JACS, H_2O), 11 (PACS, H_2O) and 12 (MACS,H_2O); concentration was 3 mg/mL in all cases.

gaseous SO_3, ClH_3SO_4/ H_2SO_4 mixture) [4,11,34,35]. In our study, the higher $-SO_3H$ density (1.7 mmol/g) was obtained in MACHT resulting from the easier sulfonation of the partially carbonsised structure formed under hydrothermal conditions [26]. Therefore, it may be concluded that sulfonation with 4-benzenediazoniumsulfonate radicals is more effective in the presence of graphitic/ordered carbons, contrary to the direct sulfonation process (conc. H_2SO_4, SO_3) reported as a more efficient strategy for non-graphitic carbons [4,5,8,11-13]. Furthermore, the efficiency of radical sulfonation was also affected by the amount of sulfonating agent. The *M. ferrea* DOWC based sulfonated carbon discussed in this chapter, MACS, prepared at 15:1 w/w ratio of sulfonating agent to AC exhibited almost 3 times higher $-SO_3H$ density those from our earlier study (MAC-SO_3H), prepared with a lower ratio of ~2:1 (Table 6.3) [25].

6.3.1.7. TGA analysis

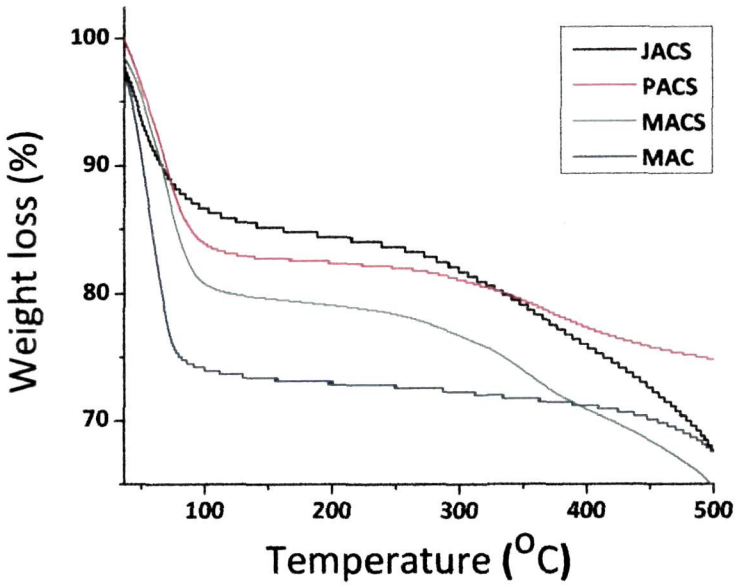

Figure 6.9. TGA patterns of the sulfonated carbon catalysts in comparison to the parent material (MAC).

All sulfonated catalysts showed excellent thermal stability upto temperatures close to 250 °C under oxygen-free conditions (Table 6.3). Based on TGA, the catalysts prepared from *P. pinnata* and *M. ferrea* DOWC were found to exhibit 3-5% better stability than the *J. curcas* based catalyst due to their more ordered structure and presence lower amounts of

surface functional groups (Table 6.3). The typical TGA patterns show two distinctive weight losses (Fig. 6); the first, more rapid loss was between 0-130 °C which might be due to loss of water and free moisture adsorbed on the catalyst surface and the second region from 240-380 °C, the 6-8% weight loss in this region was due to the removal of $-SO_3H$ groups, as this region was absent in the non-sulfonated carbons (Fig. 6.9) [25,34]. In short, sulfonation lowered the onset of thermal decomposition resulting from the incorporation of $-SO_3H$ groups on carbon surface. Following the 2nd region, weight loss continued but at a much lower rate; however, for JACS, the weight loss continued at the same rate even after 400 °C due to the removal of surface functional groups and further carbonisation of the material at high temperatures. Overall, all the materials demonstrated excellent operational stability and were suitable for applications at reaction temperatures close to 240 °C.

6.3.1.8. NH_3-TPD measurements

The typical NH_3-TPD plot of a representative catalyst, PACS is shown in Fig. 6.10 in comparison to the parent non-sulfonated carbon PAC. The total acid density calculated from TPD measurements are presented in comparison to the titration results (Table 6.3). In all experiments, two distinctive peaks were observed, a weak acid site around 140-160 °C and strong acid site 340–350 °C (Fig. 6.10). The strong acid sites were attributed to the presence of $-SO_3H$ groups whereas weak acid sites were attributed to the surface functional groups (–OH, –COOH and lactones) on AC surface [34]. The presence of the small peak at 340–350 °C in the non-sulfonated materials could most likely be accounted by the presence of phosphates in AC, also supported by FT-IR and EDX analysis (Table 6.1). However, in our experiments the TPD desorption temperature was restricted to 500 °C as the sulfonation reduced the stability of these materials and 500 °C is the maximum temperature upto which most of the $-SO_3H$ remain attached to the catalyst surface, as also stated by Kastner *et al.* [34]. It is also worth mentioning that acidities based on TPD were always 30-35% higher than those obtained by titration most likely due to the low thermal stability of these materials which resulted in leaching of $-SO_3H$, -COOH during measurements and in agreement with results previously reported in literature [14,34].

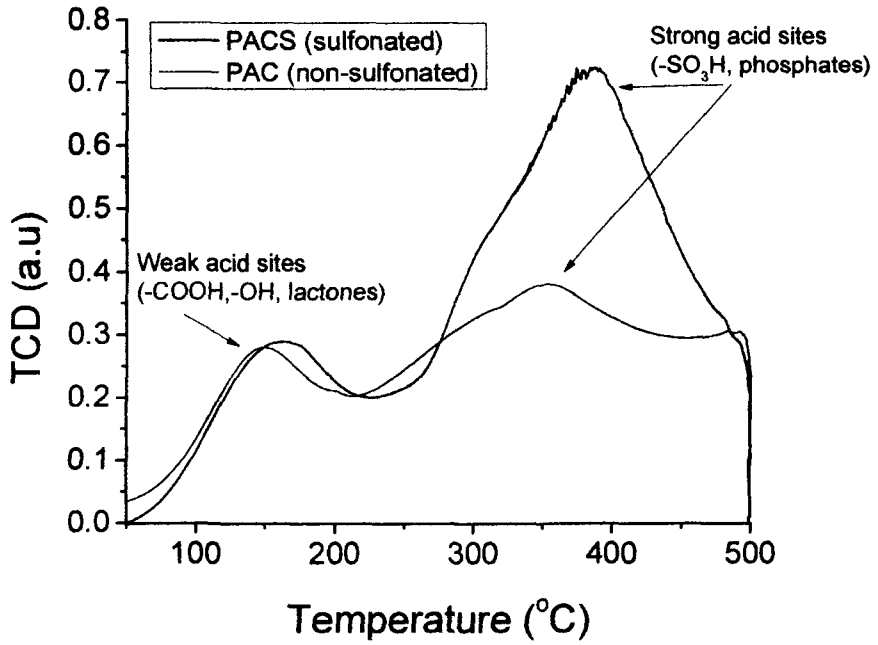

Figure 6.10. Ammonia TPD profiles of catalytic materials obtained from *Pongamia pinnata* DOCW, before sulfonation (blue line) after sulfonation (black line).

6.3.1.9. SEM and EDX element mapping

Morphologically the DOWC derived sulfonated carbons consists of irregular and non-uniform particles evident from the SEM images (Fig. 6.11), similar to the carbons reported in our previous study and supporting fact that the morphology of the carbon material remained largely unaffected by sulfonation [25]. EDX element mapping (O and S) of the sulfonated carbons prepared by radical sulfonation indicated a homogenous and uniform distribution of the various acid sites (-SO_3H, -OH and -COOH) on the catalyst surface with no non-single element clusters (Fig. 6.11). The highest S density was observed for MACS followed by PACS and JACS respectively following the order of their respective –SO_3H densities. On the other hand, the density of O (or the O containing surface functional groups) followed just the opposite order JACS>PACS>MACS, in accord with more functionalized structure of JACS.

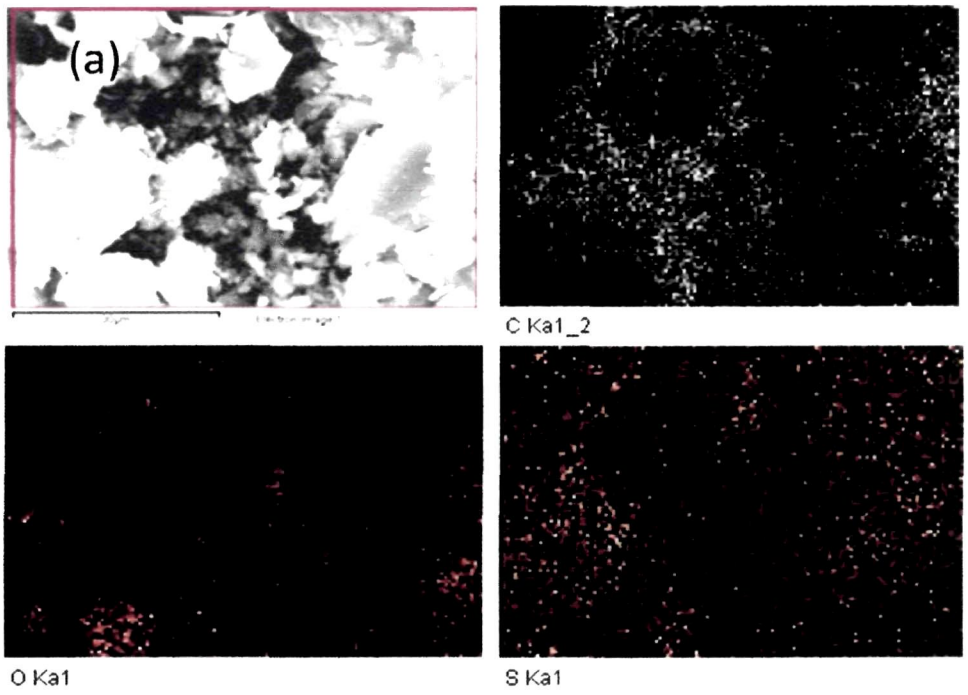
(a)
C Ka1_2
O Ka1
S Ka1
(b)
30µm
Electron Image 1
C Ka1_2
O Ka1
S Ka1

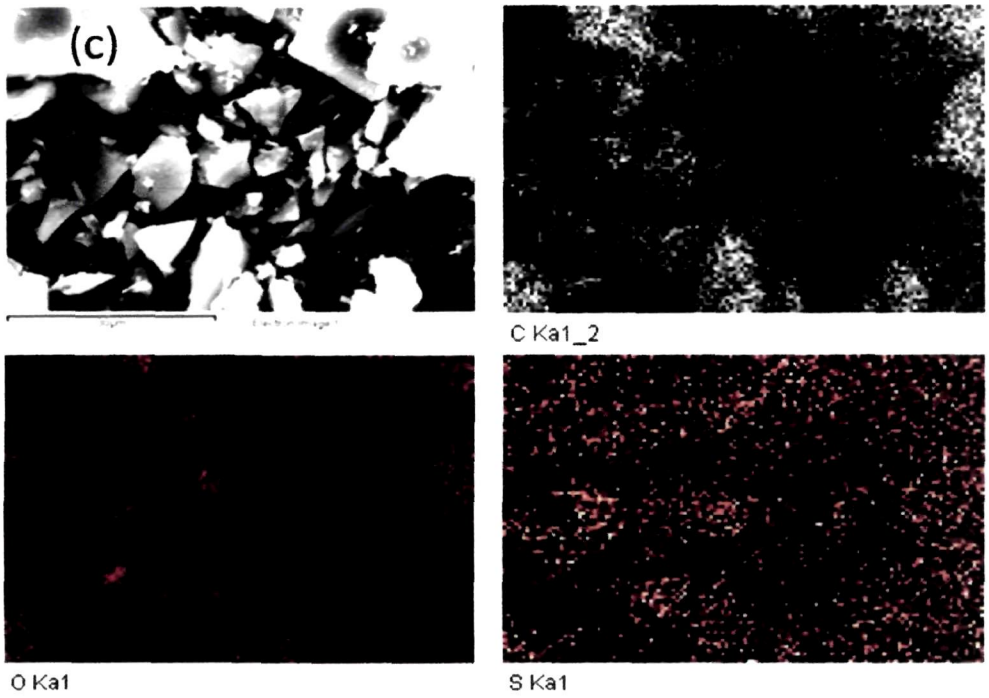

Figure 6.11. SEM images (scale 30 μm) and corresponding EDX element mapping (C, O, and S) distributions of the sulfonated carbon catalyst (a) JACS, (b) PACS and (c) MACS.

6.3.1.10. TEM analysis

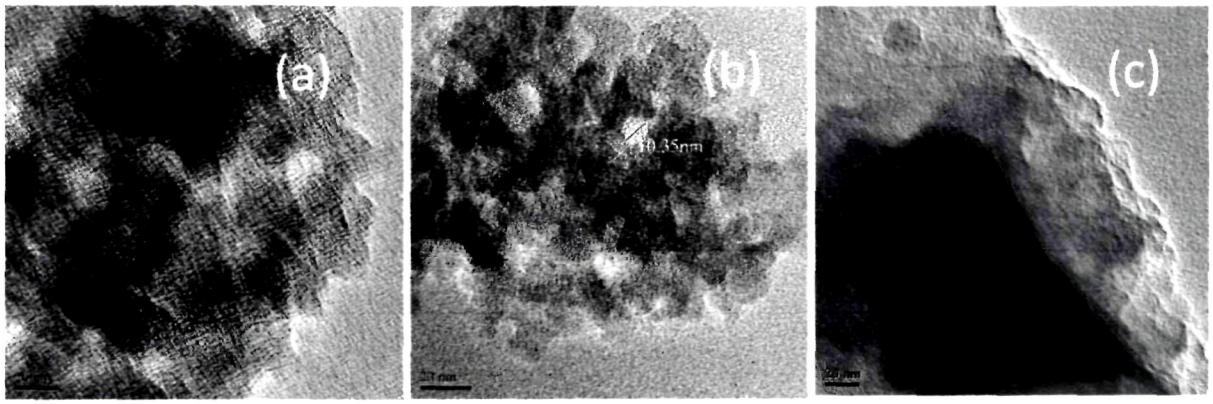

Figure 6.12. TEM micrographs of the optimum catalysts, (a) MACS, (b) PACS and (c) JACS (scale 20 nm)

TEM micrographs (Fig 6.12) of selected carbon catalysts MACS, PACS and JACS clearly show the presences of a non uniform porous structure with randomly arranged aromatic/graphitic carbon sheets in the materials, dissimilar from the microporous corncob

derived sulfonated carbons reported by Arancon *et al.* [15]. The morphology was distinctly different for JACS and MACS/PACS, a textured and coarse surface morphology observed for MACS/PACS were characteristics of a more mesoporous structure and well reflected by the higher specific surface area mesopore content in the material, whereas the former being less coarse exhibited features typical to less porous materials (Fig. 6.12 and Table 6.3) [15]. These findings are consistent with the effect of carbon source on catalyst structure.

6.3.1.11. Proposed structure of the catalytic materials

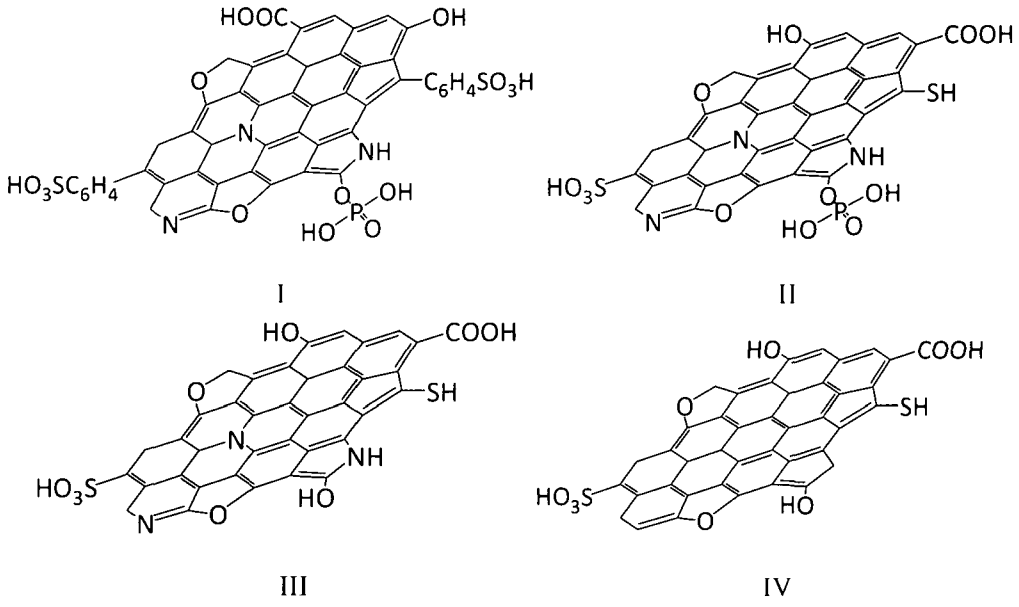

I II III IV

Figure 6.13. Proposed structure of the DOWC derived sulfonated carbons, (I) Phosphoric acid activated DOWC sulfonated with 4-benzenediazoniumsulfoante, method 1 (II) Phosphoric acid activated DOWC sulfonated with H_2SO_4 (98%), method 2 (III) Hydrothermally sulfonated DOWC with H_2SO_4 (98%), method 3 in comparison to (IV) the typical carbohydrate or sugar based sulfonated carbons, based on Hara *et al.* [4] method.

The above characterization results point to a much complex structure for the DOWC biomass derived sulfonated catalysts, different from the typical carbohydrate or sugar derived sulfonated carbons/sulfonated active carbons based on the conventional Hara *et al.* method [4]. Structurally these multifunctional materials are related more to the N-doped carbons or carbon nitrides rather than amorphous or active carbon [4]. Upon activation the

N rich DOWC carbonises into carbon nitride like films; consequently, the basic structural unit of sulfonated form of these carbon catalysts can be closely approximated by a carbon nitride sheet which has been extensively functionalized with –OH, –COOH, $–SO_3H$ or $–PhSO_3H$ and phosphate groups. The DOWC based materials may adopt any one of the three the structures I or II or III depending on preparation method (Fig. 6.13). The density and nature of surface acidic groups are directly affected by carbonisation temperature and method. Here, the H_2SO_4 treated and phosphoric acid activated DOWC (method 2) will take up structure I while the materials prepared by method 1 will adopt structure II and the hydrothermally sulfonated and carbonised materials (method 3) will take up structure III. In contrast the basic structural unit of typical carbohydrate or resin based sulfonated catalyst is a graphene sheet functionalized with –OH, –COOH and $–SO_3H$ groups (IV).

6.3.2. Catalytic activity

6.3.2.1. Oleic acid esterification

Oleic acid esterification was used as a model reaction to probe the utility of these DOWC based sulfated carbons as biodiesel catalysts. Esterifications are equilibrium reaction characterized by the combining of an alcohol and an acid to yield an ester and H_2O. It is highly reversible and the H_2O formed during the reaction also shifts the equilibrium in backward direction, thus the yield of the ester is usually improved using Le Chatelier's principle. The reaction is slow in the absence of a catalyst; sulfuric acid is a typical catalyst as it functions both as a catalyst and dehydrating agent.

Fig. 6.14 shows an overview of the catalytic properties of the various DOWC based sulfonated carbons in comparison to H_2SO_4. The results presented in Fig. 6.14(a) illustrate the superiority of the catalytic materials in comparison to H_2SO_4 and point to the occurrence of an apparent relation between catalyst structure and acidity with ester yield, as also reported for biochar based sulfonated carbons by Yu *et al.* [11] and Krestener *et al.* [34]. The highest conversions were obtained for the most porous PACS and MACS with high $–SO_3H$ density of ~1.6 mmol/g followed by the comparatively less porous and acidic JACS ($–SO_3H$ density of 1.5 mmol/g), the presence of large amount of N containing functional groups in JACS might have also contributed to deactivation of some of the acid sites resulting in lower yields. Whereas the low conversion obtained for the hydrothermally obtained MACHT could be attributed to its non-porous structure limiting diffusion and

accessibility large oleic acid molecules (length~2.4 nm) [36] to the active sites. The lowest ester yield recorded for the sulfuric acid treated $MACH_2SO_4$ catalyst was due to its low $-SO_3H$ density (Table 6.3). Furthermore, $-SO_3H$ groups in such catalyst were more easily leached upon reuse in comparisons the catalyst obtained by 4-benzenediazonium sulfonation or the hydrothermal method (Fig. 6.15), Yu *et al.* found a similar effect for activated biochar catalysts [11]. Increasing the methanol concentration obviously increased conversion for the less active JACS, $MACH_2SO_4$ and MACHT, yet it did not approach the levels achieved by MACS or PACS, Fig. 6.14(a). The order of esterification activity based on conversion was MACS >PACS >JACS >MACHT >H_2SO_4 > $MACH_2SO_4$ following combined effect of acidity and porosity. The effects of alcohol chain length on conversion

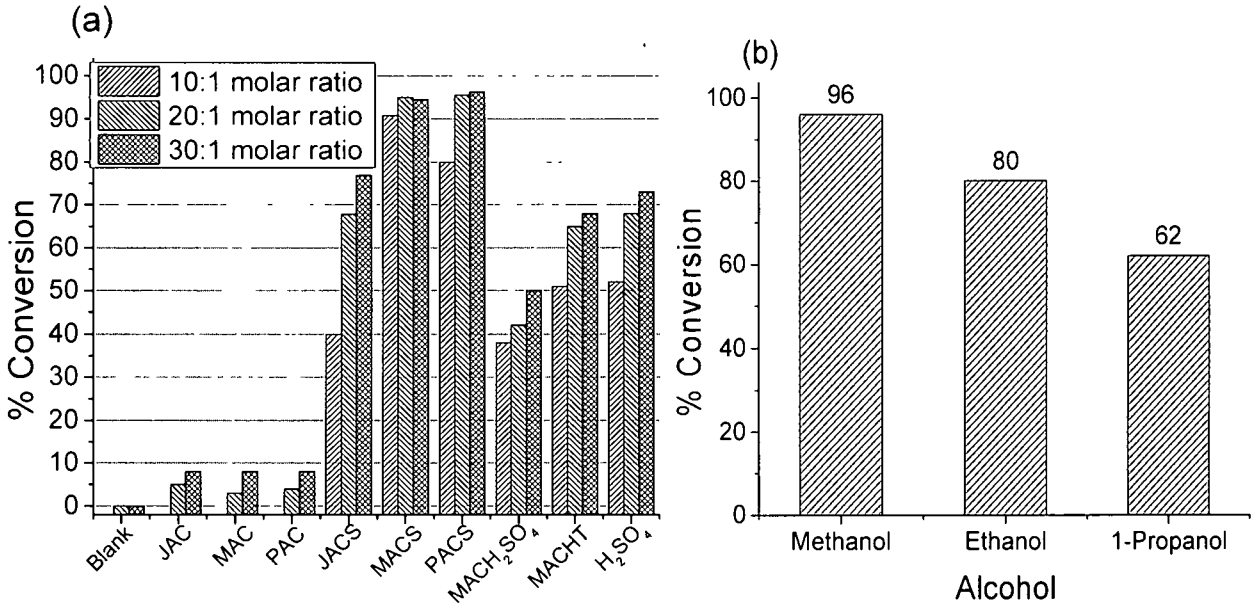

were also studied by repeating experiments with ethanol and 1-propanaol using MACS as a reference catalyst under identical reaction conditions. The conversion achieved with ethanol was only 80% and it reduced even further, 62% with 1-propanol, Fig. 6.14(b). The reduced conversions could be explained on the basis of difference in reactivities of alcohols of different carbon chains.

Figure 6.14. (a) Catalytic activity of the DOWC derived materials in comparison to H_2SO_4 and (b) Effect of alcohol chain length (investigated using MACS at 30:1 methanol to oleic acid molar ratio) as a function of oleic acid conversion.

Reaction conditions: catalyst loading was 3 wt% of acid or 0.02 g H_2SO_4 (equivalent catalytic amount of $-SO_3H$ in MACS), 10 h reaction, and temperature was 65±5 °C.

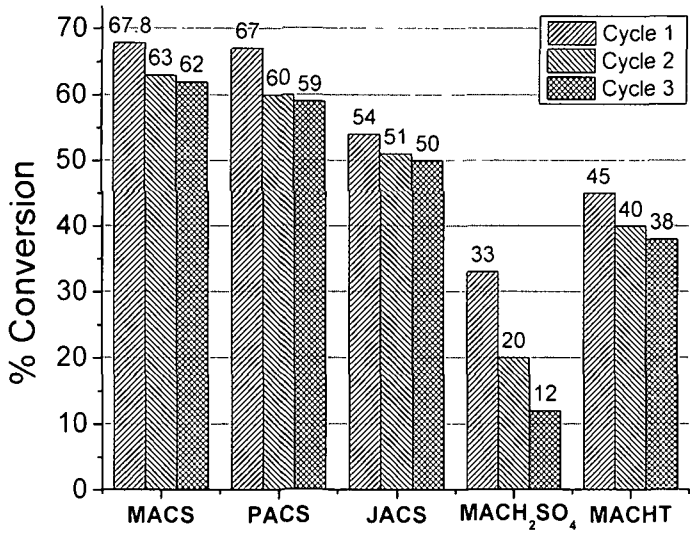

Figure 6.15. Deactivation of the DOWC derived sulfonated carbons over 3 cycles. Reaction conditions: catalyst loading was 3 wt% of acid, molar ratio of methanol to oleic acid was 30:1, 3 h reaction and temperature was 65±5 °C.

To get a better picture, the turnover frequencies (TOF) of the DOWC derived materials were determined and compared to some of the sulfonated carbons reported in literature (Table 4). Comparison of the TOF also revealed a sturdy relation between pore volume and $-SO_3H$ density with catalytic activity. The high TOF and superiority of radically sulfonated DOWC catalysts to the hydrothermal and directly sulfonated catalysts and the biochar, active carbon catalysts reported by Kastner, *et al.* [11] and Geng *et al.* [20] were consistent with the effects of pore size and $-SO_3H$ density (Table 4). Whereas the even higher TOF obtained of the sulfonated ordered mesoporous carbons (OMC) and sulfonated starbons-300; were attributed to the presence of much larger mesopores (diameter >9 nm) and higher $-SO_3H$ density in comparison to the DOWC based carbons possessing a mixed mesoporous and microporous texture [20,35].

Overall, the esterification activities of the porous, radically sulfonated DOWC derived catalysts were higher than the biochar, active carbon or carbohydrate derived catalysts. While the non-porous hydrothermally sulfonated DOWC and directly DOWC sulfonated catalysts were less active than the biochar, active carbon or carbohydrate derived catalysts (Table 6.4).

Table 6.4
Comparison of the esterification activity of the DOWC derived sulfonated carbons with carbons reported in literature

Catalyst	Source	Sulfonating agent	T / °C	Methanol to oil molar ratio	Pore volume/ cm^3g^{-1}	$S_{(BET)}$/ m^2/g	$-SO_3H$ density/ mmol/g	TOF/ h^{-1}	Ref.
AgForm-400C-SO4	AgForm 400 biochar	H_2SO_4	47	20	0.0005	338	0.45±0.03	2.4	[34]
PHC-400C-SO4	Peanut hull char	H_2SO_4	57	20	0.13	242	0.61±0.03	9	[34]
WVB-20-SO4	Wood AC	H_2SO_4	57	20	0.76	1391	0.2±0.01	10.8	[34]
BX-7540-SO4	Wood AC	H_2SO_4	60	20	0.34	967	0.10 ±0.002	33.6	[34]
WVB-20-SO3	Wood AC	Gaseous SO_3	60	20	0.63	1137	0.81±0.01	10.8	[34]
SC-CCA3	resorcinol–furfural resin and γ-Al_2O_3 as a hard template	4-BDS	65	57	0.57	623	1.70	102	[20]
Starbons-300A2-ClSO3HAH2SO4-5	Starbon-300	mixture of $ClSO_3H/H_2SO_4$	80	10	-	75	1.80	509*	[35]
S-AC	Mesoporous AC	4-BDS	65	57	0.24	318	1.42	44	[20]
JACS	Jatropha DOWC	4-BDS	65±5	20	0.23	96	1.50	35.2	Self
PACS	Pongamia DOWC	4-BDS	65±5	20	0.46	483	1.59	56.1	Self
MACS	Mesua DOWC	4-BDS	65±5	20	0.41	468	1.62	58.7	Self
MAC-SO_3H	Mesua DOWC	4-BDS	80	21	n.r	556	0.73	51.5	[25]
MACHT	Mesua DOWC	H_2SO_4,Hydrothermal	65±5	20	0.03	<1	1.73	29.2	Self
$MACH_2SO_4$	Mesua DOWC	H_2SO_4	65±5	20	0.61	690	0.19	26	Self

BDS = benzenediazoniumsulfonate, AC = activated carbon, DOWC = de-oiled waste cake, * expressed in activity/mmol SO_3H

6.3.2.2. Cellulose hydrolysis

In contrast to esterification, hydrolysis of cellulosic materials involves the breaking of glycosidic bonds in polysaccharides with H_2O to produce the building monosachhrides/sugar molecules (a valuable precursor for bioalcohols, fuels and chemicals).

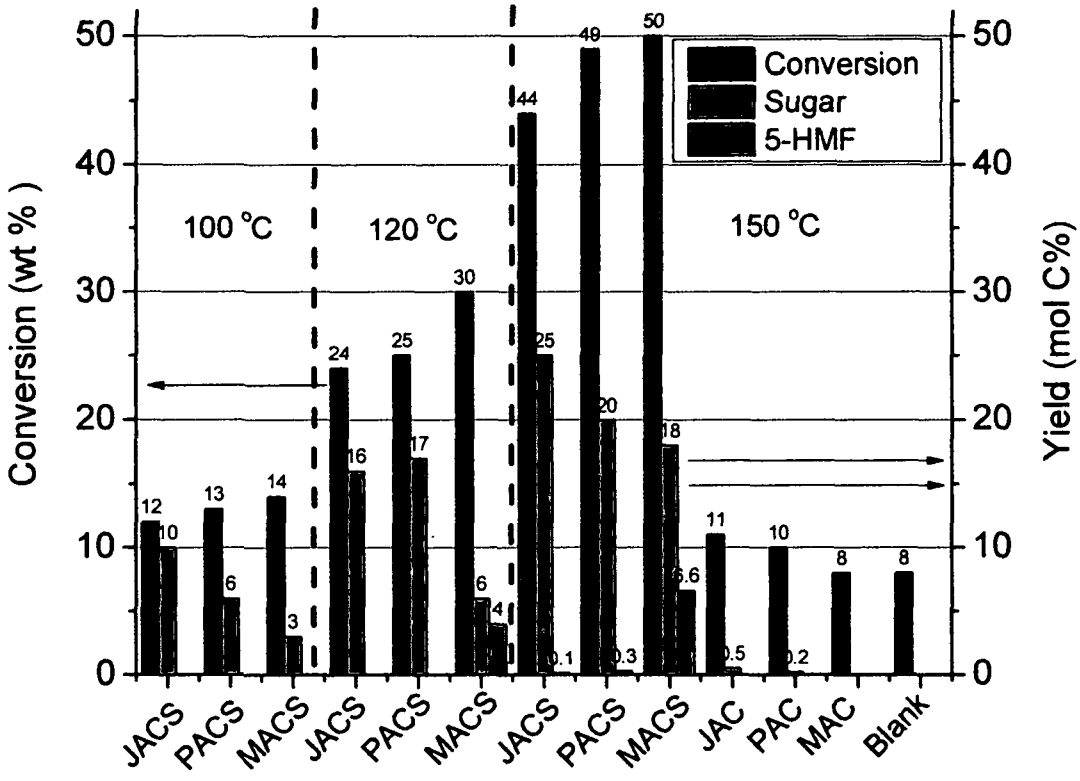

Figure 6.16. Hydrolysis of microcrystalline cellulose over DOWC derived catalytic materials. Reaction conditions: microcrystalline cellulose (crystallinity index =81%) 0.01 g, catalyst 0.01 g, deionised water 1 mL, reaction time 24 h.

The results summarized in Fig. 6.16, clearly shows the catalytic effect of the sulfonated materials when compared to their non sulfonated counterparts showing comparable activity as the blank reaction, H_2SO_4 treated carbons were not studied due to

lower stability of $-SO_3H$ groups in such materials. The increased sugar yield with temperature was consistent with earlier reports and related to the difficulties associated with getting past highly crystalline structure of microcrystalline cellulose (crystallinity index = 81%) at lower temperatures. The effect of reaction temperature on cellulose hydrolysis was investigated between 100-150 °C over the DOWC based carbons prepared by 4-benzenediazoniumsulfonate sulfonation, temperatures above 150 °C were not studied as sequential degradation of glucose to undesirable HMF, Levulinic and formic acid have been reported to occur which make sugar recovery difficult and inhibit downstream fermentation of the sugars to alcohols [37,38]. In addition to temperature, sugar yields were also affected by the catalyst properties as seen in Fig. 6.16. The more functionalized *J. curcas* and *P. pinnata* DOWC based catalysts, JACS and PACS showed superior selectivity towards the sugars with total sugar yields of 24% and 20% (mol C%) from microcrystalline cellulose at 150 °C, while to our surprise MACS, the most active esterification catalyst produced the lowest sugar yield and formed degradation products such as HMF, the general order of activity being JACS> PACS> MACS (opposite of esterification) (Fig. 6.16). This low saccharification activity MACS was probably caused by the high $-SO_3H$ and phosphate density facilitating the sequential degradation of sugars. In addition, since the material possessed a lower total acid density (lower density of –OH, –COOH groups), its ability to absorb glucans and water soluble oligomers was limited in comparison to JACS or PACS. Hara *et al.* [4,5,39] indicated that phenolic groups present in sulfonated carbons can absorb glucans and water soluble oligomers, which are then consequently hydrolyzed by $-SO_3H$ groups present on the catalyst surface to sugars. On the other hand, the superior catalytic performance of JACS and PACS could be related to the presence of higher amounts of –OH and –COOH groups, resulting in an enhanced ability of these materials to absorb glucans and water soluble oligomers [39]. Nevertheless, the sugar yields were still much lower than the values reported for sulfonated carbons in literature [28,40-42]. The lower yields could be attributed to the fact that cellulose substrate was not subjected to any pre-treatments to reduce the crystallinity, while the previous studies have used cellulose pretreated by ball-milling as substrate which are amorphous and much easier to hydrolyze [28,40-42]. However, treatments such as ball-milling require very long durations (~48 h) and can-not be considered as a realistic

approach to reduce crystallinity at large scale [43,44]. Ionic liquid (IL) pre-treatment on the other hand has been reported to be an equally effective method to reduce cellulose crystallinity and offers several additional advantages including, short pre-treatment times (1-3 h against 48-72 h for ball-milling), the feasibility of recovering100% of the used IL,

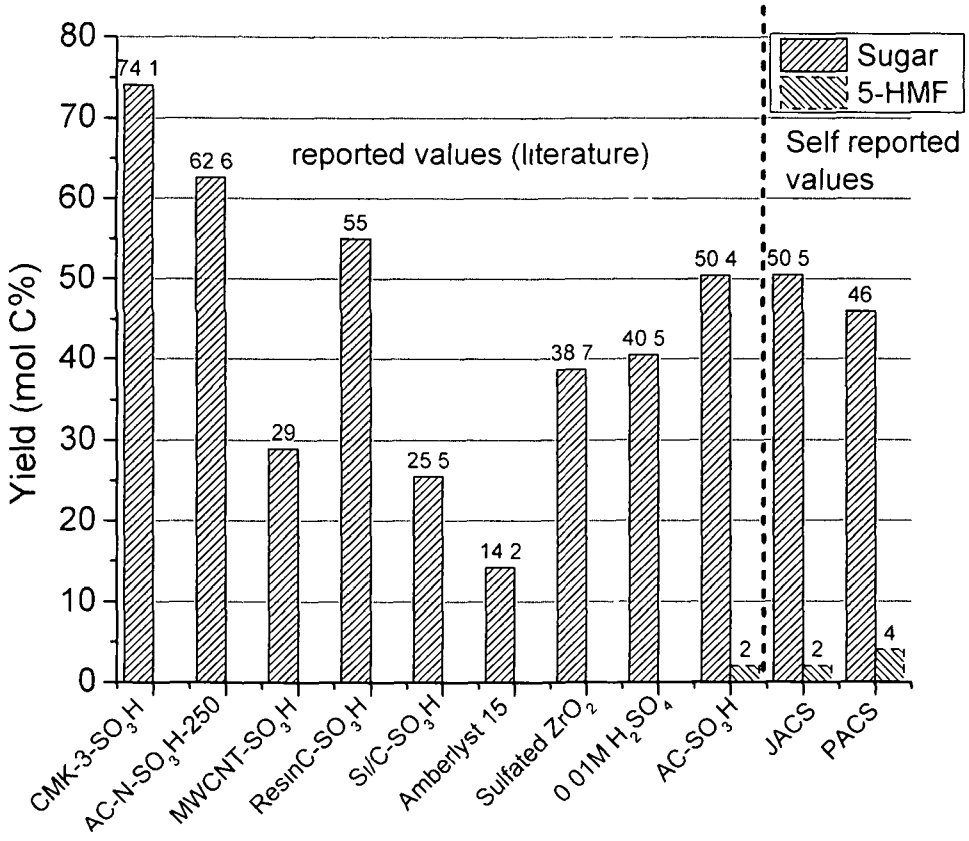

Fig. 6.17. Comparison of the saccharification activity of the DOWC-based sulfonated carbon with carbons and solid acids reported in literature. Reaction conditions: amorphous cellulose (ball-milled/ionic liquid treated): catalyst: H_2O = 1:1:1 (w/w/v), reaction time 24 h and temperature 150 °C.

ability to dissolve and instantly regenerate large quantities cellulose to its initial purity under mild conditions. The Cl^- containing idazolium ionic liquids particularly have been reported to be highly efficient in cellulose dissolution resulting from their high hydrogen bond basicity [43].

Therefore in the following experiments, reactions were performed using cellulose substrate regenerated by 1-ethyl-3-methylimidazolium chloride pre-treatment over the

most active JACS and PACS catalysts at 150 °C and their yields were also compared to the previously reported carbons. The results presented in Fig. 6.17 show two fold increase in sugar yield consistent with the lower crystallinity of the IL treated cellulose and sugar yields comparable with carbons reported in literature. JACS slightly outperformed PACS and yield 50.5% sugars. The sugar yields for DOWC based catalysts were higher than sulfonated AC reported by Onda *et al.* [28], sulfonated amorphous sugar catalyst Vyver *et al.* [40] and most of the sulfonated AC catalysts reported by Pang *et al.* [41] and comparable to the sulfonated silica/carbon nanocomposite catalyst Vyver *et al.* [40], but much lower than sulfonated CMK-3 and HNO_3 pre-treated sulfonated AC catalyst reported by Pang *et al.* [40] (Fig. 6.17). The lower yield of JACS in comparison to mesoporous sulfonated CMK-3 and sulfonated resin can be attributed to its lower surface area and pore volume, whereas for PACS it could be primarily attributed to the formation of degradation products due to its higher $-SO_3H$ density and presence of lower amounts of surface functional groups. These findings point to the need of a balanced structure with optimum mix of both strong and weakly acidic sites and a mesoporous structure for high saccharification activity of sulfonated carbons. Consequently, the combination of IL pre-treatment with hydrolysis catalyzed by sulfonated carbons could be an effective method for obtaining sugars from cellulosic materials. In a related study Zhang *et al.* [44] reported similar effect of IL pretreatment, where sugar yield increased by 4 times using 1-butyl-3-methyl imidazolium chloride pre-treated cellulose. Finally, the sulfonated carbons also exhibited excellent activity in saccharification of lignocelluloses, as indicated by 65 % sugar yield obtained from Mesua DOWC with MACS catalyst under identical reaction conditions. However, reusability studies could not be performed due to the difficulties associated with separation of unreacted cellulose from catalyst particles, resulting in overestimation of sugar yield during reusability tests, this issue was recently addressed by Zhang *et al.* [45] with magnetic Fe_3O_4@C-SO_3H catalysts.

6.3.2.3. Comparison of the effects of structure on catalytic properties

Preparation methods strongly influenced the surface properties of DOWC based sulfonated carbons, thus affecting their catalytic properties. In general, catalysts with a higher porosity, high surface area and acid site density always favored high activity. The

conventional method of sulfonation (using H_2SO_4) was found to be less effective compared to radical sulfonation (using 4-benzenediazoniumsulfoante) for preparing catalysts with said features from DOWC. High esterification rates were favored for catalyst with high –SO_3H density and porosity, those obtained by chemical activation and radical sulfonation of *M. ferrea* and *P. pinnata* DOWC while the carbons obtained hydrothermally and by direct sulfonation exhibited poor activity resulting from limited pore space and low –SO_3H density respectively. On the other hand, the more functionalized JACS obtained from *J. curcas* cakes under identical conditions excelled in cellulose saccharification resulting from its superior ability to absorb water soluble glucans, the criteria for high saccharification activity was a balanced surface structure with optimum mix of both strong and weakly acidic sites and a mesoporous structure further enhanced this. Interestingly, PACS owing to its highest specific surface area, porosity and total acid density (~higher density of –OH, -COOH groups) simultaneously exhibited high activity in both reactions. Although catalytic activity of these materials were lower than the mesoporous sulfonated carbons viz. OMC–SO_3H and CMK–3–SO_3H, they were more active than the biochar, active carbon and carbohydrate based catalysts [4,11, 13,34]. Besides, the additional advantage of these materials remains in their easy and cost effective preparations using a waste generated within biodiesel production. Further improvements in catalytic activity of these DOWC based materials could be possible by improving mesopore content and surface functional group density.

6.4. Conclusion

An effective and straight forward method to transform solid bio-wastes (DOWC) generated in biodiesel production to highly active sulfonated carbon catalysts has been demonstrated, consisting of chemical activation and radical sulfonation. Use of chemical activation was necessary to facilitate porosity and functional group development, in order to enhance the catalytic performance. The reported sulfonated carbon materials show remarkable potential as alternative and environmentally benign catalysts in the production of biofuels (biodiesel and bioalcohols). Structurally these carbons were more complicated than previously reported sulfonated carbons and contained phosphates, nitrogen compounds in addition to -SO_3H, -COOH, -OH and lactones typically present in carbohydrate, sugar or resin based sulfonated carbons. Conventional H_2SO_4 sulfonation

failed to produce catalysts with a high $-SO_3H$ density and porosity simultaneously. Radical sulfonation on the other hand was found to be more effective and produced catalysts with tenfold high $-SO_3H$ densities than H_2SO_4 sulfonation even from graphitic and ordered AC. Carbon source and amount of sulfonating agent used influenced efficiency of radical sulfonation and hence $-SO_3H$ density and catalytic activity. A high density of $-SO_3H$ groups usually resulted in higher esterification rates while a higher density of surface functional groups –COOH, –OH favored high saccharification activity as well as selectivity towards sugars. Thus, the *M. ferrea* and *P. pinnata* DOWC based catalysts with higher $-SO_3H$ density and surface area were found to be more active in esterification of oleic acid whereas the Jatropha cake based catalyst showed better activity and selectivity in cellulose saccharification.

6.5. References

1. Zheng, S. et al. Acid-catalyzed production of biodiesel from waste frying oil. *Biomass Bioenergy,*, **30**(3), 267–272, 2006.
2. Soetaert, W. & Vandamme E.J. *Biofuels In Wiley-Series in Renewable Resources*, Wiley, New York 2009.
3. Konwar, L.J. et al. Review on latest developments in biodiesel production using carbon-based catalysts. *Renew Sust Energ Rev*, **29**, 546–564, 2014.
4. Hara, M. Biomass conversion by a solid acid catalyst. *Energy Environ. Sci.*, **3**, 601–607, 2010.
5. Nakajima, K. & Hara M. Amorphous carbon with SO_3H groups as a solid brønsted acid catalyst. *ACS Catal.*, **2**(7), 1296–1304, 2012.
6. Gonçalves, M. *et al.* Glycerol conversion catalyzed by carbons prepared from agroindustrial wastes. *Ind. Eng. Chem. Res.*, **52**, 2832–2839, 2013.
7. Peng, L. et al. Preparation of sulfonated ordered mesoporous carbon and its use for the esterification of fatty acids. *Catal. Today.*, **150**, 140-146, 2010.
8. Zong, M.H. et al. Preparation of a sugar catalyst and its use for highly efficient production of biodiesel. *Green Chem.*, **7**, 434–7, 2007.
9. Budarin, V. et al. Starbons: New Starch-Derived mesoporous carbonaceous materials with tunable properties. *Angew. Chem. Int. Ed.*, **45**, 3782-3786, 2006.

10. Devi, B.L.A.P. et al. A Glycerol-based carbon catalyst for the preparation of biodiesel. *ChemSusChem.* **2**(7), 617–620, 2009.
11. Yu, J.T. et al. Development of biochar-based catalyst for transesterification of canola oil. *Energy Fuels.* **25,** 337–344, 2010.
12. Kitano, M. et al. Preparation of a sulfonated porous carbon catalyst with high specific surface area. *Catal. Lett.*, **131,** 242–249, 2009.
13. Shu, Q. et al. Synthesis of biodiesel from waste vegetable oil with large amounts of free fatty acids using a carbon-based solid acid catalyst. *Appl Energy.* **87**(8), 2589–2596, 2010.
14. Rao, B.V.S.K. et al. Carbon-based solid acid catalyst from de-oiled canola meal for biodiesel production. *Catal. Commun.*, **14**, 20–26, 2011.
15. Arancon, R.A. et al. Valorisation of corncob residues to functionalised porous carbonaceous materials for the simultaneous esterification/transesterification of waste oils. *Green Chem.*, **13,** 3162-3167, 2011.
16. Chang, B. et al. Soft-template synthesis of sulfonated mesoporous carbon with high catalytic activity for biodiesel production. *RSC Adv.*, **3,** 1987-1994, 2013.
17. Ordomsky, V.V. et al. Foam supported sulfonated polystyrene as a new acidic material for catalytic reactions. *Chem Eng. J.*, **207–208**, 218–225, 2012.
18. Ji, J. et al. Sulfonated graphene as water-tolerant solid acid catalyst. *Chem. Sci.*, **2,** 484–487, 2011.
19. Liu, R. et al. Sulfonated ordered mesoporous carbon for catalytic preparation of biodiesel. *Carbon,* **46**, 1664 –1669, 2008.
20. Geng, L. et al. Efficient carbon-based solid acid catalysts for the esterification of oleic acid. *Catal. Commun.*, **13,** 26–30, 2011.
21. Verma, M. et al. Efficacy of karanjin and phorbol ester fraction against termites (Odontotermes obesus). *Int. Biodeterior. Biodegrad.*, **65,** 877-882, 2011.
22. Deeba, F. et al. Bioprocessing of Jatropha curcas seed oil and deoiled seed hulls for the production of biodiesel and biogas. *Biomass Bioenergy,* **40,** 13–18, 2012.
23. Maarten, A. et al. Valorisation of Jatropha curcas: solubilization of proteins and sugars from the NaOH extracted de-oiled press cake. *Ind. Crop. Prod.*, **34**(1), 972–978, 2011.

24. Vernersson, T. et al. Arundo donax cane as a precursor for activated carbons preparation by phosphoric acid activation. *Bioresour Technol*, **83,** 95–104, 2002.

25. Konwar, L.J. et al. Biodiesel production from acid oils using sulfonated carbon catalyst derived from oil-cake waste. *J. Mol. Catal. A: Chem.*, In press, 10.1016/j.molcata.2013.09.031

26. Zhang, B.H. et al. Novel sulfonated carbonaceous materials from p-toluenesulfonic acid/glucose as a high-performance solid-acid catalyst, *Catal. Commun.*, **11** (7), 629-632, 2010.

27. Satyarthi, J.K. et al. Estimation of free fatty acid content in oils, fats, and biodiesel by ^{1}H NMR spectroscopy. *Energy Fuels,* **23,** 2273–2277, 2009.

28. Onda, A. et al. Selective hydrolysis of cellulose into glucose over solid acid catalysts *Green Chem.* **10,** 1033-1037, 2008.

29. Puziy, A.M. et al. Synthetic carbons activated with phosphoric acid. I. Surface chemistry and ion binding properties, *Carbon*, **40**, 1493–1505, 2002.

30. Wei, J. et al. TEM, XPS and FTIR characterization of sputtered carbon nitride films, *Surf. Interface Anal.* **28**, 208–211, 1999.

31. Puziy, A.M. et al. XPS and NMR studies of phosphoric acid activated carbons, *Carbon,* **46**, 2113–2123, 2008.

32. Nagaiah, T. C. et al. Mesoporous nitrogen-rich carbon materials as catalysts for the oxygen reduction reaction in alkaline solution, *ChemSusChem,* **5**, 637 – 641, 2012.

33. Ferrari, A.C. & Robertson J. Interpretation of Raman spectra of disordered and amorphous carbon. *Phys. Rev. B: Condens. Matter*, **61**(20), 14095-14107, 2000.

34. Kastnera, J.R. et al. Catalytic esterification of fatty acids using solid acid catalysts generated from biochar and activated carbon. *Catal. Today*, **190,** 122– 132, 2012.

35. Aldana-Pérez, A. et al. Sulfonic groups anchored on mesoporous carbon Starbons-300 and its use for the esterification of oleic acid, *Fuel,* **100**, 128–138, 2012.

36. Janaun, J.A.B. Ph.D, thesis, Development of sulfonated carbon catalysts for integrated biodiesel production, The University of British Columbia, Vancouver, Canada, 2012.

37. Larsson, S. et al. The generation of fermentation inhibitors during dilute acid hydrolysis of softwood. *Enzyme Microb. Technol.* **24**(3–4), 151–159, 1999.
38. Wu, Y. et al. Microwave-assisted hydrolysis of crystalline cellulose catalyzed by biomass char sulfonic acids. *Green Chem.,* **12**, 696–700, 2010.
39. Kitano, M. et al. Adsorption--1,4 glucans on graphene-based amorphous carbon bearing SO_3H, COOH, and OH groups, *Langmuir*, **25,** 5068 – 5075, 2009.
40. de Vyver, S. V. et al. Sulfonated silica/carbon nanocomposites as novel catalysts for hydrolysis of cellulose to glucose, *Green Chem.*, **12**, 1560–1563, 2010.
41. Pang, J. et al. Hydrolysis of cellulose into glucose over carbons sulfonated at elevated temperatures. *Chem. Commun.*, **46,** 6935–6937, 2010.
42. Yu, Y. & Wu, H. Effect of Ball Milling on the Hydrolysis of Microcrystalline Cellulose in Hot-Compressed Water, *AIChE Journal*, **57**(3), 793–800, 2011.
43. Mäki-Arvela, P. et al. Dissolution of lignocellulosic materials and its constituents using ionic liquids-A review, *Ind. Crop. Prod.*, **32,** 175–201, 2010.
44. Zhang, Q. et al. Pretreatment of microcrystalline cellulose by ultrasounds: effect of particle size in the heterogeneously-catalyzed hydrolysis of cellulose to glucose, *Green Chem.*, **15**, 963-969, 2013.
45. Zhang, C. et al. Magnetic core–shell Fe_3O_4@C-SO_3H nanoparticle catalyst for hydrolysis of cellulose, *Cellulose,* **20**, 127–134, 2013.

Conclusion and future work

Chapter 7

Chapter 7

7.1. Conclusion

The replacement of fossil and petroleum fuels by renewable alternatives such as biodiesel, bioethanol, biobutanol has become increasingly important in recent years due to environmental as well as economic concerns. In spite of being well-established processes, the main drawbacks preventing the large scale commercialization of these fuels are their higher production costs and due to involvement of complex multi step synthesis and purification steps resulting from use of homogenous catalysts. It is well accepted fact that uses of heterogeneous catalysts offer several process advantages over the homogeneous counterparts which include easy catalyst separation from product and reusability which can greatly improve the process economics. However, most of the conventional heterogeneous catalysts (alumina, zeolites, Amberlyst, sulfated zirconia etc.) are plagued by high costs and performance issues (low activity) in connection to their applications in biofuel production. Therefore, improvement in biofuels process economics may be achieved through the use of cost effective solid catalysts which can be integrated to existing biofuel production units, e.g. using of catalyst synthesized from bio-wastes or in situ generated wastes within biofuel production. This will not only eliminate the use of corrosive chemicals such as H_2SO_4, NaOH, KOH etc. but make the process environmentally benign, cost effective and greener one.

The present investigation was undertaken with the aim of bridging the cost gap in heterogeneous biofuel synthesis by developing solid catalysts from renewable sources using easily available bio-wastes. Within this work, several types of biogenic wastes viz. (i) post harvest crop residues of *Vigna radiate* plant and (ii) *Musa balbisiana* pseudo stem, (iii) mollusk shells and (vi) de-oiled waste cake residues from biodiesel production were successfully transformed into heterogeneous catalysts and applied in various reactions associated with the production of biofuels. In order to achieve the desired transformations three different approaches were applied namely, (i) calcination in Chapter 3, (ii) carbonization followed by activation and impregnation in Chapter 4 and (iii) carbonization/chemical activation followed by sulfonation in Chapter 5 & 6. The catalytic

activities were studies by employing esterification, transesterification (biodiesel production) and cellulose saccharification (bioalcohol production) as model reactions.

The heterogeneous alkali and alkaline bases discussed in Chapter 3 and 4 were employed in transesterification of vegetable oils to FAMEs (subjected FFA content in oil were less than 1 wt%). FAME yield upto 96% was achieved under optimized reaction conditions over the CaO supported active carbon (ACaO) catalyst discussed in Chapter 4. It also exhibited superior reusability and stability in comparison to neat as well doped CaO catalysts under investigated reaction conditions. The Ash (mixed alkali and alkaline oxide type catalysts) although active (~92% FAME yield) were prone to severe deactivation as the active species (K_2O and CaO) were easily leached to the reaction media.

The DOWC based sulfonated carbons discussed in Chapter 5 and 6 showed excellent activities for biodiesel production from Acidic oils (AO). The materials were also capable of selectively hydrolyzing cellulosic materials to fermentable sugars (the intermediates in bioethanol and biobutanaol production). These materials can be easily integrated into biodiesel production itself, which can sustainably reduce the process economics. The catalytic activities of the DOWC derived sulfonated carbon materials were higher than homogenous H_2SO_4 under identical reaction conditions. Transesterification activity was found to be dependent on the reaction conditions and initial FFA content in AO. Higher initial FFA content led to increased transesterification activity resulting from the increased mutual solubility of the oil and methanol. Under optimized conditions, FAME yields upto ~71% was achieved from the catalyst derived from *M. ferrea* DOWC. The structural features of these materials (surface area, acidity) were in turn influenced by preparation method and the properties of carbon source (DOWC) which ultimately affected their catalytic properties. In general, catalysts with a higher porosity, high specific surface area and acid site density always favored high activity. The conventional method of sulfonation (using H_2SO_4) was found to be less effective compared to radical sulfonation (using 4-benzenediazoniumsulfoante) for preparing catalysts with these features. High esterification rates were favored for catalyst with high $-SO_3H$ density and porosity; those obtained by chemical activation and radical sulfonation of *M. ferrea* and *P. pinnata* DOWC while the carbons obtained hydrothermally and by direct sulfonation exhibited

poor activity resulting from limited pore space and low $-SO_3H$ density respectively. On the contrary, the strongly hydrophilic materials (higher total acid/surface functional group density), those obtained from *J. curcas* and *P. pinnata* DOWC exhibited superior saccharification activity. Molar sugar yield upto 50% was reached using a combination of 1-ethyl-3-methylimidazolium chloride pre-treatment followed by subsequent hydrolysis over JACS (Jatropha DOWC derived sulfonated carbon catalyst) under optimized conditions.

7.2. Suggestions for future work

The present works could not cover many other reactions linked with biofuel production (Chapter 1, Fig. 1.4). There are scopes for further investigation on both the application and optimization part of synthesis conditions (e.g. carbonization temperature, activating agent, method etc. to improve catalytic properties) for the DOWC based sulfonated carbons discussed in Chapter 5 and 6.

One of the main interests will be to improve the transesterification activity and to examine catalytic activity of these materials in other acid catalyzed reactions leading to the production of biofuels (e.g. glycerol transformation). In our preliminary tests the sulfonated carbons reported in this study have shown excellent activity in glycerol etherification with *tert*-butyl alcohol (TBA) and studies are presently underway (Appendix I).

Magnetization of the carbon materials is another option which could make the separation of catalyst from product mixtures especially for solid state reactions.

Surface modification the DOWC based AC carbons with basic functionalities for catalytic applications in base catalyzed reactions, CO_2 capture etc. (Appendix II).

One more aspect will be screening the application of these materials in fields other than catalysis e.g. water tenement, as adsorbents.

Appendix

Appendix I

Synthesis of GTBE over DOWC based sulfonated AC

The catalytic applicability of the DOWC derived sulfonated carbons were examined in glycerol upgradation to fuel additives (GTBE) by etherification with *tert*-butanol (TBA).

A1.1. Introduction

Glycerol is an unavoidable by-product from biodiesel and soap production, although it cannot be used as a fuel or additive it can be etherified with *tert*-butyl alcohol (TBA) or isobutene in the presence of acid catalysts to mono-tertbutyl glycerol (MTBG), di-tert-butyl glycerol (DTBG), and tri-tert-butyl-glycerol (TTBG) ethers (collectively called as GTBE). Glycerol etherification with *tert*-butanol produces water as a by-product, while isobutene does not. Conversely, isobutene is very expensive compared to *tert*-butanol and requires high pressure (2 MPa) to keep it in liquid form. Klepacova *et al.* [1,4] applied several commercial solid acid catalysts such as Amberlysts (15, 31, 35 and 119), ion-exchange resins (A-31 and A-119) and large-pore zeolites (H-Y and H-Beta) to catalyze glycerol etherification with isobutene and *tert*-butanol and found that etherification with *tert*-butanol leads to lower conversion and selectivity owing to formation of water by dehydration of *tert*-butanol, deactivating the catalysts. Overall, etherification with TBA is more attractive due to lower costs and operational difficulties associated with handling highly inflammable isobutene [1-6].

Owing to their remarkable acidic properties the sulfonated carbons or sugar catalysts may have prospective catalytic applications in glycerol etherification. They have already been applied in a range of acid catalyzed reactions such as: esterification, transesterification, and hydrolysis. Recently, these sulfonic acid-functionalized carbon materials have also been demonstrated to show excellent catalytic activity in glycerol transformations (esterification and etherification), however, the etherification with isobutene showed more favorable results with better selectivity towards desired higher ethers [7-9]. Thus keeping in mind the role of sulfonated carbons in glycerol conversion, the etherification activity of the synthesized DOWC based sulfonated carbons were also evaluated using PS500 as one of the representative catalysts.

A1.2. Materials and methods

A1.2.1. Materials

Glycerol (99%, anhydrous), *tert*-Butanol (ACS grade) were purchased from Merck India Ltd. N,O-Bis(trimethylsilyl)trifluoroacetamide (99%), Pyridine (99%) and all analytical solvents were purchased from Sigma Aldrich. The PACS described in Chapter 6 was chosen as representative catalyst due to highest surface and acidity among the DOWC based sulfonated carbons.

A1.2.2. Methods

The catalytic tests were performed in batch mode in a 200 mL autoclave equipped with digital temperature indicator and magnetic stirring. In a typical reaction, 0.5 g (5 wt%) of catalyst (particle size <250 μm, pre dried at 150 °C) was added to 10 g glycerol stirred (250 rpm), followed by an addition of 32.2/73 g preheated *tert*-butanol, heated to 90 °C for desired time (1-10 h). After, completion of reaction to determine conversion of glycerol, products were analysed by GC on a TRACE™ 1300 (Thermo Scientific) equipped with FID detector and Agilent (Select Biodiesel for glycerides) GC column. The column temperature was held at 50 °C hold 1 minute, 15 °C/minute to 180 °C, 7 °C/minute to 230 °C, 30 °C/minute to 380 °C and held for 5 minute. Helium was used as the carrier gas at a flow rate of 3 mL/min. The products were subjected to silylation prior to GC analysis. In a typical process 500 mg N,O-Bis(trimethylsilyl)trifluoroacetamide was added to 100 mg product followed by addition of 10 mL pyridine, the resulting contents were hated on a oil bath at 70 °C for 1 h. The individual products were identified by GC-MS of un-silylated products due to commercial unavailability standards. GC-MS was performed on a on a Perkin Elmer Claurus 600 equipped with DB-5 MS column to achieve desired chromatographic separation. The column temperature was held at 50 °C for 1 min, then heated from 50 °C to 250 °C and the rate of increase was 5 °C/min. The carrier gas used was helium and the flow rate was maintained at 1 mL/min. The MS was scanned from 50 to 600 Da. The conversion C_{Gly} was based on glycerol concentration measured at specified time intervals from calibration curves:

$$C_{Gly}(\%) = \frac{(C_i - C_t)}{C_i} \qquad (A.i)$$

where, C_i is the initial concentration and C_t is concentration measured at time t.

Here, the selectivity to MTBG, DTBG and TTBG has been expressed as area percentages from TIC (total ion chromatogram) of GC-MS as direct comparison with standard solutions of MTBG, DTBGs and TTBG was not possible.

A1.3. Results and discussion

Fig. AI1-AI4, shows the TIC and EI mass spectrum of the sample obtained at 4 h. The product identification was based on the method described by Jamróz *et al* [10]. Almost all EI spectra were very similar to each other, typically exhibiting the base peak at m/z = 57 corresponding to fragment ion $[C_4H_9]^+$ of TBA. These spectra are slightly different from the ones report by Janaun *et al.* [8] where peak at mz = 45 corresponding to fragment ion $[C_3H_9]^+$ from $-(CH_3)_3$, was dominant. Most of the EI patters resembled those reported by *Jamroz et al.* [10], where peak the base peak was at m/z = 57.

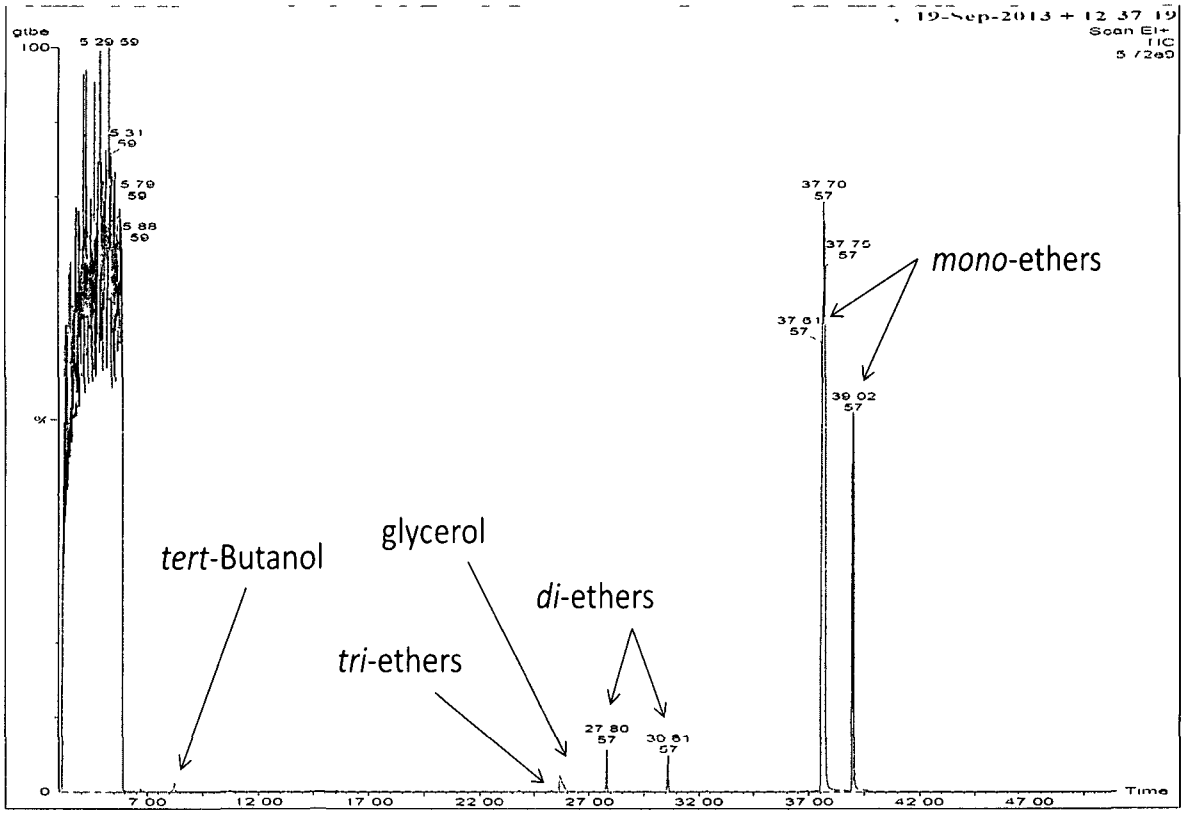

Figure AI1. Gas chromatogram of the sample obtained at 4 h.

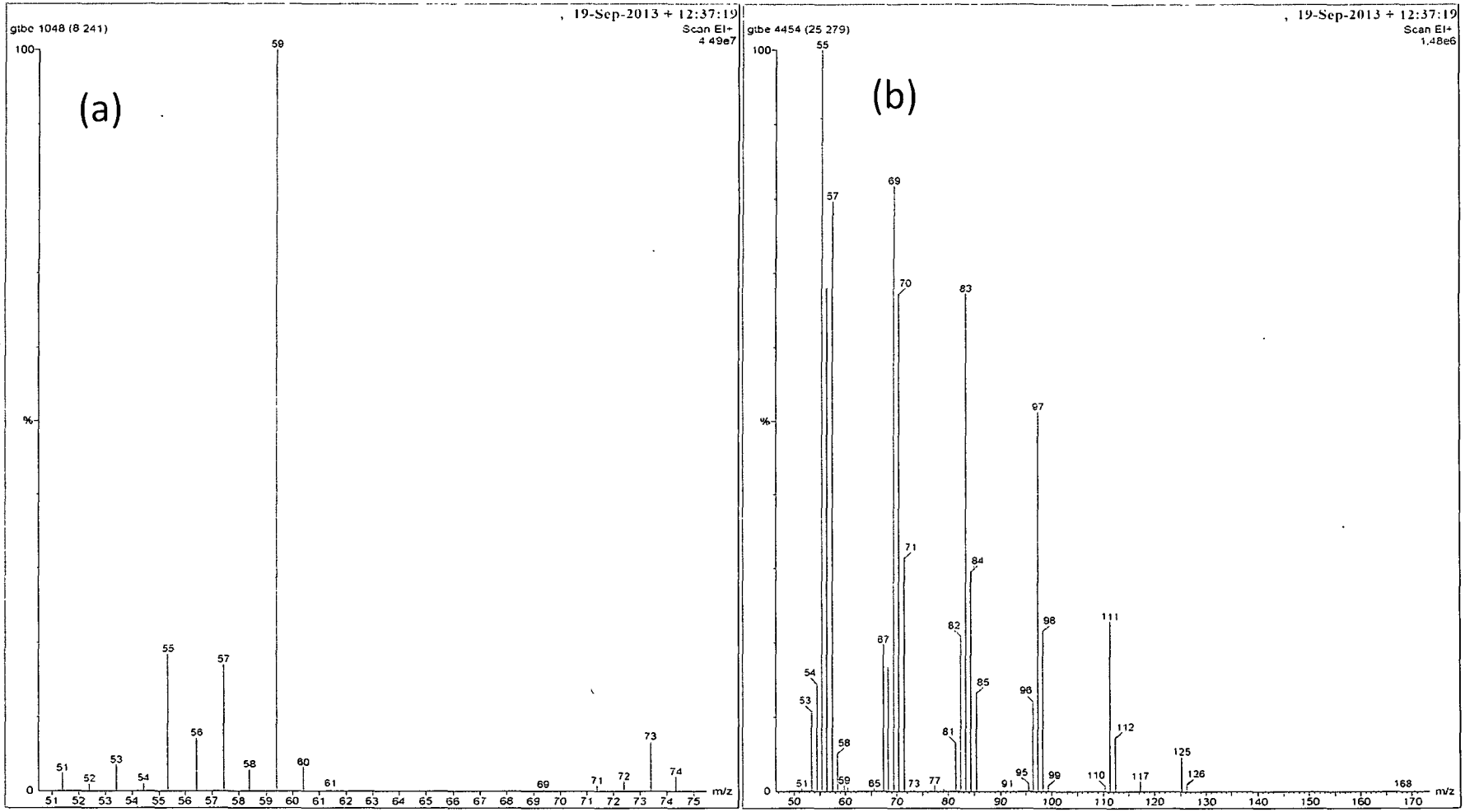

Figure AI2. EI mass spectrum of (a) TBA and (b) TTBG

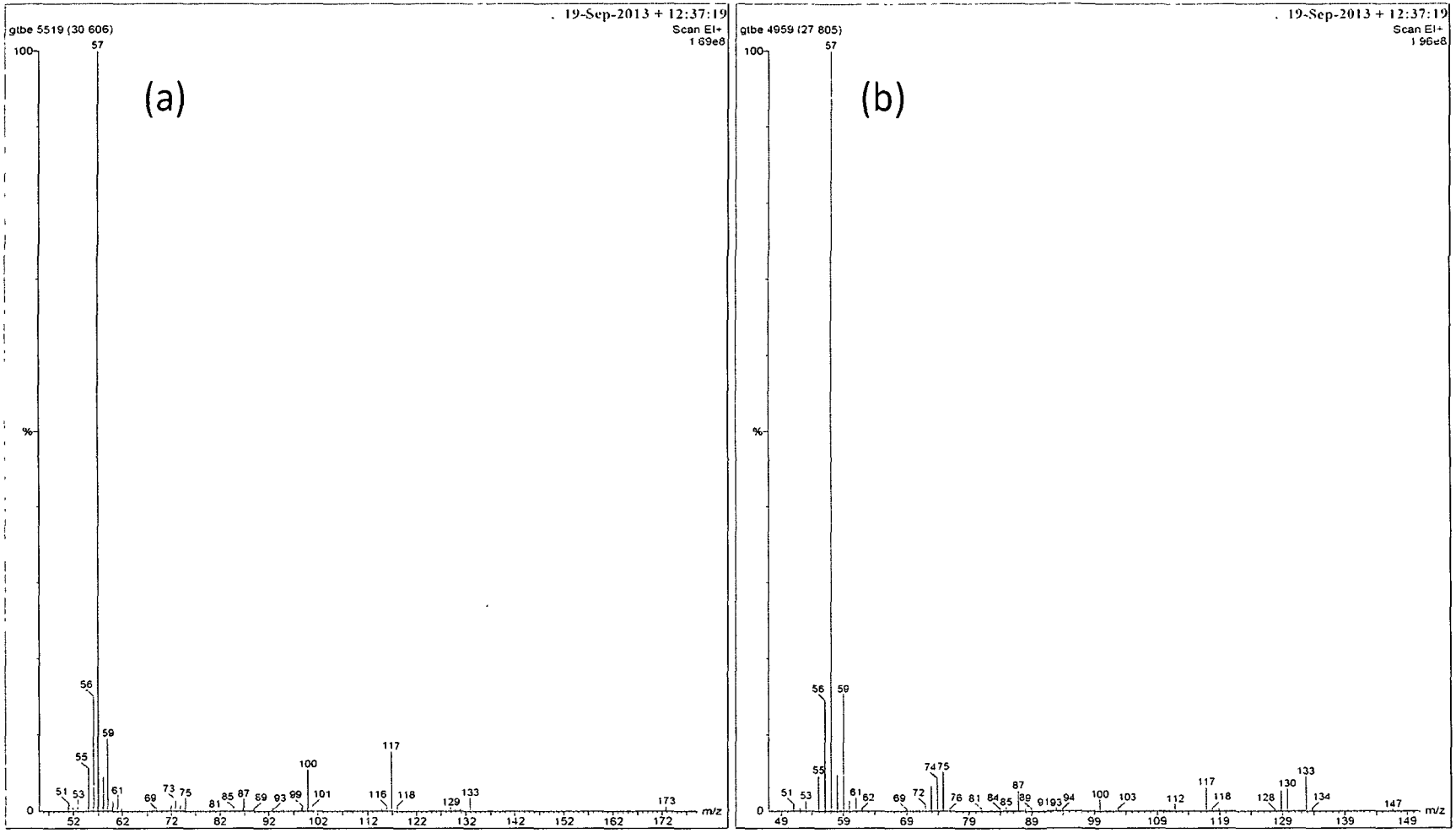

Figure AI3. EI mass spectrum of (a) DTBG and (b) DTBG isomer.

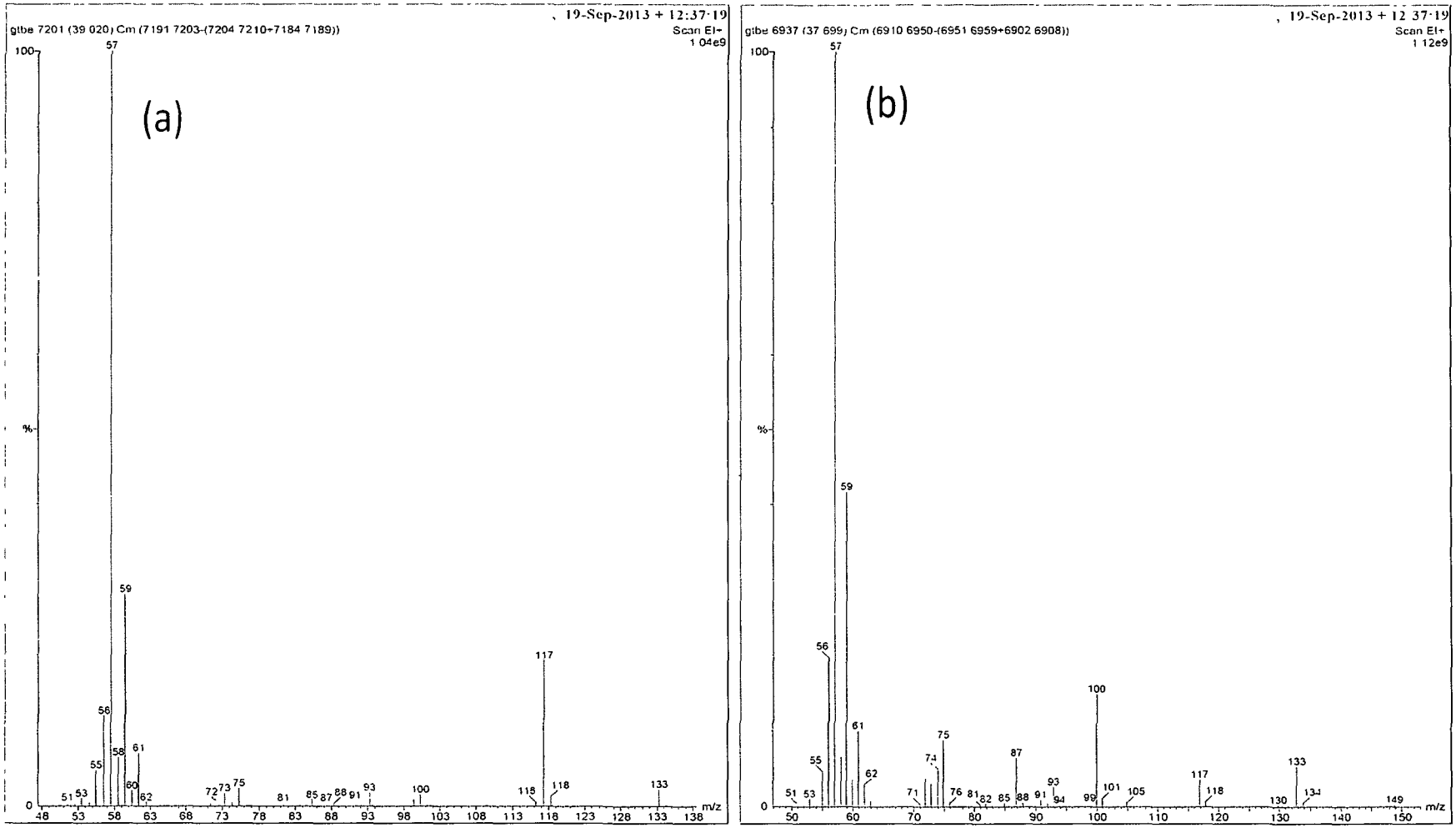

Figure AI4. EI mass spectrum of (a) MTBG and (b) MTBG isomer.

Fig. AI5 shows the catalytic activity of PACS at 90 °C as function of glycerol conversion. Conversion increased with increased reaction time and reached a steady equilibrium (94%) at 6 h, however selectivity to higher ethers (*di-* and *tri-*) steadily increased till 7 h (expressed as area percentage) beyond which it remained constant. In comparison to similar agro-industrial waste based carbons reported in literature the selectivity to higher ethers were lower most likely from the use of lower reaction temperature [7,11]. However, the improved conversion could be associated with the higher surface area of JACS (914 m^2/g) in comparison to those previously reported in literature (<1 m^2/g). On increasing molar ratio the selectivity to the *di-* ether increased but *tri-*ether selectivity did not increase significantly. Therefore, it might be possible to enhance the selectivity of higher ethers by (i) removal of water and/or (ii) increasing the reaction temperature considering the high thermal stability of the DOWC based sulfonated carbon materials.

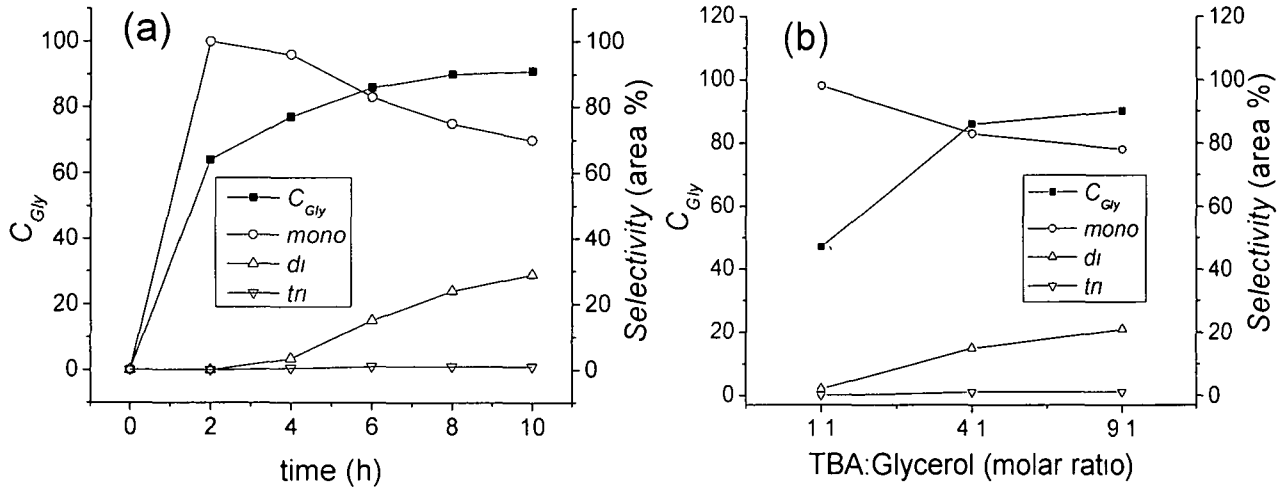

Figure AI5. (a) Glycerol conversion as a function of reaction time and (b) effect of *tert-*butanol (TBA) to glycerol molar ratio on product selectivity. Reaction conditions: catalyst = 5 wt% of glycerol, temperature = 90 °C, time = 6 h, autogenous pressure and stirring rate = 500 rpm.

A1.4. Conclusion

The DOWC based sulfonated carbons can be employed as catalysts in glycerol upgradation into fuel additives (GTBE) by etherification with TBA. The higher surface area these materials facilitated improved conversions (>90%), however, selectivity to desired higher ethers DTBG and TTBG were low most likely from the low reaction tempratures. The future prospects of the study will be improving DTBG selectivity as conversion to TTBG results in unnecessary consumption of TBA, since DTBG has fuel properties comparable to TTBG. In addition, effect of reuse and comparison with commercial zeolites and sulfonated resins will also be studied.

A1.5. References

1. Klepacova, K., et al. Tert butylation of glycerol catalyzed by ion-exchange resins. *Appl. Catal., A.*, **294**: 141-147, 2005.
2. Klepacova, K., et al. Etherification of glycerol with tert-butyl alcohol catalysed by ion-exchange resins. *Chem. Pap-Chem. Zvesti*, **60**, 224-230, 2006.
3. Klepácová, K. et al. Etherification of glycerol and ethylene glycol by isobutylene. *Appl. Catal., A.*, **328**, 1-13, 2007.
4. Klepacova, K., et al. Etherification of glycerol for diesel fuels. *Pet. Coal*, **45**, 54-57, 2003.
5. Melero, J. A. et al. Acid-catalyzed etherification of bio-glycerol and isobutylene over sulfonic mesostructured silicas. *Appl. Catal. A*, **346**, 44-51, 2008.
6. Frusteri, F. et al. Catalytic etherification of glycerol by tert-butyl alcohol to produce oxygenated additives for diesel fuel, *Appl. Catal. A*, **367**(1–2), 77–83, 2009.
7. Gonçalves, M. et al. Glycerol Conversion Catalyzed by Carbons Prepared from Agroindustrial Wastes, *Ind. Eng. Chem. Res.* **52**, 2832−2839, 2013.
8. Janaun, J. & Ellis, N. Glycerol Etherification by tert-butanol catalyzed by sulfonated carbon catalyst. *J. Appl. Sci.* **10**, 2633, 2010.
9. Zhao, W. et al. Etherification of Glycerol with Isobutylene to Produce Oxygenate Additive Using Sulfonated Peanut Shell Catalyst, *Ind. Eng. Chem. Res.*, **49** (24), 12399–12404, 2010.

10. Jamroz, M.E. et al., Mono, di, and tri-tert-butyl ethers of glycerol: A molecular spectroscopic study. *Spectroc Acta Pt A-Molec Biomolec Spectr*, **67,** 980-988, 2007.

11. Galhardo, T.S. et al Preparation of Sulfonated Carbons from Rice Husk and Their Application in Catalytic Conversion of Glycerol, *ACS Sustainable Chem. Eng.*, **1**, 1381−1389, 2013.

Appendix II

DCC aided grafting $-NH_2$ groups on active carbon

A green protocol for grafting carbon (AC) surfaces with $-NH_2$ groups was developed and applied on the *Jatropha curcas* DOWC derived AC. $-NH_2$ modification was achieved by N,N'-Dicyclohexylcarbodiimide (DCC) mediated grafting process.

AII.1. Introduction

Carbon materials have unique mechanical, electrical and structural properties which have due to which they find diverse applications in catalysis, adsorption, water, gas purification and as electrode materials. Furthermore, the surface properties of the carbon materials can be easily tuned to incorporate acidic or basic groups, which can alter their properties drastically [1]. The $-SO_3H$ modified carbons have high acidities comparable to H_2SO_4 which makes them a suitable substitute to conc. H_2SO_4 acid catalyzed reactions [1-3]. In a similar way several methods are available to produce an amine-functionalized carbon surface, which may be used to form subsequent amide linkages, hydrogen bonds, or merely to change the surface adsorption properties [1,4]. Recently, Villa *et al.* [5] used amino-functionalized carbon nanotubes as solid basic catalysts for the transesterification of triglycerides. In addition such materials can find applications as adsorbents for CO_2 removal from biogas or industrial flue gases. So, far amination of the carbon surfaces is accomplished mainly by reaction with diamines. A typical process involving three steps, (i) introduction of carboxylic groups onto the surface of carbon by oxidising it with nitric acid, followed by (ii) reaction with thionyl chloride to transform the carboxylic acid groups to the acid chlorides which are than (iii) treated with diamines to yield amine modified carbons. Activation with thionyl chloride resulted in more diamine being immobilized on the surface than reaction with nitric acid alone. It has also been shown that carbon fibers oxidized with nitric acid can be funtionalized with amine groups by reaction with tetraethylenepentamine. Both single and double-bridged forms were present on the carbon surface. Other methods include attachment by Attachment via. diazonium chemistry and n-butyllithium (nBuLi) activation methods [1,6-9].

With this prospect in mind an attempt was made to graft amines onto carbon surface by using N,N'-Dicyclohexylcarbodiimide (DCC) as a dehydrating/condensing agent to form amide bonds (Scheme A1). The uses of DCC can eliminate the use $SOCl_2$ and the number of steps involved in traditional amine grafting process (Scheme A2).

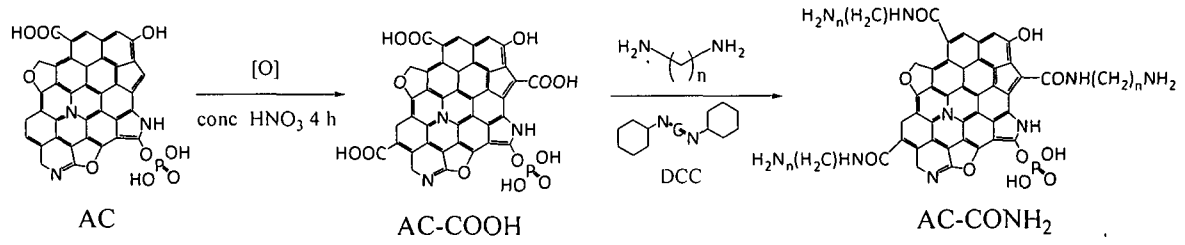

Scheme A1 Proposed route for $-NH_2$ grafting (N,N'-Dicyclohexylcarbodiimide aided)

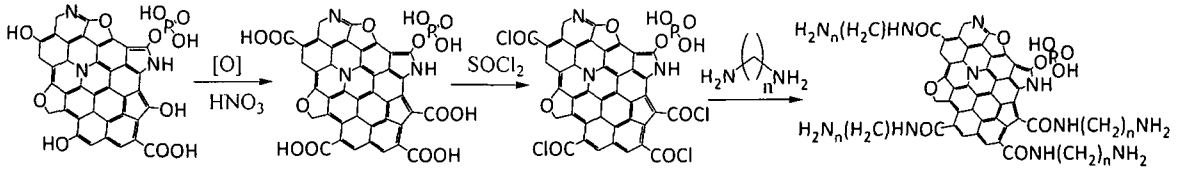

Scheme A2 Conventional route for $-NH_2$ grafting ($SOCl_2$ aided)

AII.2. Materials and Methods

AII.2.1. Materials

Oil cake press from *Jatropha Curcas* seeds were collected, ground and passed through Standard ASTM sieve (Mesh No. 60, 0.25 mm) and used as a precursor for the preparation of AC. HNO_3 (70%), tetrahydrofuran (HPLC grade) and acetone (99.5%) were purchased from Merck India Ltd. Mumbai. N,N'-Dicyclohexylcarbodiimide (≥99%) and Ethylenediamine (≥99.5%) were purchased from Sigma Aldrich. All solvents and chaemicals were used without further purifications.

The AC was prepared by chemical activation oil cake press with 50% phosphoric acid as at 500 °C under self-generated atmospheres as described earlier. For comparison unactivated carbon samples were also prepared at 500 °C as control.

AII.2.2. $-NH_2$ grafting

In a typical process, 5 g *Jatropha Curcas* derived AC was refluxed with 50 g concentrated HNO_3 for 4 h to generate –COOH groups on carbon surface. In the next step,

1 g –COOH modified carbon was refluxed with 0.33 mole (20 g) ethylenediamine (EDA) or hexaethylenediamine (HEDA) in the presence of 10 g N,N′-Dicyclohexylcarbodiimide (DCC) and 50 ml THF at 70 °C for 72 h. The resulting product was filtered washed with THF, acetone and then methanol until the filtrate became clear. The resulting amidized carbon were dried in vacuum at 110 °C for 24 h and labeled as NH_2-AC. The resulting materials were characterized by N_2-physisorption, XRD, elemental analysis and FT-IR.

AII.3. Results and discussion

The FT-IR spectrum of unmodified AC exhibit the typical bands of carbonyl groups (C=O, ~1712 cm^{-1}) and characteristic peaks of incompletely carbonised materials, near 1580 cm^{-1} attributable to aromatic ring modes. Upon oxidation, the intensity of –COOH bands increased sharply, in agreement with the success of oxidation process resulting in introduction of abundant –COOH groups on AC surface. The successful grafting of $–NH_2$ on AC was evident from shifting of this carbonyl band at 1712 cm^{-1} to 1569 cm^{-1} which confirmed the formation of amide linkages (CO-NH bonds) between EDA and -COOH groups. The increased intensity of carbonyl band in HNO_3 treated carbons was (Fig. AII1). The success of surface modifications on carbon was also indicated by the acid site densities measured by titration methods. The $–NH_2$ densities were estimated to be 2.53 and 2.26 mmol/g for EDA and HDA grafted carbons respectively, based on elemental analysis. There was almost ~96-97% reduction in specific surface area following NH_2 modification probably due to excessive loading of such groups. Thus, future prospective exists for optimization of the grafting conditions in order to achieve higher $–NH_2$ density, specific surface area and porosity simultaneously. The loss of porosity was also visible in the TEM images (Fig. AII2). The XRD patterns (not shown) exhibit a similar broad and weak (002) diffraction peak near 2θ=15-30° and resembled the previously discussed amorphous carbons (Chapter 5 and 6). No, detectable changes in XRD patterns were observed upon surface modification.

Both EDA and HEDA modified carbons (NH_2-AC) showed negligible transesterification activity at methanol to oil molar ratio of 9:1 and 65 °C, the low activity could be attributed to the low basicity of the primary amine groups and the low specific

surface area of these materials restricting the interaction between larger triglyceride molecules with active sites. Nonetheless, it could be possible to improve transesterification

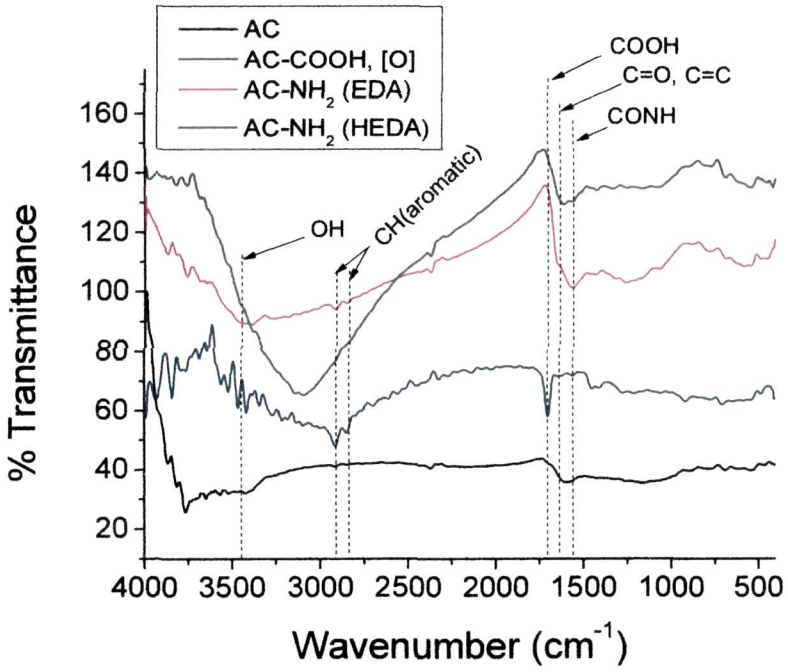

Fig. AII1. FT-IR patterns showing successful grafting of $-NH_2$ group

activity upon (i) increasing reaction temperature (ii) by grafting more basic amines (secondary, tirtery or guanidines) and (iii) increasing catalyst surface area [6]. The prospective applications of current materials may include: as sorbent for removal of carbon dioxide (CO_2), arsenic from water and as electrodes.

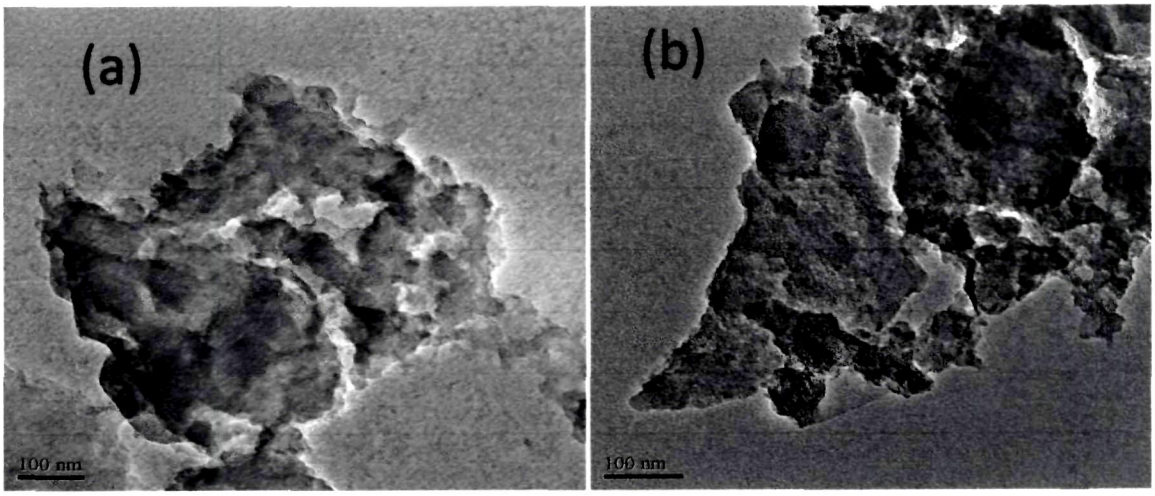

Fig. AII2.TEM images of (a) NH_2-AC (EDA) and (b) JAC showing loss of porosity upon grafting AC surface with ethylenediamine (EDA).

AII.4. Conclusion

Carbons with upto 14% N and $-NH_2$ group density of 2.4-2.5 mmol/g were obtained by DCC mediated grafting process. Use of DCC eliminates the use of $SOCl_2$ and reduces the number of steps involved. However, grafting also reduced porosity and surface area, thus, future prospective of the work will be optimization of the preparatory conditions to obtain high surface area, porosity and $-NH_2$ functionalization simultaneously.

AII.5. References

1. Stein, A et al. Functionalization of Porous Carbon Materials with Designed Pore Architecture, *Adv. Mater.*, **21**, 265–293, 2009.
2. Budarin, V, et al. Starbons: New Starch-Derived Mesoporous Carbonaceous Materials with Tunable Properties. *Angew. Chem. Int. Ed.*, **45**, 3782-3786, 2006.
3. Nakajima, K. & Hara, M. Amorphous Carbon with SO_3H Groups as a Solid Brønsted Acid Catalyst, *ACS Catal.*, **2** (7), 1296–1304, 2012.
4. Liu, G. et al. Development of non-precious metal oxygen-reduction catalysts for PEM fuel cells based on N-doped ordered porous carbon, *App. Cat. B*, **93**(1–2), 156–165, 2009.
5. Xiao, J, et al. CO_2 adsorption thermodynamics over N-substituted/grafted graphanes: a DFT study. *Langmuir.*, **30**(7), 1837-44, 2014.
6. Villa, A. et al. Amino-functionalized carbon nanotubes as solid basic catalysts for the transesterification of triglycerides. *Chem. Commun.*, 4405–4407, 2009.
7. Tamai, H, et al. Surface functionalization of mesoporous and microporous activated carbons by immobilization of diamine. *J Colloid Interface Sci.*, **295(1)**, 299-302, 2006.
8. M. Abe, et al. Amination of Activated Carbon and Adsorption Characteristics of Its Aminated Surface, *Langmuir* **16**, 5059, 2000.
9. Shafeeyan, M.S. et al. A review on surface modification of activated carbon for carbon dioxide adsorption, *J. Anal. Appl. Pyrolysis*, **89(2),** 143–151, 2010.